

**Scientific Cruise Report of the
Arctic Expedition ARK-XIII/2 of RV "Polarstern" in 1997**

**Wissenschaftlicher Fahrtbericht über die
Arktis-Expedition ARK-XIII/2 von 1997
mit FS "Polarstern"**

**Edited by
Ruediger Stein and Kirsten Fahl
with contributions of the participants**

**Ber. Polarforsch. 255 (1997)
ISSN 0176 - 5027**

**Scientific Cruise Report of the
Arctic Expedition ARK-XIII/2 of RV "Polarstern" in 1997**

**Wissenschaftlicher Fahrtbericht über die
Arktis-Expedition ARK-XIII/2 von 1997
mit FS "Polarstern"**

Ruediger Stein
Alfred Wegener Institute for Polar and Marine Research
Columbusstraße, Bremerhaven, Germany
e-mail: rstein@awi-bremerhaven.de

Kirsten Fahl
Alfred Wegener Institute for Polar and Marine Research
Columbusstraße, Bremerhaven, Germany
e-mail: kfahl@awi-bremerhaven.de

Cruise Report ARK-XIII/2, Content

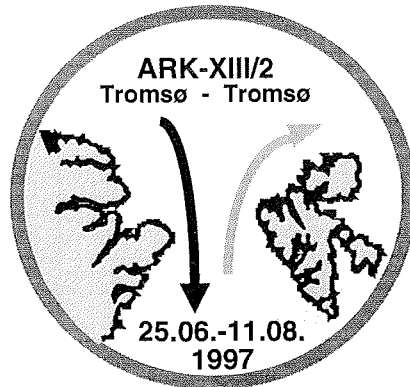
1	Introduction (R. Stein)-----	1
2	Itinerary (R. Stein)-----	4
3	Meteorological Conditions -----	13
	(K. Buhlmann, H. Sonnabend)	
4	Physical Oceanography -----	16
	(B. Rudels, R. Meyer, D. Hevekerl)	
5	Marine Biology -----	38
	(E. Rachor, H. Thiel, H. Auel, H. Bäsemann, E. Bauerfeind, S. Denisenko, E. Helmke, K. v. Juterzenka, M. Klages, U. Klauke, F. Kulescha, K. Kosobokova, S. Lischka, K. Meiners, V. O. Mokievsky, Y.B. Okolodkov, B. Sablotny, I. Schewe, V. Shevchenko, T. Soltwedel, Q. Zhang)	
5.1	Sea-Ice: Ecological Studies -----	38
	(Q. Zhang, K. Meiners, K. v. Juterzenka, S. Lischka)	
5.1.1	Sea-Ice Observations -----	39
	(Q. Zhang, K. Meiners, K. v. Juterzenka, S. Lischka)	
5.1.2	Physical and Biological Properties of Arctic Sea-Ice -----	40
	(Q. Zhang, K. Meiners)	
5.1.3	The Response of Arctic Sea-Ice Micro-Organisms to Changes of Salinity Under Different Light Conditions -----	42
	(Q. Zhang)	
5.1.4	Distribution of Organisms and Grazing Experiments with Arctic Sea-Ice Protists -----	44
	(K. Meiners)	
5.1.5	Characteristics and Biota of Small Melt Pools -----	45
	(K. v. Juterzenka, S. Lischka, K. Meiners, Y. B. Okolodkov, Q. Zhang)	
5.1.6	Sea-Ice Algae -----	47
	(Y. B. Okolodkov)	
5.2	Phytoplankton -----	49
5.2.1	Phytoplankton Ecology -----	49
	(E. Bauerfeind, Y. B. Okolodkov)	
5.2.2	Algae in Melt Pools -----	52
	(Y. B. Okolodkov)	
5.2.3	Phytoplankton: Studies on the Biodiversity, Taxonomy, Community Comparison and Biogeography -----	53
	(Y. B. Okolodkov)	
5.3	Zooplankton Ecology -----	60
5.3.1	Distribution of Mesozooplankton -----	60
	(K. Kosobokova, H. Auel, S. Lischka)	
5.3.2.	Egg Production in Pelagic Copepods -----	60
	(K. Kosobokova, S. Lischka)	
5.3.3	Ecology of Meso- and Bathypelagic Copepods in the Arctic Ocean -----	63
	(H. Auel)	
5.3.4	Meroplankton: Sampling of Zoobenthos Larval Plankton -----	64
	(E. Rachor)	
5.4	Vertical Particle Flux (E. Bauerfeind, V. Shevchenko)-----	65
5.5	Benthos -----	66
5.5.1	Epifauna/Megafauna -----	67
	(H. Thiel, K. v. Juterzenka, M. Klages, F. Kulescha, B. Sablotny)	

II

5.5.2	Macrofauna: Quantitative Assessment -----	67
	(E. Rachor, S. Denisenko)	
5.5.3	Meiobenthos-----	77
	(V. O. Mokievsky)	
5.5.4	Microbials -----	80
	(E. Helmke, U. Klauke)	
5.5.5	Activity and Biomass of the small Benthic Biota -----	82
	(T. Soltwedel, I. Schewe, V.O. Mokievsky, B. Sablotny)	
5.5.6	Sediment Community Oxygen Uptake -----	85
	(M. Klages)	
5.5.7	Experimental Studies on Echinoderms and Crustaceans -----	86
	(K. v. Juterzenka, M. Klages)	
5.6	Bird Observations -----	87
	(H. Bäsemann)	
6	Sea-Ice Sedimentology and Water Chemistry-----	90
	(D. Dethleff, V. Shevchenko)	
6.1	Sea-Ice Sediments -----	90
	(D. Dethleff)	
6.2	Snow and Melt Pond Water Chemistry -----	97
	(V. Shevchenko)	
7	Marine Geology-----	98
	(C.J. Schubert, M. Behrends, K. Fahl, H.-P. Kleiber, J. Knies, M. Levitan, M. Mitjajev, E. Musatov, G. Nehrke, F. Niessen, V. Shevchenko, R. Stein, R. Volkmann)	
7.1	Marine Sediment Echosounding using PARASOUND -----	99
	(F. Niessen, H.P.Kleiber)	
7.2	Geological Sampling, Description, and Methods Applied -----	106
7.2.1	Aerosol Sampling -----	106
	(V. Shevchenko)	
7.2.2	Sampling of the Water Column for Organic-Geochemical -----	106
	Investigations (K.Fahl)	
7.2.3	Oxygen and Carbon Isotopes Investigations of Water and -----	107
	Foraminifers (R. Volkmann)	
7.2.4	Nitrogen and Carbon Isotopes Investigations of Organic -----	110
	Material (C.J. Schubert)	
7.2.5	Sea Floor Sediment Sampling and Description-----	111
	(M. Behrends, K. Fahl, J. Knies, M. Levitan, M. Mitjajev, E. Musatov, G. Nehrke, R. Volkmann)	
7.3	Physical Properties and Core Logging -----	115
	(F. Niessen, H.-P. Kleiber)	
7.4	Lithostratigraphy and Sediment Characteristics-----	121
	(C. Schubert, J. Knies, M. Levitan, E. Musatov, R. Stein)	
7.5	Aerosols -----	136
	(V. Shevchenko)	
8	Geochemistry-----	138
	(M. Rutgers v. d. Loeff, E. Damm, M. Kühn, A. Maibaum)	
8.1	Early Diagenesis -----	138
8.1.1	Trace Metals-----	138
	(M. Kühn)	
8.1.2	Oxygen-----	138
	(E. Damm)	

III

8.2	The Benthic Nepheloid Layer-----	140
	(M.Rutgers v.d. Loeff)	
8.2.1	Transmissiometry -----	140
	(M.Rutgers v.d. Loeff)	
8.2.2	Sediment-Water Exchange (Scavenging of ²³⁴ Th)-----	144
	(M.Rutgers v.d. Loeff)	
8.2.3	Early Diagenetic Reactions in the Suspended Phase -----	145
	(M. Rutgers v.d. Loeff)	
8.2.3.1	Trace Metals-----	145
	(M. Kühn)	
8.2.3.2	Organic Constituents (Biomarker) -----	146
	(M. Rutgers v.d. Loeff)	
8.3	Radium Sampling-----	146
	(M. Rutgers v.d. Loeff)	
8.4	Surface Observations on Export Production-----	147
	(M. Rutgers v.d. Loeff)	
8.5	Methane -----	148
	(E. Damm)	
9	References -----	150
10	Annex -----	155
10.1	Station List-----	156
10.2	Weather Data-----	167
10.3	Geological Data Tables and Graphical Core Description-----	172
10.4	General Guidelines for Data and Sample Distribution and Publications -----	225
10.4.1	Physical Oceanography-----	225
10.4.2	Marine Biology-----	225
10.4.3	Sea-Ice Sedimentology and Water Chemistry-----	228
10.4.4	Marine Geology-----	229
10.4.4.1	Sediment Sample Distribution Guidelines for ARK-XIII/2 Material -----	231
10.5	List of Participants-----	233



1 Introduction (R. Stein)

Based on the excellent experiences and the success of the international multi-disciplinary scientific expeditions with the ice-breaking RV "Polarstern" into the central Arctic Ocean and adjacent Eurasian continental margin areas in 1986 (ARK-IV/3), 1991 (ARK-VIII/3), 1993 (ARK-IX/4), 1995 (ARK-XI/1), and 1996 (ARK-XII), the expedition ARK-XIII/2 was carried out to the continental margin off Svalbard, the Yermak-Plateau area, and Fram Strait (Fig.1.1).

The main components of the multidisciplinary project comprise:

- (1) oceanographic investigations to understand and quantify both the circulation and water mass transformations;
- (2) biological investigations in fundamental ecology (pelago-benthic coupling; sea-ice biology) and biogeography;
- (3) geological investigations including sea-ice research, aerosol measurements, studies of modern particle flux through the water column, and studies of short- and long-term changes in paleoenvironment; and
- (4) geochemical studies of early diagenesis as well as particle transport and chemical turnover in the benthic nepheloid layer.

The research program of this "Polarstern" Expedition will partly contribute to the EU-project "Arctic Ocean System in the Global Environment" (AOSGE).

The regional priority of the expedition was a transect east of Svalbard (transect A) and transects from the northern Svalbard continental margin across the Yermak Plateau to the East Greenland continental margin (transects B, C, D, and E) (Fig. 1.2).

Alltogether, the ARK-XIII/2 Cruise can be regarded as a very successful expedition. A huge amount of new data and samples for oceanographical, sea ice, biological, geochemical, and geological research were obtained. The present report describes the scientific program and first results of this expedition.

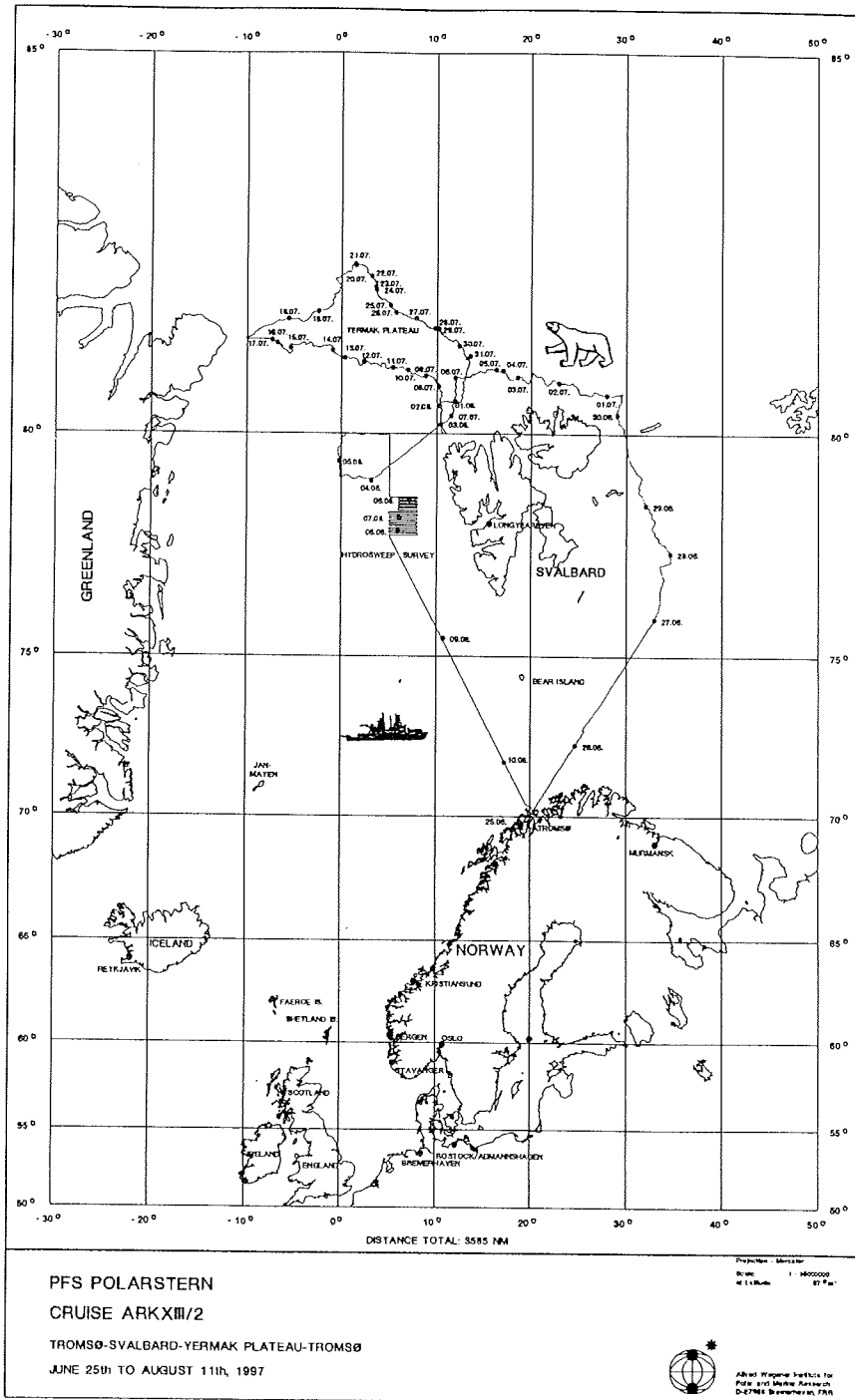


Fig. 1.1: Cruise track of RV "Polarstern" during ARK-XIII/2.

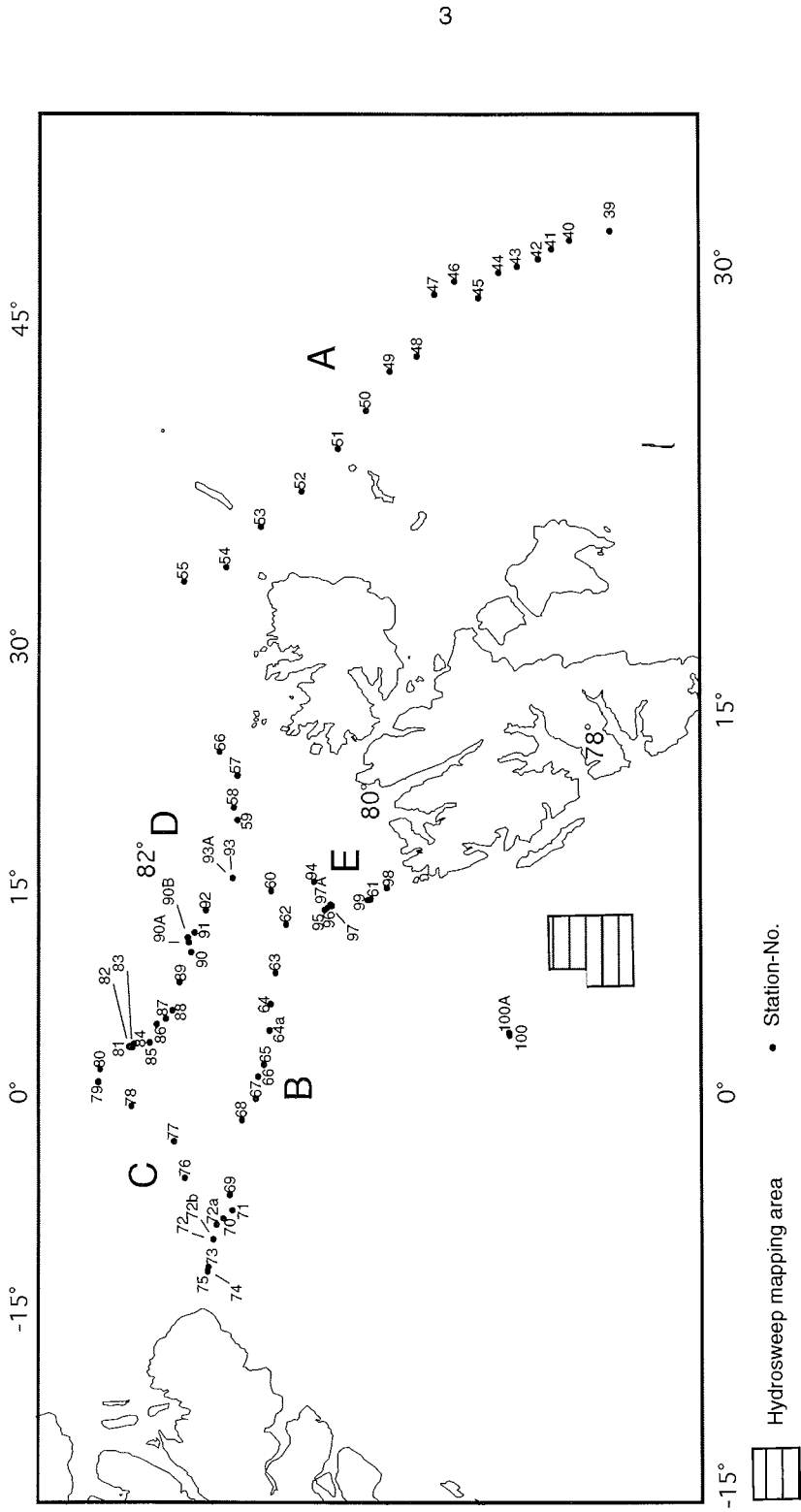


Fig. 1.2: Sampling stations of RV "Polarstern" cruise ARK-XIII/2 and major working transects A-E.

2 Itinerary (R.Stein)

On June 25, 1997, 22.30h, RV "Polarstern" left Tromsø, onboard 43 crew members and 48 scientists. After a short transit of 420 nm we reached our first station 39 of transect A ($75^{\circ} 59.9' N$, $32^{\circ} 59.4' E$; Figs. 1.2, 2.1a) in the area east of Svalbard on Friday, June 27, 1997, 09.30 UTC. During the first days, shipboard activities concentrated on oceanographical and biological measurements and sampling of the water column and sampling of near-surface sediments, using CTD/Rosette, multinet, bongonet, seafloor imaging (Fotoschaukel), epibenthos sledge, Agassiz trawl, giant box sampler (Großkastengreifer), Van-Veen-Grab, and multicorer, respectively. During transit times, aerosols were routinely collected using a pump installed on the uppermost deck of the vessel. At station 49 ($77^{\circ} 35.2' N$, $34^{\circ} 42.2' E$), a sediment trap deployed some weeks ago during Cruise ARK-XIII/1, was recovered on June 28. On July 01, at the last station of transect A (station 55, $80^{\circ} 41.4' N$, $29^{\circ} 24.4' E$; water depth of 410m), the OFOS ("Ocean Floor Observation System") was employed, a system which allows a direct observation of the sea floor by means of a video and photo camera. Despite extreme ice condition, this first test in shallow water depth was very successful. At the same station, the first sea-ice sampling program also took place on a large ice floe.

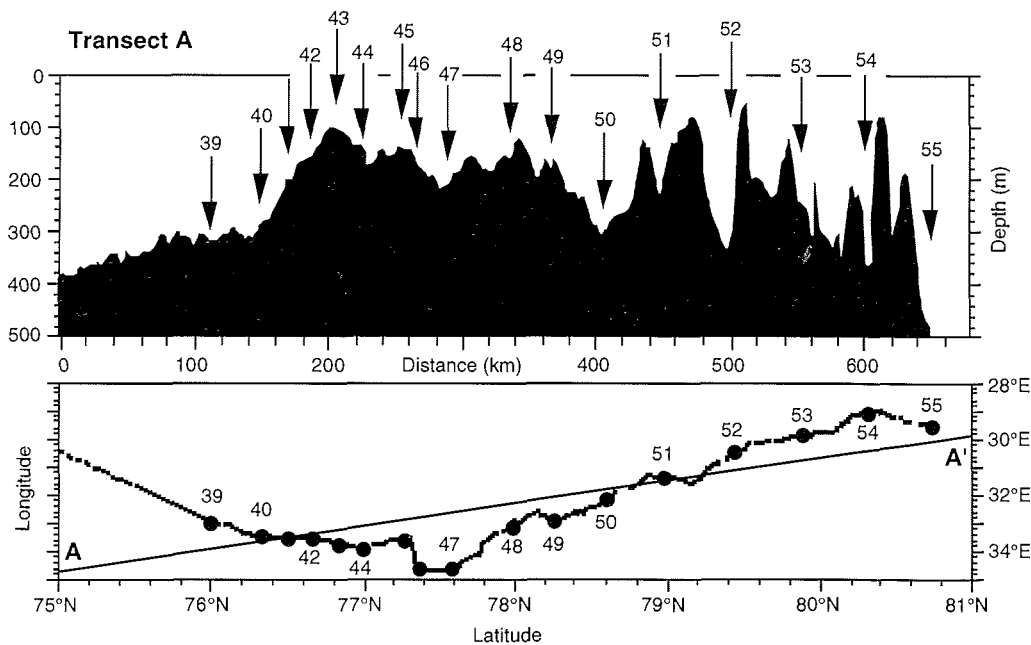


Fig. 2.1a: Depth profile of transect A and course plot with station numbers. For location of transect A see Figures 1.2 and 2.2.

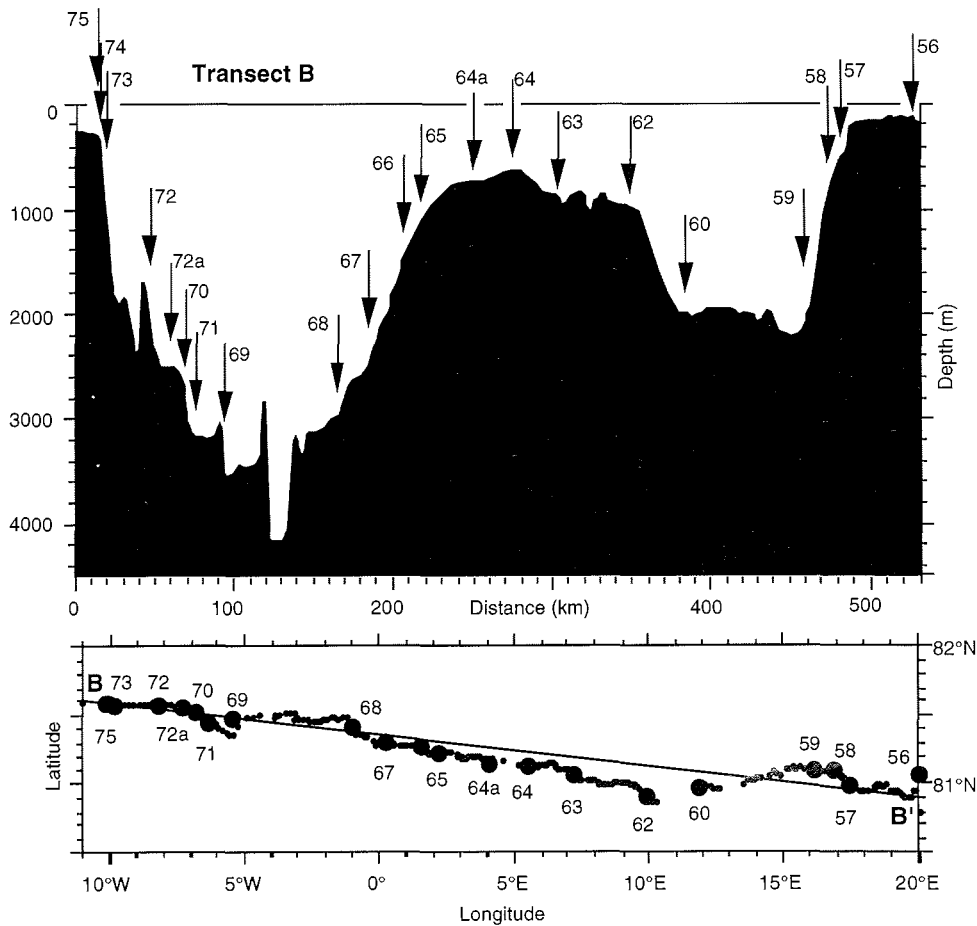


Fig. 2.1b: Depth profile of transect B and course plot with station numbers. For location of transect B see Figures 1.2 and 2.2.

Because transect A had been sampled in detail for geological studies during the 1991 "Polarstern" Cruise ARK-VIII/3, the geological activities were restricted to a few selected sampling stations of near-surface sediments.

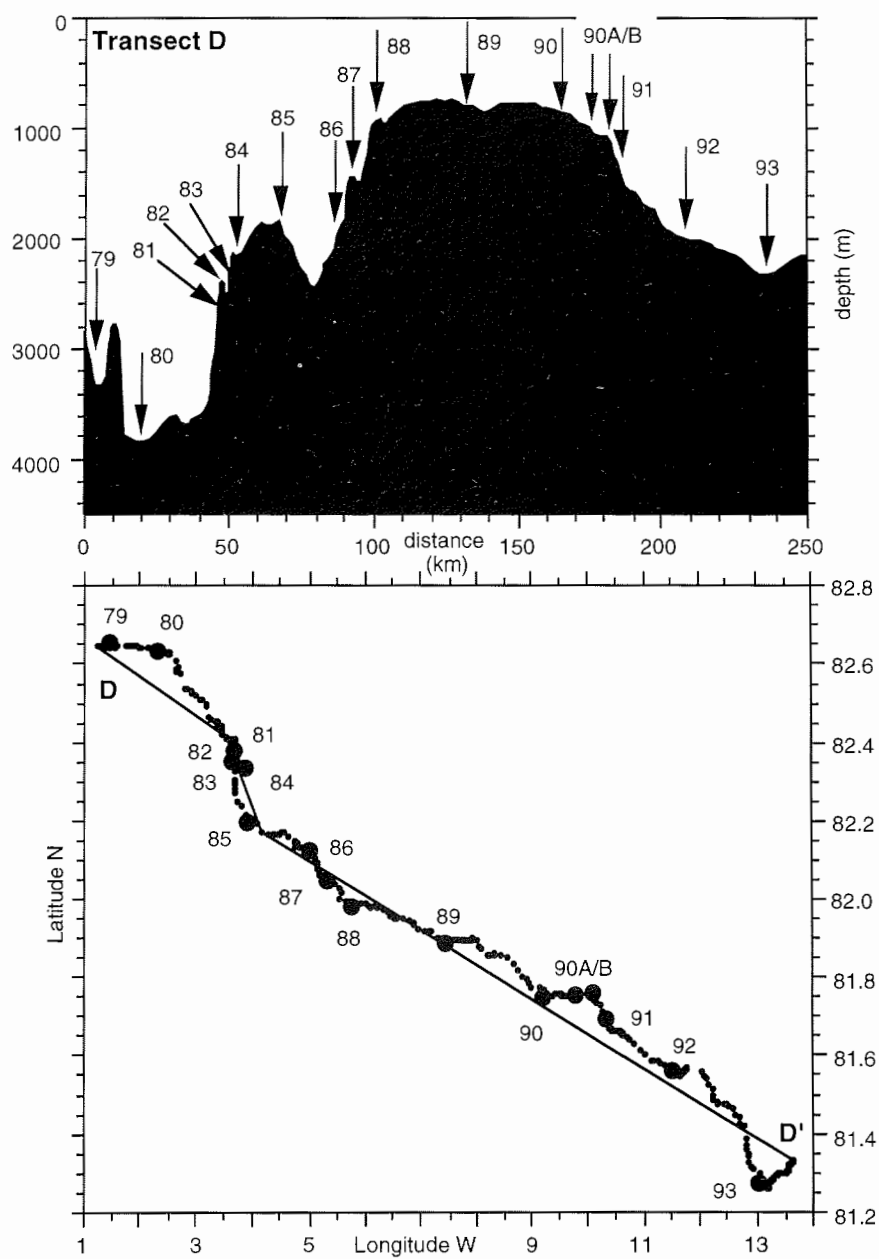


Fig. 2.1c: Depth profile of transect D and course plot with station numbers. For location of transect D see Figures 1.2 and 2.2.

Due to very strong pack ice, we decided not to proceed farther north to recover an oceanographic mooring system deployed at $81^{\circ} 26.32' \text{ N}$, $30^{\circ} 54.73' \text{ E}$ in 1991, but instead to steam to the west (transect B, Figs. 2.1b, 2.2) where the sea-ice cover should be more open according to satellite photographs (Figs. 2.3a, 2.3b). In the evening of July 02, we reached the first station of transect B (station 56; $81^{\circ} 03.7' \text{ N}$, $20^{\circ} 07.5' \text{ E}$) where only a CTD cast was taken. On the way to the next station, we stuck in heavy pack ice in the early morning of July 03. This stop of several hours was used for a sea-ice sampling station on an ice floe. In the evening we continued steaming to the west and reached station 57 ($80^{\circ} 58.7' \text{ N}$, $17^{\circ} 25.1' \text{ E}$), the first main station where an intensive oceanographical, biological, and geological sampling program was carried out.

During the following days up to July 07, three further main stations were sampled successfully. At station 59, the *in-situ* pumps for sampling of water for trace metal determinations were used for the first time during this expedition. Parallel to the station work onboard "Polarstern", a biological and sedimentological sea-ice sampling program was performed. "Dirty sea ice" was sampled on smaller ice floes reached by helicopter. After having finished the 2000 m station 60 at the lower southeastern slope of the Yermak Plateau ($80^{\circ} 58.6' \text{ N}$, $11^{\circ} 46.4' \text{ E}$) we were steaming to the south in the early morning of Sunday July 06. Our goal was to reach the ice edge north of Svalbard, 50 nm ahead of us. This excursion to the south was necessary for the deployment of a mooring system equipped with a "multisampler" and a sediment trap. Under the extreme ice conditions of our actual working transect it would have been impossible to recover the mooring system planned to do at the end of this Leg. With the "multisampler" and the sediment trap the concentration of particles in the bottom water close to the sea floor and the particle flux in the water column, respectively, should be sampled and determined. After eleven hours steaming time we reached the ice edge and deployed successfully the mooring system at $80^{\circ} 10.47' \text{ N}$, $10^{\circ} 24.48' \text{ E}$ (station 61, Fig. 2.2).

After deployment of the mooring system, we steamed back to the north into the thick pack ice. Due to the strong ice condition we reached the next station 62 of transect B at $80^{\circ} 54.2' \text{ N}$ / $09^{\circ} 53.1' \text{ E}$ on Tuesday July 08, 14.30 UTC, and started with the station work. At this station, the kastenlot was used for the first time during this expedition. Due to thick pack, we were proceeding slowly to the west. Reconnaissance flights with the helicopter were still necessary to find the right way through the pack ice. On July 10, we reached the top of the Yermak Plateau and had a main station in about 640 m of water depth (station 64; $81^{\circ} 07.7' \text{ N}$, $05^{\circ} 35.1' \text{ E}$). Based on a "Parasound" survey indicating a rough sea-floor topography and low penetration depth, we decided not to run the gravity corer at this station. The seafloor was sampled with an "Agassiz Trawl" containing only a small number of animals and stones.

Between July 12 and 15, oceanographical, biological, and geological sampling took place at the western slope of the Yermak Plateau in water depths between 1000 and almost 4000m.

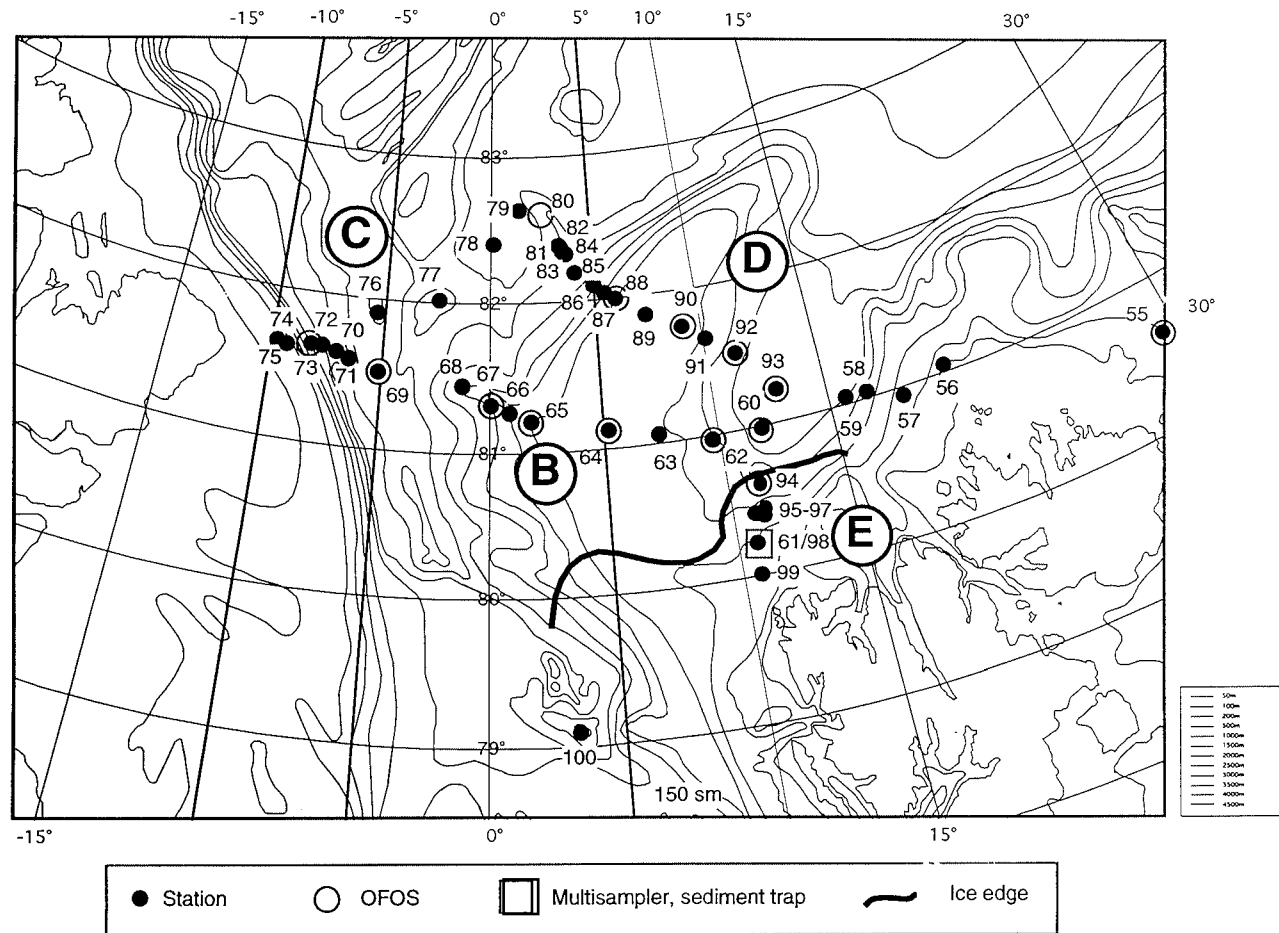


Fig. 2.2: Main working area with transects B, C, D, and E. Station numbers, stations with OFOS runs, location of mooring system (multisampler and sediment trap) and approximately position of the ice edge are indicated.

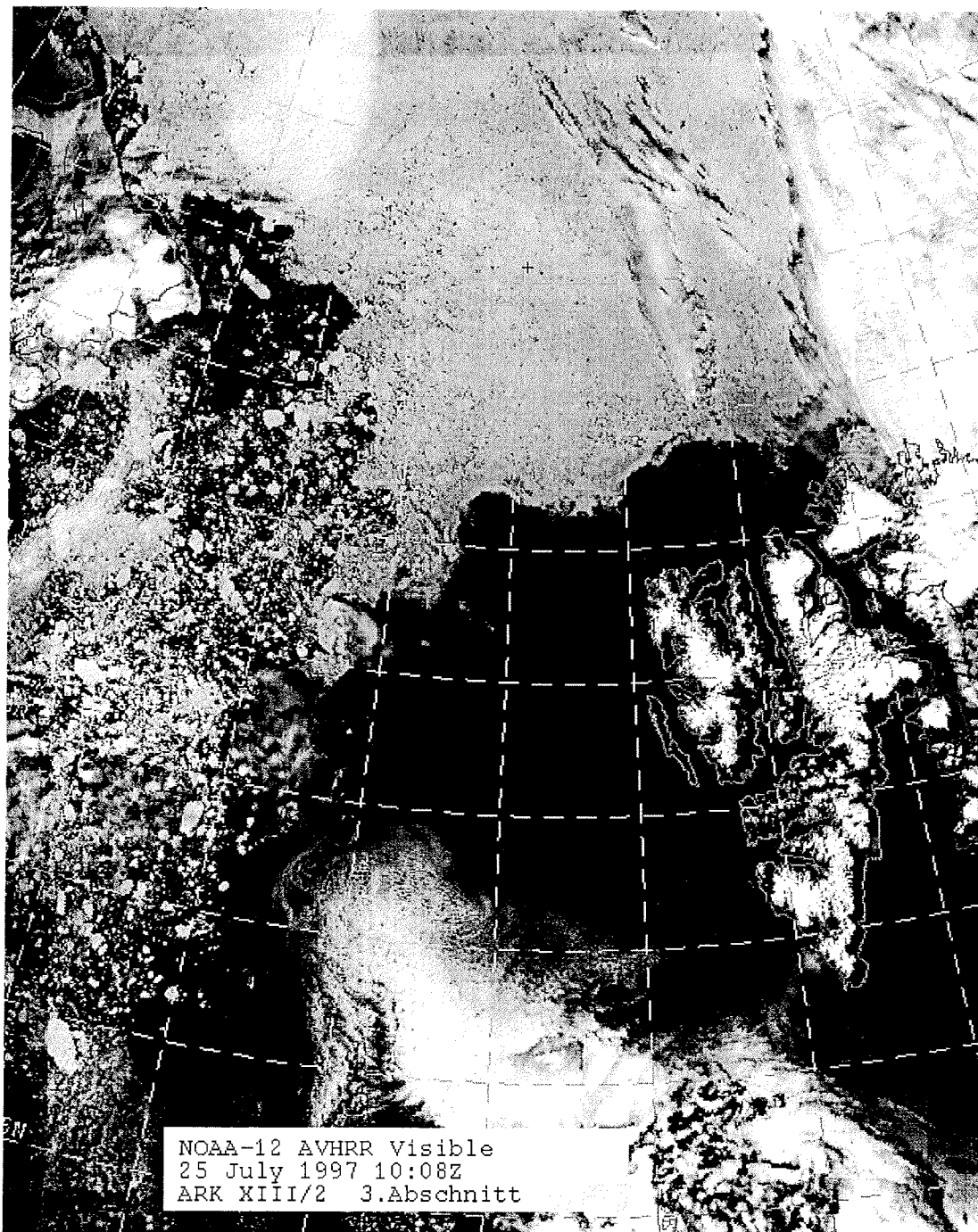


Fig. 2.3a: Satellite photograph of sea-ice situation during RV "Polarstern" Cruise ARK-XIII/2. (July 25, 1997).



Fig. 2.3b: Satellite photograph of sea-ice situation during RV "Polarstern" Cruise ARK-XIII/2. (August 06, 1997).

On transect B across the Yermak Plateau, the "Ocean Floor Observation-System" (OFOS) was used at 6 stations (Fig. 2.2). Abundant animals (brittle stars, sponges, crinoids etc.) as well as feeding and creeping traces of bivalves, gastropodes, and echinoderms were observed by means of the video camera and photographed. The population at the sea floor suggests that the Yermak Plateau area is strongly influenced by water masses from the Norwegian Sea.

On July 16, we reached the lower slope of the East Greenland continental margin. There, the ice conditions became much better (Fig. 2.3a). From July 16 to 18, stations in water depths between 3150 and 300 m were successfully sampled by all disciplines. We finished transect B with a CTD cast at station 75 (81° 35' N, 10° 07.9' W; 273 m of water depth), the westernmost point of the whole expedition, in the early morning of July 18.

Then, we were steaming northeast-wards and started with transect C (Fig. 2.2) from the east Greenland continental margin through the Lena Trough to the western flank of the Yermak Plateau. Already Friday evening our station work took place in the Lena Trough at 4150 m water depth.

On July 20, 13.30 UTC, we arrived at the northernmost point of our expedition (82° 40' N, 01° 27' E), back again in the strong pack ice, and continued with our routine station work onboard "Polarstern" and on ice floes. On our way to the southeast, ice conditions became stronger and stronger.

During the night of July 21/22, we stuck in the ice. We decided to use this stop for an OFOS run, and to have an ice reconnaissance flight next day. After this flight, we continued to go southeast because better ice conditions prevailed in the area of our next two stations.

On July 23-24, station work took place at the northwestern slope of the Yermak Plateau. At this very steep slope older (Tertiary) sediments should be cropping-out, which may be sampled by the geological gears available onboard "Polarstern". The study of these sediments would allow reconstructions of the preglacial Arctic paleoenvironment. The gravity corer used at three stations 81, 83, and 84 (transect D, Figs. 2.1c, 2.2) recovered short cores containing sediments partly older than those obtained before during this cruise. They are, however, probably not of Tertiary age as assumed from first shipboard analyses. Concerning the age of these sediments further shorebased studies will hopefully give a more precise answer.

On July 27, we already reached the top of Yermak Plateau and had a major station at a water depth of 850m where most of our sampling gears were successfully used. Due to the still very thick sea-ice cover, Agassiz trawl and epibenthos sled could not be run. Since the evening of July 28 we were working at the eastern slope of Yermak Plateau. The ice conditions became much better. Thus, in addition to the other sampling gears, the sea floor could be sampled by means of Agassiz trawl and epibenthos sled.

On July 29, at station 91, the last kastenlot core came on deck, another long sediment core with distinct variations in colour, texture, and composition, probably representing the last glacial/interglacial changes. Due to the good ice conditions we already reached the last station 93 of the transect in the

afternoon of July 30 and started with a 28-hours activity, where all oceanographical, biological, geochemical, and geological sampling gears incl. OFOS were used.

During this last week, the sea-ice group successfully sampled i) "dirty" ice in the vicinity of an AWI sediment test-field, ii) surface deposits from an iceberg and iii) muddy material from a very turbid ice floe. From the samples obtained we will learn more about sources, pathways, biological content, chemical composition and sediment inclusions of Arctic sea-ice. Close to the iceberg we sampled a 2000m² large, extremely dirty patch in the pack ice. At this site, the ice surface was covered by a sediment layer of roughly 3-4 cm thickness. The fine to medium grain-size distribution of the sampled material, its content of macroscopic organic material and its geographic location in the Transpolar Drift hint to entrainment of the sediments directly from the bottom of shallow Siberian shelf sites (e.g. Laptev Sea) through the mechanisms of anchor ice formation or vertical turbulences. According to preliminary estimates this turbid ice patch contained roughly 5-10 t.

On August 01, we reached the ice edge north of Svalbard at 80° 36' N, 12° 31' E. During the following days up to August 03, six further stations were sampled successfully on a north-south transect of the northern Svalbard continental margin at water depths between 1100 and 300 m (transect E, Fig. 2.2). At the last station 99, the multisampler and the sediment trap deployed on July 07 (station 61), could be recovered without any problem due to optimum weather conditions.

After having finished this station, "Polarstern" started her direct transit to the Molloy Deep. At 79° 6' N, 03° 6' E and a water depth of 5445 m, station 100, the deepest station of the entire expedition, took place on August 04. At this station, the "Pressure-Retaining Water Sampler" for studies of bacteria under *in-situ* conditions was used very successfully. In addition, last CTD, multicorer, giant box corer, and OFOS were run. During station work, a helicopter started its way to Longyearbyen to pick-up three AWI Hydrosweep specialists. They arrived onboard "Polarstern" at 15.15 UTC.

During the night August 04/05 we steamed northwest and reached 80° N, 0°, the starting point of the planned hydrosweep survey, on August 05, 16.00 UTC. Because the ice conditions in this area were not suitable for Hydrosweep mapping, it was decided to sail southeast for the ice-free area west of Svalbard. During the following three days up to August 08, a Hydrosweep survey was performed in the area between 78° 46' N, 5° E - 78° 46' N, 8° E and 78° N, 5° E - 78° N, 8° E (Figs. 1.1, 1.2).

In the morning of August 08, "Polarstern" left the Hydrosweep mapping area heading southeast for Tromsø. After 46 days at sea, many of them in heavy pack ice, "Polarstern" arrived at Tromsø on August 11, 7.50 Local Time, bringing to an end a scientifically very successful cruise.

Acknowledgements

All participants in "Polarstern" Cruise ARK-XIII/2 gratefully thank captain Ernst-Peter Greve and his crew, as the success of our expedition was substantially supported by their excellent cooperation and efforts.

3 Meteorological conditions (K. Buhlmann, H. Sonnabend)

Leaving Tromsø in the evening of June 25 1997 to the first research area near the pack-ice edge east of Hopen-Island the weather was sunny, visibility good and the wind northwesterly about bft 4. Between June 27 and June 30 (transect A east of Svalbard) the wind was light and variable, but most of the time the sky was overcast with some snow showers or freezing drizzle and temperatures some little below the freezing point. The visibility became poor sometimes and the first fog was observed for some hours. On July 02 the wind increased up to bft 5 from northwest with snow showers in the vicinity of an intensive low over the Barents Sea. Within the next two days the wind shifted southerly according to low pressure over Fram Strait, associated with advection of warmer air masses. On July 05 and 06 we got under influence of a large high over the Barents Sea which brought sunshine all day und night and temperatures up to +3°C. The visibility was extremely good, that we could see the mountain range of northern Svalbard from a distance of one hundred km.

During the next ten days our research area on the southern Yermak Plateau and off east Greenland lay in a large southerly airflow. Several lows with their fronts and troughs were moving from the Iceland area towards the Arctic basin, causing most of the time compact cloudiness, and often rain and fog with southerly to westerly winds between bft 3 and 6.

Between July 21 and July 31 (transect D, Yermak Plateau) dry air with light to moderate northwesterly and northerly winds affected us, and high pressure conditions increased slowly. Thus the weather became very good. From July 22 to 26 the sun was shining continuously nearly 100 hours, and the visibility was excellent.

Then, the weather situation changed again. Two depressions developed one after another over the northeastern coast of Greenland moving towards the Siberian part of the Arctic Sea. They especially brought a closed layer of low stratus with mist and occasionally fog. The wind increased up to bft 6 in front of the lows and shifted westerly with near gale force bft 7 gusting up to gale force 8 bft in the vicinity.

On August 01 the ship left the pack ice and reached open water just north of Svalbard, where we had in moist air from southernly regions two days with moderate to dense fog and some drizzle. On August 03 the fog dissipated at noon for nearly five hours caused by light southeasterly winds and foehn induced by the mountains of Svalbard. Thus, a helicopter flight to the Koldewey Station in Ny Ålesund could be realized. Just after having finished the flight another front of a low over Greenland approached from the south causing rain und fog again. During the last days of the cruise the southwesterly airflow over the northern Atlantic intensified more and more steering several lows from southern Greenland towards Fram Strait. They affected us with low stratus clouds, sometimes rain and fog, and mostly southerly winds up to bft 7.

The frequency distribution of wind directions (see 3.1) shows maxima of southerly, southwesterly and southeasterly winds according to higher pressure over Scandinavia and the Barents Sea, and lower pressure over Greenland especially in the second part of the cruise. All other directions were less frequent. Figure 3.2 shows the frequency distribution of the windspeed in Beaufort. The most frequent wind force was bft 4, followed by 3 and 5 bft.

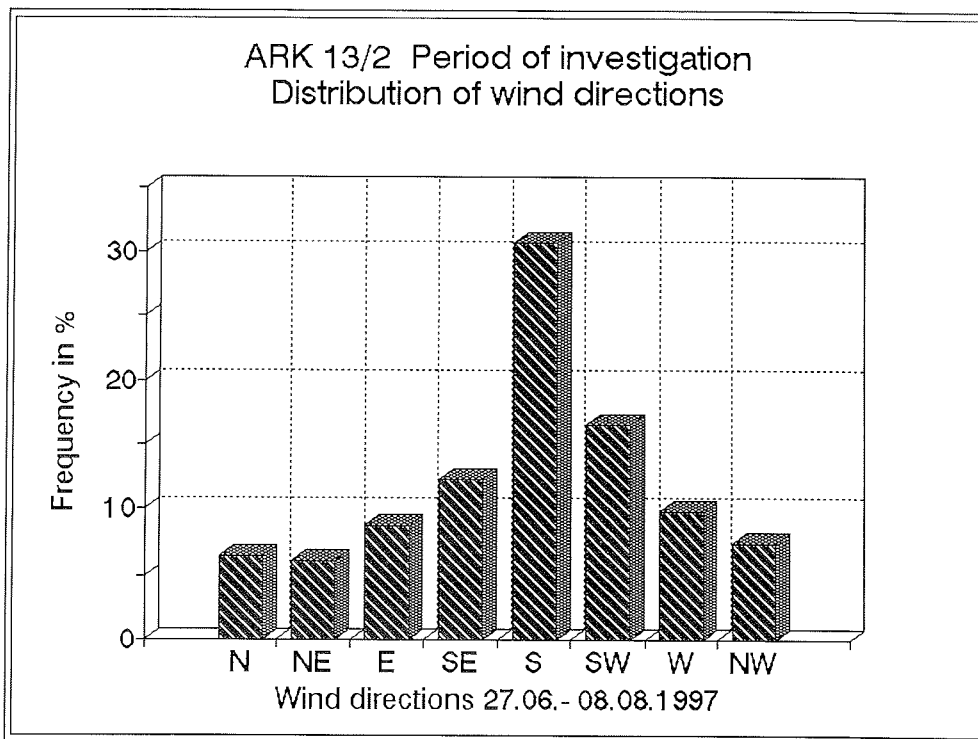


Fig. 3.1: Distribution of wind directions during the Expedition ARK-XIII/2 with RV "Polarstern".

During the whole cruise the number of days we observed fog amounts to 21. This relative high value can be explained by the great share of southerly wind directions which favour the advection of warmer and moist airmasses. The frequency of fog, however, was greater over the open water than over ice-covered areas. The temperatures over the ice-covered areas lay between +2°C and -2°C. The highest value reached +3°C, the lowest -3°C.

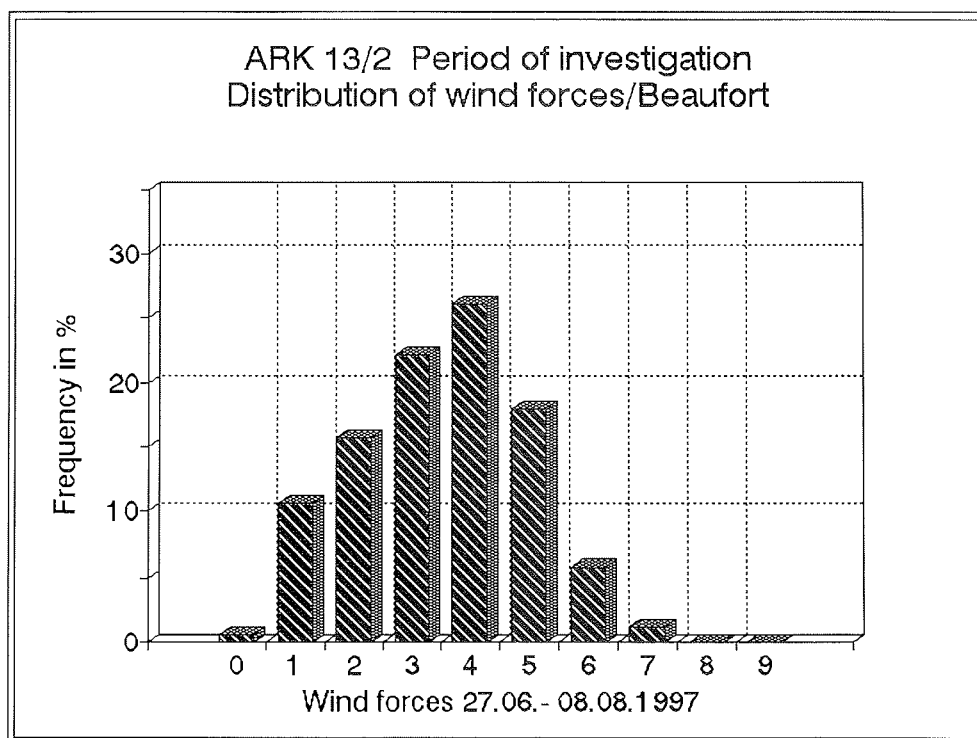


Fig. 3.2: Distribution of wind forces/Beaufort during the Expedition ARK-XIII/2 with RV "Polarstern".

A detailed list of weather observations is presented in the annex.

4. **Physical Oceanography** (B. Rudels, R. Meyer, V. Ivanov, D. Hevekerl)

Introduction

The main theme of the oceanographic work during RV "Polarstern" cruise ARK-XIII/2 was a study of the interactions between the two main inflow branches from the Norwegian Sea, entering the Arctic Ocean over the Barents Sea and through Fram Strait, respectively. As originally planned it was a joint project between FIMR, AWI, IfMHH and AARI and would be an integral part of the proposed European AOSGE programme. Because of changes in the cruise route this programme was cancelled and the work had to focus on the Fram Strait inflow branch north of Svalbard and around the Yermak Plateau. To estimate also the Arctic Ocean outflow and the recirculation of the West Spitsbergen Current in the northern part of Fram Strait a transect to the Greenland continental slope was projected. An attempt to recover two moorings, deployed north of the Barents Sea in 1991, was also considered. Because of the new working area the oceanography work has become much more relevant for the running European VEINS programme, while its importance for the shortened and postponed AOSGE programme has diminished.

Narrative

After leaving Tromsø on the night of June 26th the hydrographic work began in the Barents Sea on the 27th of June with a CTD station at 76°N 33°E in the east-west channel north of the Central Bank. This station became the starting point for a north-south hydrographic transect, A, running across the Grand Bank, passing Kong Karls Land and then up to the strait between Nordaustlandet and Kvitöya to the Arctic Ocean (for station positions see Figure 4.1). The transect repeated a biology transect taken earlier in spring during the ARK-XIII/1 cruise. Further to the north the ice conditions became heavy and the recovery of the moorings was postponed to the later part of the cruise. However, the ice conditions in the working area remained difficult and no possibility to attain the mooring positions arose.

An extensive east-west transect, B, approximately along 81° 30', was then taken from the shelf north of Nordaustlandet, across the Sofia Deep, over the southern part of the Yermak Plateau, across Fram Strait and up the Greenland continental slope. The transect work was temporarily interrupted to put out a biology-geochemistry mooring close to the northwest corner of Spitsbergen. A CTD station was taken, which was to be repeated towards end of the cruise as the mooring was recovered.

In contrast to the heavy ice encountered over the Yermak Plateau the area west of Greenland was almost ice free. However, the slow progress in the eastern part only allowed time for a symbolic northern return transect C (5 stations) across Fram Strait before the main expedition work over the northern Yermak Plateau was started. The plateau was crossed by a CTD transect, D, running northwest-southeast from the deep Nansen Basin and ending in the central Sofia Deep. The cruise then finished with a short north-south transect (E) up the Svalbard continental slope to the mooring position. A final, single station down to 5540m was taken in the Molloy Deep in Fram Strait.

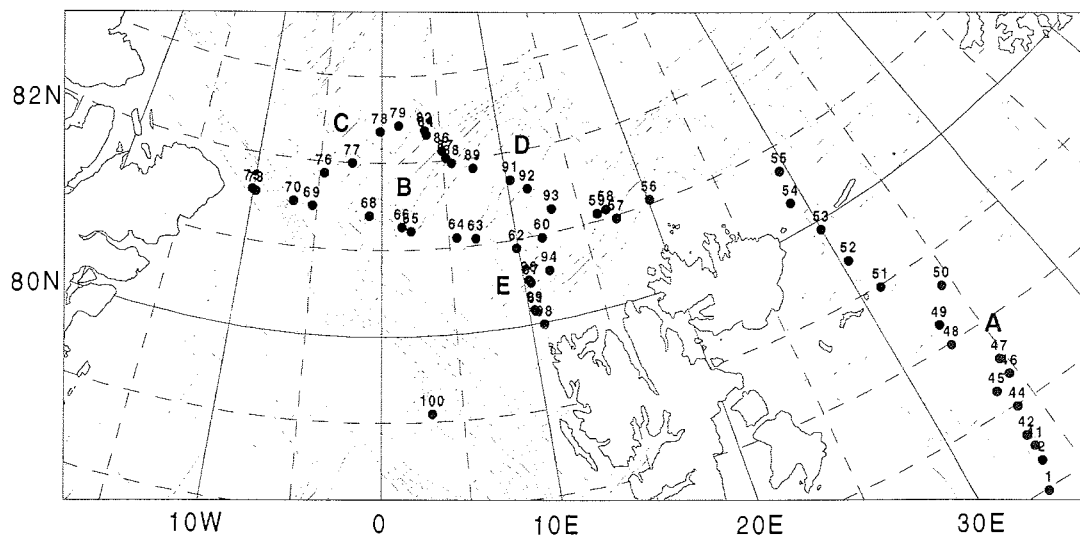


Fig. 4.1: Map with station positions

The physical oceanography programme consisted exclusively of CTD work, enhanced with water sampling and temperature measurements for calibration of the sensors. Water sampling was also made in support for other groups, especially biology, geochemistry and geology. This often led to multiple CTD casts on the stations. 57 CTD stations were taken. The exact positions of the CTD stations are given in appendix 10.1.

A Seabird SBE 911plus CTD system and a Seabird Carousel rosette sampler were used. The original conductivity cell showed 0.015-0.02 too low salinity value as compared to the bottle salinities and also appeared unstable. At station 67 the sensor finally broke and had to be replaced. Thermistor and pump were then also exchanged. The new conductivity sensor worked considerably better and the measured salinities were now much closer to the on deck calibration salinities (about 0.004 too high). At station 99, the next to last, the winch run amok on deck and brought the rosette into the block. Fortunately nobody was injured but 7 Niskin bottles were broken.

Preliminary Results

One initial aim was to obtain a CTD station net north of Fram Strait forming a closed box. Geostrophic calculations, combined with continuity constraints and some minimisation assumptions could then be applied to estimate the exchanges through Fram Strait and the recirculation of the West Spitsbergen Current in the northern part of the strait. However, because of the restricted time and the severe ice conditions the number of stations had to be reduced. The resulting large station spacing, especially on the northern return transect, will limit the accuracy of the geostrophic calculations. This work requires extensive onshore analysis and will not be considered further. The present report just gives a qualitative description of the temperature and salinity observations and offer some interpretations of the observed fields.

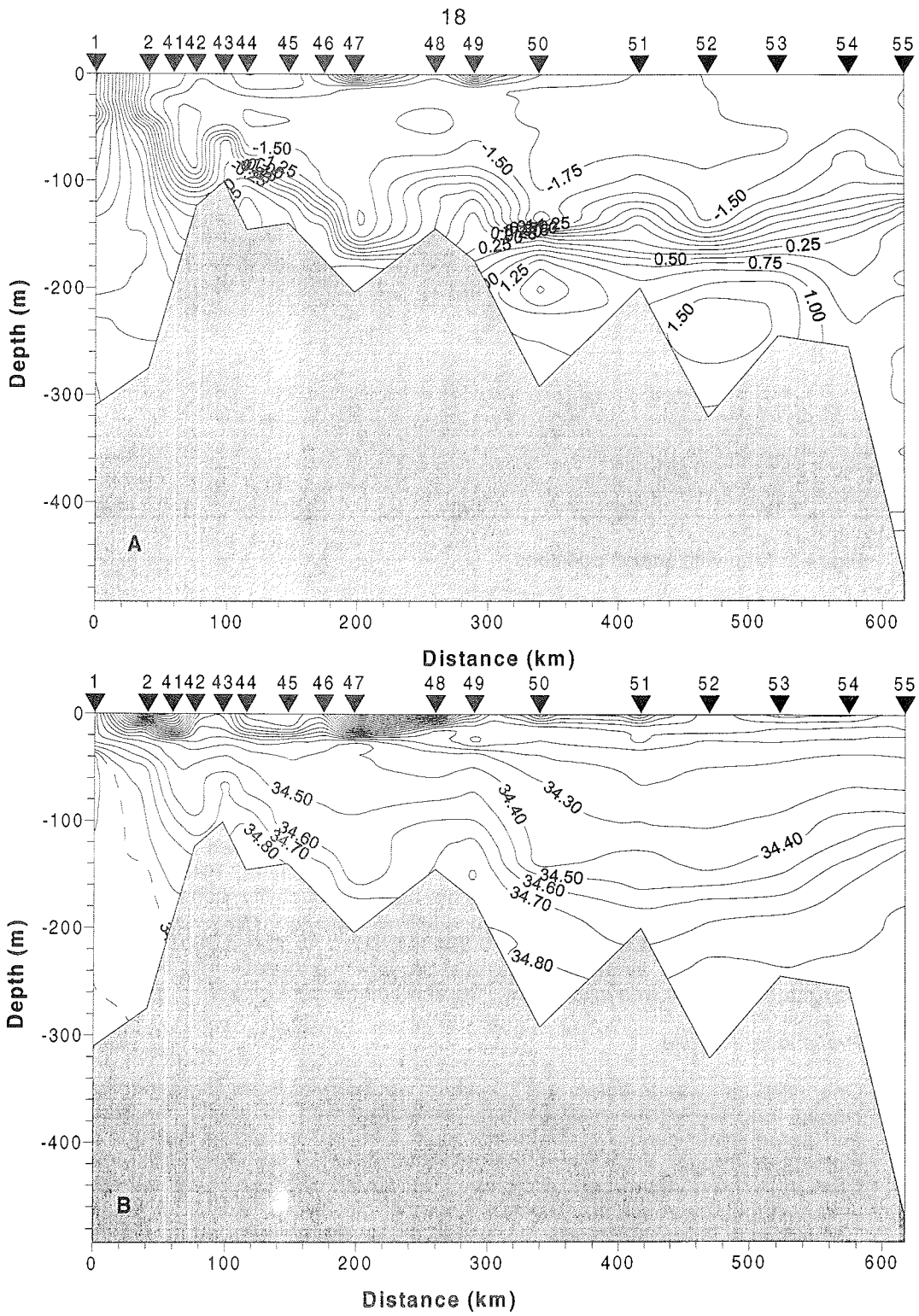


Fig. 4.2: Potential temperature and salinity sections from transect A.

The Barents Sea

The first station in the Barents Sea was taken south of the Polar Front in the area dominated by Atlantic Water entering the Barents Sea north of Norway. The front was located at the southern flank of the Grand Bank and already the second station of the transect was inside the front. The cold water over the bank north of the front did not extend to the bottom and the bottom water was above freezing (Fig. 4.2a), implying that the haline convection in winter does not homogenise the entire water column at the Grand Bank. The fairly high salinity at the bottom suggests that the bottom water derives from the south (Fig. 4.2b).

The depth of the winter convection is also in the depression northwest of the bank limited by the stratification, not by the topography. The salinity of the upper layer was somewhat lower than over the bank and the temperature and salinity of the Atlantic Water underneath were lower than south of the front (Fig. 4.2). The characteristic of the Atlantic Water north of the Grand Bank is similar to those observed north of Svalbard implying that the water enters from the north, probably through the Victoria Channel. This is in agreement with the findings by Pfirman et al. (1994).

North of Svalbard, the Sofia Deep and the Yermak Plateau

In the eastern part of transect B the Atlantic layer showed high temperatures indicating water entering from Fram Strait and following the Svalbard continental slope eastward (Fig. 4.3). On the easternmost stations some intrusions of colder, less saline water were seen. On the last transect (E) further to the west the intrusive activity was stronger and several inversions were seen in the Atlantic core (Fig. 4.4). The likely origin of the colder water mass is the shelf area north of Svalbard.

In the Sofia Deep the Atlantic Water had a temperature of 2.5 to 3 degrees (Fig. 4.3). This was colder than on the western north-south transect E (Fig. 4.5) and imply a cooling of the Atlantic Water as it flows toward the east. At the repeated CTD station (61) at the mooring position the temperature increased by 0.5 °C in little over 3 weeks. At the first cast the ice edge was just at the station position but the second time the ice edge had retreated considerably towards the north. The lower temperatures found in the east could then partly be a seasonal effect.

Over the Yermak Plateau the temperature of the Atlantic core was lower but increased on the western side of the plateau (Fig. 4.3). This would be in agreement with the accepted view that the West Spitsbergen Current splits into, at least, two streams. One entering close to Svalbard and one passing west of the Yermak Plateau, possibly recirculating westward in the strait (Bourke et al., 1988). Gascard et al. (1995) have proposed that also a third branch may be present, which flows through a deeper gap in the central part of the plateau to the Sofia Deep. Such a flow was not evident on our transect. The western core was narrow and appeared to be confined to the upper part and the western flank of the plateau. Its temperature was also lower than on the eastern part of the transect (Fig. 4.3).

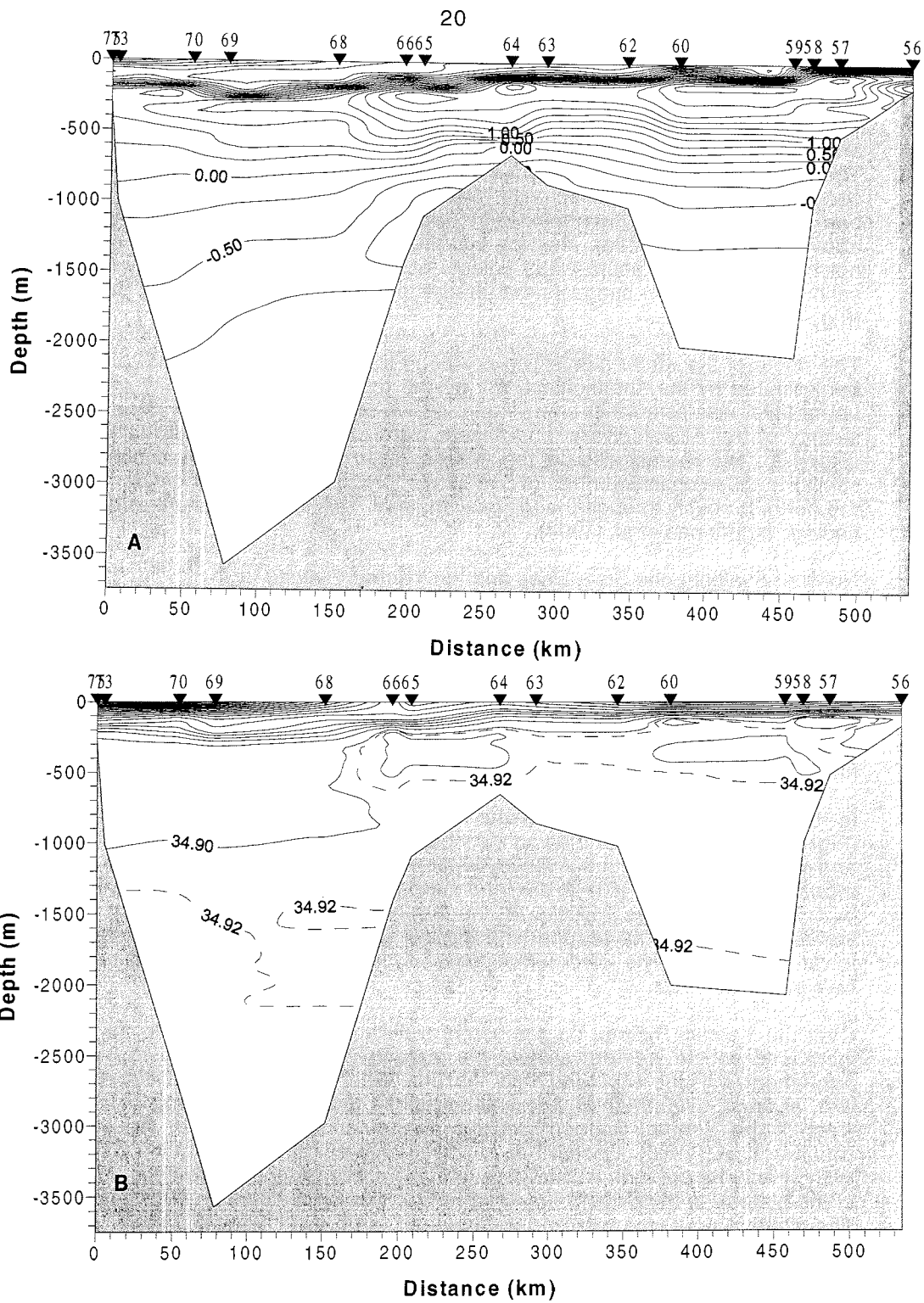


Fig. 4.3: Potential temperature and salinity sections from transect B.

In the eastern part of transect B the Atlantic Water was covered by a thin low salinity layer, probably mostly consisting of Atlantic Water diluted by sea ice melt water. In the heavy ice over the Yermak Plateau the upper layer was colder and deeper (100 rather than 50m). At the plateau the temperature and salinity were lower than in the Sofia Deep smooth over the entire water column (Fig. 4.6). The temperature and salinity profiles were also comparably smooth suggesting little lateral mixing with neighbouring waters and/or that the turbulence level in the water column is high, enhancing vertical mixing. This would imply that the cooling and freshening of the water column at the plateau is due to mechanically stirring of colder, less saline upper water into the deeper layers. Evidence of strong tidal mixing over the Yermak Plateau has been found by Hunkins (1990) and during the CEAREX experiment (Padman, 1995) as well as by numerical tidal models (Kowalik and Proshutinsky, 1994).

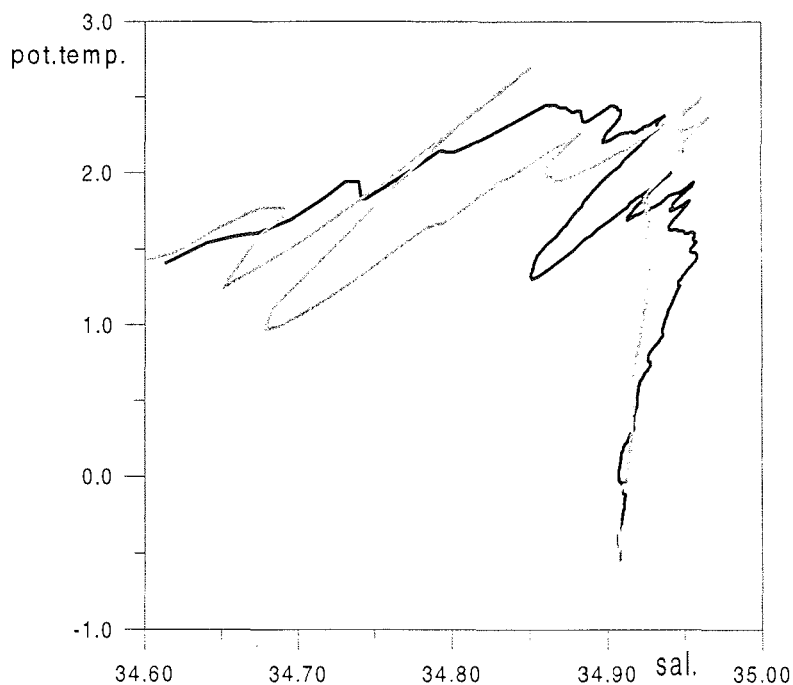


Fig. 4.4: Q-S curves for stations 58 and 94 (grey) showing the interaction between the Atlantic core and colder waters.

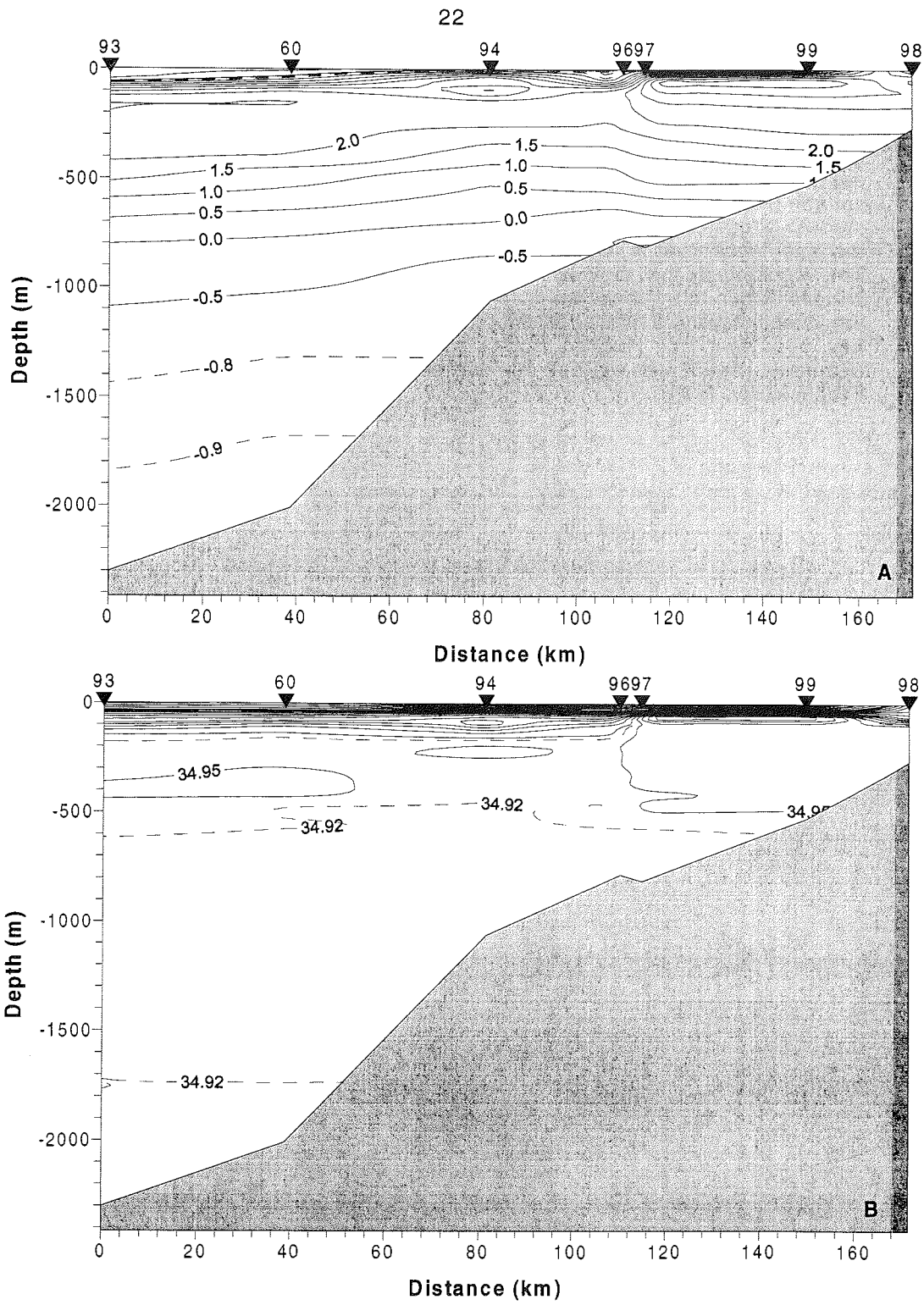


Fig. 4.5: Potential temperature and salinity sections from transect E.

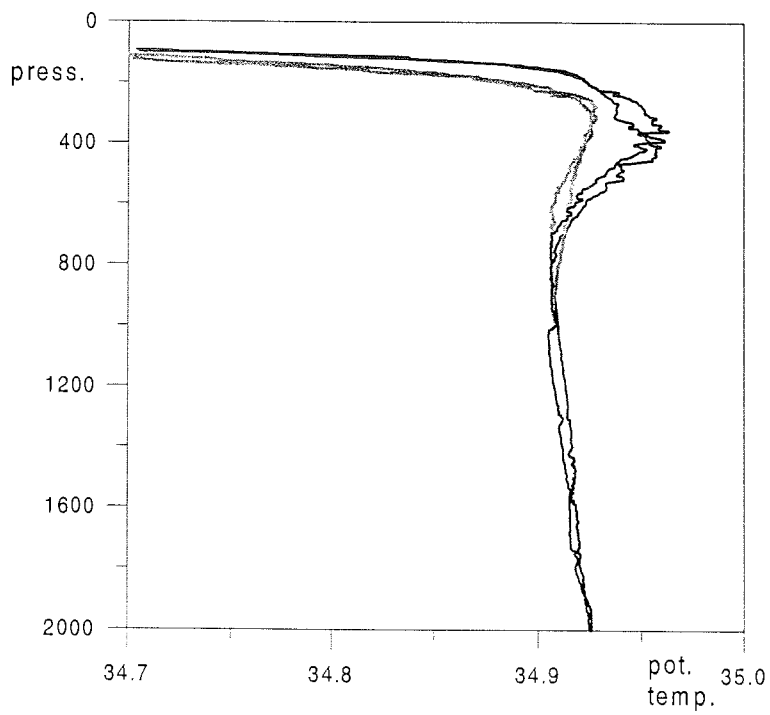
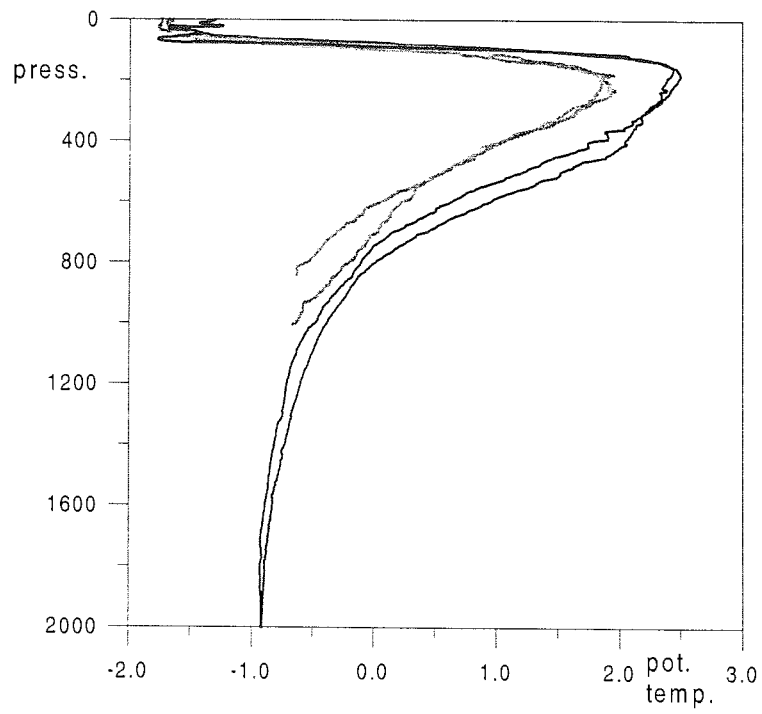


Fig. 4.6: Profiles of potential temperature a) and salinity b) for stations 59 and 93 from the Sofia Deep and stations 62 and 63 (grey) from Yermak Plateau.

Fram Strait

At the western slope of the plateau, the Atlantic Water was covered by a deep, cold upper layer. At the surface an about 20m deep layer with lower salinity and higher temperature was present because of seasonal ice melt and heating through incoming solar radiation. Deeper, at about 100m, a temperature minimum was seen showing remnants of an haline convection in winter. This cold, upper layer became gradually deeper towards the west and reached 250m in the central Fram Strait. It then again became warmer and shallower toward Greenland. The temperature in the entire 250m layer was close to freezing but the salinity profiles indicated several almost homogenous layers stacked on top of each other (Fig. 4.7). This would mean that several streams converge in the strait and their upper waters intrude into each other, pushing the Atlantic Water downward. The densest of the layers had a salinity of 34.3 and was present at most of the stations in the central part of the strait.

The lightest surface water was found in the open water area close to the Greenland continental slope. The surface salinity was as low as 31 and the upper temperature minimum was shallower than 50m-layer never. Temperature minima were present but considerably warmer than those found to the east. The deepest of these minima reached the salinity of 34.3 characteristic of the deepest temperature minimum in the eastern and central parts of the strait. This implies winter homogenised layers which have been isolated from the annual winter convection for some time and become gradually heated from below.

No warm and saline Atlantic core was observed in the strait and no indication of any strong recirculation of the West Spitsbergen Current was evident. The waters moving along the western side of the Yermak Plateau must therefore continue toward north and east. However, the water entering from the south appeared confined to a narrow wedge close to the plateau and the colder and less saline Atlantic layer and the high salinity of the deep water found in the central part of Fram Strait were more characteristic of water columns deriving from the Arctic Ocean (Fig. 4.3).

Close to the Greenland continental slope the Atlantic Layer temperature was hardly above 0.5°C and an intermediate salinity maximum found at 1700m clearly implied water from the Canadian Basin. The low salinity of the surface water also suggests that the water column in the western Fram Strait originates from the Canadian Basin (Fig. 4.3). While the Canadian Basin waters dominate the water column in the western Fram Strait on the southern transect they are not seen on the northern, C, transect. This is most likely caused by the large station spacing on the northern transect, which would leave a stream of Canadian Basin Water along the Greenland continental slope unsampled.

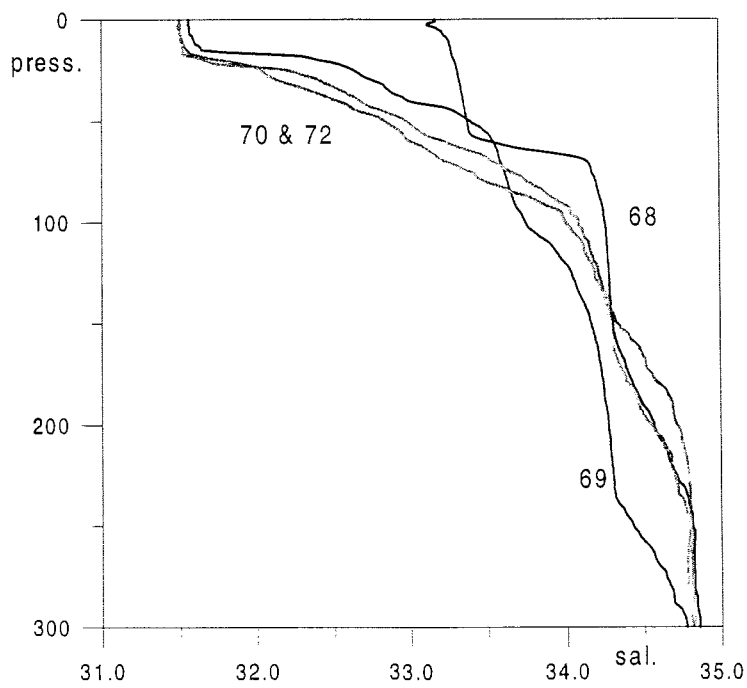
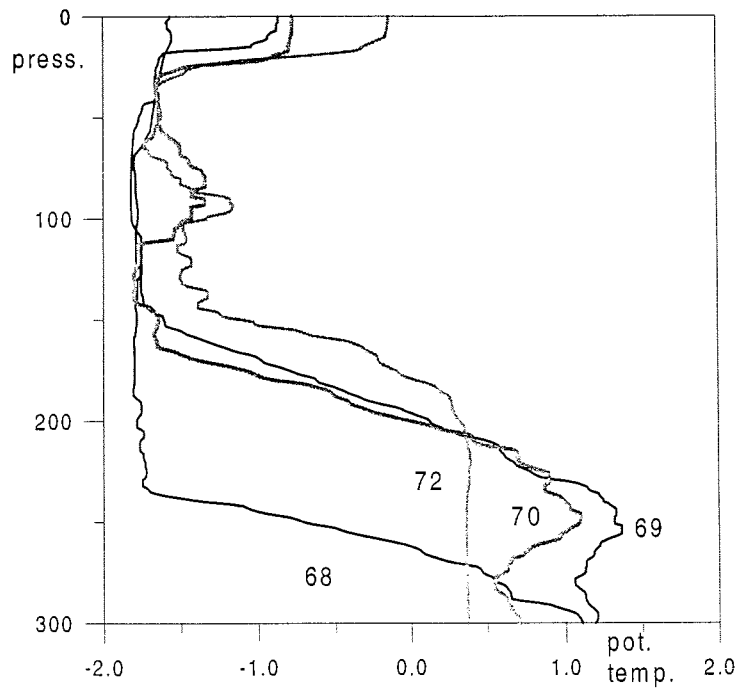


Fig. 4.7: Potential temperature a) and salinity b) profiles for the upper 300. from stations 68, 69, 70 and 72 in Fram Strait.

On transect C as well as in the central part of transect B the temperature of the Atlantic Layer was about $1.5\text{ }^{\circ}\text{C}$ (Figs. 4.8 & 4.9) suggesting Eurasian Basin rather than Canadian Basin origin. This may also be supported by the large regular inversions found in the Atlantic Layers in the central parts of both transects (Fig. 4.8). Similar inversions and layers have often been observed in the Eurasian Basin (Quadfasel et al., 1993; Rudels et al., 1994; Carmack et al., 1995) and are believed to result from the presence of two inflow streams with different characteristics. The mechanism creating these layers is not established and several explanations have been offered (Quadfasel et al., 1993; Rudels et al., 1994; Carmack et al., 1995). On the southern transect, at the boundary between the Canadian Basin and Eurasian Basin waters, the inversions were colder than in the Eurasian Basin Water column both on the southern and the northern transect and could be formed locally as the streams of Canadian Basin and Eurasian Basin waters converge in the strait.

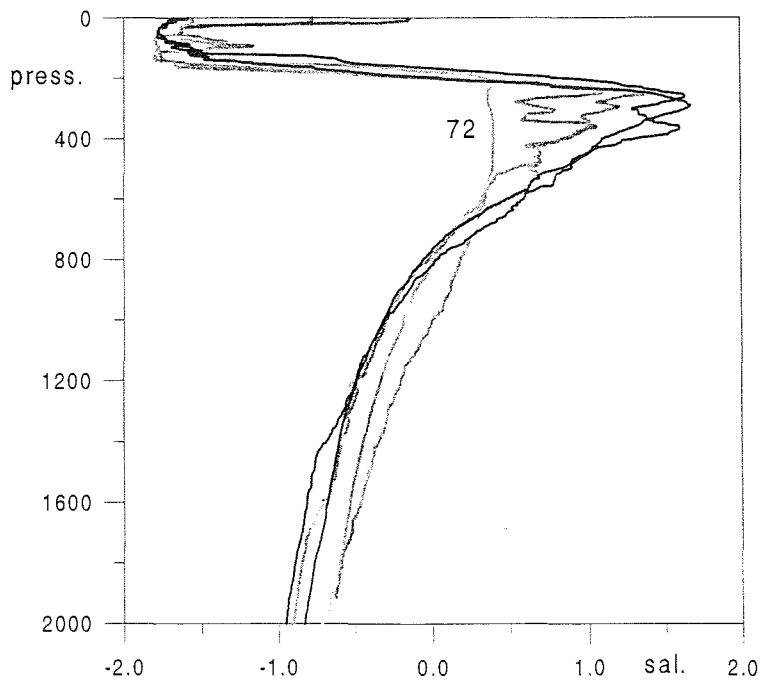


Fig. 4.8a: Potential temperature from stations 68, 70, 72, 77 and 78 in the central part of the passage. Note the smooth profile of station 72, the inversions on the other stations and the depth of the cold, low salinity surface layer.

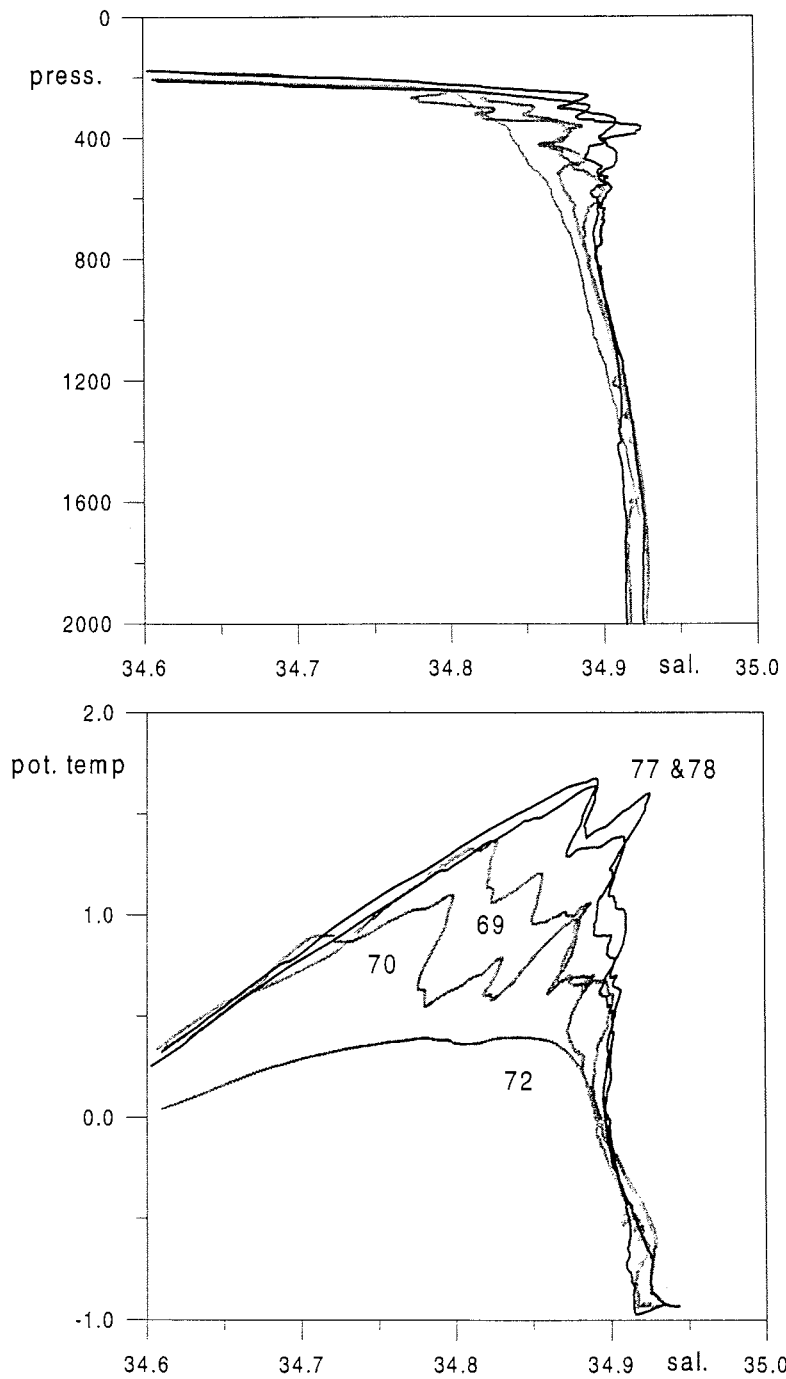


Fig. 4.8b/c: Salinity b) profiles and Q-S curves c) from stations 68, 70, 72, 77 and 78 in the central part of the passage. Note the smooth profile of station 72, the inversions on the other stations and the depth of the cold, low salinity surface layer.

The salinity and temperature profiles and Q-S curves in the central part of the strait were very similar to that found in the interior of the Nansen Basin on the ACSYS expedition with RV "Polarstern" in 1996. This is true not only for the Atlantic Layer but also for the cold surface layer (Figs. 4.8a & 4.11a). It is as deep or deeper as the Mixed Layer observed in the interior of the basin in 1996. Its temperature is close to freezing implying a recent winter homogenisation. Only little seasonal ice melt appears to have taken place. The temperature maximum of the Atlantic Layer is also displaced downward compared to the inflow in the south east as is seen by comparing transects B and C (Figs. 4.3 & 4.9). This confirms that not only ice melt and diluted Atlantic Water are present above the core of the Atlantic Layer but also that some input, presumably from the shelf areas has occurred, adding water to the upper layers and the thermocline. This is also evident from Figures 4.11a and 4.11b.

The northern Yermak Plateau.

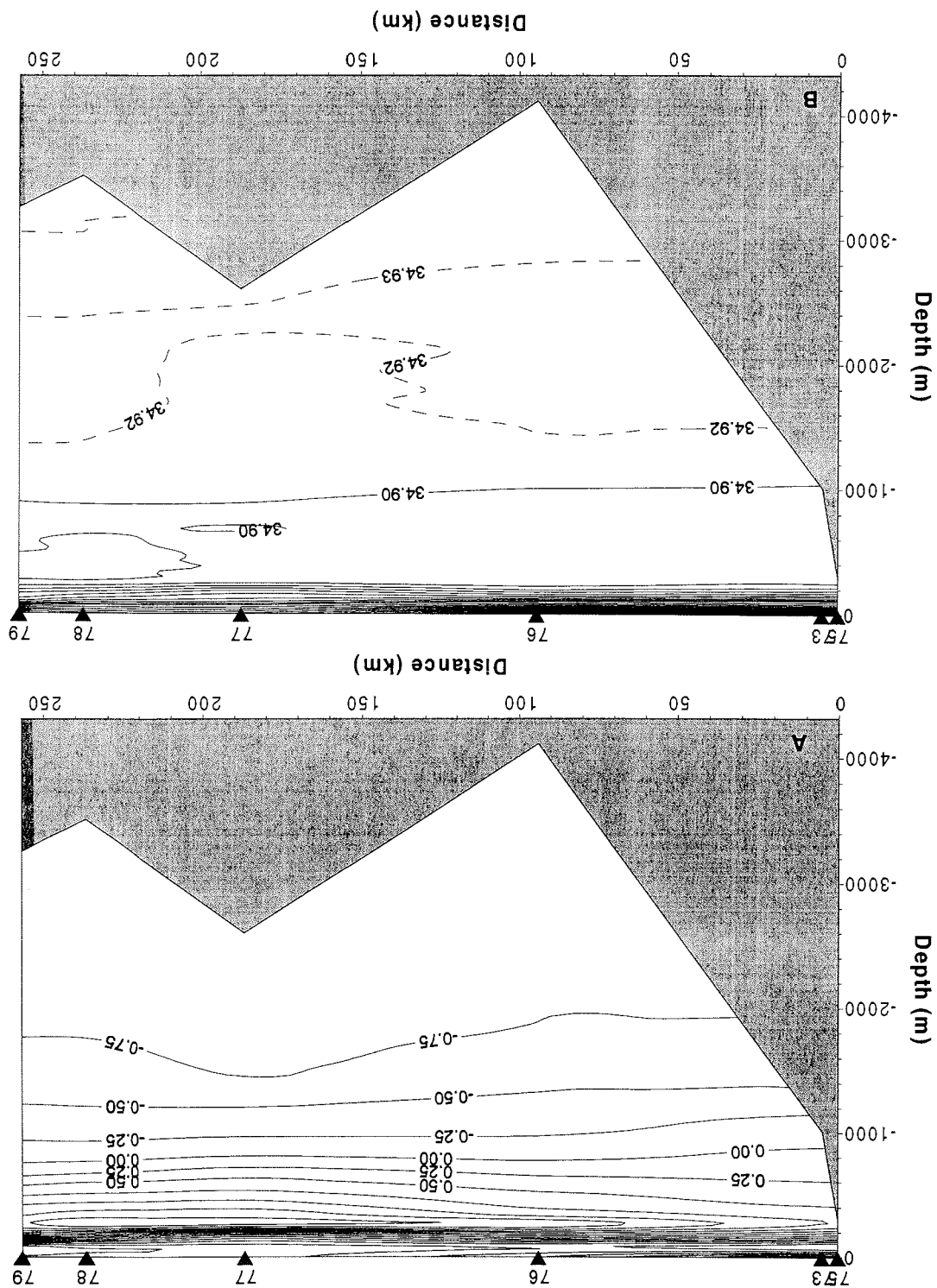
On transect D, at the north-western part of the Yermak Plateau, the upper layer became thinner closer to the slope (Fig. 4.10), perhaps indicating mixing and melting rather than winter homogenisation by freezing and haline convection. This is in the probable inflow region of the western branch of the West Spitsbergen Current and a situation similar to that to the east on the southern transect is to be expected.

The water column retained its Eurasian Basin characteristics of a deep, cold mixed layer and the regular large inversion very close to the slope of the Yermak Plateau (Fig. 4.11). Perkin and Lewis (1984) assumed that such inversions were formed locally by interaction between inflowing Atlantic Water and the Arctic Ocean water. However, the observations of similar and stronger inversions, especially in 1995 and 1996 (Rudels et al. in prep.) allows the possibility that the inversion layers are formed in the interior of the Arctic Ocean and the advected toward Fram Strait (Quadfasel et al., 1993; Rudels et al., 1994).

The difference between the assumed inflowing and outflowing water columns is not only the structure of the inversions. The inflowing Atlantic core is thicker, warmer and more saline. It is also covered by a thinner upper layer (Fig. 4.11). The comparably small difference in temperature between the assumed in- and outflow could be due to the reported recent inflow of warm Atlantic water to the Arctic Ocean (Quadfasel et al., 1991; Carmack et al., 1995), which now could have started to influence the temperature of the outflow.

The deep water becomes gradually colder closer to the slope of the Yermak Plateau and the deep water takes the characteristics of the NSDW (Fig. 4.12). Especially on stations 82, 84 and 86 a thin wedge of NSDW is seen pressed toward the flank of the plateau, implying a deep inflow from the south. NSDW cannot be identified in the Sofia Deep on the southern side of the Yermak plateau, where the deep water is clearly of Arctic origin. This would imply that the inflow is weak. However, at station 77 at the centre of transect C a temperature minimum was found at 2500m, which could be due to the presence of NSDW.

Fig. 4.9: Potential temperature and salinity sections from transect C.



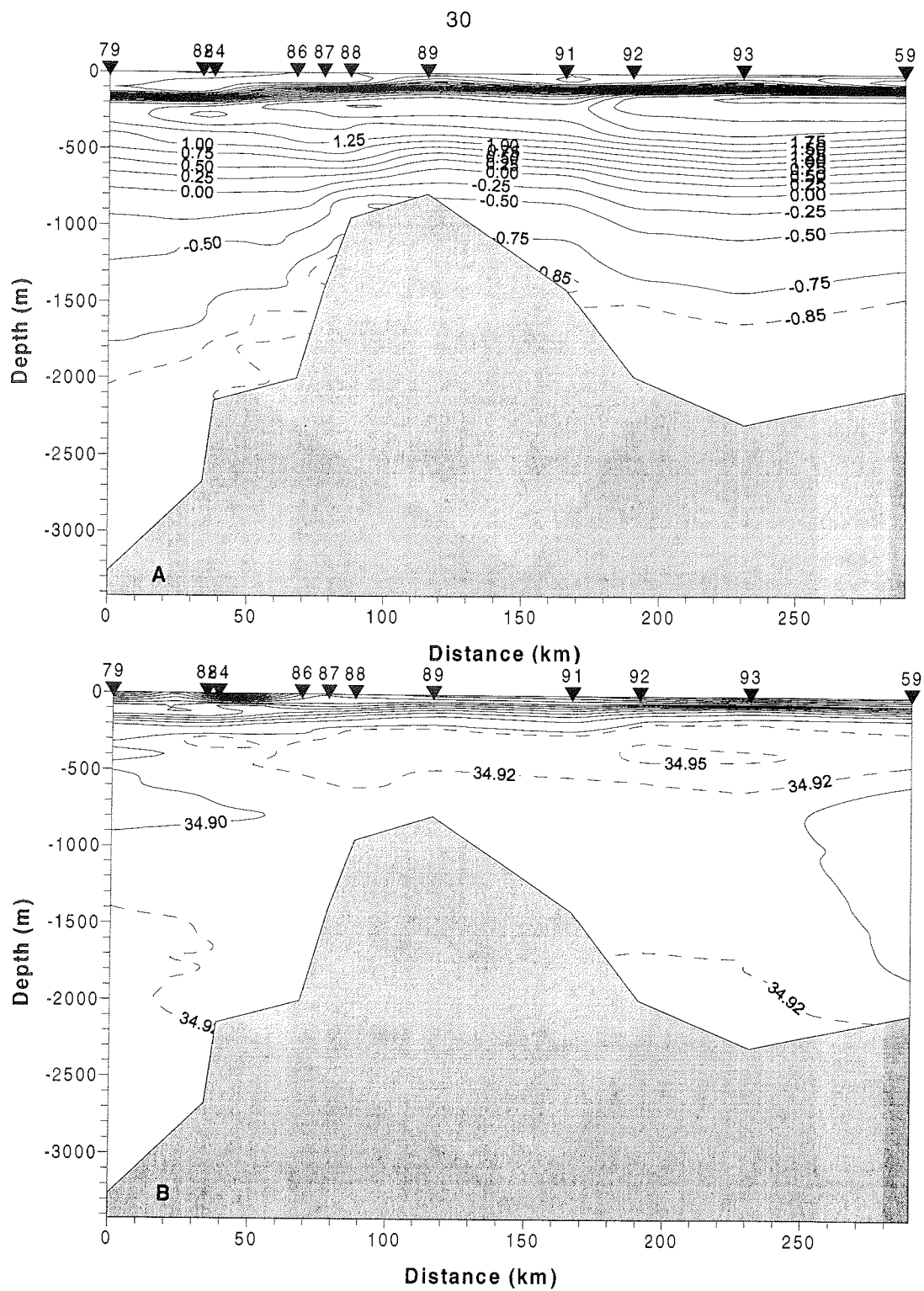


Fig. 4.10: Potential temperature and salinity sections from transect D.

At the shallower parts of the Yermak Plateau the colder water column characteristic of the plateau is found. As on transect B it is located on the Sofia Deep side of the crest and it separates the northern Atlantic core from the warmer Atlantic Water to the south. The core in the Sofia Deep has a temperature above $2.6 - 2.7^{\circ}\text{C}$ which suggests that the Sofia Deep is filled by Atlantic Water deflected from the southern inflow stream. Another possibility could be the inflow through the gap of the Yermak Plateau discussed by Gascard et al. (1995).

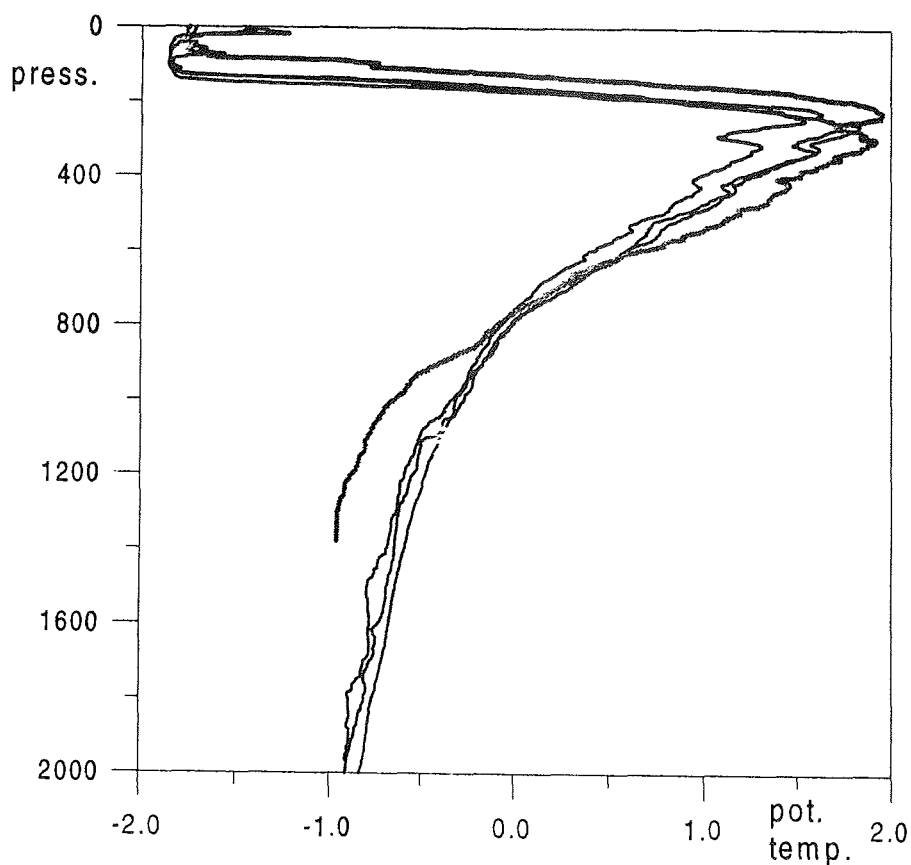


Fig. 4.11a: Potential temperature from stations 79, 82, 84 and 87 (grey) north of the Yermak Plateau. They show the more regular inversions on the northern stations and the thicker, warmer and more saline Atlantic core on the southern station (87).

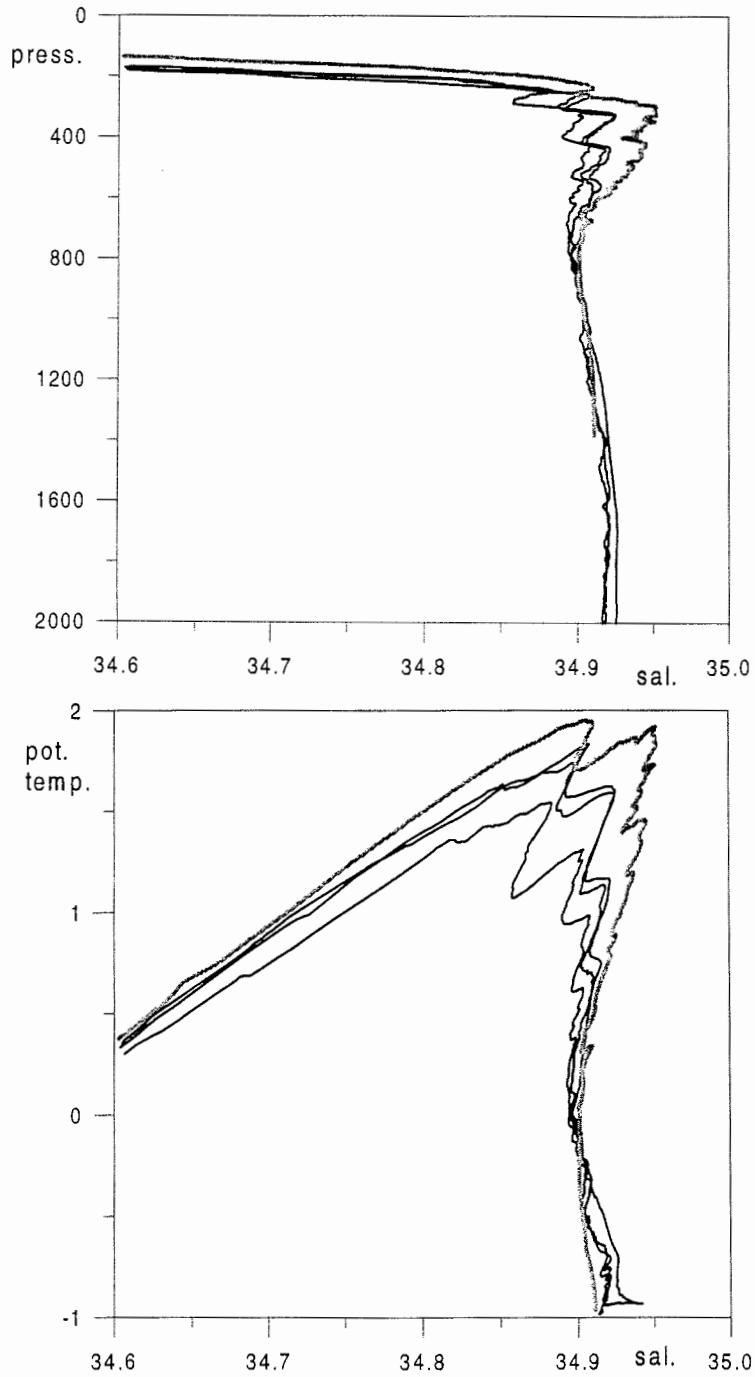


Fig. 4.11b/c: Salinity b) profiles and Q-S curves c) from stations 79, 82,84 and 87 (grey) north of the Yermak Plateau. They show the more regular inversions on the northern stations and the thicker, warmer and more saline Atlantic core on the southern station (87).

The Molloy Deep.

The final station taken in the Molloy Deep was close to the Polar front. The surface water was cold (about 1-2°C) but a temperature > 4°C at 50m and the high salinity in the Atlantic Water showed that apart from the surface water, the upper 500m derived from the south. Below the Atlantic Layer a low salinity layer with increasing salinity and decreasing temperature with depth characteristic of the Arctic Ocean Upper Polar Deep Water was found (Fig. 4.13). It was bounded below by a weak salinity and temperature minimum, which could mean the presence of a small volume of Arctic Intermediate Water from the Greenland Sea to the south. Below this minimum the weak, intermediate salinity maximum of diluted CBDW was found and the deeper water column was dominated by water from the north. This is to be expected since the Molloy Deep is north of the 2600m deep sill in Fram Strait. Beneath the CBDW the temperature decreased while the salinity remained fairly constant until the salinity stratified Eurasian Basin Deep Water was encountered. Below 3000m the potential temperature and salinity remained constant or decreased slightly, suggesting that the deepest connection between the Molloy Deep and the Arctic Ocean has a depth of 3000m. The small salinity and temperature decrease over more than 2000m could be instrumental rather than real. However, the water column remained statically stable during the decrease.

Summary and discussion.

In Table 4.1 the distributions of a few water mass characteristics are summarised. The table gives the depth, temperature and salinity of:

1. The upper temperature minimum indicating the depth of the last winter convection.
2. The temperature maximum showing the characteristics of the Atlantic Layer.
3. The salinity maximum also indicative of the Atlantic Layer.
4. The intermediate salinity minimum, which in the Arctic Ocean water column reveals the presence of the inflow over the Barents Sea. In the Nordic seas to the south it shows the presence of Arctic Intermediate Water formed mainly in the Greenland Sea.
5. The bottom water indicating the likely origin of the deepest layers. Cold and low salinity water derives from the south, warmer more saline from the Arctic Ocean. The Canadian Basin Deep Water is there the warmest and most saline.

The values are not always relevant for the shelf areas where several layers are not present.

Some conclusions can be drawn from the present observations. The temperature of the Atlantic inflow on the eastern part of the transect is lower than the maximum temperatures that have been observed in the interior of Arctic Ocean on several recent expeditions (Quadfasel et al., 1991; Carmack et al. 1995). This could indicate that at least temporarily the inflow of warmer Atlantic water has ceased. However, since the temperature at the repeat station northwest of Svalbard had increased by 0.5°C between the two observations the lower temperature could partly be a seasonal variations.

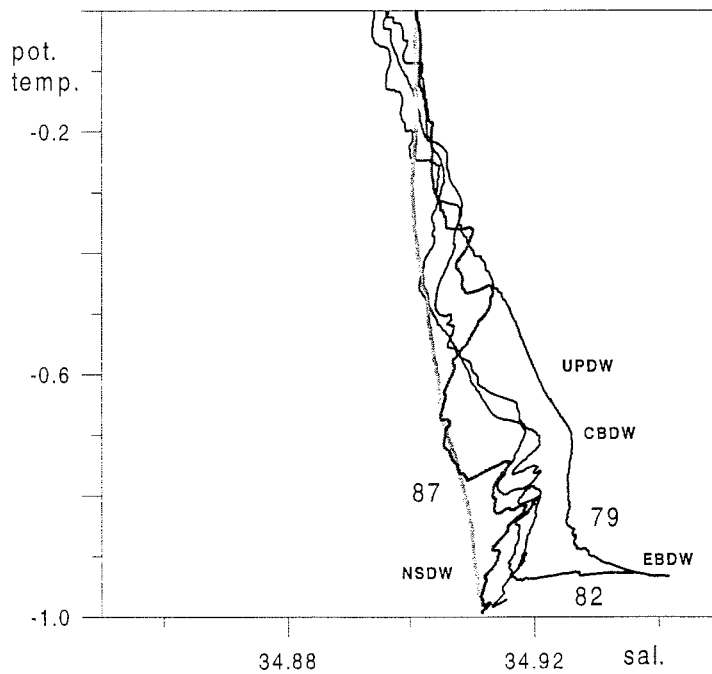


Fig. 4.12: Blown-up Q-S diagram showing the colder less saline Norwegian Sea Deep Water close to the slope (station 87), the constant temperature and increasing salinity of the Eurasian Basin Deep Water, the intermediate salinity maximum caused by the Canadian Basin Deep Water and the slope with decreasing temperature and increasing salinity typical for the Upper Polar Deep Water (station 79). The intermediate stations indicate lateral mixing of the deep waters.

The small freshwater content, the large depth of the mixed layer, and the absence of a halocline in the Arctic Ocean water column is similar to what was observed in 1996 in the interior off the Eurasian Basin (Schauer et al., in prep.). The mixed layer depth is still larger north of Fram Strait than in the interior. This could partly be due to the convergence of different outflow streams, which would suppress the underlying waters. It shows that the high salinity mixed layer is present over a large area of the Eurasian Basin or that it has been advected toward Fram Strait during the last year.

Table 4.1: The depth, temperature and salinity of the upper temperature minimum, the temperature maximum, the salinity maximum, the intermediate salinity minimum and the bottom values.

Layer:	Temp. min.			Temp. max.			Sal. max.			Sal. min.			Bottom			
	Stat.	press.	theta	sal.	press.	theta	sal.	press.	theta	sal.	press.	theta	sal.	press.	theta	sal.
39	**	**	**	**	34	3.12	34.893	61	2.21	34.995	**	**	**	301	0.74	34.920
40	26	-1.26	34.456	163	1.26	34.951	165	1.26	34.951	**	**	**	265	0.95	34.940	
41	48	-1.77	34.474	**	**	**	**	**	**	**	**	**	185	0.90	34.913	
42	62	-1.79	34.509	**	**	**	**	**	**	**	**	**	118	-0.18	34.893	
43	28	-1.69	34.398	**	**	**	62	-0.22	34.708	**	**	**	91	-0.16	34.707	
44	40	-1.78	34.425	**	**	**	141	0.59	34.844	**	**	**	143	0.59	34.844	
45	43	-1.74	34.374	**	**	**	**	**	**	**	**	**	135	0.29	34.773	
46	39	-1.72	34.394	158	0.22	34.762	160	0.22	34.762	**	**	**	169	0.19	34.762	
47	141	-1.82	34.507	**	**	**	**	**	**	**	**	**	194	0.36	34.763	
48	48	-1.80	34.343	133	-0.53	34.676	**	**	**	**	**	**	133	-0.53	34.676	
49	46	-1.71	34.363	**	**	**	**	**	**	**	**	**	152	0.16	34.785	
50	96	-1.84	34.312	202	1.78	34.773	**	**	**	**	**	**	280	0.85	34.836	
51	53	-1.81	34.167	**	**	**	**	**	**	**	**	**	188	0.94	34.598	
52	64	-1.83	34.190	240	1.78	34.813	302	1.33	34.832	**	**	**	310	1.24	34.830	
53	62	-1.80	34.208	222	1.49	34.770	**	**	**	**	**	**	236	1.48	34.780	
54	1	-1.66	33.671	**	**	**	**	**	**	**	**	**	332	0.88	34.813	
55	24	-1.77	34.134	289	1.06	34.840	356	1.01	34.845	419	0.68	34.816	454	0.69	34.839	
56	10	-1.38	33.826	97	1.63	34.805	100	1.63	34.807	**	**	**	167	-0.20	34.719	
57	2	-1.20	33.593	136	2.48	34.913	372	1.92	34.948	398	1.45	34.906	506	1.28	34.926	
58	3	-0.73	33.463	81	2.45	34.843	494	1.45	34.938	856	-0.41	34.887	972	-0.53	34.888	
59	66	-1.77	34.313	163	2.44	34.894	358	2.04	34.943	1031	-0.56	34.885	2069	-0.93	34.905	
60	19	-1.68	33.384	148	2.49	34.890	324	2.23	34.943	775	-0.02	34.886	1975	-0.92	34.910	
61	2	1.39	33.204	110	3.85	34.985	173	3.59	35.008	492	1.18	34.930	512	1.17	34.932	
62	13	-1.70	33.956	229	1.96	34.887	318	1.60	34.906	934	-0.57	34.887	1005	-0.67	34.887	
63	26	-1.77	34.280	202	1.85	34.874	314	1.53	34.908	805	-0.58	34.886	839	-0.64	34.887	
64	37	-1.79	34.212	159	2.19	34.908	424	1.53	34.940	578	0.03	34.888	636	-0.02	34.890	
65	77	-1.81	34.192	267	2.08	34.953	303	1.96	34.957	730	-0.19	34.879	1064	-0.88	34.889	
66	86	-1.83	34.220	224	2.28	34.928	472	1.52	34.947	864	-0.46	34.880	1395	-0.99	34.891	
67	94	-1.84	34.282	275	1.85	34.855	361	1.66	34.923	1060	-0.52	34.880	2428	-0.95	34.905	
68	74	-1.80	34.171	253	1.37	34.827	576	0.60	34.936	431	0.68	34.866	2964	-0.92	34.936	
69	89	-1.82	33.674	333	1.30	34.840	594	0.61	34.937	**	**	**	3574	-0.92	34.937	
70	130	-1.80	34.233	246	1.10	34.795	477	0.70	34.933	426	0.61	34.860	2714	-0.91	34.933	
72	65	-1.73	33.130	374	0.40	34.840	599	0.34	34.928	**	**	**	1912	-0.63	34.928	
73	107	-1.68	33.891	273	0.77	34.815	599	0.26	34.902	**	**	**	1100	-0.19	34.902	
74	100	-1.72	33.855	302	0.82	34.856	495	0.43	34.873	**	**	**	495	0.43	34.873	
75	100	-1.74	33.774	249	0.68	34.810	275	0.63	34.832	**	**	**	275	0.63	34.832	
76	41	-1.70	32.592	258	1.50	34.885	601	0.35	34.937	415	0.68	34.870	4170	-0.92	34.937	
77	45	-1.78	33.837	291	1.67	34.890	370	1.60	34.932	471	0.90	34.890	2575	-0.93	34.932	
78	62	-1.79	33.900	259	1.64	34.890	474	0.93	34.943	721	0.10	34.895	3517	-0.93	34.943	
79	99	-1.85	34.298	244	1.54	34.882	428	0.98	34.942	**	**	**	3258	-0.93	34.942	
82	99	-1.86	34.294	258	1.83	34.907	329	1.60	34.936	733	0.13	34.896	2778	-0.93	34.934	
84	73	-1.86	34.281	256	1.74	34.899	333	1.58	34.925	783	0.00	34.896	2118	-0.97	34.916	
86	61	-1.80	34.221	216	1.92	34.888	433	1.33	34.936	767	-0.02	34.901	1983	-0.99	34.912	
87	65	-1.77	34.201	224	1.95	34.905	326	1.84	34.952	871	-0.29	34.901	1380	-0.97	34.911	
88	60	-1.80	34.206	213	2.11	34.919	417	1.42	34.941	771	-0.41	34.904	913	-0.83	34.909	
89	26	-1.71	33.869	198	1.93	34.905	387	1.35	34.938	750	-0.33	34.908	774	-0.36	34.908	
90	15	-1.75	33.698	226	1.83	34.916	313	1.54	34.931	779	-0.53	34.908	819	-0.61	34.909	
91	17	-1.76	33.651	254	1.88	34.922	336	1.67	34.934	789	-0.35	34.906	1398	-0.86	34.917	
92	21	-1.73	33.581	188	2.47	34.916	394	1.89	34.956	924	-0.35	34.904	1966	-0.92	34.930	
93	17	-1.70	33.161	182	2.50	34.920	408	2.06	34.960	847	-0.13	34.906	2276	-0.93	34.933	
94	21	-1.31	32.793	83	2.70	34.851	229	2.37	34.965	738	-0.21	34.905	1025	-0.71	34.908	
96	14	-1.01	32.731	81	2.46	34.862	247	2.07	34.949	712	-0.38	34.905	767	-0.49	34.907	
97	3	-0.78	32.874	48	3.76	34.966	163	2.99	34.997	703	-0.24	34.906	792	-0.53	34.907	
98	49	2.89	34.583	102	3.63	34.974	160	3.24	35.000	**	**	**	257	2.48	34.990	
99	2	0.12	32.445	57	4.42	35.015	60	4.42	35.016	489	1.04	34.944	512	1.01	34.944	
100	3	1.63	32.825	26	4.85	34.747	52	4.25	35.031	800	-0.04	34.896	5534	-0.97	34.924	

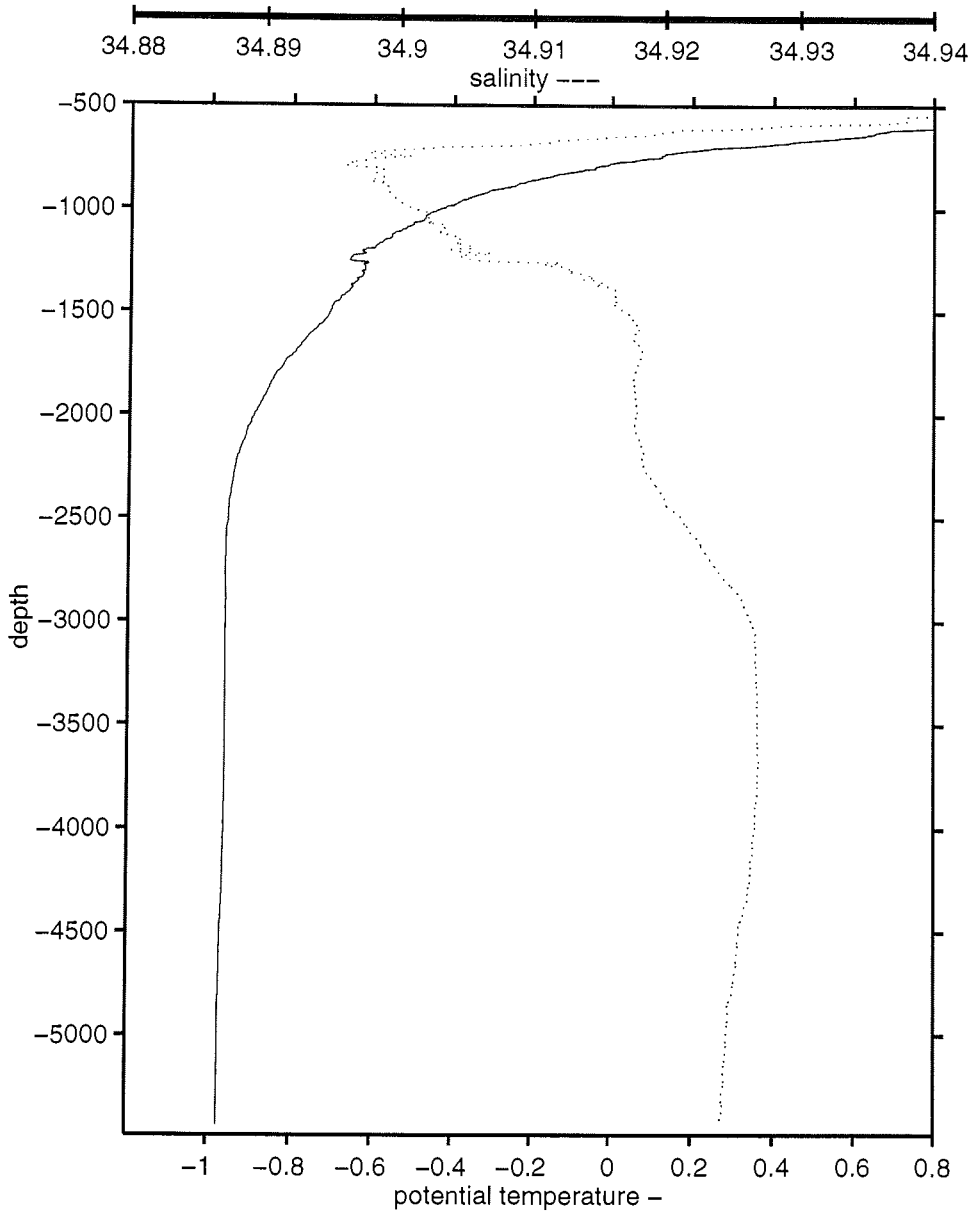


Fig. 4.13a: Potential temperature and salinity profiles from the deeper (below 500m) part of station 100 in Molloy Deep. The Arctic Ocean deep waters, UPDW, CBDW and EBDW (see text Fig. 4.12) are seen as well as a weak temperature minimum possibly indicating the presence of Arctic Intermediate Water from the south.

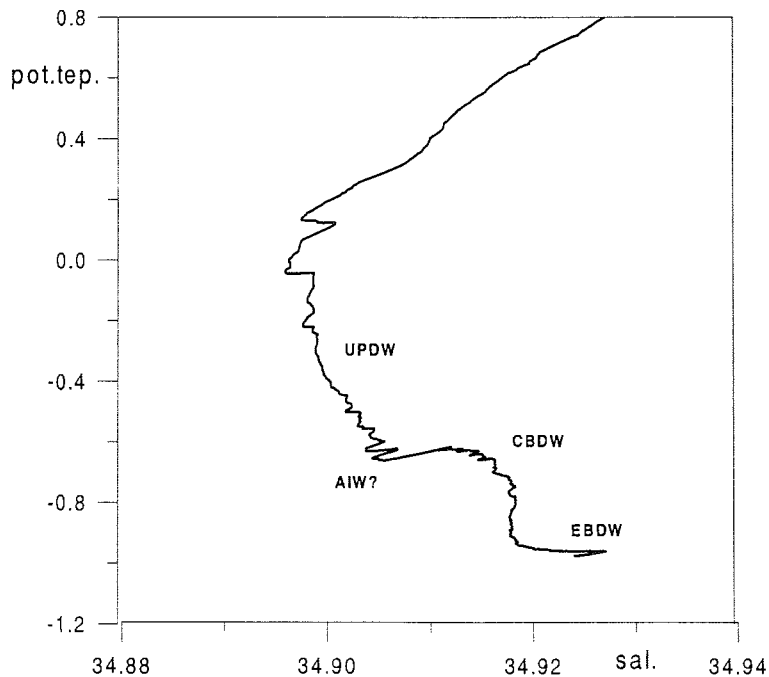


Fig. 4.13b: Q-S curves from the deeper (below 500m) part of station 100 in Molloy Deep. The Arctic Ocean deep waters, UPDW, CBDW and EBDW (see text Fig. 4.12) are seen as well as a weak temperature minimum possibly indicating the presence of Arctic Intermediate Water from the south.

The Atlantic Layer deriving from the Canadian Basin was cold and had smooth temperature and salinity profiles. It implies that the reported pulse of warm Atlantic Water has not made a complete tour around the Arctic Basin. However, the Eurasian Basin Waters showed higher temperatures than on the Oden transect between the Morris Jesup Plateau and the Yermak Plateau taken in 1991 showing that the part of the high temperature pulse, which is confined to the Eurasian Basin now has reached the outflow region of the Nansen and Amundsen Basins.

The interleaving structures observed in the water column were remarkably similar to those found in the Nansen Basin north of the Kara Sea on the ACSYS cruise in 1996. They were more evolved though, having weaker minima and now have been advected from the ACSYS positions, it would imply that at least one return stream could have as large velocity as 4cm/s. This appears very high. However, a funnelling effect may be present as the streams from the different regions converge, allowing part of the flow to accelerate as it approaches Fram Strait. This would leave the Amundsen and Canadian Basin waters in the backwater causing them to attain a comparably higher residence time.

5 **Marine Biology**

(E. Rachor, H. Thiel, H. Auel, H. Bäsemann, E. Bauerfeind, S. Denisenko, E. Helmke, K. v. Juterzenka, M. Klages, U. Klauke, K. Kosobokova, F. Kulescha, S. Lischka, K. Meiners, V. O. Mokievsky, Y.B. Okolodkov, B. Sablotny, I. Schewe, V. Shevchenko, T. Soltwedel, Q. Zhang)

The high Arctic ecosystems are assumed to respond most sensitively to any unusual environmental change including persistent climatic trends. The biological investigations during ARK-XIII/2 are regarded as a contribution to the better understanding of the Arctic marine ecosystems, which is a prerequisite for any realistic predictions about responses of populations and systems to environmental changes. Moreover, it is challenging enough that the coupling and functioning of the main sub-systems (ice - pelagial - benthal) are insufficiently described and understood so far.

The cooperation of a great diversity of biological research teams on board "Polarstern", therefore, offered a unique opportunity to contribute to the understanding of the functioning of the Arctic marine system. It is expected that the results of the different compartment studies can be put together at a later stage to build-up energy flow models for selected areas (central to northern Barents Sea, Yermak Plateau with its neighbouring deep-sea areas), also as a main input to the international research program "AOSGE".

The general strategy during the cruise was to sample along transects which covered strong regional gradients, i.e. across the continental slopes and the marginal ice zones. Thus, differences due to these gradients could be discerned.

5.1 **Sea-ice: Ecological Studies**

(Q. Zhang, K. Meiners, K. v. Juterzenka, S. Lischka)

Sea-ice floes are the habitat for the so-called sympagic community which consists of algae, bacteria, protists and metazoans. During this expedition we studied physical and biological properties of ice floes to characterize the seasonal changes occurring in the spring-summer transition. Ice samples were obtained by means of ice coring. A total of 12 stations were sampled during this expedition. Only one station was sampled in the northernmost area of the Barents Sea during transect A, all other sampling activities focused on the ice floes around the Yermak Plateau in the northeast of Greenland Sea during transects B, C and D. In the eastern part of the Yermak Plateau area (east of 13°E), first year ice floes were sampled. In its middle and western parts of the Yermak Plateau area, we got multi-year ice floes and insights into the release of organic matter from the ice. Due to increasing occurrence of melt pools we started to sample this special habitat on ten stations.

Based on these two different kinds of ice floes, first of all, our data set will allow a detailed comparison of biomass and communities in first-year versus multi-year ice. Secondly, the results will be included into data sets from earlier "Polarstern" expeditions to describe the seasonal cycle of ice biota development in Arctic seas.

5.1.1 Sea-Ice Observations

(Q. Zhang, K. Meiners, K. v. Juterzenka, S. Lischka)

A total of 66 observations on the state of the sea-ice cover were made while the ship was steaming in ice-covered waters. We determined the percentages of certain ice types (new ice - young ice - first-year ice - multi-year ice) as well as sizes of ice floes, snow thickness, sediment load and occurrences of melt pools.

In the Barents Sea, we observed only first year ice. As an example, the average ice-cover distribution along the northwards going transect A is given in Figure 5.1.

First-year ice thickness ranged from 50 to 180 cm with a strong increase toward the north. The average floe size diameter increased towards the north from less than 10m at the southernmost observation point to more than 1000m at the northernmost location. No new ice formation was observed along the transects A and B and most of the observation points along the transects C and D due to the polar summer air temperature (around -3.2°C to 2.0°C), but at the northernmost points along the transects C and D, new ice was forming to a small amount between the multi-year ice floes.

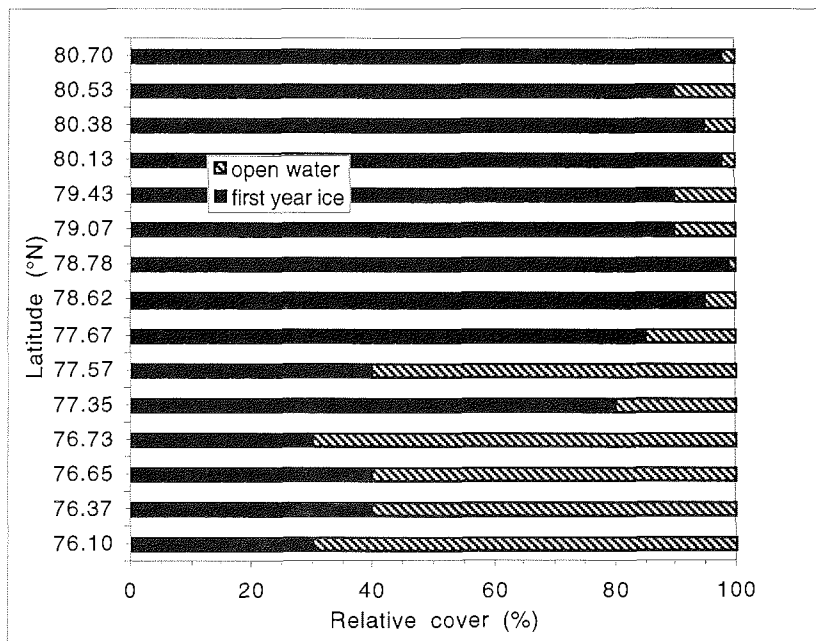


Fig. 5.1: Ice cover along the northward heading transect A of ARK-XIII/2.

The ice cover in the area of the Yermak Plateau was dominated by first-year ice floes, only in the western part it was covered with multi-year ice floes. Open water without any ice was observed in the north-western Greenland Sea. At

almost all locations we recorded floes including sediment. Ice floes were covered with melt pools from 1% to 80% during the entire expedition. Their sizes ranged from 1m² to more than 1000m². This gave us the opportunity to study the ecology of small melt pools (details described in section 5.1.5).

We frequently observed strong coloration of ice floes due to the occurrence of algae. Not only the bottom sides but also internal layers of ice floes showed a slight brownish color. Therefore we hypothesize that the formation of internal layers also occurs frequently in Arctic seas as described for Antarctic regions. However, we did not have the opportunity to study such floes by taking ice cores.

5.1.2 Physical and Biological Properties of Arctic Sea-Ice (Q. Zhang, K. Meiners)

At 12 stations we sampled several ice cores to measure vertical profiles of the following parameters:

- ice temperature
- ice bulk salinity
- chlorophyll *a* and phaeopigment concentrations
- abundances of organisms (bacteria, protists, metazoans).

The organism abundance will be analysed in the home laboratories. *In-situ* and on board "Polarstern" we determined the first 3 parameter sets mentioned above. An interesting example of the available data set is given for ice station 57/184 (Fig. 5.2). There we found two internal peaks of algal biomass as expressed in Chlorophyll *a* concentrations occurring in the sub-bottom layer and the middle part of the ice core. The temperature of the top parts of this ice core was relatively high (-0.3°C), which presented the summer values. Lowest temperatures were mostly observed in the middle part of the ice cores, while a warming of the ice surface occurred. Typically, only one peak of algal biomass appeared in the bottom parts of the ice floes. The highest peak of algal biomass was recorded as 50.0 mg Chlorophyll *a* m⁻³ ice at station 79/202.

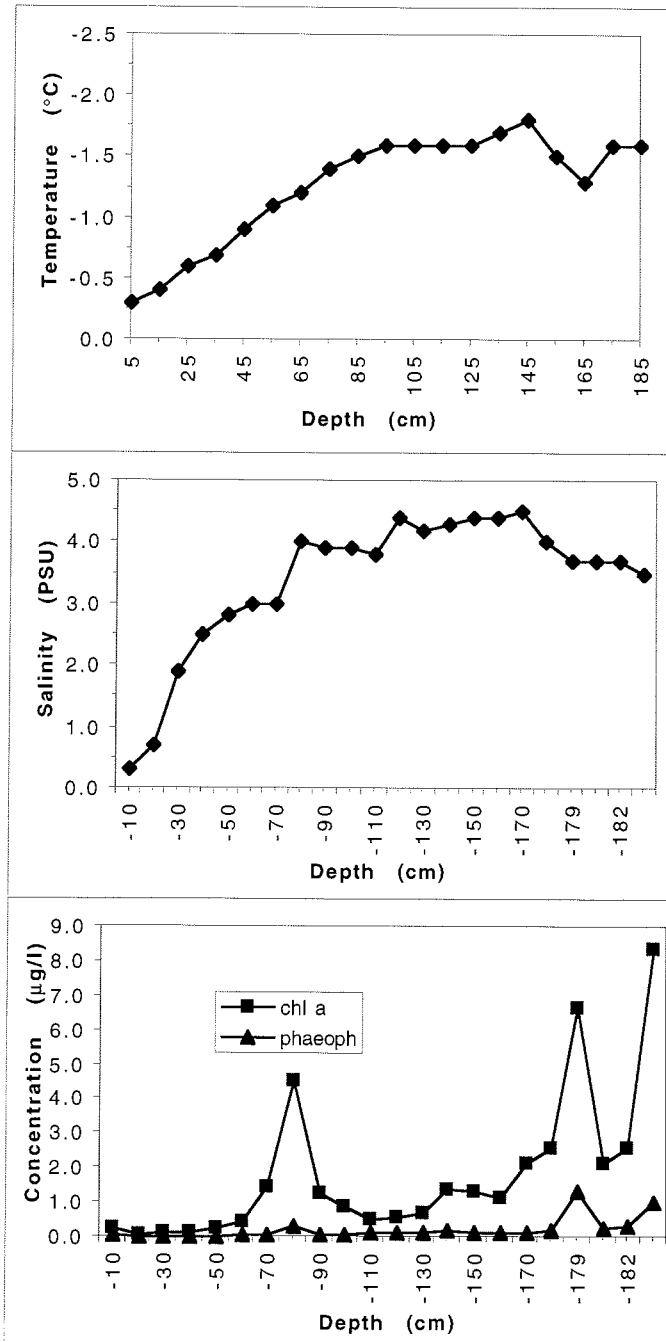


Fig. 5.2: Vertical distribution of temperature, salinity and algal pigments in the ice floe at station 57/184.

5.1.3 The Response of Arctic Sea-Ice Micro-Organisms to Changes of Salinity Under Different Light Conditions (Q. Zhang)

Polar marine ecosystems are subject to strong seasonality and interannual variability of environmental factors especially ice cover and irradiance. Sea-ice covers between 7-14 million km² of the Arctic Ocean are a crucial parameter for the modelling of environmental changes in polar areas. Microalgae from the water column and the sea ice are important primary producers in polar oceans, in which diatoms are dominant and contribute more than 90% to the total microalgal biomass. The seasonal development of the polar marine algae is mainly controlled by abiotic parameters. The onset of microalgal growth in spring is dependent on the increase of the available light intensities after the dark polar winter.

Micro-organisms that inhabit the interstices and underside of sea ice are exposed to wide variations of salinity, in particular during the periods of brine drainage and ice melting. Numerous studies at Arctic, Antarctic and sub-Arctic sites have shown that light is the principal factor limiting the onset and early development of bottom ice algal blooms. It was reported that four Arctic diatoms were euryhaline and maintained growth rates of 0.6 to 0.8 divisions per day over a salinity range of 10 to 50psu.

During the RV "Polarstern" cruise legs ARK-XIII/1 and 2, we carried out an experiment to study the salinity tolerance of Arctic algae in a range of 1 to 100psu under natural light conditions. The results showed that most species of the natural ice microalgal community in the Greenland Sea exhibited net growth within a range of 4 to 74psu, and that the maximum net community growth rate was at 20psu. Data on the responses of Arctic sea-ice micro-organisms to changes in salinity lower than that of normal seawater under different light conditions are limited.

Our experiment was designed to study the response of Arctic sea-ice micro-organism, i.e. algae and bacteria, to salinities below normal Arctic seawater. For that purpose ice cores were taken from an ice floe at the location of 77°22'N, 0°22'E during ARK-XIII/1 in the Greenland Sea. The top 10cm segments melted and filtered through a 0.2µm Nuclepore filter were used as the low salinity melt water (LSMW, 0.2psu). The bottom 2cm sections thawed in an excess of 0.2µm filtered seawater were used as the natural Arctic sea-ice micro-organisms. Larger metazoans were excluded by filtration through a 60µm silk mesh.

The eight steps of salinity were achieved by the addition of LSMW to normal Arctic sea water (34.2psu). 200ml of the melted bottom sea-ice water with the natural sea-ice biota was added to 1000ml medium. After mixing, the end salinity was measured with a WTW-salinometer. The final eight steps of salinity were 4.7, 8.3, 12.8, 16.6, 21.4, 25.2, 29.6 and 33.1psu. The samples were divided and filled into Corner polystyrene tissue culture vials with a volume of 250 ml each and cultured at a temperature of 0°C at four different light conditions (for details, see Fig. 5.3).

The cultivation was maintained for 25 days. Subsamples (25 ml) were collected every five days after the start of the experiment and were fixed with borax-buffered formaline of 1% final concentration. Then a 10 ml subsample was filtered onto 0.2µm Nuclepore filters and stained with DAPI. At the end of

the cultivation, the algal pigments were measured with a Turner 10-AU Fluorometer.

On board, video records for later analysis of the species composition of the algae, the bacterial sizes, shapes and abundance were made using a Zeiss Axiovert 135 inverted light and epifluorescence microscope, equipped with a Sony DXC-930P 3-CCD video camera and a Sony SVO-9500MDP recorder. Details will be analyzed at the home lab in the IPÖ Kiel.

Chlorophyll a concentrations on the 25th day (Fig. 5.3) were higher at 33.1psu with normal or lower irradiance of 24 hours light. The differences of the Chlorophyll a concentrations are not significant at all the eight steps of salinity with a light:dark cycle (light condition). The algal abundances at the 20th and 25th days show similar changes (Fig. 5.4).

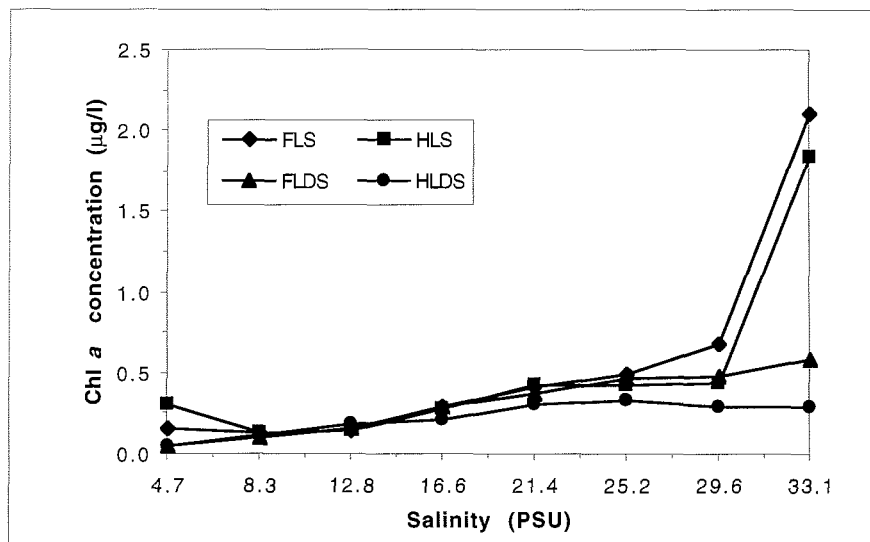


Fig. 5.3: The Chlorophyll a concentrations at the 25th day after culture. FLS means normal irradiance ($41.61\mu\text{E}/\text{m}^2\text{s}$) with 24 hours light; FLDS means normal irradiance ($41.61\mu\text{E}/\text{m}^2\text{s}$) with a light:dark cycle of 14:10 hours; HLS means lower irradiance ($14.74\mu\text{E}/\text{m}^2\text{s}$) with 24 hours light, and HLDS means lower irradiance ($14.74\mu\text{E}/\text{m}^2\text{s}$) with a light:dark cycle of 14:10 hours.

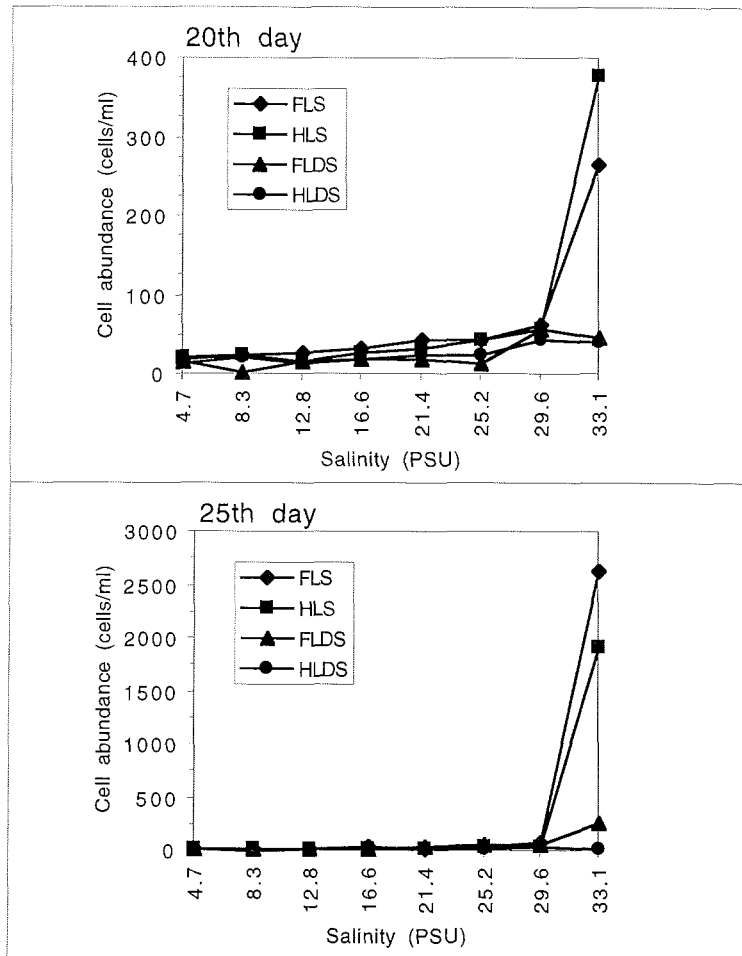


Fig. 5.4: The algal abundance at the 20th and 25th day after culture. FLS means normal irradiance ($41.61\mu\text{E}/\text{m}^2\text{s}$) with 24 hours light; FLDS means normal irradiance ($41.61\mu\text{E}/\text{m}^2\text{s}$) with a light:dark cycle of 14:10 hours; HLS means lower irradiance ($14.74\mu\text{E}/\text{m}^2\text{s}$) with 24 hours light, and HLDS means lower irradiance ($14.74\mu\text{E}/\text{m}^2\text{s}$) with a light:dark cycle of 14:10 hours.

5.1.4 Distribution of Organisms and Grazing Experiments with Arctic Sea-ice Protists (K. Meiners)

In order to improve the knowledge about the vertical distribution of sympagic organisms we took one ice core in the northern Barents Sea and 11 ice cores in the Yermak Plateau area in the north Greenland Sea. The ice cores were used to determine the abundances and biomasses of bacteria, protists and meiofauna. The ice cores were cut into sections of 1-20 cm length and melted in the dark by addition of filtered seawater to avoid osmotic stress. After

melting samples were subsampled and fixed either with formalin (1% final concentration) or with Bouin's fluid. Bouin-fixed samples will be used for the investigation of meiofauna and for taxonomic work on ciliates. This work will be done in the home laboratories at IPÖ. Formalin-preserved samples were filtered onto 0.2 µm and 0.8µm polycarbonate filters and stained with the fluorescence stain DAPI. These filters will be analyzed using epifluorescence microscopical techniques to obtain data of bacteria and protists. The estimated biomass of heterotrophic protists will be used to calculate the grazing impact of this group by general allometric equations.

These indirect estimates will be compared with the results of direct grazing measurements which were performed during the cruise by using fluorescently labelled bacteria (FLB) and fluorescently labelled algae (FLA). FLB and FLA were added to melted bottom ice sections. We measured the long-term disappearance of FLB and FLA within the samples to provide data about the grazing impact of the total community. Experiments were run as time course experiments, and the disappearance of labelled prey was observed over a period of 24 hours. Subsamples were taken after 0, 6, 12, 18 and 24 hours. Subsamples were fixed with formalin and also stained with DAPI. The decrease of the concentration of FLB and FLA will be determined by epifluorescence microscopy in the home laboratories.

In addition to this program we took bottom sections for the cultivation of a variety of sympagic algae, protozoan and metazoans. The cultivated organisms will be used for further taxonomic work and additional grazing experiments (using the serial dilution method) in the home laboratories.

5.1.5 Characteristics and Biota of Small Melt Pools

(K. v. Juterzenka, S. Lischka, K. Meiners, Y. B. Okolodkov, Q. Zhang)

In addition to the work on sea-ice biota within the ice, which is described in the previous chapters, a total of 10 small bluish melt pools was investigated during the cruise. Samples of surface water and water from the bottom of the pools as well as ice samples were taken for analyses of Chlorophyll *a* and phaeopigments, nutrients and quantitative evaluation of algal cells and bacteria. Pigment concentrations were measured on board according to Arar & Collins (1992) using a Turner design fluorometer. Water samples for nutrient analysis were frozen and stored at -30°C. Quantitative water samples were fixed with formaldehyde (final conc. 1%), and a subsample was filtered on 0.2 µm polycarbonate filters and stained with DAPI for subsequent countings of bacteria. Further analysis of these samples will take place in the laboratory at IPÖ. Taxonomical investigations on living microflora in pool bottom water and ice samples were carried out by Y. B. Okolodkov (Chapter 5.1.6).

The maximum diameter of the pools investigated ranged from approx. 0.5 m to 8 m, the maximal depth from 11 cm to 42 cm (further characteristics are given in Table 5.1). All pools contained freshwater, but pool no.2 showed a slightly enhanced conductivity of 0.6 mS in its bottom water.

Table 5.1: Characteristics of melt pools sampled during ARK-XIII/2.													
pond no.	station no. 44/	day of the year	position		approx. size (m)		shape	colour	max. depth	comments	ice floe: size of ice floe	ice thickness (cm)*	cover by melt ponds (%)
			latitude	longitude	length	diameter							
1	62	189	80°54. N	29°29. E		0,56	kidney-like	bluish, some sediment	16 cm (with slush)		100-1000m	200	30
2	64	191	81°7.6 N	5°36.2 E	5	2	irregular, elongated	bright bluish, "clean"	10 cm in holes	lots of air bubbles in bottom ice	100-1000m	200	50
3	66	194	81°17.4 N	0°20.1 E	6 to 7	5	elongated/oval	bluish-grey-greenish	15 cm	overfrozen; rainy day rainwater on top	100-1000m		30
4	69	196	81°26.9 N	5°23.5 W	7	2,5	oval with protrusions	bright blue - grey	15 cm	pool overfrozen (d=5cm)	100-1000m	350	10 to 20
5	77	200	82°0.0 N	2°26.0 W	7	4	elongated/oval	nice blue, grey spots	32 cm	pool overfrozen (d=2-3cm) filled with slush bottom ice soft/slushy	100-1000m	250	20
6	79	202	82°38.5 N	1°31.9 E	6	3,5	amoeboid	grey-blue	14 cm	pool overfrozen (d=0.5 cm)	> 1000m	240	10
7	83	204	82°19.5 N	3°41.3 E	6 to 7	3 to 5	elongated/irregular	bluish-grey	22 cm	pool overfrozen (d= 0.6 cm)		280	
8	83	205	82°19.5 N	3°41.3 E	3	3,5	heart-shaped	bright blue	11 cm (40 cm in crack)	divided in the middle by crack		280	
9	89	208	81°54. N	7°50. E	2	8	elongated	blue	20 to 21 cm in small cracks			212	
10	93	211	81°16. N	13°02. E	3,5	2,5	oval	grey-blue-greenish	42 cm	dirty ice; lumps of aggregated material at the bottom of deep melt holes at the edge of pool		160	20 to 30
												200	

* length of cores at drilling location

5.1.6 Sea-Ice Algae (Y.B. Okolodkov)

In Arctic sea-ice the highest densities of populations of ice-associated organisms including algae have been observed in the lowermost layer (Horner, 1985; Okolodkov, 1989, 1990, 1992a, b, 1996; Gradinger et al., 1991). To study the species composition of algae inhabiting this layer and to evaluate them quantitatively in fresh, not fixed samples, was one of the purposes of sea-ice studies during the ARK-XIII/2 expedition on board RV "Polarstern".

Material and Methods

Nine samples of the lowermost 10-cm layer taken with a SIPRE auger (inner diameter of 9 cm) were cut immediately (within a minute) from ice cores at nine stations located in the northern Barents Sea, NE of Svalbard (Station 54/181), in the area N of Svalbard (Stations 57/184 and 59/186) and W and SW of the Yermak Plateau (Stations 62/189, 64/191, 65/194, 79/202, 90/208 and 93/211) in the period June 30 - July 30, 1997. Ice thickness varied between 153 and 247 cm (first- and two-year ice), snow cover being 3 to 20 cm. The samples were let to melt in plastic bottles at 5°C in a refrigerator. Two litres of filtered sea water were added to every section of the cores (ca. 660 ml) before melting to avoid osmotic shock of delicate flagellates (Garrison and Buck, 1986). After melting, the algae in the samples were concentrated through 1 µm Nucleopore filter, using a reverse-filtration device, to ca. 40 ml. Before being counted the concentrated algae were stored in a refrigerator in dark from several hours to five days. Counting was made in a Hydro-Bios 3-ml chamber under the inverted microscope Axiovert 135 (for more detailed characteristics of the optics used, see chapter 5.2.3).

Results and Discussion

The total number of cells found in the lowermost 10 cm of the cores varied from 5.94×10^4 to 7.43×10^5 cells per litre of melt water (cells/l). Flagellates constituted 10.7% to 86.8% and diatoms 13.2% to 89.3% (Table 5.2). The species composition and dominances varied between different cores.

The dominance of a heterotrophic flagellate of 4.5-5.5 µm in diameter at stations 65 and 54 (31.9% and 24.0% of the total number of cells, respectively) can partly be explained by the fact that counting was made 2 to 5 days after sampling. Dividing cells of the heterotrophic flagellate were found and the process of asexual reproduction lasted a few minutes. Most likely, the population increased rapidly under favourable conditions after sampling. Samples from stations 57 and 59 are alike to a greater extent. In both cases, a chlorophyte *Chlamydomonas* sp. prevailed constituting 13.6% and 17.9%, respectively. The dominance and viability of this freshwater algae, which is more characteristic of the flora of melt pools on Arctic ice floes can be explained by intensive melting of the ice in July leading to the formation of under-ice melt ponds which are common in the Arctic Ocean (Gradinger, 1996). Various pennate diatom species constituted the bulk of the algal population at both stations. A relatively high percentage of diatoms at station 64 (75.3%), station 62 (54.0%) and station 90 (52.9%) belonged to the *Nitzschia frigida* community which included two epiphytic diatom species,

Attheya septentrionalis and *Synedropsis hyperborea* attaching to the cells of *N. frigida* especially in the case of ageing community. For example, at station 64 the share of *A. septentrionalis* was 25.1% and that of *S. hyperborea* was 23.0%, where many cells of *N. frigida* were found decaying. The highest percentage of flagellates at station 65 was mainly due to flagellates 3-5 µm in diam. (unfortunately, auto- and heterotrophic flagellates were not discriminated). At station 79, two species were responsible for the bulk of algal population: green globular cells of 11-13 µm in diameter (possibly, akinetic cells of *Chlamydomonas* sp.) - 55.2%, and a diatom *Pseudo-nitzschia* cf. *delicatissima* - 14.4%. At Station 93, along with abundant flagellates, a pennate diatom *Navicula kariana* dominated numerically (4.0×10^4 cells/l or 29.1%) and obviously in biomass being a relatively large-sized alga.

It was previously found that the seasonal succession in the lowermost layer of ice in Fram Strait, during a 3-week period in May 1988, went from the prevalence of autotrophic diatoms to the dominance of heterotrophic flagellates (Gradinger et al., 1992). Our preliminary results did not confirm the published data, probably because of the heterogeneity of the materials obtained.

Table 5.2: Quantitative characteristics of algal populations in the lowermost 10-cm layer of the ice in the waters of Svalbard and Fram Strait, in the period June 30 - July 30, 1997, during the ARK-XIII/2 cruise of RV "Polarstern"

Station number	Date	Total number of cells per litre of melt ice	% of diatoms	% of flagellates
54/181	30.06	7.43×10^5	51.6	48.4
57/184	03.07	4.33×10^5	68.3	31.7
59/186	05.07	3.21×10^5	54.6	45.4
62/189	08.07	4.63×10^5	46.0	54.0
64/191	10.07	3.67×10^5	75.3	24.7
65/194	13.07	5.94×10^4	13.2	86.8
79/202	21.07	5.82×10^5	35.2	64.8
90/208	27.07	4.43×10^5	52.9	47.1
93/211	30.07	1.36×10^5	89.3	10.7

5.2 Phytoplankton

5.2.1 Phytoplankton Ecology (E. Bauerfeind, Y. B. Okolodkov)

One goal of the biological studies of this cruise was to gain further insights into the pelago-benthic coupling and production in the study area. For this purpose sampling in the water column as well as studies of vertical particle flux were conducted. In the upper water column samples were taken in 8-10 discrete depths with the rosette water sampler. Subsamples were filtered for the analysis of chlorophyll *a*, particulate organic carbon and nitrogen, particulate silica, and the determination of seston content. Samples were also taken for the quantitative analysis of phytoplankton and its composition. Further samples were taken for the determination of the inorganic dissolved nutrients (phosphorus, nitrogen and silica). From the latter, information about the production history in the water column of the study area can be obtained, and from the difference to the winter nutrient concentrations the amount of production can be estimated.

Altogether, samples were obtained at 33 stations. During the cruise only measurements of chlorophyll *a* concentrations and analysis of phytoplankton composition could be performed. All other samples were fixed and stored refrigerated until analyses in the home laboratory.

Results

At the beginning of the cruise samples were taken along a south-north transect (transect A) in the Barents Sea in the same area where sampling was performed already during May 1997. By comparing the results of the two transects we will be able to get information about the temporal development of plankton and its production in this area.

Vertical distribution of chlorophyll *a* concentrations along transect A showed a maximum in 30 to 40m (Fig 5.5). Maximum concentrations of up to 5.6 µg/l were measured at station 42, whereas surface concentrations were less than 0.3 µg/l. This distinct vertical distribution pattern may be associated with frontal processes in the area. However, detailed information about this will only be available after thorough analysis of the hydrographical data. Chlorophyll *a* was distributed more evenly in the upper water layer in the northern ice-covered part of transect A. In this region concentrations between 0.5 and 1 µg/l were measured. Phytoplankton composition along transect A was mainly dominated by diatoms (see 5.2.3). Only at stations 39 and 42 flagellates were also present in higher amounts (*Dinobryon balticum* and *Phaeocystis pouchetii*).

Along transect B (Yermak Plateau-Fram Strait) again low concentrations of chlorophyll *a* (< 0.5µg/l) were observed in the ice-covered part of the transect. A plankton bloom was noticed at the ice edge (station 69) and in the ice-free region towards the coast of Greenland. In this region chlorophyll *a* concentrations of 3-4.5 µg/l (Fig. 5.6) were present in the upper 20-30m of the water column exhibiting also low salinity values. This bloom, dominated by the Arctic diatom *Chaetoceros socialis*, was most probably induced when the

nutrient-rich water originating from the ice-covered areas in the North became exposed to sunlight in the ice-free areas south of 82-83°N.

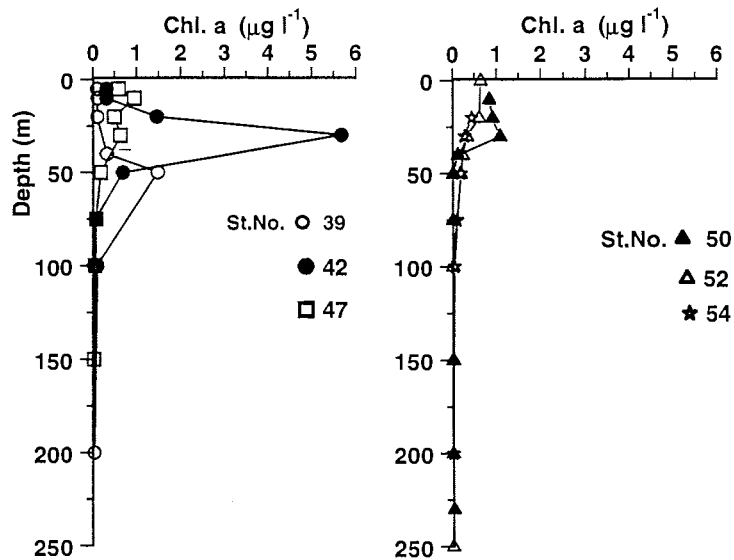


Fig. 5.5: Vertical distribution of Chlorophyll *a* at selected stations in the Barents Sea (transect A).

At the southern end of transect D (stations 94-99) a plankton bloom (Chlorophyll *a* concentrations 2-3 $\mu\text{g/l}$) was also noticed and could be traced to a distance of 44 km from the ice edge. This bloom was dominated by flagellates (*Dinobryon balticum* and *Phaeocystis pouchetii*) and represented a later stage in plankton succession.

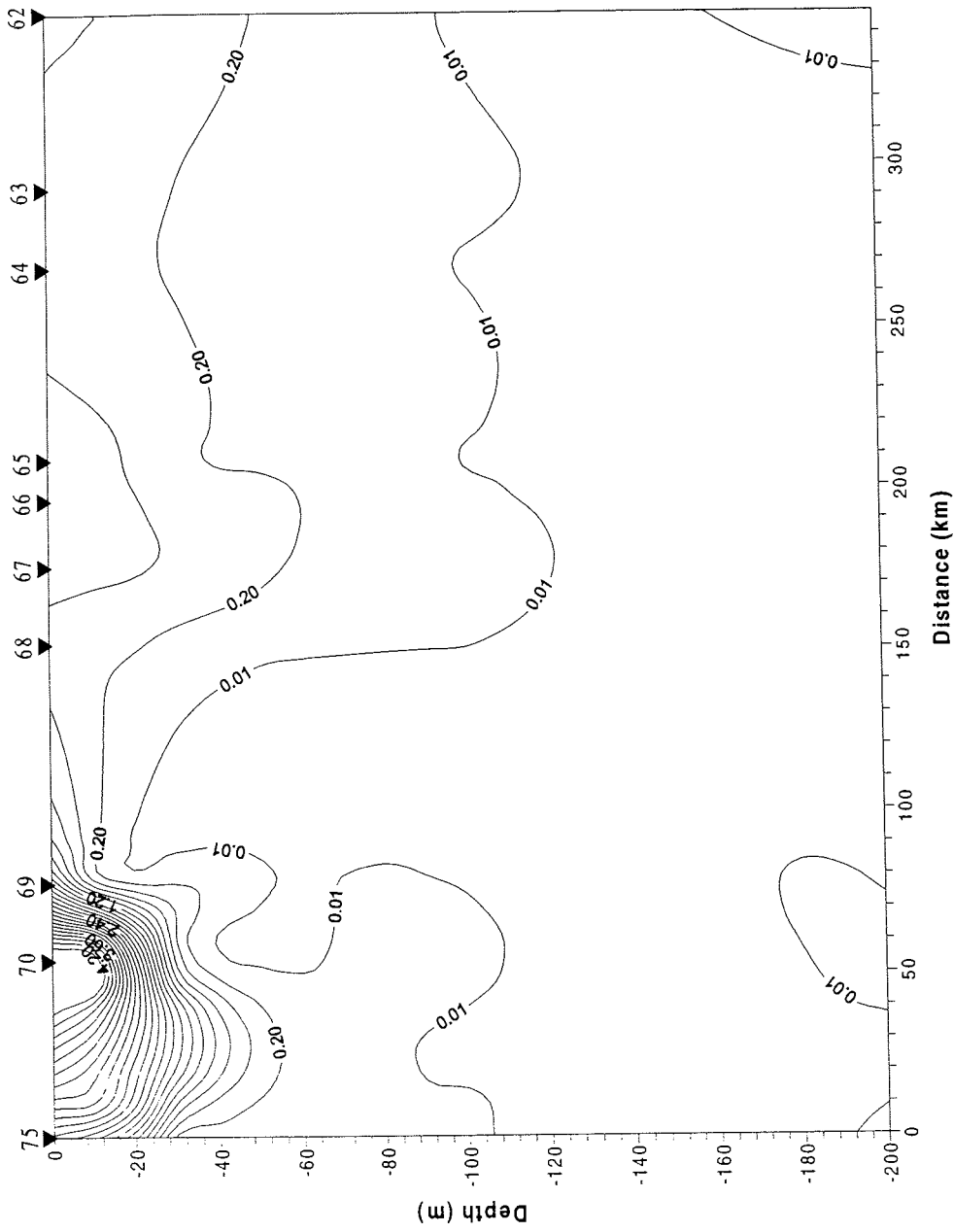


Fig. 5.6: Chlorophyll a concentrations along transect B (Yermak Plateau - Shelf of Greenland).

5.2.2 Algae in Melt Pools (Y. B. Okolodkov)

In the Arctic, melt pools may cover 50-60% of the sea ice (Horner et al., 1992). First studies on the biota inhabiting pools were carried out by Nansen (1906) who found a variety of diatoms and ciliates there and hypothesised about the origin of them in the pools. Data on the Arctic melt pool ecosystem are scarce and limited to the eastern Chukchi Sea and the northern Barents and Greenland Seas (Bursa, 1963; Okolodkov, 1997). More detailed data on the melt pool ecosystem were obtained in the area of the East Greenland Current between 71°N and 82°N in the summers of 1993 and 1994 during "Polarstern" cruises. To learn more about the algal species composition and viability of algae in melt pools was one of the aims of the facultative programme of studies on melt pools during the ARK-XIII/2 cruise.

Twelve melt pools on the pack ice were studied for the species composition of unicellular algae and heterotrophic flagellates. All melt pools represented freshwater ponds. Samples of bottom water and bottom ice were quantitatively investigated. In some pools, lumps of white or grey colour were collected from the holes up to 2 cm in diameter in the bottom ice. The lumps were composed of primarily marine planktonic and ice-associated species. The diatoms found could not be proved viable, although some of them still contained the cell content residues and probably contributed to the total chlorophyll a concentration.

The total number of algal cells varied from 10^2 to 1.7×10^5 cells per litre of bottom water or melt bottom ice (cells/l). The most diverse flora was found in bottom ice of melt pool 3 (station 66) on July 13, located on a two-meter thick ice floe. Three freshwater chlorophyte species were found, *Chlamydomonas* cf. *nivalis* reaching concentration of 9.9×10^4 cells/l and another abundant species - 6.3×10^4 cells/l. In the bottom ice of melt pool 8 (station 83) the concentration of *C. cf. nivalis* reached 2.8×10^4 cells/l, while it was completely absent in the bottom water. The total number of cells in the bottom ice exceeded that in the bottom water by a factor of 59. In melt pool 10 (station 93), on July 30, the concentration of *C. cf. nivalis* reached 4.0×10^3 cells/l in bottom water and 7.4×10^3 cells/l in bottom ice. Apart from chlorophytes, two peculiar dinoflagellate species were found. One of them was also observed in the surface water among ice floes at stations 79 and 90 with salinity being 18.4 and 13.5, respectively. Dinoflagellate cysts morphologically similar to those described by Meunier (1910) from the eastern Barents Sea and the western Kara Sea under the name *Echinus minus*, were observed in melt pool 9 (station 90), their concentration being 1.1×10^4 cells/l. Epifluorescence technique did not confirm the presence of chlorophyll inside the cells (in fresh samples taken from the water column the cysts clearly contained chlorophyll). Apart from these, the resting cysts of the chrysophyte *Dinobryon faculiferum* were found in some melt pools.

Usually, the concentration of living algae was essentially higher in the bottom ice compared with the bottom water in the same pool. Also, heterotrophic zooflagellates provisionally referred to the class Kinetoplastidea were common. In some melt pools amoeboids were observed.

Thus, melt pools on Arctic ice can be prevailed by autotrophic or heterotrophic unicellular flagellates in summer. For diatoms originated from sea water, melt pools form "grave-yards", where their remainders are an abundant food for heterotrophic organisms.

5.2.3 Phytoplankton: Studies on the Biodiversity, Taxonomy, Community Comparison and Biogeography (Y. B. Okolodkov)

Despite of the detailed studies on phytoplankton ecology in Fram Strait and its vicinity, information on the diversity of algae in the water column is still fragmentary. During many dozens of years, the Arctic, especially its ice-covered areas, have been considered as the realm of diatoms. In polar regions, athecate or naked dinoflagellates have been a neglected group of planktonic organisms until recently. More detailed studies on the dinoflagellate diversity in the European Arctic were carried out at the beginning of the century (Meunier, 1910; Wulff, 1919). During the last years it was shown for the southern Norwegian Sea and the northern Barents Sea that at least in summer the number of dinoflagellate species can exceed that of diatoms (Okolodkov, 1993, 1997). Dinoflagellates are more diverse and more abundant in the tropical seas. About 1400 to 1800 dinoflagellate species constitute marine phytoplankton in the world ocean (Sournia et al., 1991). Some 250 dinoflagellates have been recorded in the Arctic (Okolodkov and Dodge, 1996). Several new athecate dinoflagellate species were described recently from the European Arctic seas (Okolodkov, 1997). The data obtained from the northern Barents Sea in July-August 1996 allow us to conclude that there are dozens of naked dinoflagellate species undescribed yet. One of the main purposes of phytoplankton studies during the ARK-XIII/2 cruise on board RV "Polarstern" was to study the species composition of planktonic algae with special emphasis on dinoflagellates.

Material and Methods

For taxonomical studies, phytoplankton was sampled at 34 stations from June 27 to August 4, 1997. Usually, at every station a hand net, mouth 17 cm, mesh size 20 μm , was towed from the depth of 30 m to the surface. In addition, 3 to 8 l of surface water taken with a plastic bucket were filtered through a 1 μm pore size Nuclepore filter using a reverse-filtration device. In total, 61 samples were collected by the hand net (34 samples) and the bucket (27 samples). Concentrated material was examined under the inverted microscope Axiovert 135, Carl Zeiss. 5/0.15, 20/0.50, 40/0.75 and 100/1.30 (immersion oil) Plan-Neofluar objectives and a condenser, numerical aperture 0.55, were used. A wide range of light microscopy methods was applied, including bright and dark field illumination, phase and interference contrast as well as epifluorescence when studying the living algae. Algae were measured and identified mostly to the species level. About 110 drawings of some 60 dinoflagellate species were made. Approximately 1400 pictures of phytoplankton species, mostly naked dinoflagellates, were made using camera Contax 167MT, Kyocera Corp., Japan.

Results and Discussion

Biodiversity and Taxonomy

A list of algal taxa found during the cruise is given in Table 5.3. In average, from 40 to 60 algal species were distinguished at every station. Very often, the number of dinoflagellate species exceeded that of diatoms due to athecate dinoflagellates. At some stations, e.g. at station 92, among densely located ice floes, the number of dinoflagellate species in the water column exceeded that of diatoms by the factor of 2; the total number of algal species reaching 70. High diversity of dinoflagellates was due to athecate species. Moreover, at some stations such as station 92, naked dinoflagellates clearly dominated in biomass, at least in the surface layer. The highest biodiversity of planktonic algae was observed at station 100 where more than 100 species were distinguished. Dinoflagellates contributed 56 species, which is likely related to Atlantic waters. A number of new, undescribed species were examined in detail. Descriptions of new athecate dinoflagellate species accompanied with drawings and photographs will be published elsewhere, together with the data obtained during the cruises on board RV "Oceania" and "Lance" in July-August 1996 to the ice-edge zone east of Svalbard and to Kongsfjorden, the western coast of Spitsbergen. Detailed morphological data for a presumably new species of thecate dinoflagellates of the genus *Protoperidinium* were obtained. The species has been previously known from the marginal ice zone (MIZ) of the Barents Sea (cruises of RV "Lance" in 1995 and 1996). Thus, the subsidiary role of dinoflagellates in relation to diatoms in the high Arctic seas should be reconsidered.

The taxonomy of other flagellate groups except dinoflagellates in the Arctic has been more poorly investigated so far. One should note that the species found belong to different classes of algae (cryptophytes, chrysophytes, dictyochophyceans, prymnesiophytes, euglenophytes, chlorophytes, and prasinophytes).

A few types of cysts of dinoflagellates and chrysophytes were found, and their morphology was examined using the light microscopy. A peculiar heterotrophic flagellate was found, which combines the morphological features of dinoflagellates (dinocaryon and sulcus) and euglenophytes (spirally striated covering similar to a pellicule). Its morphology and swimming behaviour were examined. It has been previously recorded from the NE Atlantic, with the use of the scanning electron microscopy in 1994. More thorough examination of literature is needed to be sure whether it is a known species or a new genus or a higher rank taxon.

Distribution Patterns, Dominances, and Biogeography

A peculiar community was found near station 79 during a helicopter flight. In the surface layer with a salinity of 18.4, the community consisted of typically marine and freshwater species. The latter appears to originate from melt pools on ice floes. Apart from the chlorophytes of the order Volvocales, a few athecate dinoflagellate species characteristic of freshwater melt ponds were observed. The community under discussion can represent an inoculum transported to other areas with ice floes, since it contained different kinds of resting unidentified cysts.

Table 5.3: List of algal taxa found in the northern Barents and Greenland Seas and Fram Strait in water column, sub-ice assemblages and melt pools during the "Polarstern" ARK-XIII/2 cruise in June 27 - August 04, 1997.

Dinoflagellata:

Actiniscus pentasterias (Ehrenberg) Ehrenberg, internal skeleton
Alexandrium ostenfeldii (Paulsen) Balech et Tangen
A. tamarense (?), theca
Amoebophrya sp. (endoparasite in *Gyrodinium lachryma*)
Amphidinium cf. *herdmanae* Kofoid et Swezy
A. sphenoides Wulff
Amphidinium sp. 1
Amphidinium sp. 2
Amylax triacantha (Jørgensen) Sournia
Ceratium arcticum (Ehrenberg) Cleve var. *arcticum*
C. fusus (Ehrenberg) Dujardin var. *fusum*
Cochlodinium cf. *brandtii* Wulff
C. helicoides Lebour
C. cf. helix (Pouchet) Lemmermann
C. cf. pupa Lebour
Dinophysis acuminata Claparède et Lachmann
D. norvegica Claparède et Lachmann
D. pulchella (Lebour) Balech
D. rotundata Claparède et Lachmann
Echinum majus Meunier (a dinoflagellate cyst)
E. minus Meunier (a dinoflagellate cyst)
Gonyaulax spinifera (Claparède et Lachmann) Diesing
Gymnodinium abbreviatum Kofoid et Swezy
G. cf. arcticum Wulff
G. elongatum Hope
G. endofasciculum Campbell
G. gracile Bergh
G. cf. groenlandicum
G. ostenfeldii Schiller
G. cf. wulffii Schiller
Gymnodinium spp.
Gyrodinium cf. *aureolum* Hulburt
G. cf. crassum (Pouchet) Kofoid et Swezy
G. cf. fusus (Meunier) Kofoid et Swezy
G. cf. lachryma (Meunier) Kofoid et Swezy
G. cf. nasutum (Wulff) Schiller
G. cf. pellucidum (Wulff) Schiller
G. cf. rubrum Kofoid et Swezy
G. spirale (Bergh) Kofoid et Swezy
Gyrodinium spp.
Heterocapsa rotundata (Lohmann) Hansen
Heterocapsa sp.(?)
Katodinium glaucum (Lebour) Loeblich III
Katodinium sp.
Micracanthodinium claytonii (Lohmann) Deflandre, with and without spines
Oxytoxum sp.

Table 5.3, cont.

Pentapharsodinium dalei Indelicato et Loeblich III
Peridiniella catenata (Levander) Balech
P. danica (Paulsen) Okolodkov et Dodge
Prorocentrum minimum (Pavillard) Schiller
Proterothropsis vigilans Marshall
Protoceratium reticulatum (Claparède et Lachmann) Bütschli
Protodinium sp. (?)
Proto-peridinium bipes (Paulsen) Balech
P. brevipes (Paulsen) Balech
P. cf. cerasus (Paulsen) Balech
P. conicoides (Paulsen) Balech
P. depressum (Bailey) Balech
P. cf. islandicum (Paulsen) Balech
P. cf. mite (Pavillard) Balech
P. cf. ovatum Pouchet
P. pallidum (Ostenfeld) Balech
P. pellucidum Bergh
P. cf. pyriforme (Paulsen) Balech subsp. *pyriforme*
P. cf. steinii (Jørgensen) Balech
Proto-peridinium sp.
Scrippsiella trochoidea (Stein) Steidinger et Balech
Torodinium robustum Kofoid et Swezy

Bacillariophyta:

Actinoptychus senarius (Ehrenberg) Ehrenberg
Attheya septentrionalis (Østrup) Crawford in Crawford et al.
Bacterosira bathyomphala (Cleve) Syvertsen et Hasle in Hasle et Syvertsen
 Centrales gen. sp. (*Stellarima* sp.?)
Chaetoceros atlanticus Cleve
C. borealis Bailey
C. concavicornis Mangin
C. convolutus Castracane var. *convolutus*
C. convolutus Castracane f. *trisetosum* Brunel
C. decipiens Cleve
C. debilis Cleve
C. fragilis Meunier
C. furcellatus Bailey
C. gracilis Schütt
C. socialis Lauder
C. teres Cleve
C. wighamii Brightwell
Corethron cryophilum Castracane
Coscinodiscus cf. *oculus-iridis* Ehrenberg
Cylindrotheca closterium (Ehrenberg) Reimann et Lewin
Dactyliosolen fragilissimus (Bergon) Hasle
Diploneis litoralis (Donkin) Cleve
Entomoneis kjellmanii (Cleve) Poulin et Cardinal
E. kryophila (Cleve) Okolodkov
E. paludosa (W. Smith) Reimann var. *hyperborea* (Grunow) Poulin et Cardinal

Table 5.3, cont.

Eucampia groenlandica Cleve
Fossula arctica Hasle, Syvertsen et von Quillfeldt
Fragilariopsis cylindrus (Grunow) Krieger in Helmcke et Krieger
F. oceanica (Cleve) Hasle
Hantzschia weyprechtii Grunow in Cleve et Grunow
Haslea crucigeroides (Hustedt) Simonsen
H. cf. kjellmanii (Cleve) Simonsen
Melosira arctica (Ehrenberg) Dickie
Navicula directa (W. Smith) Ralfs in Pritchard var. *directa*
N. kariana Grunow in Cleve et Grunow
N. cf. novadeciapiens Hustedt
N. pelagica Cleve
N. septentrionalis (Grunow) Gran
N. cf. transitans Cleve
N. cf. trigonocephala Cleve
N. valida Cleve et Grunow
N. vanhoeffenii Gran
Nitzschia angulatrix W. Smith
N. cf. granii Hasle
N. frigida Grunow in Cleve et Grunow
N. laevissima (Grunow) Grunow
N. promare Medlin in Medlin et Hasle
Pinnularia quadratarea (Schmidt) Cleve
Plagiotropis sp.
Pleurosigma cf. clevei Grunow in Cleve et Grunow
P. cf. stuxbergii Cleve et Grunow
Porosira glacialis (Grunow) Jörgensen
Proboscia alata (Brightwell) Sundström
Pseudogomphonema arcticum (Grunow ex van Heurck) Medlin
P. groenlandicum (Østrup) Medlin
Pseudo-nitzschia cf. delicatissima (Cleve) Heiden in Heiden et Kolbe
P. seriata (Cleve) H. Peragallo in H. et M. Peragallo
Rhizosolenia borealis Sundström
R. hebetata Bailey f. *hebetata*
R. hebetata Bailey f. *semispina* (Hensen) Gran
Stenoneis cf. inconspicua (Gregory) Cleve
Synedropsis hyperborea (Grunow) Hasle, Medlin et Syvertsen
Thalassiosira antarctica Comber
T. bioculata (Grunow) Ostenfeld
T. gravida Cleve
T. nordenskioeldii Cleve
Thalassiosira sp.
Thalassiothrix longissima Cleve et Grunow in Cleve et Möller

Table 5.3, cont.

Chromophyta:

Cryptophyceae:

Cryptomonas sp.

Chrysophyceae:

Dinobryon balticum (Schütt) Lemmermann

D. belgica Meunier

D. faculiferum (Willén) Willén, with resting cysts

Meringosphaera mediterranea Lohmann

Pseudokephyrion sp.

Dictyochophyceae:

Dictyocha speculum Ehrenberg

Prymnesiophyceae:

Emiliana huxleyi (Lohmann) Hay et Mohler in Hay et al.

Phaeocystis pouchetii (Hariot) Lagerheim

Chlorophyta:

Euglenophyceae:

Euglenophyceae gen. sp.

Prasinophyceae:

Pterosperma sp.

Pyramimonas spp.

Chlorophyceae:

Chlamydomonas sp.

Choanoflagellidea (zooflagellates):

Bicosta minor (Reynolds) Leadbeater

B. spinifera (Thronsen) Leadbeater

Calliacantha longicaudata (Leadbeater) Leadbeater

C. natans (Grøntved) Leadbeater

Parvicorbicula socialis (Meunier) Deflandre

Unicellular organisms of uncertain taxonomic position:

Leucocryptos marina (Braarud) Butcher

Green globules (chlorophycean akinetes?)

Flagellates unidentified

Another peculiarity is the absence of large-sized naked dinoflagellates such as *Gyrodinium spirale*, *G. rubrum*, *Gymnodinium endofasciculum*, *G. gracile* and *G. abbreviatum* in the northern ice-covered areas.

Epifluorescence method allowed us to study about 50 dinoflagellate species and to discriminate between autotrophic and heterotrophic dinoflagellates.

Among loricate chrysophytes, the presence of two closely related, but morphologically different species, *Dinobryon balticum* and *D. belgicum*, was confirmed. For *D. faculiferum*, the formation of resting spores was recorded.

New findings of biogeographical value were made. An athecate dinoflagellate *Proterytropsis vigilans* is firstly recorded for the Eurasian Arctic. Many planktonic species are recorded for the study area for the first time.

The relative abundances, numerically dominant and subdominant species were determined at every station. During the cruise, three "bloom" events were recorded: (1) at station 42 in the MIZ of the northern Barents Sea; (2) at stations 70, 72, 73 and 75 in the "polynya", NE of Greenland; (3) at stations 94, 96 and 99 in the MIZ between the Yermak Plateau and Spitsbergen. The species composition as a whole as well as the composition of dominant and subdominant species varied with place. In the Barents Sea, *Thalassiosira gravida*, *Phaeocystis pouchetii*, *Fragilariopsis oceanica* and *Dinobryon balticum* were most abundant. In the "polynya" near the Greenland coast, *Chaetoceros socialis* prevailed, *F. oceanica*, *Chaetoceros wighamii* and *Thalassiosira* cf. *antarctica* being subdominant. In the MIZ, north of Spitsbergen, *P. pouchetii* and *D. balticum* dominated, *C. socialis* and *C. fragilis* being subdominant at station 99. All three events were likely spring phytoplankton "blooms" related to the MIZ.

Phytoplankton was sampled at different stages of seasonal succession. The presumably earlier stage was observed near Greenland where short chains of *C. socialis* not united to bush-like colonies and young colonies of *P. pouchetii* were found. In the other two cases, primarily old colonies of *P. pouchetii* and *D. balticum* characteristic of more advanced stages of seasonal succession were encountered.

In other cases, various algal species were recorded as dominant: *Thalassiosira bioculata* (stations 63, 64, 65 and 68), *T. antarctica* and *T. nordenskioldii* (stations 47, 57 and 58), *Fragilariopsis oceanica* (stations 47, 50, 52, 54, 57, 58 and 65), *Pseudo-nitzschia* cf. *delicatissima* (stations 68, 77, 79 and 82), *Chaetoceros gracilis* (station 84), *C. convolutus* (station 59), *Gymnodinium* species (stations 88, 91 and 92), *Dinobryon balticum* (station 90), and a flagellate autotrophic alga of uncertain taxonomic position (station 93). Some other species were recorded as subdominant: *Dictyocha speculum* (stations 47 and 64) and *Nitzschia frigida* (stations 50 and 54). More comprehensive information on the species composition of planktonic algae is available from stations 39, 42, 47, 50, 52, 54, 57-59, 61, 63-65, 68, 70, 72, 73, 75, 77, 79, 82, 84, 87-94, 96, 99 and 100.

5.3 Zooplankton Ecology

5.3.1 Distribution of Mesozooplankton

(K. Kosobokova, H. Auel, S. Lischka)

During the expedition ARK-XIII/2 the regional and vertical distribution of mesozooplankton was studied in the waters off the Svalbard archipelago. Multiple opening/closing net samples (Multinet, mesh size 150µm; Hydro-Bios Kiel) were collected at 25 stations along three transects in the Barents Sea, across the Yermak Plateau and onto the East Greenland Shelf. Three to five standard water layers (0-25, 25-50, 50-100, 100-200, 200 m-bottom) were sampled on the Barents Sea shelf (transect A) depending on the water depths. At the deep stations on the Yermak Plateau and the East Greenland Shelf (transects B and C) two successive vertical casts of the Multinet were taken from the bottom and 300 m to the surface. In the Barents Sea sampling was repeated at the same stations as during the first cruise leg ARK-XIII/1a, so that the seasonal succession from early spring (May) to summer (July) could be investigated. This is also a contribution to the AOSGE-project.

The investigations focused on the influence of different water masses on the zooplankton distribution. Especially the Barents Sea and Fram Strait are characterised by the inflow of relatively warm Atlantic water masses into the Arctic Ocean. Therefore boreal species of Atlantic origin (e.g. *Calanus finmarchicus*, *Pareuchaeta norvegica*) are abundant in those regions. In contrast, the zooplankton community on the East Greenland continental slope was poor and dominated by polar species (e.g. *Calanus glacialis*, *Pareuchaeta glacialis*). The analyses of the collected samples will be continued at AWI (Bremerhaven), IORAS (Moscow) and IPO (Kiel).

5.3.2 Egg Production in Pelagic Copepods

(K. Kosobokova, S. Lischka)

Copepod egg production is a valuable measure of the availability of food. Accordingly, our studies will contribute to the joint work on the intensity of pelagic coupling, again a contribution to the AOSGE-project.

Material and Methods

Copepods for egg production experiments were collected by bongo net (mesh size 200 and 310 µm) from the entire water column at the stations with depths less than 1500 m, and from the 0-1500 m water layer at the deeper stations. On the transect A in the Barents Sea egg production experiments were carried out with *Calanus glacialis*, *Metridia longa* and *Pseudocalanus minutus*.

To measure the average egg production rates in the first two species experiments were carried out on groups of 25-30 females. The females were sorted out from the bongo catches immediately after capture and placed in 200 ml plexiglas insets having false bottoms of mesh (300 - 500 µm) to separate eggs from females. These were then suspended in 250 ml TPX jars containing filtered sea water. Average egg production during the first 24 hours

was used as a measure of the actual rate in the field (*in-situ* egg production rate).

To measure the individual clutch size and intervals between subsequent spawning events, experiments were carried out on single females of the same species 30 individual females of *C. glacialis* and 5-20 *M. longa* females from each station were kept in microbiological cell wells in filtered sea water for 5-6 days. They were checked once per day, eggs were counted and faecal pellets were removed. From 9 to 24 individual females of *P. minutus* were also kept in microbiological cell wells filled with filtered sea water. The females were observed daily for egg production, size of the clutches, for time of nauplii hatching and intervals between subsequent spawning events. The longest observation time was 36 days. Individuals were fed regularly with phytoplankton or cultures of ice algae. Egg production experiments with *M. longa* and *P. minutus* were also carried out at several stations of the transects B and C, whenever these copepods were present in the plankton.

The effect of starvation on egg laying was studied on groups and individual females of *C. glacialis* and *M. longa* during 5-6 days. At the deep stations (depths more than 500 m) adult females of meso- and bathypelagic copepods were sorted out from the bongo catches immediately after capture and checked for the states of gonad maturity. Ripe females were cultivated in cell wells with filtered sea water as long as possible. They were fed with small copepods and phytoplankton only in small amounts. In total, females of 13 copepod species were observed (*Gaetanus tenuispinus*, *G. brevispinus*, *Heterorhabdus norvegicus*, *Chiridius obtusifrons*, *Aetideopsis rostrata*, *A. multiserrata*, *Scaphocalanus magnus*, *Augaptilus glacialis*, *Spinocalanus longispinus*, *Tharybis groenlandicus*, *Pareuchaeta norvegica*, *P. glacialis* and *P. barbata*) to estimate the individual clutch size, spawning intervals, and nauplii hatching time. All egg production experiments were carried out in a cooled room at temperature of 0°C.

Preliminary Results

Calanus glacialis dominated zooplankton biomass at almost all stations along transect A except station 39. Up to 97% of *C. glacialis* females at stations 42-55 were in ripe condition. Average egg production rates ranged between 50-68 eggs/female*day in ice-free areas and 26-40 eggs/ female*day in the ice-covered area (Fig. 5.7). *C. glacialis* females produced clutches with rather regular 2-days intervals. Individual clutch size ranged between 6 and 157 eggs per female, however most females produced clutches with more than 50 eggs (Fig. 5.8). The high values of the *in-situ* egg production rate, overwhelming domination of ripe females and large individual clutch sizes indicated high reproductive activity of the *C. glacialis* population in the northwestern Barents Sea during the period of our investigations.

Under starvation conditions the egg-laying in *C. glacialis* ceased after 3-4 days. The number of egg-laying females decreased dramatically by the 3rd day of starvation (Fig. 5.9). This kind of response to starvation conditions indicates that spawning in *C. glacialis* was strongly related to the phytoplankton availability during the studied period.

M. longa showed very low spawning activity on the Barents Sea shelf in the beginning of July. Most females had unripe gonads and did not produce eggs. Three weeks later in the area of the Yermak Plateau the percentage of mature *M. longa* females had increased indicating the later beginning of the reproductive season in this species compared to *C. glacialis*. Individual *M. longa* females produced 23-88 eggs per spawning event.

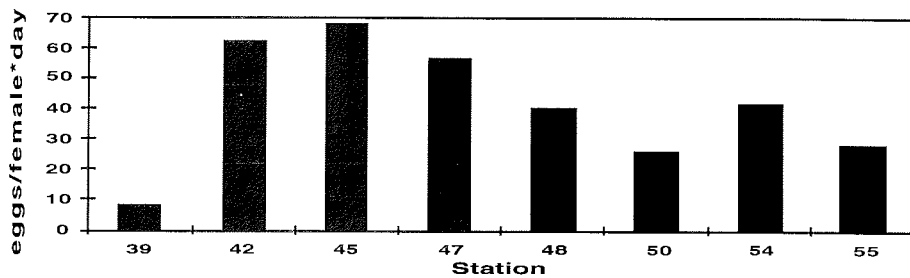


Fig. 5.7: Average egg production rate of *Calanus glacialis* in the Barents Sea

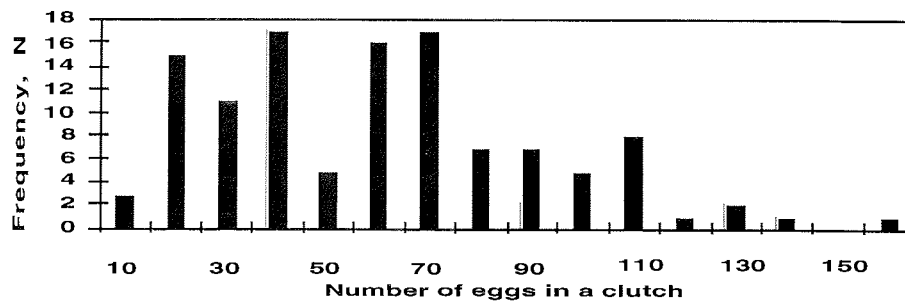


Fig. 5.8: Individual clutch size of *Calanus glacialis*

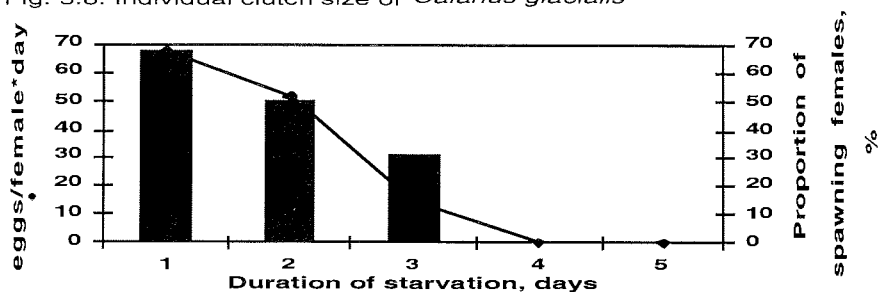


Fig. 5.9: Average egg production rate of *Calanus glacialis* under starvation conditions (bars) and proportion of egg-laying females (line)

Pseudocalanus minutus showed rather high spawning activity with an average of 58% egg-producing females after 12 days of observation time (Fig. 5.10). However, most active spawning was observed at stations in the Barents Sea where up to 94% of the females laid eggs. This was probably due to very good feeding conditions. The average egg number per clutch was 11, ranging from one single egg up to 39 (Fig. 5.11). Nauplii appeared after 9 to 10 days from egg production. *P. minutus* females also produced subsequent clutches after hatching of the nauplii, but the intervals between these clutches were very different for individuals.

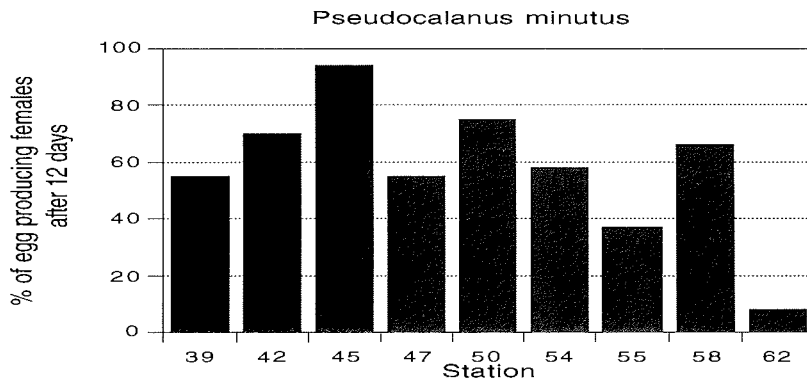


Fig. 5.10: Proportion of spawning *Pseudocalanus minutus* females

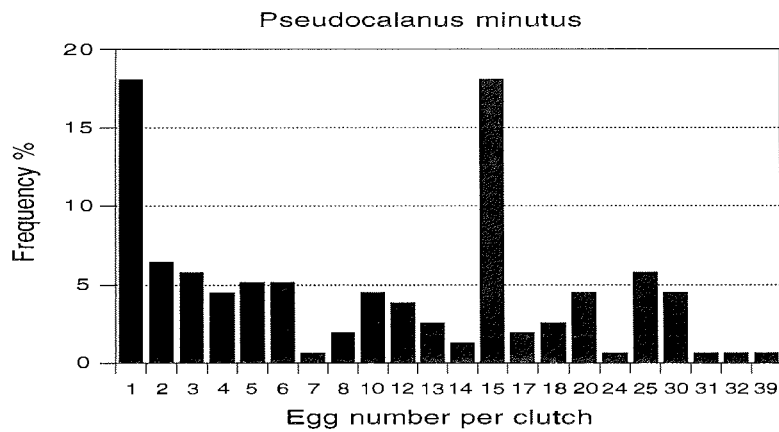


Fig. 5.11: Individual clutch size of *Pseudocalanus minutus* females

5.3.3 Ecology of Meso- and Bathypelagic Copepods in the Arctic Ocean (H. Auel)

Introduction

As a part of the international AOSGE project the distribution and the life cycles of mesozooplankton organisms were studied. The investigations concentrated on the spatial and ecological niches of meso- and bathypelagic copepods, whose adaptations and life strategies are still unknown. In addition, the feeding behaviour of these mainly omnivorous and carnivorous species and their effect on the carbon and energy flux from the epipelagic to the benthic realm were studied (kryo-pelago-benthic coupling).

Material and Methods

Abundance and vertical distribution of meso- and bathypelagic copepods of the families Euchaetidae and Aetideidae were studied by multinet casts on two transects from Fram Strait onto the East Greenland Shelf and from the southern Nansen Basin onto the western Yermak Plateau, respectively.

Additionally, individuals for experiments and biochemical analyses were collected at 24 stations with a bongonet (200, 310 μm). The organisms were identified to species level and sorted according to developmental stage, gonad maturity and body size. The samples were immediately frozen at -80°C . A total of more than 1000 samples was collected, including ctenophores, pteropods, copepods, euphausiids, decapods, and amphipods.

To investigate the feeding behaviour and energy demand of deep-sea copepods feeding and starvation experiments were conducted in a cooling container on board. These studies will be supported by biochemical analyses (lipid content and composition) and respiration measurements at IPO.

Preliminary Results

Altogether, 11 copepod species of the two bathypelagic families Euchaetidae and Aetideidae were identified. Closely related species inhabit different depth strata, to avoid interspecific competition. The carnivorous copepods, *Pareuchaeta norvegica* and *P. glacialis* ranged from the surface to 500 m depth. Below 500 m *Pareuchaeta barbata* and *P. polaris* were more abundant. *Chiridius obtusifrons* and *Gaetanus brevispinus* were the dominant aetideid copepods in polar regions, whereas *Gaetanus tenuispinus* and *Aetideopsis multiserrata* dominated in areas with stronger Atlantic influence. The bathypelagic realm below 1000 m was characterised by a different copepod community, including *Aetideopsis rostrata*, *Chiridiella reducta* and *Pseudochirella spectabilis*.

5.3.4 Meroplankton: Sampling of Zoobenthos Larval Plankton (E. Rachor)

Many macro-zoobenthos species have pelagic larvae (meroplankton), the occurrences and developmental success of which are triggered by seasonal influences like light intensity (and day length), water temperature (water masses, currents) or/and food availability. The occurrence of larvae is also regarded as indicator of the seasonal (nutritional) state of the parent benthos population. Our knowledge about the appearance of such larvae and the duration of the pelagic phase in Arctic waters is very poor. Within the research field of coupling processes between the pelagial and benthic, fine mesh plankton was therefore collected for detailed analyses of larvae occurrences.

For this purpose, an Apstein handnet with 20 μm meshes was used for surface (0-20m) water sampling at the stations 39, 47, 50, 52, 57, 58, 61 and 99 in shallow waters around Svalbard (thanks are due to Yuri Okolodkov). Samples, stratified over the whole water column, were additionally obtained by a multinet with 63 μm meshes (stations 47, 52, 61, 99, thanks to H. Auel).

Moreover, the upper net hauls of the epibenthic sled at the stations 47 and 50 with meshes of 90 μm were taken in addition to study the near-bottom (hyperbenthic) occurrence of larvae.

These samples will be used for a comparison of larval plankton during ARK-XIII/1 in May-June with that of late June, especially along the Barents Sea transect. The repetition of multinet sampling at station 61 (i.e. 99) north off Spitsbergen will allow a comparison with larval occurrences even by the end of July.

In addition to the analyses of the plankton material, potentially parent animals obtained by trawling (Agassiz trawl) and grab sampling will be studied for their gonadal stage to find out whether larvae were advected or may have been spawned in the sampling area, indicating, thus, a possible food input triggering the benthos spawning.

5.4 Vertical Particle Flux (E. Bauerfeind, V. Shevchenko)

Knowledge about flux of biologically produced particles to depth and finally to the seafloor is rare in the Arctic. This holds true especially for particles that are produced in the ice, at the bottom of the ice and by ice-associated organisms. In order to gain better information about this ice-associated flux a set of 4 sediment traps (diameter 12 cm) was moored on ice floes at 4, 10, 20 and 40 meters beneath ice floes in areas of varying ice coverage. The duration of the deployment could be prolonged substantially by using helicopters for deployment as well as the recovery of the traps. Altogether 7 successful deployments (Table 5.3) were performed during the cruise. First macroscopic inspection of the samples revealed considerable flux rates at all depths, however with differences between the stations. Detailed information will be available after biochemical, chemical and microscopic analyses in the land-based laboratories.

A time series sediment trap (diameter of collecting funnel 0.5 m^2) was moored in cooperation with the geochemical working group at the beginning of the cruise (July 6, 1997) close to the ice edge at $80^{\circ}10.47'N/10^{\circ}24.48'E$ in a water depth of 523 m. The sediment trap was located 100 m above the seafloor and 60 m above a multisampler (see Chapter 8) that was incorporated in the same mooring. The sediment trap was programmed to sample in 48 h intervals, starting on July 07. The mooring was recovered successfully at August 3, and 13 samples were obtained. First visual inspection of the samples revealed an increase of the sedimentation at the end of July/beginning of August. During this period also a change in color of the sedimented particles was noticed which is indicative for the sedimentation of undegraded phytoplankton material. Besides the biochemical and microscopic examinations the flux of Thorium will also be analyzed in these samples after return to the laboratory.

Table 5.3: Dates and positions for deployment and recovery sediment traps moored at ice floes

Deployment				Recovery			
	Date	Time	Position	Date	Time	Position	Duration
SSF No. 1	05.07.97	01:20	81 06.00N 16 11.9E	06.07.97	00:16	81 96.8N/ 16 09.7 E	23 h
SSF No. 2	10.07.97	20:30	81 07.7N 05 34.1E	11.07.97	18:45	81 07.02N 06 03.99E	23 h
SSF No. 3	12.07.97	11:50	81 14.0N 02 24.7E	15.07.97	10:55	81 17.77N 04 58.13E	71 h
SSF No. 4	16.07.97	14:00	81 31.28N 06 48.74w	17.07.97	13:30	81 32.27N 07 09.3W	23.5
SSF No.5	19.07.97	14:00	82 17.52N 00 43.72W	21.07.97	13:30	82 16.28N 00 41.67W	47.5 h

5.5 Benthos

Introduction (E. Rachor)

Benthos comprises all organisms living at the surface of the sea floor as well as those dwelling in the sediments, sometimes even down to depths of one metre. As a boundary subsystem, the benthos is characterized by strong biological activities, which have to be understood before any predictions of transformation and burial processes of organic matter can be made.

A great variety of sampling gears were used during the cruise to investigate structural features of the benthos (from the large epifauna by imaging and trawl sampling to all kinds of "endo-organisms" - bacteria, micro-, meio- and macro-fauna - , mainly obtained by coring gears).

Measurements of biochemical activity rates and of sediment core oxygen uptake rates were performed in addition to evaluate the significance of benthic organisms for the transformation of directly sedimented or advected organic matter, and to build-up energy flow budgets for a selection of the investigated areas (e.g. across the marginal ice zones). Laboratory studies e.g. on behaviour, food uptake and substrate decomposition rates as well as oxygen uptake will be used to fill gaps of the research done already on board "Polarstern".

5.5.1 Epifauna/Megafauna

(H. Thiel, K. v. Juterzenka, M. Klages, F. Kulescha, B. Sablotny)

The size class of the megafauna is defined by its detectability on seafloor photographs. By this it is largely restricted to epifauna.

Imaging was achieved by an OFOS (Ocean Floor Observation System), equipped with an Osprey OE 1323 video camera, four floodlights with 400 W together, a still camera Benthos 372 A, carrying a 37 mm objective and a Benthos flash unit 383 Th with two flashlights of 400 Ws together.

The video black & white low level camera was used to control the OFOS above the seafloor. A weight, hanging down from the frame indicates optimal photographic distance and also serves as a comparative size indicator. The still camera was loaded with a Kodak Ektachrome 200 ASA film of 30 m length providing nearly 800 shots. The camera was triggered on command.

Usually, the OFOS is towed with a speed of 1 nm/h about 3 m above the seafloor, when this is expected to be rather flat. This method was applied outside the ice at two stations, however, with only 1 m distance from the seafloor to adjust to the other stations. The slack in the wire dampened the ship's movement to some extent, but it could not be avoided that OFOS hit the seafloor several times, creating a large plume.

In the ice towing of the OFOS was only possible on a single station, but the towing distance available was less than 0.5 nm. At all other 14 stations OFOS success relied on the drift of the ice, which was up to 0.5 nm/h. At several occasions the drift diminished during the OFOS employment, in one case even down to zero. The distances covered during the single stations varied due to these conditions. Because the flash had a minimum frequency of 4 seconds, single objects could be imaged twice. This would probably help in the identification of objects, e.g. of fish species, which are generally seen on the photographs from their back, making a determination to species level difficult or even impossible.

Preliminary results are based on the video images and short pieces of still photo film developed onboard for testing image quality. The material may be divided according to depth for all of the stations along transects B and D, except for stations on the Greenland slope (transect B) and in the Molloy Deep (5400 m), a separated station south of the working area.

Stations on transects B and D (cf. Fig. 2.2) fall into four groups:

A.) Station 64 (660 m) and station 88 (1420 m) although of different depths are characterized by large filter feeders like *Umbellula spec.*, Pennatulacea, Crinoidea and Actiniaria, and by Ophiuroidea and a few sea urchins on and partly buried in the sediment.

B.) Stations 62, 63, 65, 90 and 94 at 900 m to 1050 m depths show smaller Crinoidea, many Ophiuroidea of several species, some sea urchins of the species *Pourtalesia jeffreysi*, and a few burrows of a slender isopod.

C.) Stations 60, 67, 84, 92 and 93 at depths of 2040 - 2300 m are marked by many holes borrowed by isopods and tracks of *P. jeffreysi*, partly imaged in the process of sediment reworking, rather much burrowed in the head of their tracks. Ophiuroidea are also present.

D.) Stations 69 and 80 at 3200 m and 3800 m, respectively, exhibit very few specimens of small holothurians and a very distinctive animal track. The specimens crawl in the sediment, opening the sediment surface in long central cracks with some side branches, and then seem to surface (for feeding?) and produce long depressions branching off from a central line. No specimens were seen associated with these tracks.

The horizontal similarity between stations seems to correspond to the general observation that species and communities have a wide horizontal distribution along continental slopes, but their vertical distribution is limited. There was some subjective impression that stations on the western slope of the Yermak Plateau were somewhat richer in species abundance than on the eastern slope, compared within the same depth ranges. However, this imagination could not be verified by the video images and the few frames available so far.

Whereas all stations mentioned were characterized by a soft mud, the station on the steep, current swept Greenland slope, at depths between 560 m and 800 m, showed stones, gravel and sand. A few ophiuroids and regularly single specimens of an actinarian were observed.

Station 100 at 5400 m depth completed the OFOS deployments with a great surprise: Towing the OFOS along a transect of about 2.5 nm, it was realised that the seafloor was covered with a high density of loosely distributed small (about 4 cm long) holothurians. They gave the impression of a rather random distribution, however, this must be analysed later in detail. Additionally, large and small specimens occur in this population, a rare observation in the deep sea. A few developed still photos demonstrated the occurrence of amphipods, and only a careful analysis can divide them from the younger generation of the holothurians. This soft bottom habitat is now and then, on average every 90 m, interspersed by some hard substrate: a small piece of wood, a piece of iron (?) and somewhat consolidated clay (?). These hard(er) substrates were inhabited by loose aggregations of actinarians.

Additionally, still photography was applied within the Yermak Plateau area (water depth 830 to 2200 m) by means of an underwater photoprobe (Photosea 70). From the drifting ship, a series of 25 to 40 photographs was taken at 9 stations by subsequent lowerings of the system to trigger the camera at each bottom contact (for details of design and operation see Piepenburg & v.Juterzenka 1994). The photographs will be analyzed in the home lab with special emphasis on small scale distribution patterns of abundant epibenthic species and their activity patterns (locomotion, feeding modes). The results shall be compared with data obtained by the OFOS at the same stations.

A small isopod, caught at station 58 (water depth approx. 700 m) and transferred into a tank containing sediment, started to burrow after a while and produced a hole with a non-symmetric opening. This hole was similar to the holes observed by the OFOS at several stations. Large specimens of the

ophioroid *Ophiopleura borealis* produced characteristic traces in the tank sediment and on the seafloor.

Originally, the charter of a Remotely Operated Vehicle (ROV), was planned for this expedition, but finally it could not be realized. The OFOS had to be mobilized as a substitute. Earlier the question was discussed, whether a ROV would be a suitable system to be employed under Arctic ice conditions. The experience gathered during this expedition with the OFOS verifies the assumption that even under severe ice conditions the ROV would have been deployed with great success. Already without any drift the ROV would have excess to a circular area of about 2000 m². Additionally it must be realized that ROVs are equipped with more functions and abilities. The video images are displayed in colour and give more online information for better immediate use. The photographic system with zoom objectives allows close-up photos with more details. The ROV can collect samples for direct comparison with the images, and it may carry a number of other tools for measurements at the seafloor. As a general result of this cruise it must be stressed that a ROV can be used safely in the central Arctic Ocean and that new and fascinating results can be expected from its employment. Research on the seafloor and in the bottom-near water layer in the Arctic Ocean should be done regularly by employing a ROV. This equipment would be highly useful as well to help in the recovery of freefall systems under the ice.

Agassiz trawl (AGT) and epibenthic sled (EPS) were used in order to obtain samples and living specimens of selected species as well as information about the species composition of epibenthic communities. However, due to heavy sea-ice conditions prevailing in the area of investigation trawls were only used at 5 and 9 stations for AGT and EBS, respectively. After sampling with AGT a representative subsample of approx. 20 l was taken and sieved over 1 and 0,5 mm mesh size in order to describe the species composition.

The EBS consists of two net devices which are designed to sample epibenthic and suprabenthic organisms: a lower (epi-) net and an upper (supra-) net which is located 30 cm above the lower net case. Usually mesh sizes of 500 µm for the lower net and 300 µm for the upper net used (exception: stations 42 and 49 in the Barents Sea with a mesh size of 90 µm for the upper net). The EBS was used at four stations of transect A (Barents Sea; water depth 160 - 450m), one station of transect B (Barents Sea slope; 780 m), one station of transect D (Yermak Plateau; 1090 m) and the three stations at the slope north of Svalbard (1000 - 480 m).

In the Barents Sea and the adjacent slope (stations 42, 47, 49, 55, 58), epibenthic echinoderms caught by the EBS were dominated by the brittle stars *Ophiocten sericeum* and *Ophiacantha bidentata*. This finding correspond with the results of former studies in the Barents Sea (Anisimova, 1989; Piepenburg & Schmid, 1996). High abundances of peracarid crustaceans, pantopods and decapods, at least at certain locations, were obvious.

The catch obtained at the Yermak Plateau (station 90A) contained a few specimens of *Ophiocten* sp. At the slope north of Svalbard (stations 94, 96, 99), *Ophiocten sericeum* predominated at a water depth of 1000 m (station 94), whereas at 770 m (station 96) only a few specimens were found. AGT at this station showed a population of large *Ophiopleura borealis* which were not

caught with the epibenthic sled. At 500 m (station 99), a high abundance of small *Ophiura* sp. and ophiuroid juveniles were obvious.

Trawl catches were preserved in buffered formaline (final conc. 4%). Subsamples of abundant echinoderm species were taken from each trawl to identify size and age structure as well as seasonal growth patterns by means of size frequency as well as growth band analyses. These investigations will be carried out in the home lab and will be accompanied by stomach content analysis. Some specimens were frozen at -30°C to accompany epibenthos samples taken for stable isotope analysis in 1996. Living specimens of abundant echinoderm species were transferred to tanks and kept in a cooling container (see Chapter 5.6.7.)

The most abundant ophiuroid species in the area investigated are characterized by a planktic larval stage (*Ophioplutei*). After finishing metamorphosis in the water column, they are sinking down to the seafloor (postlarvae). To look for these early stages of development, the upper 0.5 cm of MUC cores (diameter 60 mm) were taken at stations 49, 58, 79, 87, 94, 96 and 99 and preserved in formaline (conz. 4%) for analysis (see also Chapter 5.3.4).

5.5.2 Macrofauna: Quantitative Assessment (E. Rachor, S. Denisenko)

Introduction

Macro-endofauna (infauna) including animals living on the sediment surface which are adequately sampled by grab and box samplers were quantitatively collected as a contribution to

- the description of structural features of benthic communities along the investigated transects (across the marginal ice zone, down the continental slopes and across the Yermak Plateau including the adjacent deep Fram Strait and Nansen Basin waters). These features include species composition, abundances and biomass, diversity and feeding types. The data will be used for building up energy flow budgets of the total benthos (see especially Chapter 5.5.6).
- the analysis of biogeographical distribution patterns, especially to compare the westernmost continental slope fauna of the Nansen Basin and of the Yermak Plateau with that of Siberian areas. Material obtained by EPS and AGT will also be included into the evaluations.
- the quasi-synoptic description of macrozoobenthos communities along a section from the Murman coast up to the continental slope of the northern Barents Sea. For this purpose, data of the Barents Sea transect will be combined with those of the first leg (ARK-XIII/1a, May 1997) and with data obtained south of this transect by the Murmansk RV "Dalnie Zelentsy" along the "Kola Section" (also during May).

Material and Methods

Samples were obtained from large box samplers (0.25 m²), including sub-sampling by inserted boxes of 1/44 m²; or from Van-Veen-grabs (0.1 m²); and from incubated multicorer tubes. They were sieved on 250µm meshes (upper

sediments layer, as a rule 0-2 cm) and on 500 μ m (layers deeper than 2 cm). As far as possible, sediments and fauna were gently brought into suspension before sieving, while the remaining parts were sieved with more water pressure. The material was preserved in sea water with 4 % formaldehyde, buffered with a saturated borax solution. The main evaluations will be done in the home lab.

The locations of the box and grab samples are indicated in the map (Fig. 5.12). Van-Veen-grabs were taken only along transect A (at 5 stations); giant box corers (GKG) were obtained at altogether 44 stations.

First Results

In total, quantitative samples were obtained at 49 stations. A part of the small box subsamples were pre-sorted and preliminarily analysed with respect to species richness (numbers of distinguishable taxa) and abundances. These analyses brought about several trends according to water depths, longer-term ice coverage and, as it seems, specific regional hydrological and sedimentological regimes. Some results of these analyses are summarised in Tables 5.4, 5.5, 5.6; and the trends along the southern (B) and northern (D) transects across the Yermak Plateau are depicted in Figures 5.13 and 5.14.

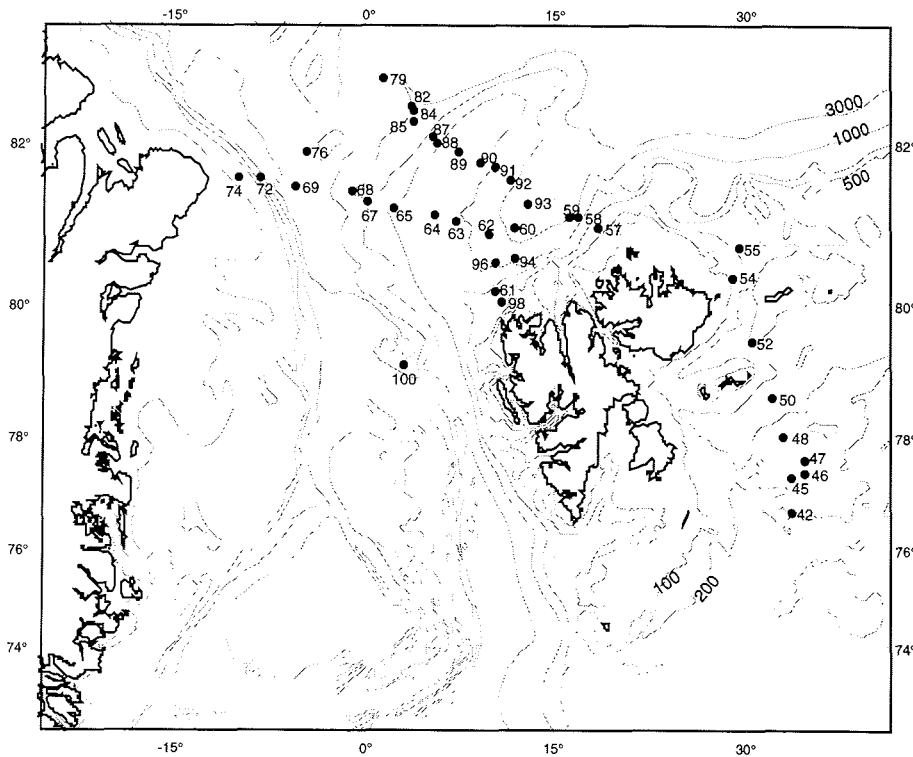


Fig. 5.12: Map of infauna sampling stations.

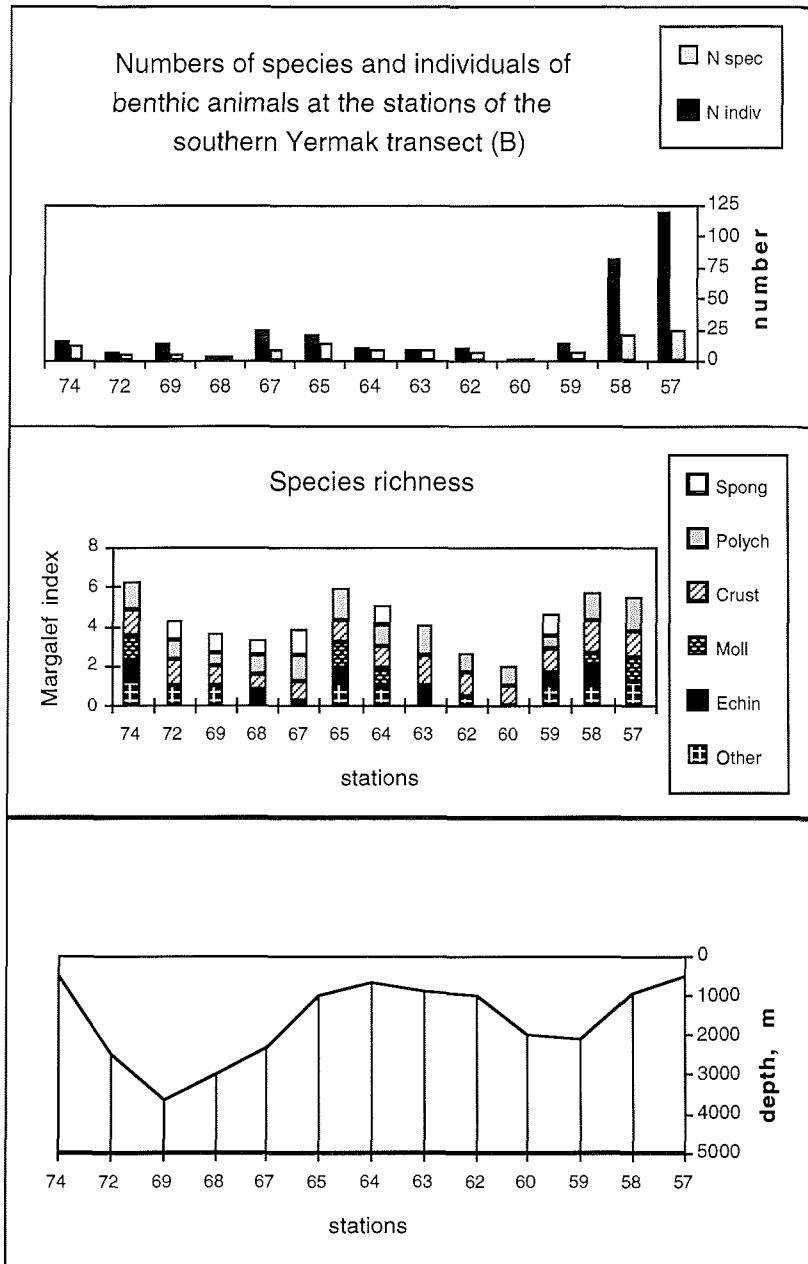


Fig. 5.13: Numbers of species and individuals, and species richness along the transect B.

For a preliminary analysis of species richness of macro-infauna Margalef indices (M) were calculated:

$$M = S / \log_2(N-1),$$

where S - total species number, N - total individual number.

They show that the most common taxonomic group on all stations, the Polychaeta, are, accordingly, the main contributors to species richness, irrespective of depth. Then the Crustacea follow, but they were practically not found at depths of more than 3000 m. Mollusca were collected only on elevations of the sea floor including the slopes, at depth less than 2000 m. Spongia and Echinodermata do not show distinct depth distribution patterns in their richness, while species seem to be distributed along depth belts down the continental slopes. Such a belt zonation pattern is well known from the literature and was depicted e.g. for the Laptev Sea in the 1995 „Polarstern“ cruise report (Rachor, 1997). The analyses of the samples from the slopes of the Yermak Plateau indicate a similar belt pattern there (see also 5.5.1).

Another well known distribution feature are the decreases in abundances and, accordingly, biomass with water depth increasing towards the deep sea plains. This general trend is well seen in Figures 5.13 and 5.14 (see also 5.5.3).

Since the Yermak Plateau area investigated is normally covered by pack ice during the whole year, species richness and abundances seem to be reduced there (e.g. when compared with the shelf slope stations north of Svalbard). Moreover, there are some indications in preliminary results that the western slope fauna of the plateau may be richer than that of the eastern slope (in the lee of the plateau), which may be explained by stronger Atlantic water advection (and food particle importation) along the western slope (see chapter 8).

Further analyses of samples have to be done to support or reject hypotheses about the possible reasons of macro-infauna distribution and richness/poverty patterns especially in the Yermak Plateau area.

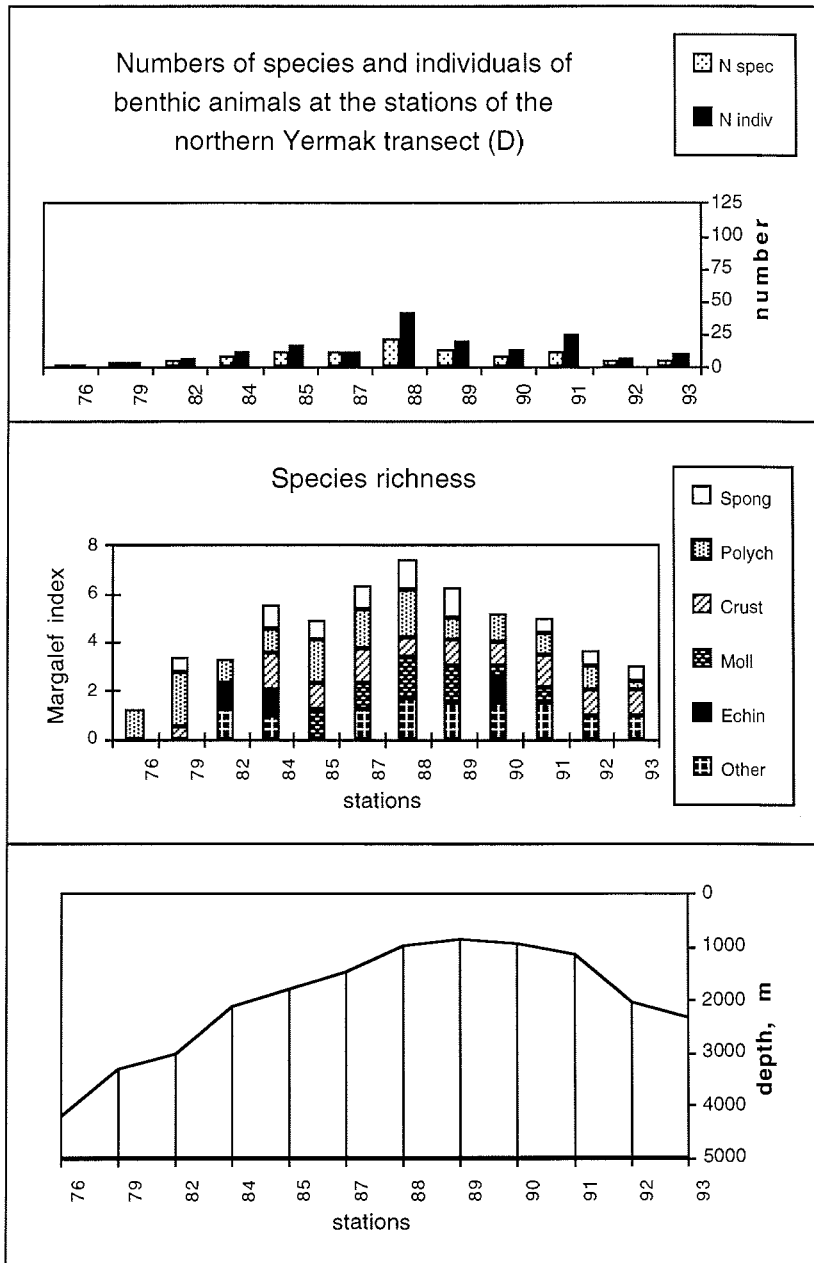


Fig. 5.14: Numbers of „species“ and individuals, and Margalef species richness along the transect D.

Table 5.6: Macrozoobenthos species and individual numbers along Barents Sea S-N-Transect ARK-XIII/2 (from infauna box samples, 1/44 m²).

Stat. No.	N. of Spitsbergen							
	4 2		4 7		5 2		9 6	
Water Depths (m)	150		212		325		794	
<i>Taxon</i>								
Spongia	0		1 1		0		0	
Cnidaria			0		0		0	
Nemertinea	1	2	1	1	1	1	0	
Nematoda (large)	1	1	0		0		0	
Sipunculida	0		0		0		1 3	
Echiurida	1	1	0		0		0	
Priapulida	0		0		0		1 1	
Polychaeta	12	32	3	7	13	75	10 61	
Pogonophora	0		0		0		1 1	
Mollusca								
Bivalvia	3	18	4	16	5	10	4 15	
Gastropoda	1	1	1	1	0		1 1	
Others	0		0		0		1 2	
Crustacea								
Amphipoda	5	5	1	1	2	2	3 6	
Isopoda	1	1	0		0		1 2	
Tanaidacea	0		0		1	1	1 1	
Cumacea	3	7	1	2	2	4	0	
Others	1	6	0		1	1	1 2	
Echinodermata	0		0		1	1	1 1	
Bryozoa	1	1	0		0		0	
Misc.	0		0		0		0	
Sum	30	74	12	29	26	95	26	96
	spp. ind.		spp. ind.		spp. ind.		spp. ind.	

5.5.3 Meiobenthos (V. O Mokievsky)

The term "meiobenthos" means small Metazoans belonging to the size class of 100 µm up to 1 mm. According to different authors, the lower limit of this group varies from 100 down to 50 or even 42 µm which leads to different results in quantitative estimates. From ecological point of view, meiobenthos consists of two main components - permanent meiobenthos (eumeiobenthos) which includes smallest Metazoa, and temporal, or pseudomeiobenthos, represented by juveniles and larvae of macrobenthic organisms. In terms of taxonomic composition, eumeiobenthos is a well recognizable set of high taxa, such as nematodes, harpacticoid copepods, ostracods and many others. The great role of this group in benthic ecological processes is undoubted, but

still is really unknown especially in the deep-sea realm. Only a few of quantitative data dispersed over the World Ocean are available till now. Much less is known about taxonomic composition and spatial structure of meiobenthic communities. In the deep seas of the High Arctic there are only data from the Ymer-80 expedition, which were collected north off Svalbard.

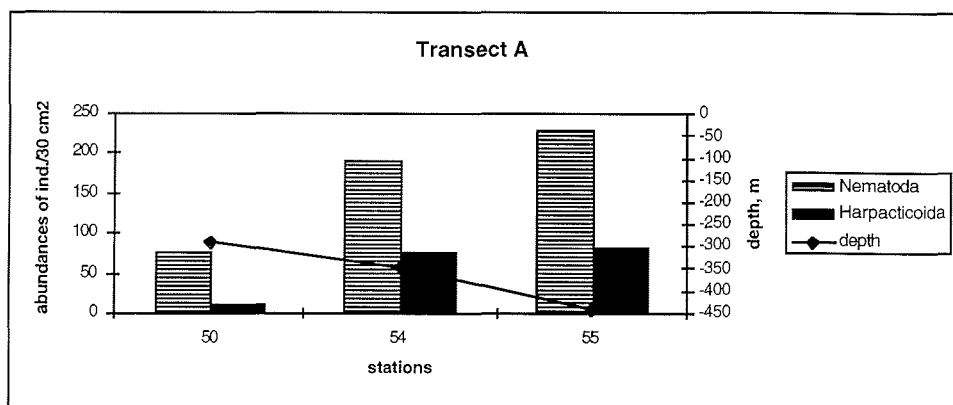


Fig. 5.15: Distribution of meiobenthos taxa on Spitsbergen shelf.

During the ARK-XIII/2 cruise quantitative meiobenthos samples were collected along two transects crossing the Yermak Plateau and a third one near the Spitsbergen Archipelago. Abundance of meiobenthos and its taxonomic composition were the main goals of this study. For these purposes, meiobenthos samples were collected on almost each benthic station using multicorer with tubes of 29.3 cm². The upper two centimeters of sediments were sieved through a 50 μ m mesh, and animals were counted under a stereoscopic microscope. Thereafter all organisms were preserved for further taxonomic analysis. The number of samples varied from one to 11. Totally, 33 samples were processed aboard and 24 were preserved without processing. For more precise reconstruction of benthic size spectrum, another set of samples was also collected at the same stations. There, three subsamples of 3 cm² were taken from multicorer tubes down to a depth of 5 cm. Each subsample was divided in one centimeter layers which were preserved in 4% formol separately.

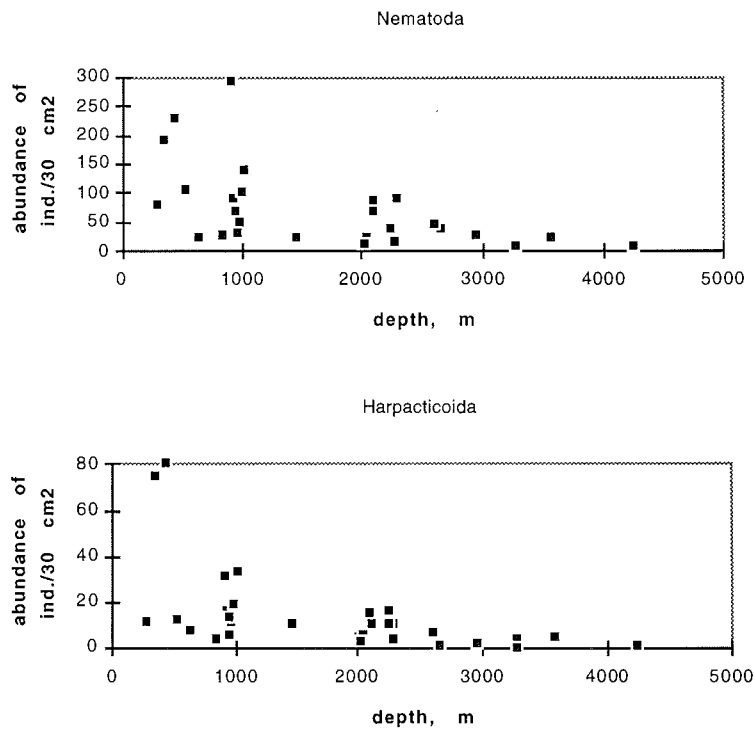


Fig.5.16: Abundance of nematodes and harpacticoids at different depths.

In the samples 19 taxa including both true meiobenthic organisms and organisms of intermediate size between meio- and macrobenthos such as small amphipoda, sponges, cumaceans and isopods of about 1.5 - 2 mm or less, were found. Nematodes and harpacticoids were most common and abundant in the meiobenthos. Nematodes were found everywhere, the latter were present in almost all samples. Other eumeiobenthic animals (Kinorhyncha, Turbellaria, Ostracoda, Tanaida, Halacarida, Hydrida, Aplacophora and Gastrotricha) represented rather small numbers. Pseudomeiobenthos including juveniles and larvae of Bivalvia, Gastropoda, Priapulida and Holoturiodea, occurred in some samples. The main peculiarities of meiobenthos distribution are shown here for nematodes and harpacticoids as most abundant and representative groups.

Along the Barents Sea transect A (stations 42-55) meiobenthos was richest and most abundant; all common meiobenthic taxa were found in a significant number. The abundance of most important groups such as nematodes and harpacticoids increased with the depth down to 600 m (Fig. 5.15). Kinorhyncha were also present on this transect in significant numbers (30-50 ind/30 cm²). The taxonomic composition on the Yermak Plateau is nearly the same, but the population density of meiobenthos is several times less in

average. Many groups were represented by very small numbers of organisms. The abundance of meiobenthos shows a good correlation with bottom relief and also confirm the well known fact of decreasing population densities with depth (Fig.5.16). However, this main trend might be altered significantly by local variation in environmental factors controlling the species' abundances. Spatial heterogeneity in sediment composition, hydrodynamics, productivity of overlying water masses and others lead to large variation in species abundance and taxonomic diversity even within the same station (Fig. 5.17a). Transects C and D crossing the Yermak Plateau north of transect B represent the same type of distribution but with relatively small numbers of organisms (Fig. 5.17b).

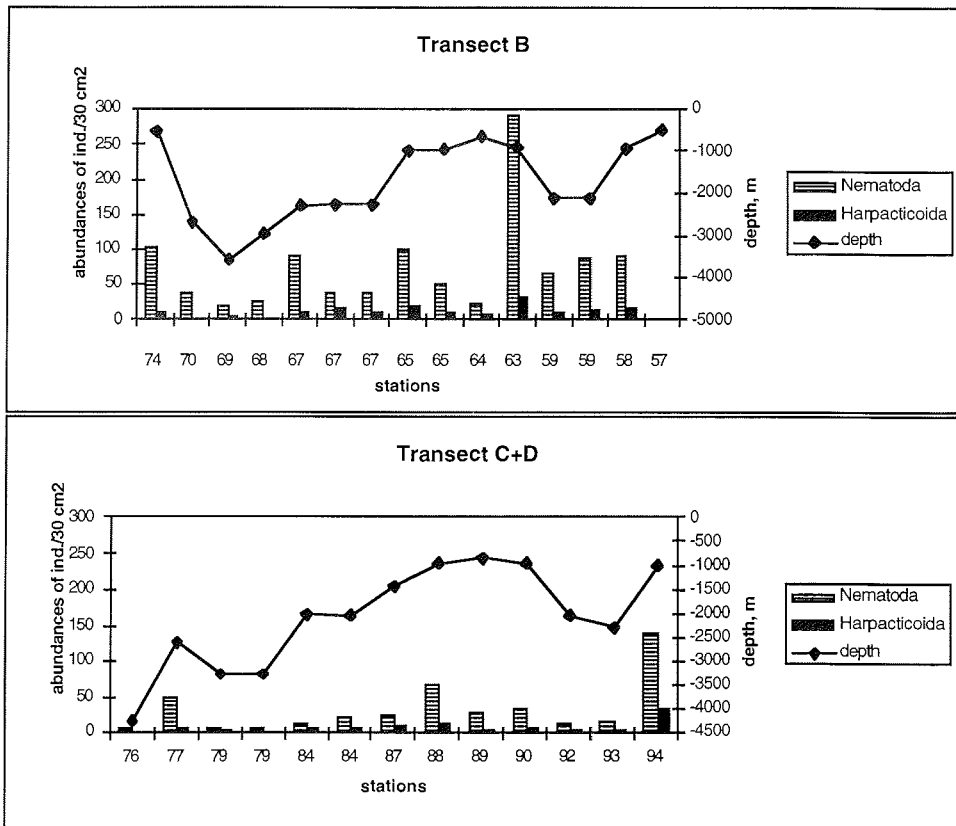


Fig. 5.17a/b: Meiobenthos distribution along Fram Strait transects.

5.5.4 Microbials (E. Helmke, U. Klauke)

Until now very little is known about microbial communities and processes in the Northern Polar Ocean. This is especially true for the deep pelagic and benthic zone but applies also for the surface area including sea ice. In contrast to the Southern Ocean, where we conducted previous studies, the Northern Polar Ocean has a vast permanent sea-ice cover and is subjected to a strong

lateral import of terrigenous material. Whether these different conditions cause differences in structure and activity of the microbial communities of the two polar oceans was the central question of our studies.

We focused on the benthic microbial communities and laid special emphasis on the deep-sea flora. With respect to pelago-benthic coupling pelagic and sea-ice communities were also considered.

Surface sediments as well as the overlying water were sampled from the multicorer at three stations on transect A and at 21 stations on transects B, C and D as well as in the Molloy Deep. Water samples from different depths were taken from CTD bottles at one station of the transects B and D as well as in the Molloy Deep. Sea-ice and surface-water samples were collected at eight different stations along the route.

In general the following parameters were determined in sediment, water, and sea ice samples:

- total bacterial counts
- bacterial biomass
- viable bacterial counts
- secondary production by means of ³H-thymidine and ³H-leucine
- glucose turnover

Additionally, sediment samples were prepared for the determination of water content, C/N ratio and protein content. ATP was extracted from surface-water and sea-ice samples.

Viable counts were determined by means of different methods and cultural approaches applying various temperatures, pressures and substrate qualities and quantities. The cultures represent the basis for isolation work, i.e., for the analysis of the bacterial community structure. Information about quantity and role of the allochthonous and autochthonous bacterial components will further be provided by the activity measurements conducted at different temperatures and hydrostatic pressures.

Concerning the structure of bacterial deep-sea communities the existence and role of decompression-sensitive bacteria were analysed. A prerequisite for this study was a recently developed water sampler which concentrated bacterial cells *in-situ* and brought them up to the surface maintaining *in-situ* pressure. The pressure-retaining water sampler was deployed at four stations. On board, the concentrated water samples of the Molloy Deep and of a 3000 m station were subdivided with negligible pressure loss; the subsamples were subjected to different experimental conditions. The final evaluation of these experiments will be done in the home laboratory. Most of the other assays and experiments with sediment, water, and sea-ice samples are also only to be conducted or finished in the home laboratory.

Preliminary results are available from the activity measurements of the water and sea-ice samples. These indicate that the adaptation of the sea-ice flora from the Northern Polar Ocean to cold temperatures is less pronounced than of that from the Southern Ocean.

With respect to the deep-sea flora sampled with decompression we got close adaptations to deep-sea conditions with the bacterial community of the Molloy Deep. On the other hand, the bacterial flora of a 4000m station in the sea-ice

covered northern region showed no barophilic response. However, final evidence about depth adaptation related to nutrient supply will not be obtained before the entire material is worked up.

5.5.5 Activity and Biomass of the Small Benthic Biota (T. Soltwedel, I. Schewe, V.O. Mokievsky, B. Sablotny)

Benthic deep-sea ecosystems are fueled by the input of organic matter sinking vertically through the water column or being advectively transported. We hypothesize that for large areas of the deep, perennial ice-covered Arctic Ocean (i.e. deep-sea regions adjacent to uncovered continental margins) the advectively mediated food energy is of higher importance than the vertically derived energy. This should stand in contrast to open-ocean systems. Investigations of the pathways for organic substances and of benthic processes, and a comparison with results from other deep-sea regions, will contribute to a better understanding of the functioning of the benthic deep-sea ecosystem of the Arctic Ocean.

The quantitative assessment of bacteria, nano- and meiofauna organisms, and the analysis of a series of biogenic sediment compounds will allow to obtain substantial information on the ecological status of the benthic system. Sediment-bound chloroplastic pigments equivalents, CPE (i.e. chlorophyll *a* plus degradation products) were determined to quantify (vertical and/or lateral) organic matter input from primary production. Differences in activities and biomass within the sediment samples were assessed by a series of biochemical assays commonly used in ecological investigations of the deep sea. To evaluate bacterial exoenzymatic activities, esterase and aminopeptidase turnover rates were determined with the fluorogenic substrates fluorescein-di-acetate (FDA) and methyl-cumarinyl-amide (MCA), respectively. Rather labile macro-molecules like adenylates (i.e. ATP, ADP and AMP), DNA and phospholipids were analyzed specifically as indicators for 'living biomass', i.e. small sediment-inhabiting organisms; more stable compounds like particulate proteins were determined to estimate the bulk of 'living' plus 'dead biomass', i.e. organisms and the proportion of detrital organic matter in the sediments.

Sediment sampling was done with a multicorer (MUC), allowing the collection of almost undisturbed sediment samples essentially for investigations at the sediment-water interface. The MUC was equipped with a video camera for online control, bearing the opportunity to survey the sampling area for a certain period of time and to place the gear selectively at a distinct location, however only within the drift direction of the ship and instrument. Moreover, the real-time control of the MUC allowed to react, at least to a certain extent, if the instrument did not work properly during the sampling process at the seafloor. Generally, the video pictures impressively demonstrated the importance of real-time control for benthic sampling programs. Due to their enhanced mobility and their multi-purpose functionality, the use of a Remotely Operated Vehicle (ROV) for future projects is highly recommended.

The observation and sampling program was adjusted to the requirements of the entire cruise schedule. A total of 32 stations on four transects were sampled within this project. Subsamples for faunistic investigations and for

biochemical analyses were taken using small piston-style corers (5 ml and 20 ml disposable syringes) down to 5 cm sediment depth. To evaluate small-scale variations, three replicates from each MUC (randomly sampled from different MUC tubes) were analyzed for the various parameters. Subsamples were sectioned horizontally in 1-cm-layers and analyzed separately to investigate gradients within the sediment column.

Nano/meiofauna and bacteria samples were preserved for later investigations in the home laboratory. Biochemical analyses for estimating heterotrophic activity in the uppermost centimetres of the sediments were done on board to avoid losses in activity during storage. Sediment samples for the determination of chloroplastic pigments and total adenylates were also analyzed on board, whereas all other samples for biomass determinations were stored in a deep freezer for later analyses in the home institute.

Preliminary results already show some clear trends in the data, e.g. generally decreasing values within the sediment column, a clear tendency for declining values with increasing water depth of sampling stations, and also differences between various topographic regions.

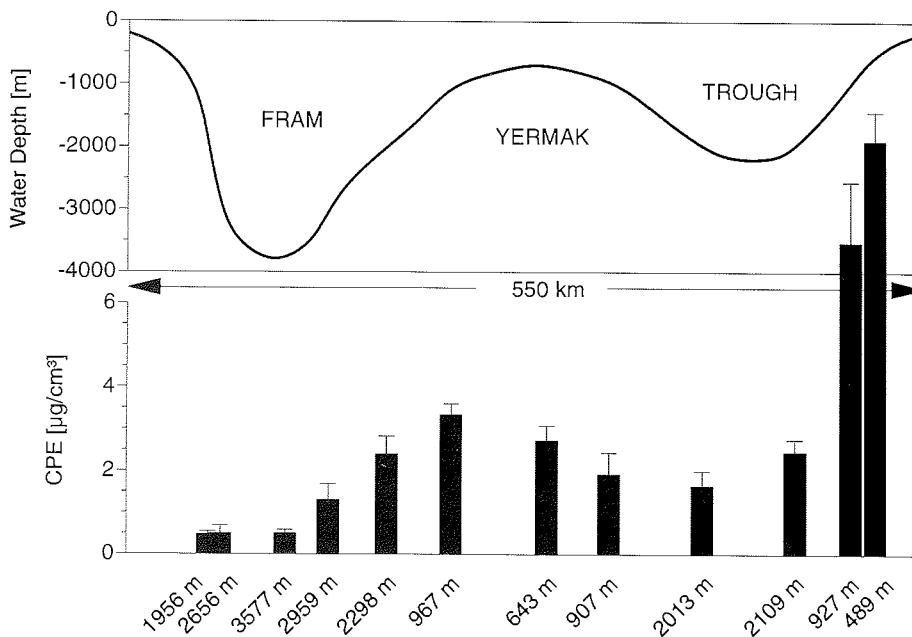


Fig. 5.18: Sediment-bound chloroplastic pigment equivalents (CPE) on stations along transect B.

For instance, concentrations of sediment-bound chloroplastic pigments (indicating the input of phytodetritus to the seafloor) on transect B crossing the Yermak Plateau at about 81°N generally followed the depth contour (Fig. 5.18), with increased values on shallowest stations, lower values in the trough to the east of the plateau and lowest concentrations in Fram Strait sediments. Comparing pigment values on stations with similar water depth (i.e. 1000 m and 2000 m stations on the eastern and western slope of the Yermak Plateau), we found higher values on the western side of the plateau, suggesting higher sedimentation rates on this slope. Pictures taken with the OFOS (Ocean Floor Observation System; see 5.5.1.) showing extremely high numbers of holes borrowed by isopods at stations on the western slope of the Yermak Plateau may confirm an enhanced input of organic matter in this region.

Except for two stations (57, 58) on the continental margin northeast of Svalbard, a highly significant correlation was found between organic matter input (indicated by sediment-bound pigments) and bacterial exoenzymatic activity (e.g. potential esterase activity, FDA; Fig. 5.19) indicating a close pelago-benthic coupling. Stations 57 and 58 showed comparably high pigment values (7-10 µg/cm³). The high relative proportion of intact chlorophyll *a* at these stations point to (relatively) 'fresh' material and a most recent sedimentation event of phytodetrital organic matter, and a still lacking „benthic reponse“ to this event.

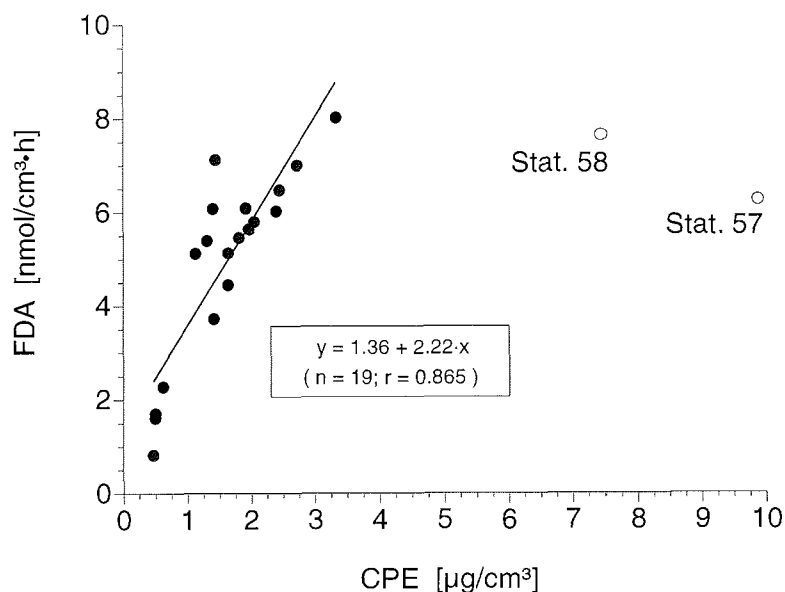


Fig. 5.19 Correlation between organic matter input (indicated by sediment-bound chloroplastic pigments) and bacterial exoenzymatic activity (FDA).

A comparison of preliminary results produced within this study with first meio- and macrofauna evaluations carried out on board (see 5.5.2. and 5.5.3.) already exhibited rather good correlations. However, a detailed ecological description of the benthic community on the Yermak Plateau and in adjacent regions will be available after the completion of further faunal and biochemical analyses planned for the different projects.

5.5.6 Sediment Community Oxygen Uptake (M. Klages)

In order to improve our knowledge concerning energy transfer from the pelagic zone into the benthos as well as within the benthic ecosystem of the Barents Sea experiments on "Sediment Community Oxygen Consumption" (SCOC) were performed. Multicorer tubes (60 mm in diameter) collected at 30 stations along the main transects were incubated for a minimum of 36 hours up to 5 days. Depending on the penetration into the sediment the overlying water column was reduced in order to improve the ration between water volume and sediment surface. The oxygen content, salinity and temperature was measured soon after sampling. Oxygen content was measured using microelectrodes and the coulometry as described by Peck & Uglow (1991). After incubation at $1 \pm 0,5$ °C the final oxygen content and the temperature were measured. The overlying water was removed and fixed with formalin (final conc.: 4 %). The sediment core was divided into three sections of 2 cm thickness each and also preserved in formalin-seawater solution. These samples will be investigated at the institute for meiofauna, juvenile macrofauna and bacteria. Some preliminary calculations on oxygen consumption for selected stations indicate that the absolute consumption rates are comparable to results previously published by Piepenburg et al. (1996) for Barents Sea benthic communities (see Fig. 5.20).

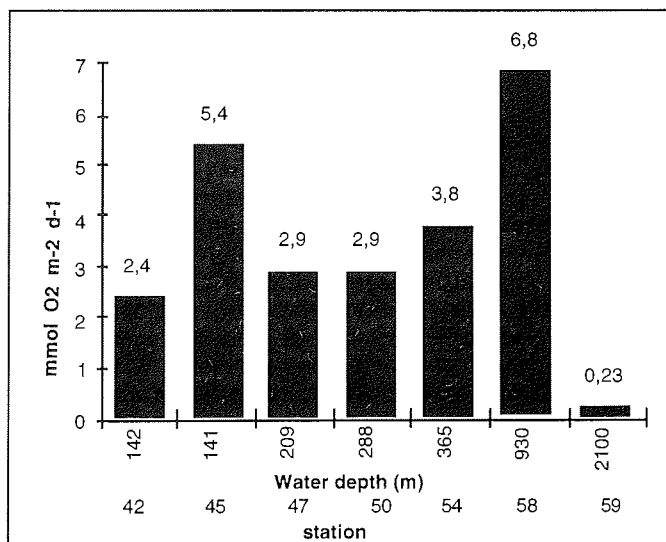


Fig. 5.20: Preliminary results on "Sediment Community Oxygen Consumption" (SCOC).

5.5.7 Experimental Studies on Echinoderms and Crustaceans

(K. v. Juterzenka, M. Klages)

The material collected with AGT and EBS (see Chapter 5.5.1) contained specimens of target species which are in the main focus of running projects at the AWI and the IPO in the framework of the AOSGE project. Therefore, ophiuroids, asteroids, decapod shrimps and amphipods were sorted out for life maintenance and transferred subsequently into two laboratory containers.

Benthic communities are dependent on the input of organic matter which is produced within the euphotic zone, but can be laterally distributed over long distances until reaching the seafloor. Growth and production as well as activity patterns of zoobenthic organisms are related to the concentration, quality, and availability of food. To assess their food preferences and feeding modes, feeding experiments with varying food sources were performed on board and will be continued in the home laboratory.

During feeding experiments on board, natural phytoplankton samples obtained by a handnet were used as suspended food source to simulate input of organic matter as caused by a sedimentating phytoplankton bloom. The experiments focused on the ophiuroid species *Ophiacantha bidentata* and *Ophiopleura borealis* and took place in a tank as well as a small flume (1m in length). During the experiments, pigment concentration in the water was monitored by taking samples for subsequent analysis of Chlorophyll *a* and phaeopigments. Selected individuals were taken from the experimental tank after a period of 4 to 6 hours and stored frozen to analyse their stomach contents.

Ophiuroids which were marked with the fluorescent marker substance calcein during ARK-XIII/1 (B. Bluhm), were kept during the cruise and will be transported back to the home lab. Since calcein binds to the calcareous skeletal structures of organisms and therefore leaves a "starting mark" for a determined growth period, this method allows a direct assessment of growth.

A total of 130 specimens of decapod crustaceans, belonging to 3 species (*Sclerocrangon ferox*, *Pandalus borealis*, *Sabinea septemcarinata*), are kept alive in aquaria. Additionally, another 50 specimens were deep frozen at -125 °C for lipid content analysis and quantification of metabolites, and approx. 150 specimens were preserved in formalin. These specimens will be used for a new approach in age determination of crustaceans by means of "Fluorescent Ageing Pigments" using the autofluorescence characteristics of these chemical compounds accumulating during time. The deployment of baited traps, useful instruments for collecting scavenging amphipods and other invertebrates, failed during our leg due to ice conditions, water depths and cruise track. However, several specimens of *Anonyx nugax*, a common scavenging Arctic species were collected with AGT and EBS. These specimens will be used within a running project on the food fall localization strategy of necrophagous amphipods in oligotrophic marine environments. 56 specimens of pantopods are kept alive (after first check most likely of the genera *Nymphon* and *Boreonymphon*) for planned respiration measurements and histological investigations (for phylogenetic purposes). Additionally, some specimens of other taxonomic groups such as anthozoans, crinoids,

gastropods, bivalves and isopods, are also kept in aquaria for detailed studies on ecophysiology in the home institutes.

5.6 Bird Observations (H. Båsemann)

Introduction

Seabirds play an important role in the Arctic food web. Most of them are on the end of the food chain and can transport considerable amounts of nutrients to the land. For example, 50 000 Little Auks breeding accumulate each year some 100 tons of excrements around their colonies (Mehlum 1989). Very little is known about the sea-bird distribution in ice-covered areas (Brown 1989). Therefore, it is very important to know how many birds live there and to which species they belong.

Counting from a ship includes many problems. The weather plays an important role as well as the status of the ship, i.e., whether it is moving or on station. In addition some of the bird species are very curious: they stay a more or less long time near the ship before they fly to their feeding or nesting grounds. At least one Fulmar accompanied the ship for five days. According V. Mokievski the bird showed a unique expression of his feathers, so it was easy to identify. J. A. van Franeker (1990) reported on „Methods for counting seabirds at sea: A plea for comparative research“, where the discussed problems involved.

Every day roughly between 12:00 und 13:00 UTC, systematical quantitative observations with binoculars from the uppermost deck („Peildeck“) took place. The observation began with a status around „Polarstern“ to see how many birds are there. In addition between 08:00 und 22:00 UTC the occurrences of birds which passed the ship were registered. This counting provided qualitative information (that they are just there). To some degree one can extract also relative abundances. During most of the days the long time observation resulted in higher species numbers. There was only one day without any bird.

Results

The observations began on June 27 and ended on August 08. In total 1946 individuals from 20 bird species were observed (Table 5.7).

Nearly every bird species that was until now described in the region between Svalbard and NE-Greenland (Mehlum, 1989) was observed. Brünnich's Guillemots (*Uria lomvia*) and Common Guillemots (*Uria aalge*) were grouped together, because it was very difficult to distinguish them from the ship. But most of the Guillemots must be Brünnich's G., because the main breeding place for Common G. is Bear Island further south. Also the Pomarine Skua (*Stercorarius pomarinus*) and Arctic Skua (*Stercorarius parasiticus*) are taken as one group. The most important sign – the tail feathers – were hardly to see from great distances.

During the first part of the cruise including transect C up to ten different bird species were seen at one counting. This number decreased to 2 to 4 species and even less in distances from land greater than 110 to 120 miles. On the way back from Greenland the transect D confirmed this observation. When low numbers close to Svalbard were observed there was bad and foggy weather. Highest numbers of species and individuals could be seen on clear days and – in addition – when the ship was moving. The turning ice flows provide a lot of food to the birds.

The only species that could be seen at the ship during the whole cruise was the Fulmar. It appeared close to the Svalbard coast in high numbers, sometimes more than 100 over the day. It was not possible to see an exchange between birds at the ship and those coming from land or other areas of the high sea. In literature it was mentioned that in the north dark brown Fulmars are more common than light gray individuals. This could be confirmed. There were definitely no white examples in distances more than 116 miles from land. Surprisingly the number of Fulmars did not increase with approach to Greenland. That was also valid for all the other birds. The reason may be that the open water at the northeasterly coast of Greenland did not provide enough food, or there were no bird colonies in this part of the Greenland coast. It was tried to prove this by helicopter flights, but due to foggy weather this was not possible.

During the cruise the birds main food, the Polar cods (*Boreogadus saida*) and small crustaceans, were seen in high numbers in the pack ice. This was not the case near Greenland.

There is a great difference in species composition between near-shore and high-sea assemblages. Related to the edge of the pack-ice and the coast are first of all Guillemots (*Uria lomvia* and *U. aalge*), Little Auks, Glaucous Gulls and Kittiwakes. Skuas and Greater Black-backed Gulls are also restricted to the edge of the pack ice and to coastal waters (Brown 1989).

Along transect D the number of Guillemots was clearly lower than along transect B. The reason could be the end of the breeding season on Svalbard. On August 08 a number of young Guillemots with one of their parents were observed already some 60 miles from the coast.

Typical for far distances to the coast are Ross' Gulls and Ivory Gulls. The latter are very common in the ice because they follow the polar bears and feed on their remains such as seal carcasses and bear droppings. Ross' Gulls were seen in relative great numbers on transect D, up to 6 to 10 birds during one day. Mehlum (1989) reported on one possible breeding success of Ross' Gulls on Cape Linné on Svalbard. Normally Ross' Gulls were flying randomly around the ship searching for food. But on August 02, two Ross' Gulls were observed on a direct way from and to the Svalbard coast that was 40 miles away. On our visit in Ny Ålesund two Dutch ornithologists reported that Ross' Gulls are breeding on Mofen Island north of Svalbard. Their normal breeding area is East Siberia and northern Canada. Black Guillemots and Arctic terns were observed both near the coast and far away. The terns, however, did not occur in high numbers.

A very rare observation was made on August 07. A Tufted Puffin (*Lunda cirrhata*) came very close to the ship. Thus, it could be easily identified. This species normally is restricted to the North Pacific. The relative high number of observed Ross' Gulls north and northwest from Svalbard and the Tufted Puffin may reflect the „trend of recolonization of the Arctic after the last ice age“ (Brown 1989).

I would like to thank Vadim Mokievsky, Eike Rachor and Hjalmar Thiel for their helpful discussions.

Table 5.7: Greatest Distance from Svalbard and observed total bird numbers, derived from 1 hour daily observations.

Species	Distance (sm)	Number
Fulmar (<i>Fulmarus glacialis</i>) Eissturmvogel	170	349
Skuas (<i>Stercorarius pom. + paras.</i>) Raubmöwen	26	1
Longtailed skua (<i>Sterc. longicaudus</i>) Falkenraubmöwe	57	3
Great Skua (<i>Stercorarius skua</i>) Große Raubmöwe	26	4
Sabine's Gull (<i>Larus sabinii</i>) Schwalbenmöwe	57	2
Glaucous Gull (<i>Larus hyperboreus</i>) Eismöwe	92	75
Iceland Gull (<i>Larus glaucoides</i>) Islandmöwe	61	1
Great Black-backed Gull (<i>Larus marinus</i>) Mantelmöwe	57	1
Kittiwake (<i>Rissa tridactyla</i>) Dreizehenmöwe	125	753
Ross' Gull (<i>Rhodostethia rosea</i>) Rosenmöwe	170	21
Ivory Gull (<i>Pagophila eburnea</i>) Elfenbeinmöwe	170	62
Arctic Tern (<i>Sterna paradisaea</i>) Küstenseeschwalbe	154	6
Guillemots (<i>Uria aalge + U. lomvia</i>) Lummen	116	318
Black Guillemots (<i>Cephus grylle</i>) Gryllteist	116	82
Little Auk (<i>Alle alle</i>) Krabbentaucher	104	256
Puffin (<i>Fratercula arctica</i>) Papageientaucher	50	15
Tufted Puffin (<i>Lunda cirrhata</i>) Gelbschopf Hornlund	40	1
Common Eider (<i>Somateria mollissima</i>) Eiderente	37	-

6 Sea-Ice Sedimentology and Water Chemistry (D. Dethleff, V. Shevchenko)

6.1 Sea-Ice Sediments (Dirk Dethleff)

Background and Scientific Targets

Arctic sea ice widely contains fine-grained sediments either incorporated as layers and diffusively distributed clouds or enriched in surficial patches after one or several melting cycles. The geological importance of sediment inclusions in Arctic sea ice has been demonstrated by various studies conducted in the US-Canadian shelf seas and, particularly, in the Siberian Laptev Sea (e. g. Dethleff et al. 1993, Dethleff 1995, Reimnitz et al. 1993a). Accordingly, shelf surface deposits are entrained into newly forming ice through turbulent processes of suspension freezing thereby leading to strong regional shelf erosion. The incorporated material is exported from the shelf seas and, after melt release, contributes significantly to the sedimentary budget of the Arctic Ocean and the Northern European Atlantic.

Extremely little is known about turbid sea-ice formation on the Kara and Barents shelves and its subsequent export and dispersion to adjacent marginal seas, the central Arctic Basin and Fram Strait. According to recent drift buoy experiments and numerical modeling results, new - and potentially sediment laden - sea ice can be exported e. g. from the Kara Sea to the Barents Sea and towards the Arctic mediterranean.

The main purposes of our field work are:

- quantification and qualification of sediments in Barents Sea and Central Arctic Ocean ice
- identification of sedimentological similarities (quantitative and qualitative sample composition, coarse- and silt grain size distribution, clay mineral assemblages) between sea-ice sediments in the Kara and Barents Seas and in the Central Arctic Ocean
- tracing possible transport pathways of sea-ice sediments from the Kara Sea into the Barents Sea and/or the Fram Strait region based on sedimentological parameters in surface deposits and sea-ice entrained material in source and melt regions
- identification and interpretation of processes active to entrain sediment into Arctic sea ice using sedimentological parameters (sand/silt/clay ratios, silt distribution, clay mineralogy)

Field Work and Laboratory Analyses

Sea-ice observations were carried out during helicopter flights and from the vessel bridge. Ice sediments were obtained along the R/V "Polarstern" transect i) from ice cores (melting and filtration), ii) from enriched, patchy distributed surface layers, iii) from different layers of tilted floes in ice ridges and iv) from melt water ponds and cryoconite holes.

Smear slides were prepared from sea-ice and ice-berg sediments in order to obtain first evaluation of grain size distribution and sedimentological composition of the sampled material.

Further laboratory methods and quantitative analyses will include determination of sand/silt/clay percentages (wet sieving and Atterberg separation), silt grain size distribution (LaserGranulometer or/and Sedigraph), clay mineral assemblages (X-ray diffractometry), and organic-carbon content and composition. Investigation of the silt fraction under the Scanning Electron Microscope will focus on qualitative sample composition.

Preliminary Results

During ARK-XIII/2 cruise, ice works were carried out at a total of 38 stations (Table 6.1). At 11 stations, an entire core-length of 20.3 m sea-ice was drilled, sawed into chunks, melted and filtered.

Table 6.1: List of ice stations during ARK-XIII/2 cruise.

Station #	Geo station	Date/JD	Latitude	Longitude
1	-	28.6./179	77°55.15'N	33°20.94'E
2	helicopter	30.6./181	80°10.83'N	28°45.68'E
3	helicopter	30.6./181	80°11.56'N	28°53.98'E
4	helicopter	30.6./181	80°43.00'N	29°29.42'E
5	helicopter	2.7./183	80°45.31'N	21°31.06'E
6	helicopter	2.7./183	80°44.53'N	21°28.21'E
7	helicopter	2.7./183	80°50.68'N	21°04.89'E
8	PS2830	3.7./184	80°59.09'N	18°31.58'E
9	PS2832	5.7./186	81°06.40'N	16°14.72'E
10	helicopter	6.7./187	80°59.50'N	11°59.17'E
11	helicopter	6.7./187	81°00.26'N	12°23.25'E
12	helicopter	6.7./187	81°02.44'N	12°46.26'E
13	PS2834	8.7./189	80°54.81'N	09°49.32'E
14	PS2835	10.7./191	81°07.68'N	05°34.11'E
15	helicopter	12.7./193	81°24.93'N	02°31.52'E
16	helicopter	12.7./193	81°19.64'N	01°30.52'E
17	helicopter	12.7./193	81°15.67'N	02°17.38'E
18	PS2838	13.7./194	81°17.78'N	00°23.17'E
19	PS2840	15.7./196	81°26.01'N	05°21.91'W
20	helicopter	19.7./200	81°59.88'N	01°15.01'W
21	helicopter	19.7./200	82°09.11'N	01°55.14'W
22	helicopter	19.7./200	81°59.56'N	02°34.43'W
23	helicopter	20.7./201	83°05.88'N	04°18.69'W
24	helicopter	21.7./202	83°06.11'N	03°44.99'W
25	PS2849	21.7./202	82°38.52'N	01°31.43'E
26	helicopter	24.7./205	82°19.16'N	03°42.52'E
27	helicopter	24.7./205	82°26.26'N	03°04.72'E
28	helicopter	24.7./205	82°26.37'N	04°41.83'E
29	PS2853	24.7./205	82°36.12'N	03°14.75'E
30	helicopter	27.7./208	81°49.93'N	06°53.21'E
31	PS2857	27.7./208	81°54.11'N	07°54.89'E
32	helicopter	28.7./209	81°29.23'N	11°40.70'E
33	helicopter	28.7./209	81°40.55'N	11°59.99'E
34	helicopter	28.7./209	81°35.12'N	11°53.68'E
35	PS2860	30.7./211	81°16.03'N	13°10.74'E
36	helicopter	31.7./212	81°19.91'N	12°50.48'E
37	helicopter	31.7./212	81°30.03'N	11°37.69'E
38	helicopter	31.7./212	81°15.04'N	12°05.63'E

Additionally, 5 cores of different lengths were taken at two stations close to an artificial sediment-test-field installed by AWI-colleagues in 1995. The ice cores were drilled in order to carry out detailed sedimentological and chemical analyses on the sampled material at AWI-laboratories, Bremerhaven. Furthermore, over 100 dirty sea-ice surface samples were collected for AWI and GEOMAR.

Table 6.2: Grain size distribution of collected material.

Station #	Sand %	Silt %	Clay %	Sediment type	Remarks
1	5	60	35	clayey silt	brown
2	<5	>60	35	clayey silt	-
3	85	10	5	sand	-
4	35	40	25	s. clay. silt	-
5	5	60	35	clayey silt	-
6	5	50	45	clayey silt	-
7	5	50	40	clayey silt	-
8	5	80	15	clayey silt	-
9	15	70	15	clayey silt	-
10	10	60	30	clayey silt	-
11	15	70	15	clayey silt	-
12	10	60	30	clayey silt	-
13	<5	>80	15	clayey silt	ridge
14	30	50	20	s. cl. silt	ridge
15	20	60	20	clayey silt	ridge
16	35	50	15	s. cl. silt	ridge
17	35	50	15	s. cl. silt	ridge
18	15	60	25	clayey silt	-
19	-	-	-	-	-
20	15	60	25	clayey silt	surface
21	25	60	15	s. cl. silt	surface
22	15	70	15	silt	surface
23	5	65	30	clayey silt	surface
24	20	60	20	s. cl. silt	surface
25	25	60	15	s. cl. silt	surface
26	<5	>80	15	silt	surface
27	15	70	15	silt	iceberg
28	10	60	30	clayey silt	surface
29	20	60	10	sandy silt	dirty pond
30	15	60	25	clayey silt	surface
31	15	60	25	clayey silt	surface
32	<5	>70	25	clayey silt	surface
33	<5	>80	15	silt	surface
34	10	70	20	clayey silt	surface
34a	85	10	5	sand	surface
35	15	70	15	silt	surface
36	5	70	25	clayey silt	surface
37	5	70	25	clayey silt	surface
38	5	70	25	clayey silt	surface

The drilled ice cores had lengths between 0.8 and 3.0 m. At few sampling sites the ice cover was not penetrated due to scientific purpose or unfavorable conditions. The ice thicknesses varied from 1.5 m to 3.5 m and increased from east to west in the northern Fram Strait. Five of the ice cores (nine including the AWI material, which had a total length of 6.82 m) contained visible inclusions or even very turbid sections. High abundances of ice inclusions were mostly restricted to the upper

30-60 core cm which can be explained through turbulent sediment incorporation during new ice formation; sediment inclusions occurring in the lower part of the cores might be due to floe rafting in an early stage of ice development in the shallow Siberian source areas or might result from under-ice incorporation into multi(second)-year ice through tidal pumping or current-induced resuspension of surface material.

As observed, the pack ice east and north of Svalbard and in the eastern part of the northern Fram Strait was the most turbid (Fig. 6.1). On transect A, several large pressure ridge fields of as much as 15-20 km² extent were observed SE and E of Spitsbergen in the Barents Sea. Parts of these areas consisting of first and multi-year ice floes, contained very dirty sea ice. At N80°59.50'/E11°59.17', extremely dirty sea-ice was observed from the helicopter extending over an area of as much as 100-200km². The ice regime N of Spitsbergen is strongly influenced by the Siberian Branch of the Transpolar Drift System, which transports large amounts of sediment from the shallow Siberian shelf seas to the European North Atlantic. This phenomenon was already documented through data obtained by Nürnberg et al. (1994). High abundances of freshwater diatoms in the Siberian and central branch of the Transpolar Drift during ARK-XIII/2 cruise additionally corroborate the assumption that the ice-incorporated material sampled north of Svalbard was entrained at shallow, near-coastal sites in the Siberian Arctic (e. g. Kara and Laptev Seas; compare Abelmann 1992).

Smear-slide analyses of ice surface sediments reveal generally fine-grained composition of the material with partly more than 90% in the fraction <63µm (Table 6.2). The sampled sediments consist mainly of silt-sized Quartz and Feldspar. Partly, iron-organic-clay aggregates, clay minerals and microorganisms reveal also high abundances (20-30%), while rock fragments, mica and heavy minerals generally are less abundant (Fig. 6.2). Coarse-grained sea-ice sediment was sampled at different stations north of Svalbard (transect A) and on transect D north of Fram Strait (Table 6.2, Fig. 6.2). The sandy material points to entrainment of surface deposits through anchor ice formation or bottom adfreezing. The fine-grained material was probably incorporated by turbulent oceanic mechanisms such as thermohaline convection, Langmuir circulation, wave action and tidal pumping.

Generally high abundances of very angular to subangular clastic material in the silt fraction of sea-ice sediment samples obtained during ARK-XIII/2 lead to the assumption that irregularly shaped, fine-grained particles are preferably activated from the shelf surface or the near-bottom nepheloid layer through hydrodynamic processes. Additionally, irregularly shaped particles - according to Stokes' law - have lower settling velocities than spherical bodies of the same mass and thus, once agitated, may remain longer in suspension. Due to interaction with buoyant rising frazil ice crystals (Reimnitz et al. 1993b) or lifted by helical oceanic vortices such as Langmuir-circulation and thermohaline convection (Dethleff 1995), the angular particles may be floated upward and collected in the grease-ice cover on the water surface. Additionally, the turbulent water masses may be forced through wedge-like streaks of frazil and suspended particulate matter can be entrapped and enriched in the grease-ice cover in areas of downward motion of convective cells (Dethleff 1995). Collection efficiency of filtration and scavenging processes in western Arctic shelf areas were modeled and discussed e. g. by Osterkamp & Gosink (1984).

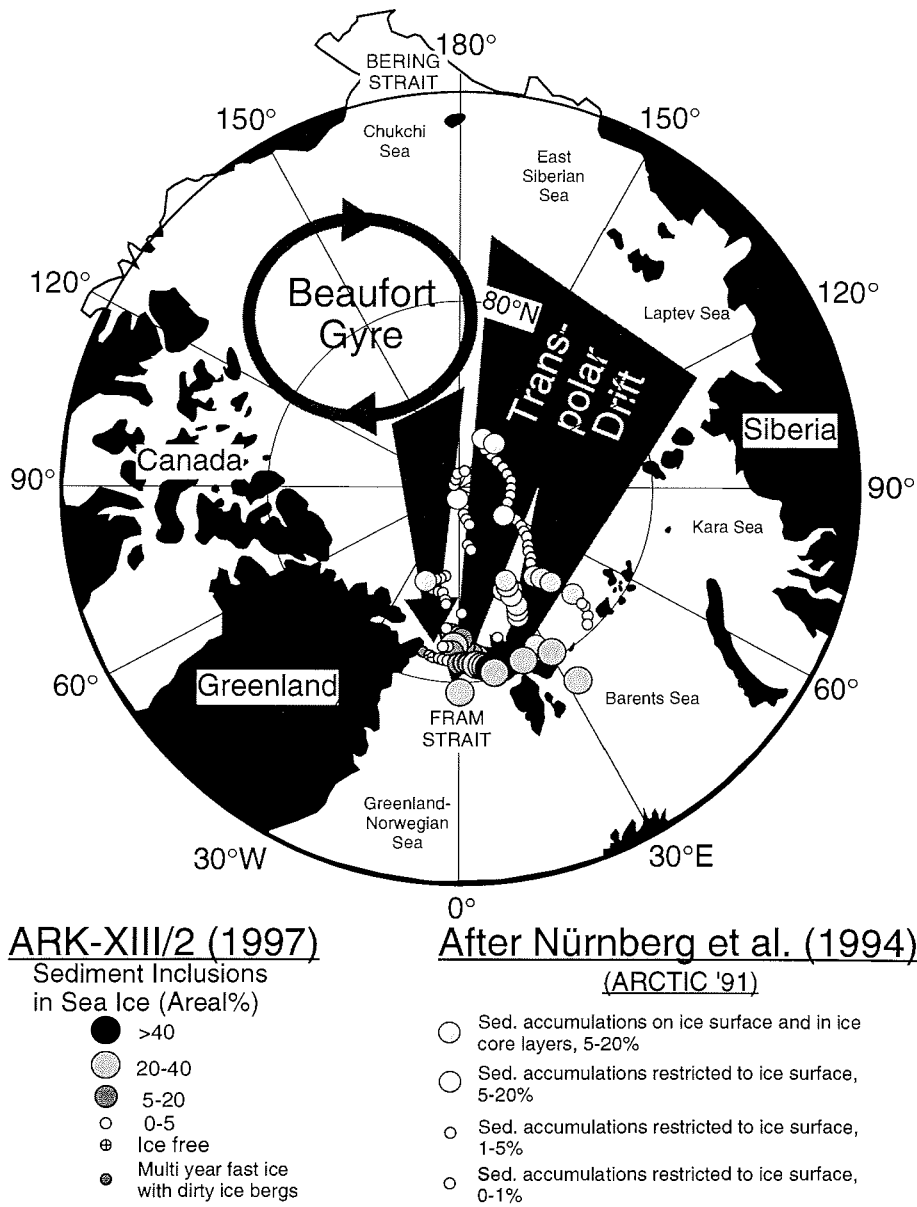


Fig. 6.1: Observed sediment concentrations on/in Barents Sea and central Arctic pack ice.

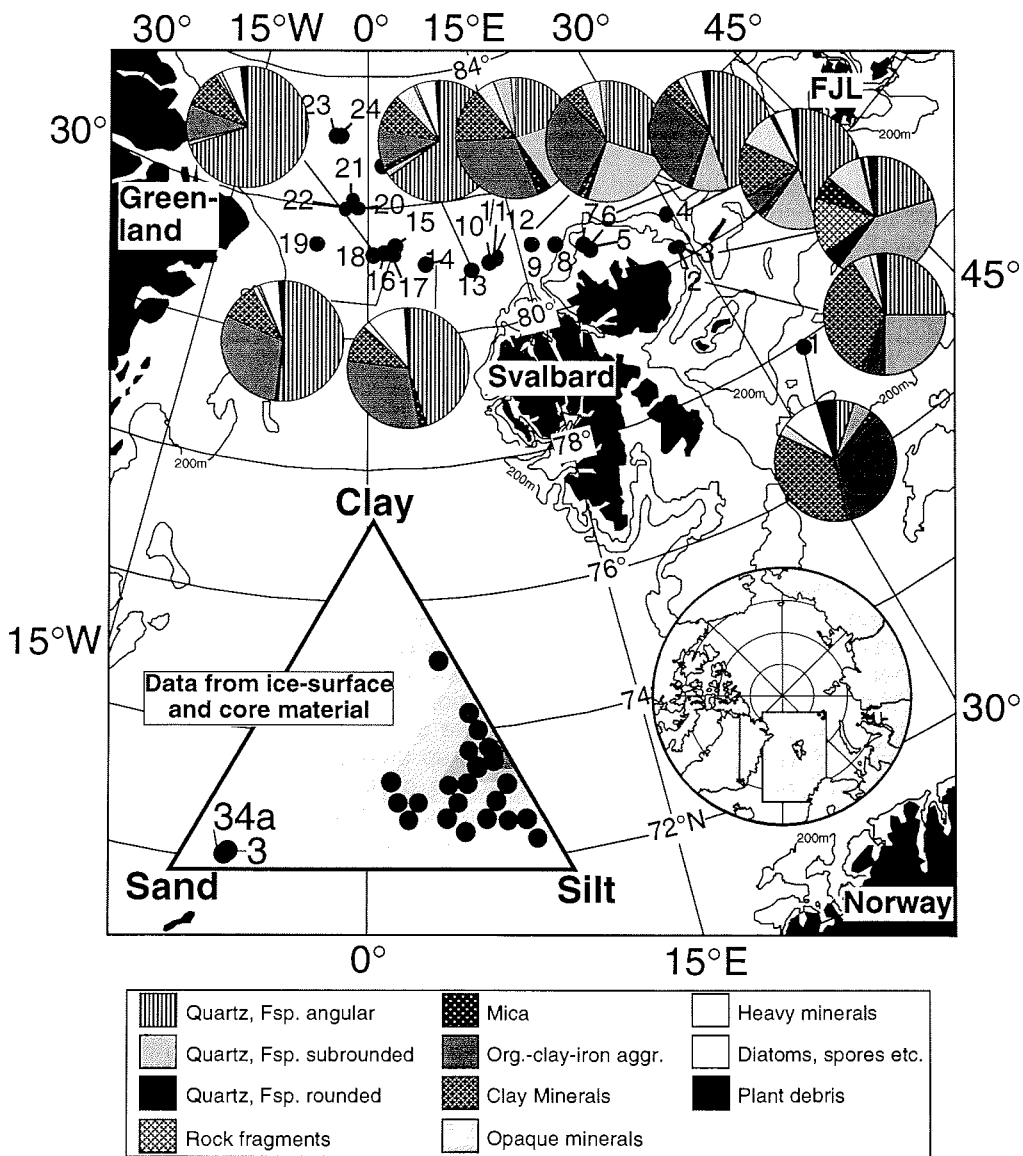


Fig. 6.2: Preliminary grain-size distribution and composition of ice sediments from the ARK-XIII/2 cruise based on smear-slide analyses.

On contrary, less abundances or even the absence of subrounded to well rounded clastic particles - particularly in the silt fraction of sea-ice sediments - might be due to faster settling of spherical material after agitation or resuspension. Higher percentages of rounded to well rounded clastic material were mainly found in the coarse fraction of few sea-ice sediment samples. This feature hints again to entrainment processes such as anchor ice formation or bottom adfreezing at shallow, near-coastal sites in the surf zone or even very close to the beach.

Towards Greenland (transect B), the ice thicknesses increased from roughly 2 m to as much as 3.5 m, whereas the percentage of the ice coverage and the content of visible ice-inclusions decreased rapidly. The near coastal area northeast of Greenland was unusually ice free due to persistent westerly winds and relatively warm atmospheric conditions over Greenland in the middle of July ($T_{\text{sea}} -0.7^{\circ}\text{C}$; $T_{\text{air}} >10^{\circ}\text{C}$). According to daily remote sensing observations, this area of open water extending N and NE of Greenland to a latitude of around 84°N might not be regarded as an extension of the southerly recurrent NE Water Polynya due to two reasons: i) the NE Water Polynya did not occur during ARK-XIII/2 cruise period and ii) the open water was not entirely surrounded by closed pack ice and thereby cannot be classified as a polynya, but simply as "open water". The coastal zone of NE Greenland was characterized by a narrow band of multi-year fast ice containing large turbid ice floes and small icebergs.

At $82^{\circ}26.26'\text{N}/03^{\circ}04.72'\text{E}$ on transect (D) we sampled sediments from a(n) (tilted?) iceberg. The sediment on the surface of the iceberg appeared red and contained considerable traces of a yet unidentified light-red, mechanically rounded mono crystal. Close to the iceberg we sampled a 2000m^2 large, extremely dirty patch in the pack ice. At this site, the ice surface was partly covered by a sediment layer of roughly 3-4 cm thickness, and a sediment-borne island arose in the middle of the central melt water pond. Besides crumbly and puffy sediment aggregates on the top of small rises we observed melt water meanders discharging into shallow ponds thereby heaping-up delta-like depositions through settling of clastic material. The fine to medium grain-size distribution of the sampled material, its content of macroscopic organic material and mica, and its geographic location in the Transpolar Drift hint again to entrainment of the sediments directly from the bottom of near-coastal, shallow Siberian shelf-sites (e.g. Laptev Sea) through the mechanisms of anchor ice formation or vertical turbulences. According to preliminary estimates, this turbid ice patch contained roughly 5-10 t (1 lorry!) of sediment which gives an idea of how much material - annually as much as several 10s of mill. t - can be transported by sea ice from the remote Siberian Arctic shelf seas to Fram Strait.

Acknowledgements

The author is indebted to AWI Bremerhaven and to the chief scientist of RV "Polarstern" cruise ARK-XIII/2, Dr. Ruediger Stein, for providing the opportunity to participate in the expedition. Furthermore, I would like to thank Michael Levitan for discussion and improvements on the smear-slide data. I gratefully thank both the helicopter and vessel crews for their immense support during the sea-ice studies.

6.2 Snow and melt pond water chemistry (V. Shevchenko)

Snow and water from melt ponds samples were collected for chemical composition studies. Date and position of sampling are listed in Table 6.3. On ice-floes samples of the upper 2 cm layer of snow and water from melt ponds were collected for chemical analysis (macrocomponents and trace elements). For sampling we used precleaned bottles, a plastic shovel, and plastic bags. Samples were stored in the refrigerator at -30 °C until processing in home laboratory. Ion chromatography and atomic absorption spectrophotometry will be carried out by Dr. M. Kriews (AWI, Bremerhaven). The obtained data will be used for estimates of deposition of chemical components to the Arctic Ocean surface from the atmosphere. Snow samples for determination of ^{10}Be were also collected. ^{10}Be will be analysed by Dr. C. Strobl (Institut für Umweltphysik, Universität Heidelberg). Samples of particulate matter, contained in snow, were collected by filtration of melted snow water through preweighted filters. After weighing at GEOMAR, Kiel, concentrations of particulate matter will be determined. Later scanning electron microscopy with X-ray microanalysis will be carried out to study the composition of individual particles.

Table 6.3: Sampling of snow and water on ice-floes.

Date	Coordinates		NN of stations				T, °C
	Latitude (N)	Longitude	Snow*	Snow**	PM#	Water##	
28.06	77°55.2'	33°20.9'E	1				-1.1
30.06	80°10.8'	28°45.7'E	2	1			-0.3
30.06	80°43.0'	29°29.4'E	3	2		1	-0.7
2.07	80°45.3'	21°31.1'E	4			2	-1.8
3.07	80°59.1'	18°31.6'E	5	3		3	0
5.07	81°06.4'	16°14.7'E		4		4	0.4
6.07	80°59.5'	11°59.2'E		5		5	1.4
8.07	80°54.5'	9°50.3'E				6	1.3
10.07	81°07.7'	5°34.1'E	6	6		7	0.4
12.07	81°14.0'	2°25.1'E				8	-0.4
13.07	81°17.5'	0°20.2'E				9	0.5
15.07	81°26.4'	5°23.1'W	7	7	7	10	-0.8
16.07	81°31.9'	6°48.9'W	8	8	8	11	-2.6
19.07	82°15.5'	0°43.7'W	9	9	9	12	-0.7
21.07	82°38.6'	1°31.4'E		10	10		0.2
22.07	82°14.6'	5°13.8'E	10	11	11	13	0.4
23.07	82°19.6'	3°42.2'E		12	12		0.1
25.07	81°46.9'	6°19.6'E		13	13	14	0.2
27.07	81°54.1'	7°54.9'E	11	14	14	15-a	-0.8
-/-	-/-	-/-				15-b(+)	-0.8
-/-	-/-	-/-				15-c(+)	-0.8
28.07	81°29.6'	11°48.2'E	12	15	15	16	-2.1
28.07	81°40.5'	10°24.3'E		16	16	17	-1.9
30.07	81°16.1'	13°11.0'E		17	17	18-a	1.6
-/-	-/-	-/-				18-b(+)	1.6

*Snow for chemical analysis, **Snow for ^{10}Be analysis, #Particulate matter contained in snow studies, ##Water from melt ponds for chemical analysis, -/- the same, (+) Water samples NN 15-b, 15-c, and 18-b were collected from melt ponds located in fields of sediment laden ("dirty") ice.

7 Marine Geology

(C.J. Schubert, M. Behrends, K. Fahl, H.-P. Kleiber, J. Knies,
M. Levitan, M. Mitjajev, E. Musatov, G. Nehrke, F. Niessen,
V. Shevchenko, R. Stein, R. Volkmann)

Major objectives of the marine geological programme are to perform high-resolution studies of changes in paleoclimate, paleoceanic circulation, paleoproductivity, and former sea-ice distribution by investigations along the Eurasian continental margin and in the adjacent Arctic Ocean basins. The late Pleistocene and the Holocene records are of main interest, as the Arctic Ocean is regarded of great significance for the global climate system. Furthermore, in the Yermak Plateau area, pre-Quaternary sediments are cropping out, which could even be cored with coring gears onboard "Polarstern" and which would allow to study the long-term history of the Mesozoic and Cenozoic Arctic Ocean and its environmental evolution from a warm polar ocean to an ice-covered polar ocean.

For these purposes, detailed stratigraphical, sedimentological, mineralogical, and geochemical analyses of surface and sub-surface sediment samples are to be made, taken by the giant box corer, the multicorer, the kastenlot corer, and the gravity corer. In addition, the water column was sampled using *in-situ* pumps and sediment traps. During transit times, aerosols were routinely collected using a pump installed on the uppermost deck of the vessel. The close cooperation of the geology group with the biological and other disciplines on board will allow a better understanding of recent sedimentation and transformation processes, which is necessary for the interpretation of the geological records.

Research objectives will concentrate on:

- high-resolution stratigraphic analyses of the sediment sequences (isotopic stratigraphy, AMS 14-C-datings, amino-acids, magnetic susceptibility);
- studies of terrigenous sediment supply (grain size; clay, light, and heavy minerals; organic compounds; geochemical tracers);
- studies of the fluxes of terrigenous and marine organic carbon (total organic carbon, C/N ratios, hydrogen and oxygen indices, stable carbon and nitrogen isotopes, maceral composition, biomarker);
- reconstruction of paleoproductivity by tracer analyses (biomarkers, biogenic opal, stable isotopes, etc.);
- studies of reactions of marine biota to environmental changes;
- studies of physical properties (magnetic susceptibility, wet bulk density, porosity, shear strength);
- study of specific sedimentary environments with detailed PARASOUND surveys.

If possible, coring positions were carefully selected using PARASOUND to avoid areas of sediment redeposition and erosion.

7.1 Marine Sediment Echosounding Using PARASOUND (F. Niessen, H.P.Kleiber)

Scientific Objectives and Technical Settings

Bottom and sub-bottom reflection pattern obtained by PARASOUND characterize the uppermost sediments in terms of their acoustic behavior. This can be used to interpret the sedimentary environments and their changes in space and time. During ARK-XIII/2 the aims of PARASOUND profiling were (i) to select coring locations for gravity and box cores, (ii) to identify lateral differences in sedimentary facies, (iii) to characterize and correlate seismic units in order to assess the variability of sediment thicknesses in the major geological working area.

The hull-mounted PARASOUND sediment echosounder was in 24-hours operation along all cruise tracks starting from 27 June 1997 (76°20' N, 33°29' E) until completion of the Hydrosweep survey on 08 August 1997 (77°54' N, 05°06' E). The PARASOUND system (Krupp Atlas Electronics, Bremen, Germany) generates two primary frequencies between 18 and 23.5 kHz transmitting in a narrow beam of 4°. As a result of the interaction of the primary frequencies within the water column, a secondary frequency is created based on the parametric effect. The parametric frequency is the difference frequency of the two primary waves transmitted. During ARK-XIII/2 the parametric frequency was set to 4 kHz. This allowed subbottom penetration up to 100 m with a vertical resolution of ca. 30 cm. The parametric pulse length was set to 2 under normal operating conditions. Under extreme conditions, such as above steep slopes and while operating in heavy sea ice, the pulse length was increased up to 8. Recorded seismograms were independently digitized by two different systems: (i) by the PARASOUND system for simultaneous printing on a chart recorder (Atlas Deso 25) and (ii) by the PARADIGMA system (Spiess, 1992) for tape storage and post-processing. The settings of the PARADIGMA system were as follows: sampling rate 25 μ s, trace length 133 or 266 ms, block size 10640 byte, format "SEG-Y packed" (Spiess, 1992).

Conditions During the Investigation

On the Barents Sea shelf (transect A) the echosounding conditions were quiet good because of no (or only limited) sea-ice cover, shallow water depth and relatively flat relief. On transects B to D the quality of seismograms is mostly poor because of the heavy ice conditions (strong noise level and frequent ice ramming of the vessel). Moreover, recording of echoes within the narrow beam often failed because of the extreme steepness of the slopes of the Yermak Plateau and in the area of the Fram Strait Fracture Zone including the Molloy Deep. The only exceptions providing good working conditions were within the almost ice-free area NE of Greenland and in the areas south of the sea-ice edge under gently dipping slope conditions. This includes the area of the Hydrosweep survey.

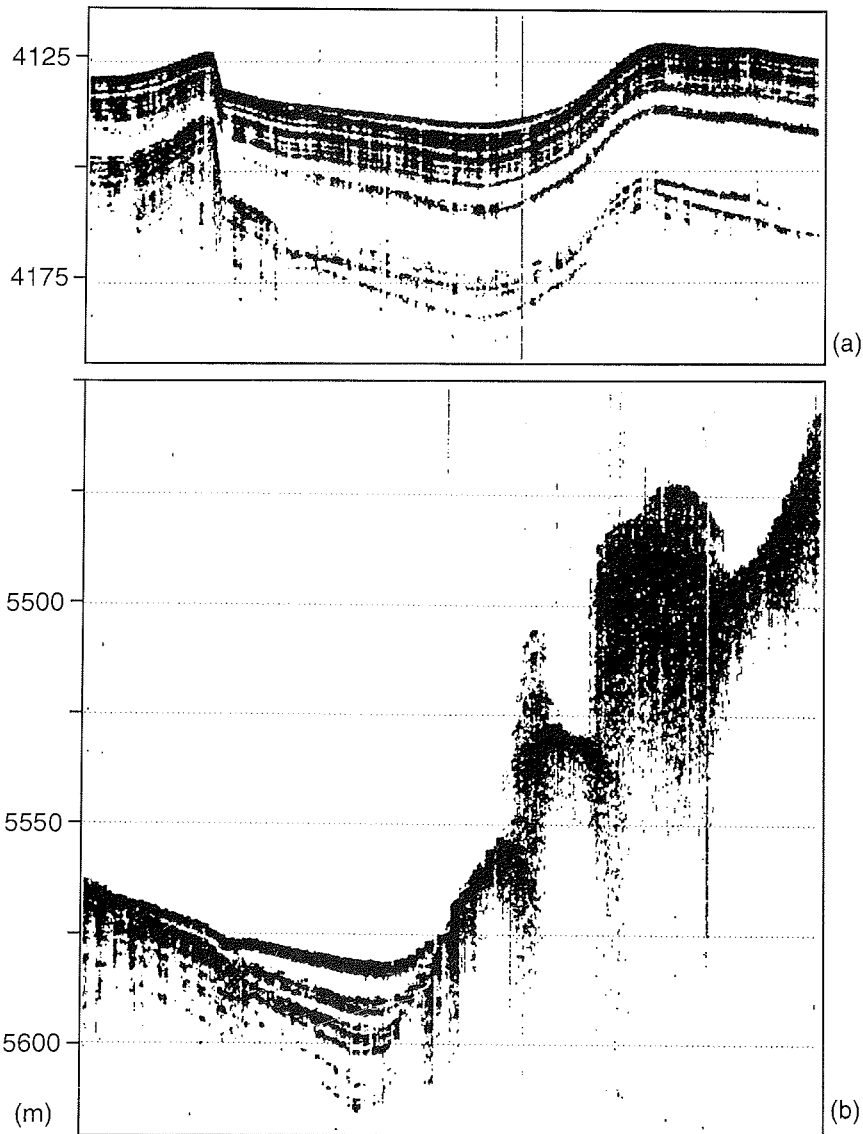


Fig. 7.1: Deep Sea areas. (a) PARASOUND record near $79^{\circ}08'N$, $2^{\circ}45'W$ (transect B). Section length 8.5 km. (b) PARASOUND record near $81^{\circ}30'N$, $3^{\circ}10'W$ (Molloy Deep). Section length 5.5 km.

Seismic Facies and Units

Along transect A, a typical Barents Sea shelf situation was observed which is well known from various investigations described by mostly Scandinavian and other research groups. On transect A, there are two areas distinguished: a southerly

regime to latitude $79^{\circ}28' N$ dominated by facies interpreted as ice-ploughed diamict or truncated bedrock, and a northerly regime near the Svalbard archipelago, characterized by more distinct morphology related to moraine ridges (see Fig. 2.1a, bathymetric transect A). An unconsolidated (Holocene?) cover is at the most a few meters thick or absent. In the main working area of the geological program, along the transects B and D across the Yermak Plateau and Fram Strait, there are generally three different acoustic reflection patterns observed which show striking similarities on both the southern (B) and northern (D) transects. These include:

- stratified sediments of different acoustic characteristics (deep-sea areas, Yermak Plateau, slopes of Greenland and Spitsbergen)
- hummocky structures with no or limited penetration (top of the Yermak Plateau)
- indistinct echoes from steep submarine slopes (Yermak Plateau and along the Fram Strait Fracture Zone)

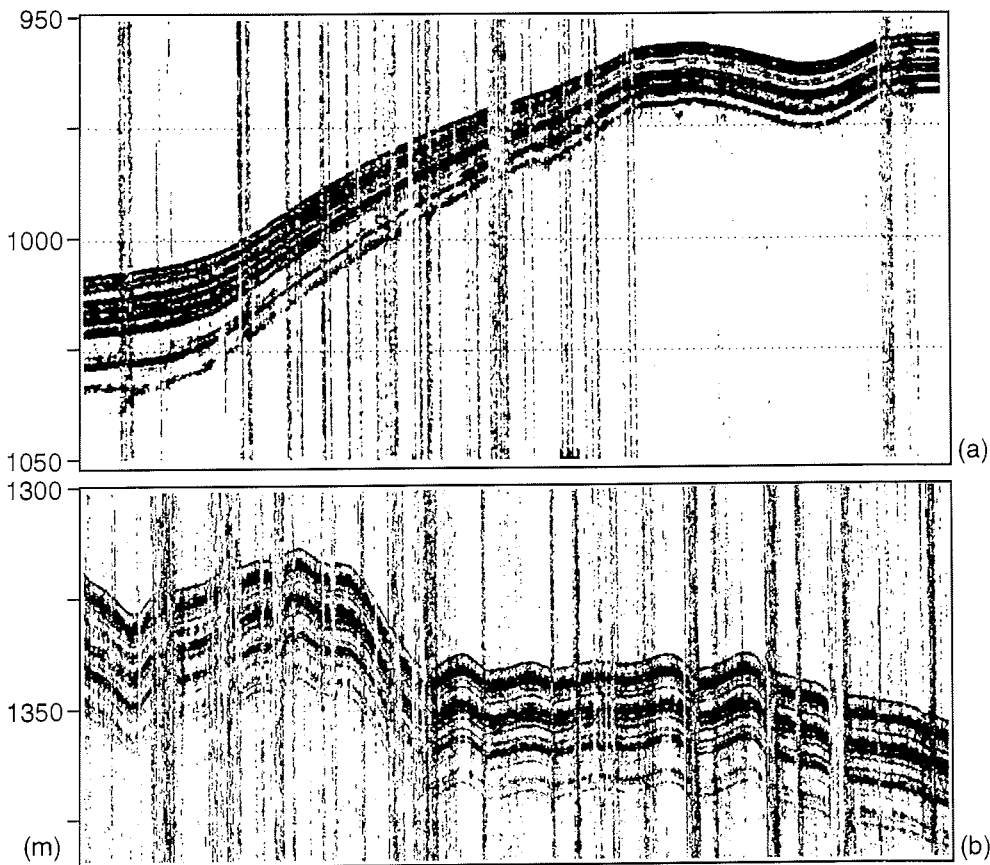


Fig. 7.2: Low (a) and high (b) accumulation areas of transect B. (a) PARASOUND record near $80^{\circ}33'N$, $11^{\circ}47'E$. Section length 1.8 km, (b) PARASOUND record near $81^{\circ}45'N$, $10^{\circ}10'E$. Section length 3 km.

The stratified sediments are described in more detail because they were selected and cored using different geological sampling equipment. They also allow a preliminary facies interpretation based on the PARASOUND records. Deep-sea areas of more than 4000 m water depth were crossed on transect B and within the Molloy Deep. In both cases, the observed sediments are well stratified and intercalated with distinct lenticular-shaped layers which are acoustically transparent (Fig.7.1). The latter are typical for debris flows and suggest redeposition from the surrounding slopes and thus relatively high rates of sedimentation. Particularly in the Molloy Deep, at about 5450 m water depth, all strata pinch out against the slope (Fig.7.1b) which implies that turbidites may be common in the sequence.

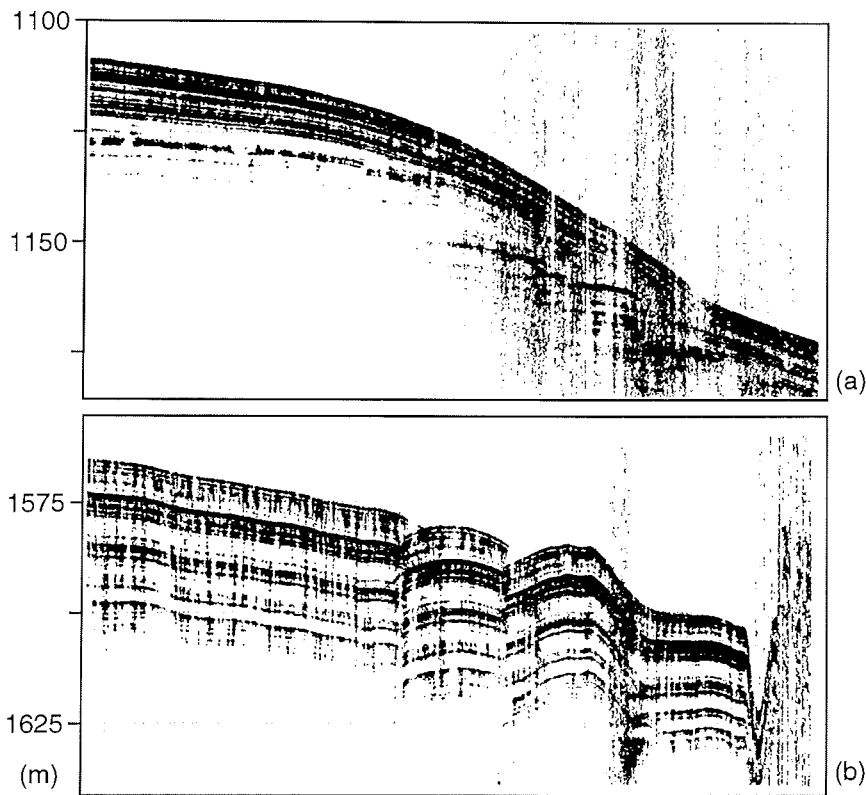


Fig. 7.3: Low (a) and high (b) accumulation areas of transect D. (a) PARASOUND record near $81^{\circ}45'N$, $10^{\circ}10'E$. Section length 1 km, (b) PARASOUND record near $81^{\circ}15'N$, $1^{\circ}41'E$. Section length 4 km.

On the slopes of Greenland and Spitsbergen, and, in particular, across the Yermak Plateau, a subdivision into two stratigraphic units is obvious in most profiles. A lower unit of weak reflectors is conformably or unconformably overlain by a package of well stratified beds, characterized by higher backscatter from distinct reflectors. The boundary of the two units is well seen when the upper unit is more condensed with thicknesses of less than 15 m. For example, Figures 7.2a and 7.3a (transect B and D, respectively) show clear evidence of the unit boundaries in two sections between 950m and 1200m water depth on the upper eastern slopes of the Yermak Plateau. Figure 7.3a is indicative for an unconformity between the two units because the reflectors of the lower unit appear to be truncated at the downslope area of the section whereas the upper unit is undisturbed. In most areas, however, as demonstrated by the example in Figure 7.2a, the transition between the two units is conformable.

Along transects B and D, these units can be followed laterally over longer distances. This allows the detection of high accumulation areas where the upper unit can reach sediment thicknesses of more than 30 m (Fig. 7.2b and 7.3b from transects B and D, respectively). In such areas, the distinction between the units is sometimes difficult or the lower unit is not seen because of insufficient penetration of the 4 kHz pulse. It is interesting to note that such high accumulation areas are often characterized by a relatively transparent top layer of 4 to 7 m in thickness (Fig. 7.2b). Sediment cores obtained during the cruise indicate that Holocene deposits can reach thicknesses of that magnitude in these areas. A first assessment of the lateral variability of the thicknesses of the seismic units across the southern Yermak Plateau is presented in Figure 7.4c. The graph indicates that areas of high accumulation are particularly common at the western end of the Yermak Plateau and, in places, along the continental slope of Greenland (Fig.7.4).

In most areas of high accumulation, the sediment packages appear to be intact and stable. Nevertheless, in places, stair-case rotational faulting of unconsolidated muds of the upper unit is observed (Fig. 7.3b). This may indicate instability. Thus high accumulation areas may function as potential source areas for submarine slumping and, subsequently, the deposition of debris flow deposits as observed in the deep-sea records of the area investigated. A distinct V-shape feature, which truncates into the sediments of the upper unit, is associated with the above faults (Fig. 7.3b right-hand side). It may be interpreted as slump scar or channel which also suggests lateral downslope transportation of sediments. Lateral variability of unit thicknesses (upper and lower units) over relatively short distances can be observed in many sections across the Yermak Plateau. For example, for both sections showing condensed thicknesses of the upper unit (Fig. 7.5), the thickness may increase from only 5 m to more than 15 m over a lateral distance of only a few kilometers. In Figure 7.5a an extreme case of lateral thinning from near the eastern top end of the Yermak Plateau (eastern slope) is shown where the entire package thins from 25 m to about 10 m thickness over only 1.5 km of lateral distance without any major unconformity or truncation seen in the section. It is obvious that strong lateral thinning occurs often in shallower water depth near the crest of the plateau (900 to 1200 m of water depth) as compared to the adjacent deeper areas characterized by high accumulation (1300 to 1700 m water depth). This may suggest that the observed differences in

facies are related to relatively small-scale lateral currents (e.g. tidal currents and/or eddies from larger-scale oceanic circulation). Similar thinning of the sedimentary cover is also observed on the Svalbard Slope (Fig. 7.5b).

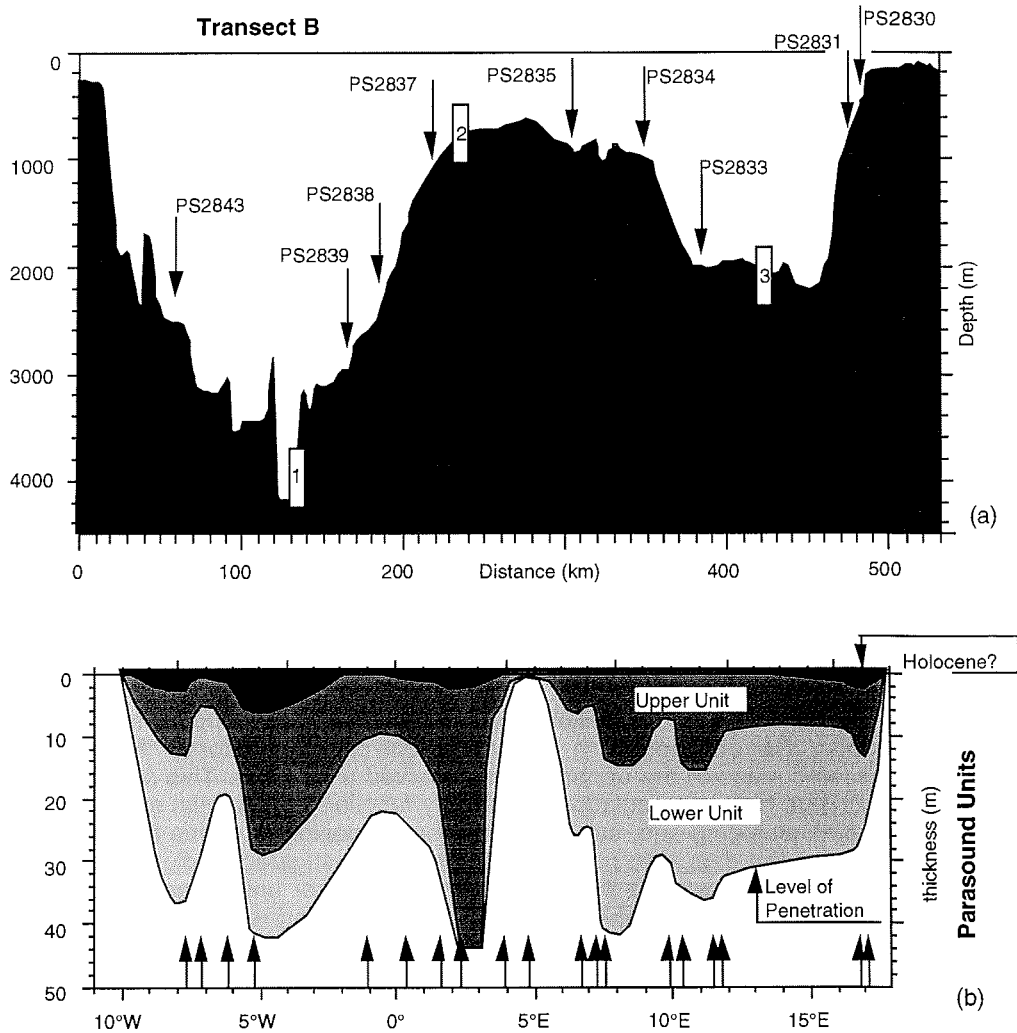


Fig. 7.4: Bathymetry and coring locations (a) and PARASOUND unit thicknesses (b) of transect B. The locations of PARASOUND profiles presented and discussed in the report are marked in (a) by boxes 1-3.
 Box 1: PARASOUND profile of Figure 7.1.a;
 Box 2: PARASOUND profile of Figure 7.2.b;
 Box 3: PARASOUND profile of Figure 7.2.a.
 The arrows in (b) indicate where unit thicknesses were measured. Data is interpolated between the arrows.

This observation is consistent with that fact that on the top of the plateau limited penetration to only a few meters at the most is recorded. This suggests no major sedimentary cover near the crest and may indicate winnowing by currents. Therefore these areas may function as a possible source for the deposition of sediments in high accumulation areas. In addition, the top of the plateau is characterized by hummocky structures. Reflections from hummocks are often associated with diffraction hyperbolae which indicate small-scale topography within the PARASOUND footprint. Therefore, the shape of the hummocks cannot be resolved in detail by the PARASOUND system which makes an interpretation of their origin difficult.

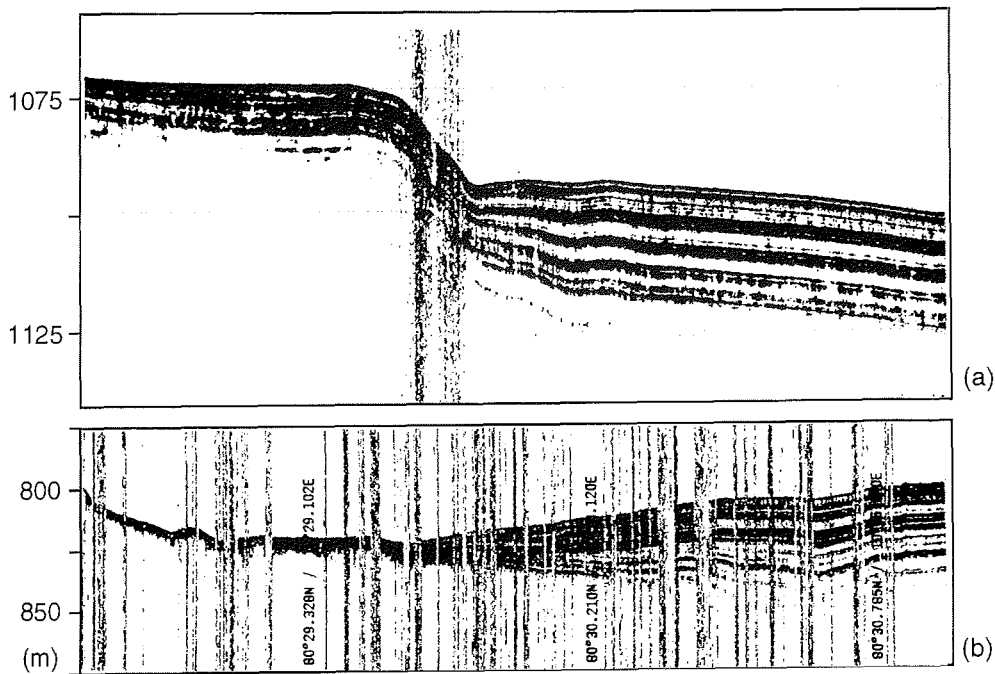


Fig. 7.5: Areas with strong lateral variability of unit thicknesses. a) PARASOUND record near $81^{\circ}44'N$, $9^{\circ}48'E$. Section length 1.5 km, b) PARASOUND record near $80^{\circ}30'N$, $10^{\circ}28'E$. Section length 2.8 km.

Indistinct or diffuse and mostly very weak echoes are typical for the steep slopes of the Yermak Plateau and other steep morphological features related to the Fram Strait Fracture Zone. On many slopes of the investigated area, the slope angle is around or above 4° so that no subbottom information is available from such terrain.

7.2 Geological Sampling, Description, and Methods Applied

7.2.1 Aerosol Sampling (V. Shevchenko)

Sampling of aerosols for elemental analysis was carried out aboard RV "Polarstern" approximately 20 m above sea level by pumping of air through AFA-HA filters (about 8 m³ per hour). To exclude contamination from the ship, sampling was interrupted when the relative wind direction was not opposite to the ship heading. No samples were collected during rain and snow. During the expedition 8 samples were collected (see Table 10.1). Elemental composition will be studied by instrumental neutron-activation analysis (INAA).

Measurements of aerosol size distribution were carried out at 66 sites (see Table 10.2) using PC-218 photoelectrical particle counter (Royco, USA). In each series, 3 parallel measurements of particle concentrations in the ranges of 0.5-1; 1-2; 2-3; 3-5; 5-10 µm were done.

7.2.2 Sampling of Water Column for Organic-Geochemical Investigations (K. Fahl)

In-situ Pumps

The sampling of the water column was carried out with so called *in-situ* pumps (Challenger Oceanic Systems and Services -COSS-, UK). The *in-situ* particulate sampler is designed to filter over one cubic metre of water in one hour at midwater depth in the open ocean. The aim is to provide sufficient quantities of particulate material for subsequent analysis of chemical moieties - in this case biomarkers - to obtain more informations about the degradation of biomolecules which were synthesized by special organisms. In general the volume sampled depends on the concentration of the suspended matter, the duration of pumping and the porosity and matrix of the filters. For the investigations of biomarkers precombusted Whatman GF/C filters (293 mm) were used.

In general the sampling was carried out at 3 stations per transect. The pumping depths (Table 7.1) were selected according to the CTD (conductivity, temperature, depth) transect. The analytical investigations will be done in the home laboratory.

In addition samples for the organic geochemical investigations from the water column were covered by Niskin bottles attached to a CTD-sonde to study biomarker gradients in the nepheloid layer (see Chapter 8) and by one sediment trap which represents a 4-week period.

Table 7.1: Station list of *in-situ* pump sampling during the RV "Polarstern" Expedition ARK-XIII/2

Station	AWI-No.	Water Depth (m)	Pumping depth (m)
044/059	PS2832	2081	150, 300, 1500, 2000
044/062	PS2834	2834	200, 300, 700, 1010
044/064	PS2836	641	100, 200, 600, 630
044/067	PS2838	2432	200, 300, 2000, 2410
044/070	PS2841	2774	250, 350, 1800, 2700
044/079	PS2849	3265	284, 680, 1800, 3100
044/084	PS2853	2150	250, 750, 2165
044/089	PS2857	840	400, 700, 805
044/093	PS2861	2300	200, 400, 2000, 2240

7.2.3 Oxygen and Carbon Isotopes Investigations of Water and Foraminifers (R. Volkmann)

Water Sampling

Water samples for stable isotope investigations ($\delta^{18}\text{O}$, $\delta^{13}\text{C}$) were taken from the rosette bottles as a vertical profile from the bottom of the water column to the upper 20m (Table 7.2). The exact choice of the depths depended on the temperature and salinity profile determined by conductivity/temperature/depth-probe (CTD). The depth interval at deep stations usually was 20m, 40m, 80m, 100m, 150m, 300m, 500m, 1000m, 1500m etc., at shallow stations (Yermak-Plateau, shelves) a closer interval in the upper 200-300m was used. To avoid exchange of atmospheric CO_2 with the gas in the water sample, the water was immediately filled in glass bottles and the glass was closed with silicon paste and tape. Additionally, the samples were stored cool and dark. $\delta^{18}\text{O}$ will be analysed at IUP (Institut für Umweltphysik, Heidelberg), $\delta^{13}\text{C}$ at the Leibniz-Labor, Kiel University .

Multinet Tows

Multinet plankton tows were used for sampling living planktonic foraminifers in the upper water column by means of a Kiel-multinet (Hydrobios Cooperation Kiel), an open-closing device with a 0,25m² square-shaped opening that allows to take five nets within one haul. The nets of 64 μm mesh size were towed vertically with a speed of 0,5m/s down and 0,3m/s up. The regular depth intervals were 500-300m, 300-200m, 200-100m, 100-50m, and 50-0m. The catch was preserved in a 4% buffered formalin seawater solution (sample pH > 8,0) and stored at 0°C. After the cruise the planktonic foraminifers will be picked out by pipette and treated with bengal-rosa-ethanol solution for distinguishing "living" (protoplasma-containing) and "dead" (empty) shells. Living species of *Neogloboquadrina pachyderma* (sinistral) will be measured for stable isotopes ($\delta^{18}\text{O}$, $\delta^{13}\text{C}$) at the Leibniz-Labor, Kiel

University. Additional species distribution and habitat of other planktonic foraminifers will be studied.

Table 7.3: Sample list for oxygen and carbon isotope investigations.

station	AWI- No.	depth (m)	water samples	multinet	surface samples (GKG)	sea ice samples
44/039		300	x	x		
44/042	PS 2822	150			x	
44/047	PS 2824	213			x	
44/052	PS 2827	323	x	x	x	
44/054	PS 2828	332	x	x		
44/057	PS 2830	519	x	x	x	x
44/058	PS 2831	970	x	x	x	
44/059	PS 2832	2077	x	x	x	x
44/060	PS 2833	2001	x	x	x	
44/062	PS 2834	1018	x	x	x	x
44/063	PS 2835	861	x	x	x	
44/064	PS 2836	649	x	x	x	x
44/065	PS 2837	1038	x	x	x	
44/067	PS 2838	2310	x	x	x	
44/068	PS 2839	2991	x	x	x	
44/069	PS 2840	3569	x	x	x	
44/070	PS 2841	2675	x	x		
44/074	PS 2846	524	x	x	x	
44/076	PS 2847	4130	x	x	x	
44/077	PS 2848	2538	x	x	x	
44/079	PS 2849	3238	x	x	x	x
44/082	PS 2851	2927			x	
44/084	PS 2953	2008	x	x	x	x
44/085	PS 2854	1806			x	
44/087	PS 2855	1414	x	x	x	
44/088	PS 2856	936			x	
44/089	PS 2857	827	x	x	x	x
44/090	PS 2858	931			x	
44/091	PS 2859	1135	x	x	x	x
44/092	PS 2860	1182			x	
44/093	PS 2861	2198	x	x	x	x
44/094	PS 2862	1100	x	x	x	
44/095	PS 2863	795			x	
44/096	PS 2864	777	x	x	x	
44/097	PS 2865	821			x	
44/098	PS 2866	274	x	x		
44/099	PS 2867	519	x	x	x	
44/100	PS 2868	5413	x	x	x	

Surface Samples

Two sediment samples were skimmed off the surface of undisturbed box cores (50cmx50cmx60cm). One sample was frozen at -30°C for qualitative analyses (species distribution) after the cruise, the other sample was sieved in 4 fractions: 63-125µm, 125-250µm, 250-500µm, >500µm. *Neogloboquadrina pachyderma* (sinistral) were picked out of the fraction 125-150µm for measuring stable isotopes. The results will be compared to those from the water samples and correlated with the results of the water column.

Ice Samples

To investigate the stable isotopes of living planktonic foraminifers in the sea ice, 10 ice samples were obtained by coring. The lower 10cm of the ice cores were separated, melted and preserved with 4% buffered formalin-tapwater solution and stored at 2°C.

Investigations of stable isotopes of planktonic foraminifers allow a reconstruction of water mass parameters and give paleoceanographic information. The left coiling *Neogloboquadrina pachyderma* (sinistral) is the most common species in the polar regions. Its test isotopic signal reflects the isotopic composition of the water masses around and provides an important proxy of past polar ocean environment and ecology (salinity, temperature, Atlantic water advection, river run-off, ice cover). The second most common species are *Neogloboquadrina pachyderma* (dextral) and *Globigerina quinqueloba*.

The amount of living planktonic foraminifers depends on the ice cover and water depth. Their abundance increases with deeper water because of their reproduction cycle in the upper 500m of the water column. On the shelf (transect A) with water depths <300m, planktonic foraminifers are very rare or absent. The maximal amount was obtained in the middle section of transect B and at every station of the short transect (E) north of Svalbard due to the absence of ice coverage and higher water depths. In the ice-covered area of the eastern part of transect B and the whole transects C and D, less species were found. Absolut abundances will be determined in the home laboratory.

In Arctic sea ice planktonic foraminifers are generally rare. Only two species of *Neogloboquadrina pachyderma* (sinistral) were found in the ice samples at station 79 and one species in the ice sample of station 89. Due to their rare amount their isotopic signal has no influence on the isotopic signal planktonic foraminifers reflecting in surface sediments and sediment cores.

7.2.4 Nitrogen and carbon isotopes investigations of organic material (C.J. Schubert)

Recent investigations of carbon isotopes in surface and near surface sediment samples of the Arctic Ocean (Schubert et al. in prep.) have revealed isotopic values indicating a high abundance of marine organic components. This observation contradicts results suggested by organic geochemical parameters (Stein et al., 1994; Schubert, 1995) which hint to a mainly terrigenous source of the organic matter in Arctic Ocean sediments.

Nitrogen isotopes of organic matter in sediments have been suggested by several authors to be indicative for nutrient distributions in surface waters and/or distinction of marine versus terrestrial organic matter. First measurements on surface and near surface samples of the Arctic Ocean (Schubert et al. in prep.) looked quite promising to be able to differentiate between higher and lower nutrient content of surface waters. Both isotopes need to be investigated in detail in different settings to understand the signal in the underlying sediments. Later, these results should give new insights in interpreting the distributions of these isotopes during glacial/interglacial changes.

To study the complete spectrum of occurrences of carbon and nitrogen isotopes in organic matter from sea-ice (icebergs), surface waters, deep water, zooplankton to the sediment, all different settings were sampled during ARK-XIII/2. In sea ice and icebergs, sediments which have been entrained during ice formation were sampled via Helicopter or at ice stations directly from the ship and frozen at minus 30°C. Since most of the biomass in sea ice was found at the lowermost part of the ice in contact to the surface water, the lowermost ten centimeters (600-700ccm) of ice cores were melted, filtered on GFC-filters and also frozen at minus 30°C. Melt ponds which are common features on sea ice in the Arctic Ocean and formed during several melting and freezing cycles, could contain high amounts of biomass in form of algae (e.g. *Nitzschia*). 500ml bottles were filled with meltwater-pond water containing algae, filtered on GFC-filters and frozen at minus 30°C. Surface waters (30-0m water depth) was prepared in the same way. On several stations copepods (~10 organisms) which were caught on the way from the sea bottom to the surface via Bongonet (20µm diameter), were isolated and frozen in glass vials (-30°C). Additionally, on each geological station surface sediments were taken and also frozen at minus 30°C. All samples will be investigated onshore via mass spectrometer analysis. Some of the samples will also undergo organic geochemical i.e. biomarker investigations for comparison with the isotopic composition. In Table 10.3 (Annex), all samples incl. sampling location are listed.

7.2.5 Sea Floor Sediment Sampling and Description

(M. Behrends, K. Fahl, J. Knies, M. Levitan, M. Mitjajev, E. Musatow, G. Nehrke, R. Volkmann)

Sampling of Near-Surface Sediments

Surface sediments were taken routinely at almost all geological stations (Fig. 7.6) with the giant box corer (GKG; 50x50x60 cm). The surface sediments of the GKG were sampled for stable isotope measurements in foraminifers and sedimentological, micropaleontological, and geochemical investigations. In addition, three plastic tubes (12 cm in diameter) and one plastic box (cross section of 7.5 x 15) covering the entire sediment column gained by GKG were taken for sedimentological, geochemical, and stable isotope investigations, and for archiving at AWI.

At all stations, the AWI multicorer ("MUC"; manufactured by Fa. Wuttke, Henstedt-Ulzburg) with eight tubes of 10 cm in diameter was used. The penetration weight of the MUC is 250 kg.

MUC cores were sampled as follows, depending on the number of cores filled with sediment:

- 2 tubes for investigation of benthic foraminifers and stable isotopes. Sediment samples were taken at 0-1, 1-2, 2-3, 3-4, 4-5, 7-8, 10-11, and 14-15 cm and subsequently mixed with bengal-rosa-ethanol-solution to stain living organisms;
- 1 tube for sedimentological investigations of the coarse fraction onboard.

Coring and Sampling of Long Sediment Cores

The gravity corer (SL) and the kastenlot corer (KAL) were used to obtain long sediment cores. The gravity corer has a penetration weight of 1.5 t, and a core barrel segment length of 5 m with a diameter of 120 mm. The core barrels used during ARK-XIII/2 had lengths of 5 and 10 m. The length of the obtained cores vary between 165 and 656 cm (Fig. 7.7). The kastenlot (Kögler, 1963), a gravity corer with a rectangular cross section of 30x30 cm, has a penetration weight of 3.5 t and a corebox segment sized 30x30x575 cm (manufactured by Hydrowerkstätten Kiel). The length of the box core boxes used was 11.75 m plus about 30 cm for the core catcher. The great advantage of this kastenlot is the wall-thickness of only 0.2 cm. Because of the great cross-sectional area (900 cm²) and the small thickness of the walls, the quality of the cores was generally excellent. The length of the obtained cores vary between 652 (PS2856-5) and 876 cm (PS2837-5) (Fig. 7.7).

Ten of the gravity cores (i.e., all KAL cores and six of the SL-gravity cores) were opened, described, and sampled onboard Polarstern (Fig. 7.7). Before opening of the SL cores, core logging was performed (see chapter 7.3). Sampling of SL cores was performed for shorebased stratigraphical, sedimentological, geochemical, and micropaleontological studies (AMS¹⁴C dating, water content, wet-bulk density, stable isotopes, XRD, grain size, carbonate, organic carbon, microfossil assemblages, etc.).

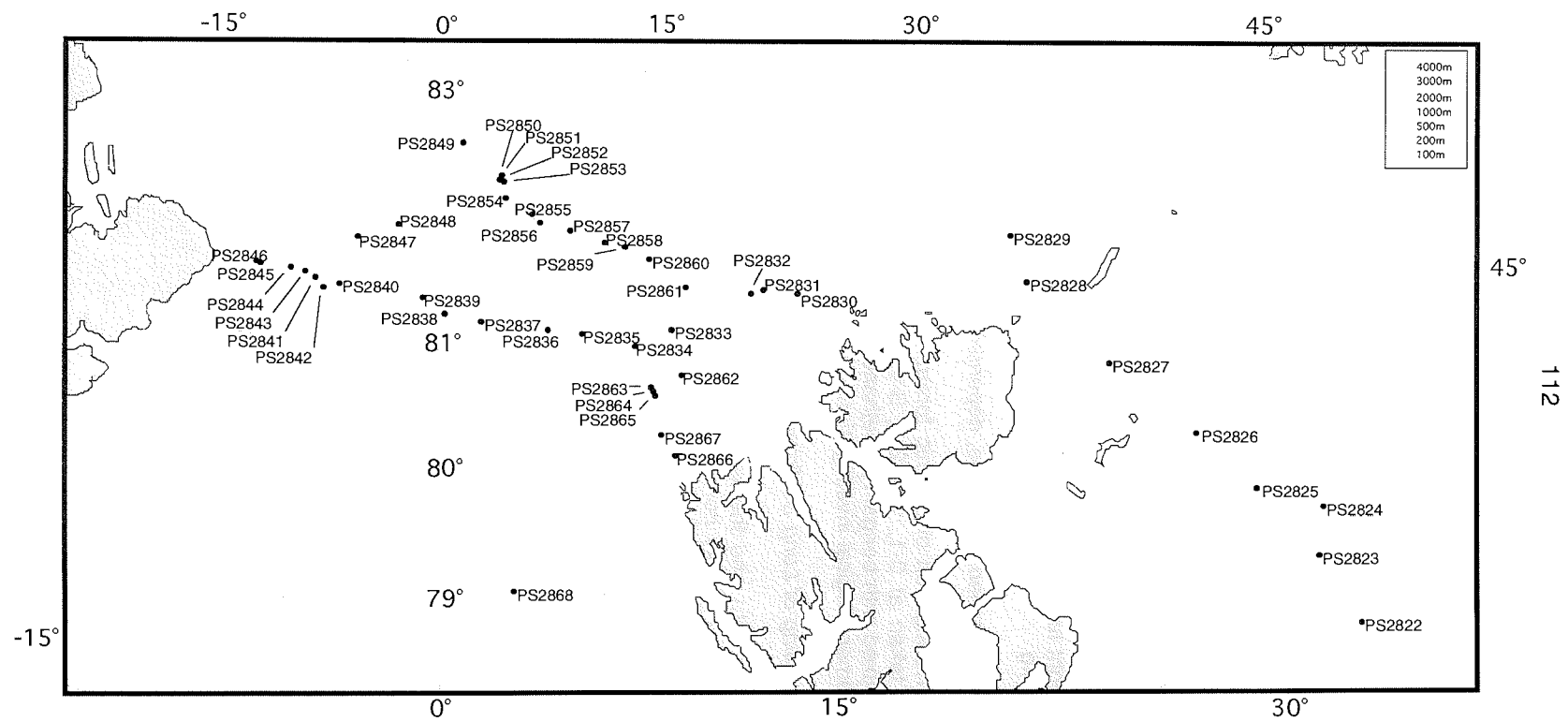


Fig. 7.6: Map indicating geological sampling stations.

Sampling of the KAL cores for the same investigations was performed as follows: three plastic boxes (100x16x7.5 cm) covering the entire core (AWI Archive; AWI geochemistry, sedimentology, mineralogy, and stable isotopes; GEOMAR sedimentology and stable isotopes). One plastic box (100x9x7.5 cm) covering the entire core was taken for core logging (see Chapter 7.3) and afterwards deep-frozen at -30°C for organic-geochemical studies to be later performed at the home laboratory. In addition, single samples were taken from the entire core for specific mineralogical and micropaleontological studies (Shirshov Institute, VNIIO).

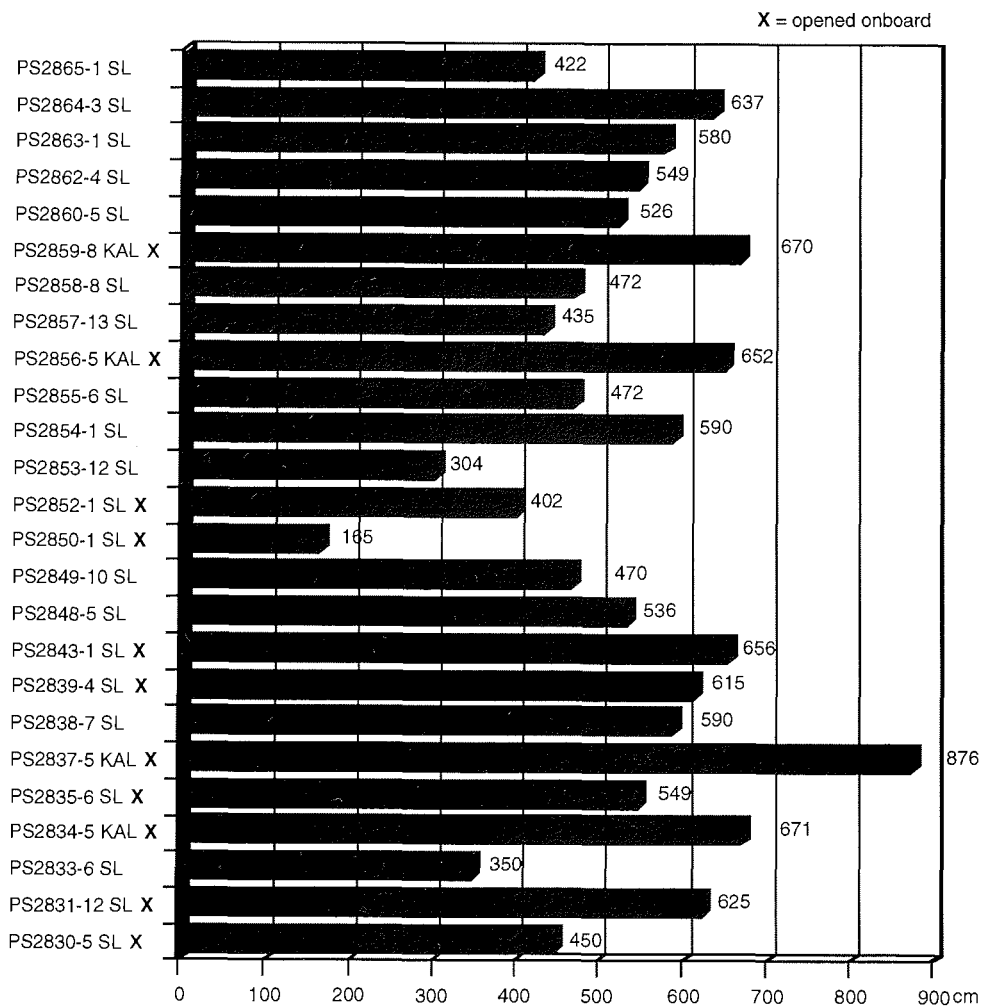


Fig. 7.7: Lengths of kastenlot (KAL) and gravity corer (SL) cores. Cores marked with "X" were opened, described, and sampled onboard "Polarstern".

Sediment Description and Characterization

(a) Visual core description

The sediment cores were routinely photographed and described, and are graphically displayed within the annex. Sediment colors were identified according to the "Munsell Soil Color Chart". Smear-slide investigations were performed to obtain estimates of the grain size and sediment composition (i.e., biogenic and terrigenous components) and for the classification of the sediment type (e.g., silty clay, sandy silt, etc.; see Annex Chapter 10.3).

(b) Coarse fraction (> 63 μm) analysis

Bulk sediment samples from several MUC cores were washed through a 63 μm sieve and dried. On a selected set of samples, the coarse-fraction composition was analysed using a binocular microscope.

(c) Radiographs

Sediment slabs of 0.5 cm in thickness were taken continuously from KAL and all opened SL cores. X-ray images will be produced from these slabs at AWI in order to elucidate sedimentary and biogenic structures and to determine the number of coarse-grained detritus >2 mm for evaluation of the contents of ice-rafted debris (IRD) (for method see Grobe, 1987).

7.3 Physical Properties and Core Logging

(F. Niessen, H.P. Kleiber, G. Nehrke)

During ARK-XIII/2 physical properties were determined on whole cores by logging (P-wave velocity, wet bulk density and magnetic susceptibility) and on discrete samples after core opening (wet bulk density). Physical properties of marine sediments are important parameters for the interpretation of the sedimentary record.

Magnetic susceptibility is commonly used as an indicator of lithological changes (e.g. Nowaczyk, 1991). It is defined as the dimensionless proportional factor of an applied magnetic field in relation to the magnetization in the sample (here measured in SI units). In marine sediments changes in susceptibility are normally controlled by variation in the content of magnetite. Magnetite has a significant higher susceptibility ($k = +10^{-2}$) than most common minerals (-10^{-6} to $+10^{-6}$). In marine environments of high latitude areas, magnetite is mostly derived from terrigenous input and/or volcanic ashes. The content of magnetite depends on its dilution by marine components such as carbonates and opal. It may also be related to the sediment porosity because water is weakly diamagnetic with susceptibility values close to zero. Magnetic susceptibility may be used as an indicator for marine versus terrestrial origin of the sediments. Together with logs of other physical properties, magnetic susceptibility records are useful for lateral core correlation.

P-wave velocity and wet bulk density can be used for the calculation of synthetic seismograms in order to compare the cored sedimentary record with high resolution seismic profiles obtained with the PARASOUND system. The aim is a better understanding of the sound reflection behavior of marine sediments. This is controlled by the contrasts of acoustic impedance in the sediment sequence. Acoustic impedance is defined as the product of density and P-wave velocity.

Wet bulk density (WBD) is the density of the total sample, including pore fluid or:

$$WBD = M_t/V_t,$$

where M_t = total mass and V_t = total volume. Units are reported in $Mg\ m^{-3}$ which is numerically equivalent to $g\ cm^{-3}$.

Porosity can be calculated from wet bulk density and grain density ($GD = 2.65\ g\ cm^{-3}$) (Weber et al., 1997):

$$P_0 (\%) = \frac{(GD - WBD)}{(GD - 1.026)} * 100$$

It is an important variable required for calculation of sediment accumulation rates ($g\ cm^{-2}\ ky^{-1}$). Calculated fractal porosities ($\% * 0.01$) of the sediment cores are presented in the annex of this report (Chapter 10.3).

Continuous Whole-Core Logging of Wet Bulk Density, P-wave Velocity and Magnetic Susceptibility

Wet Bulk Density and P-wave velocity and magnetic susceptibility were measured in 1-cm intervals on gravity and kastenlot cores taken during the cruise. We have used the "Multi Sensor Core Logger (MSCL-14)", manufactured by Geotek (UK), which allows the determination of core diameter, P-wave travel time, gamma-ray attenuation and magnetic susceptibility. The system is automated (PC based) and designed for non-destructive logging of up to 1.3 m long whole-core sections. In case of kastenlot cores, polystyrene boxes (size inside 82.5 x 72 x 1000 mm) were logged which were previously filled with sediments by pushing the boxes into the cores shortly after the kastenlot was opened. Because the loop sensor used has a different response to varying core diameter, all magnetic susceptibility values determined on kastenlot boxes are corrected.

magnetic susceptibility (10^{-5} SI) = measured value (10^{-5} SI) / K-rel

K-rel is given for gravity cores (SL) and kastenlot cores in Table 7.5 according to the correction instructions for the Bartington MS2 sensor systems. The data is expressed in SI-units, although no correct volume susceptibility can be assessed due to the loop sensor geometry.

A detailed description of the MSCL system is given by Kuhn (1995), its calibration is described by Niessen (1997) and Weber et al. (1997). The characteristics are summarized in Table 7.5. During the time of the cruise the gamma ray attenuation was calibrated to density using aluminum, graphite and water. The raw data was processed using the Geotek Software Version 3.0. Additionally, a Kaleidagraph Macro was improved during the cruise in order to calculate the correction for count rate effects on the attenuated gamma data as described in Weber et al. (1997).

Wet Bulk Density on Discrete Samples

A constant volume tube of 10 cm³ was used to sample sediments for density determination. The tube was carefully pushed into the sediments of kastenlot cores, then cut out, trimmed and weighed. To compensate for ship's motion, mass was determined using a technique of differential counterbalancing on twin top loading electronic balances (Childress & Mickel, 1980). The computerized precision electronic balance system used during this cruise was kindly provided by GEOMAR Technologie GmbH, Kiel. After determination of the total (wet) mass and volume, samples were stored for later freeze drying and determination of dry mass in the home laboratory.

Preliminary Results

Preliminary results demonstrate that the densities calculated from MSCL measurements correlate with those determined on discrete samples (Fig. 7.8). The correlation coefficient is 0.92, although, on average, the MSCL densities are slightly higher than those of discrete samples (Fig.7.8). For the entire area under

investigation, there is a positive correlation of MSCL wet bulk density and P-wave velocity. Wet bulk densities and P-wave velocities range from 1.3 to 2.4 g cm⁻³ and 1450 to 2000 m s⁻¹, respectively. Usually, high values form distinct peaks and may be related to IRD. There is very little variability of the above range within the entire area under investigation.

Table 7.5: Multi Sensor Core Logger (MSCL-14) specifications used during ARK-XIII/2.

P-wave Velocity and Core Diameter	
Transducer diameter	5 cm
Transmitter pulse frequency	500 kHz
Transmitted pulse repetition rate:	1 kHz
Received pulse resolution	50 ns
P-wave travel-time offset	8.47 μ s (KAL, 2*3 mm box wall thickness) 7.79 μ s (SL, 2*2.5 cm liner wall thickness)
Density	
Gamma ray source	Cs-137
Source activity	356 MBq
Source energy	0.662 MeV
Collimator diameter	5 mm
Gamma detector	Scintillation Counter (John Count Scientific Ltd.)
Magnetic Susceptibility	
Loop sensor type	MS-2B (Bartington Ltd.)
Loop sensor diameter	14 cm
Alternating field frequency	0.565 kHz
Magnetic field intensity	approx. 80 A/m RMS
Loop sensor correction coefficient	
SL	2 (113 cm ² core cross section)
K-rel	
Loop sensor correction coefficient	
KAL	0.82 (59.4 cm ² box cross section)
K-rel	

Core to core correlations can be carried out using wet bulk density data. This correlation is based on the fact that sediments which have an estimated age of isotopic stages 2, 4 and, in particular, 6 show significantly higher values than average. This is well seen in cores PS2835-6, PS2838-7 and PS2839-4 from transect B (Fig. 7.9). In contrast, stages with interglacial climatic conditions such as 5 and 1 are characterized by values lower than average. For example, a relatively thick Holocene cover of about 2.5 m thickness is indicated in the top uppermost of core PS2837-5 (Fig. 7.9).

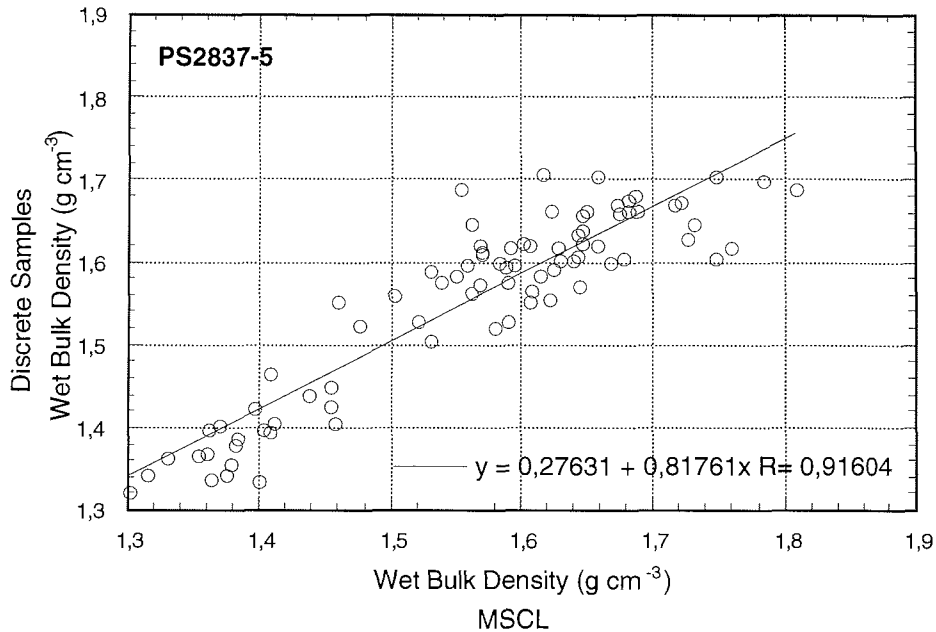


Fig. 7.8: Correlation of MSCL and discrete sample data (wet bulk density (g cm⁻³)) of core PS2837-5.

Along transect B, the correlation of the physical properties suggests significantly lower sedimentation rates towards the eastern end of the transect. This is consistent with both the results of the geological work and the sediment-reflector correlation obtained from PARASOUND data. Variable sediment accumulation is also indicated by the density records along transect D (Fig.7.10). There were severe technical problems with the susceptibility sensor which could not be overcome during the cruise. This problem caused sudden shifts in amplitude on 10 to 15 % of the data as well as strong zero drifts for some of the cores. Substantial drift corrections and partly re-measurements of the sediments have still to be carried out. For this reason, no susceptibility data is presented in this report. The data will be available on request from the data bank PANGEA of the AWI in Bremerhaven. Generally, magnetic susceptibility ranges between 100 and 500 with some peaks up to about 600 (10⁻⁵ SI). There is an anti-correlation of magnetic susceptibility and wet bulk density which is best seen in the data oscillations of sediments with an estimated age of isotopic stages 5 to 7. The susceptibility oscillations would be even stronger after correction for porosity because susceptibility in sediments with lower porosity (higher density) would increase and vice versa. Therefore, higher densities and lower susceptibilities in glacial stages suggest significantly different sediment compositions compared to interglacial conditions. A distinctive sediment layer with an age of 21-23 kyrs which was found in several cores from the Fram Strait area (see Fig. 7.16) is often also associated with very low magnetic susceptibility values of about 100 (10⁻⁵ SI).

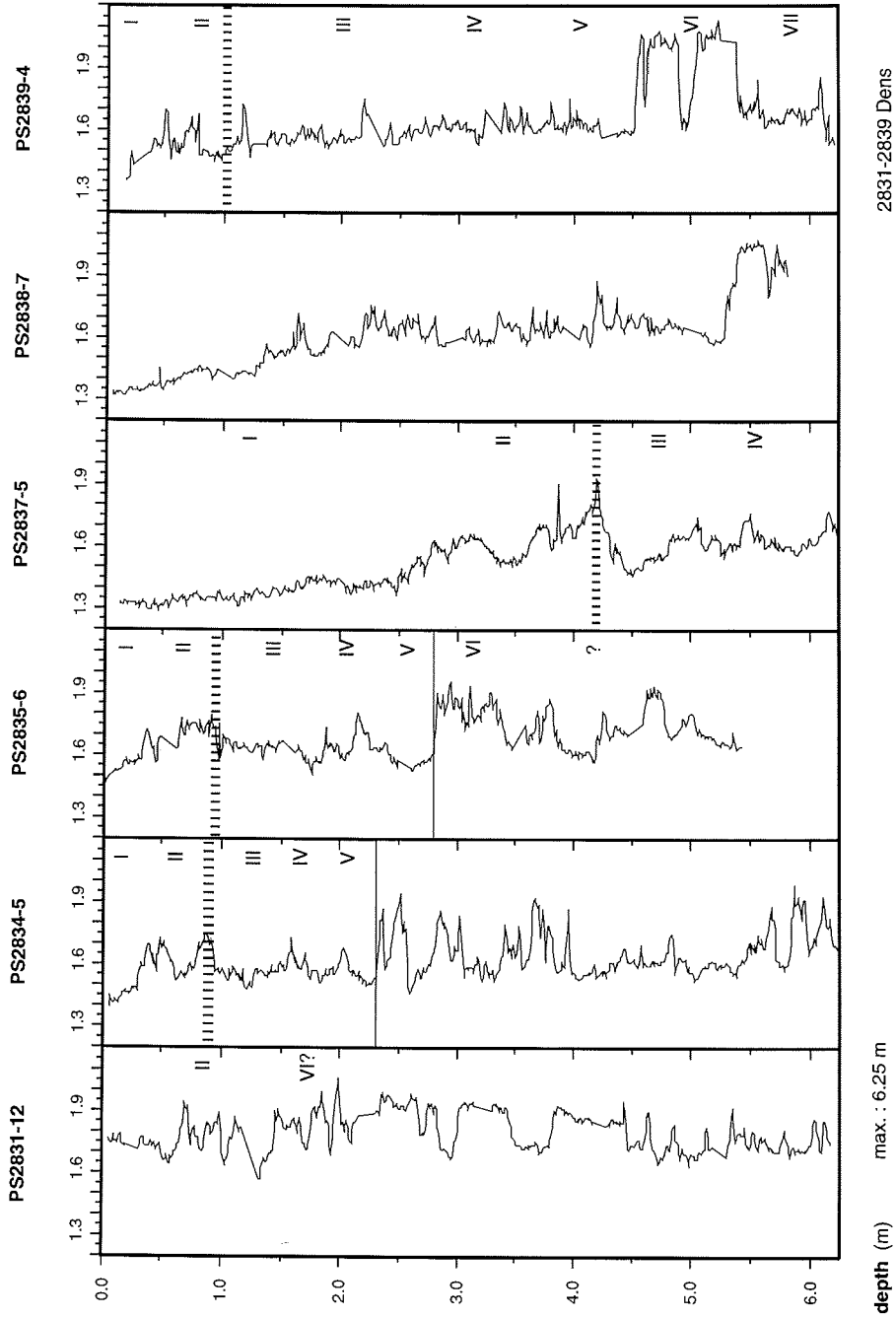


Fig. 7.9: Lateral correlation of wet bulk density data (MSCL) of cores from transect B. Roman numbers indicate estimated preliminary oxygen isotope stages as described in Chapter 7.4. Note that core PS2738-7 was not opened and described yet.

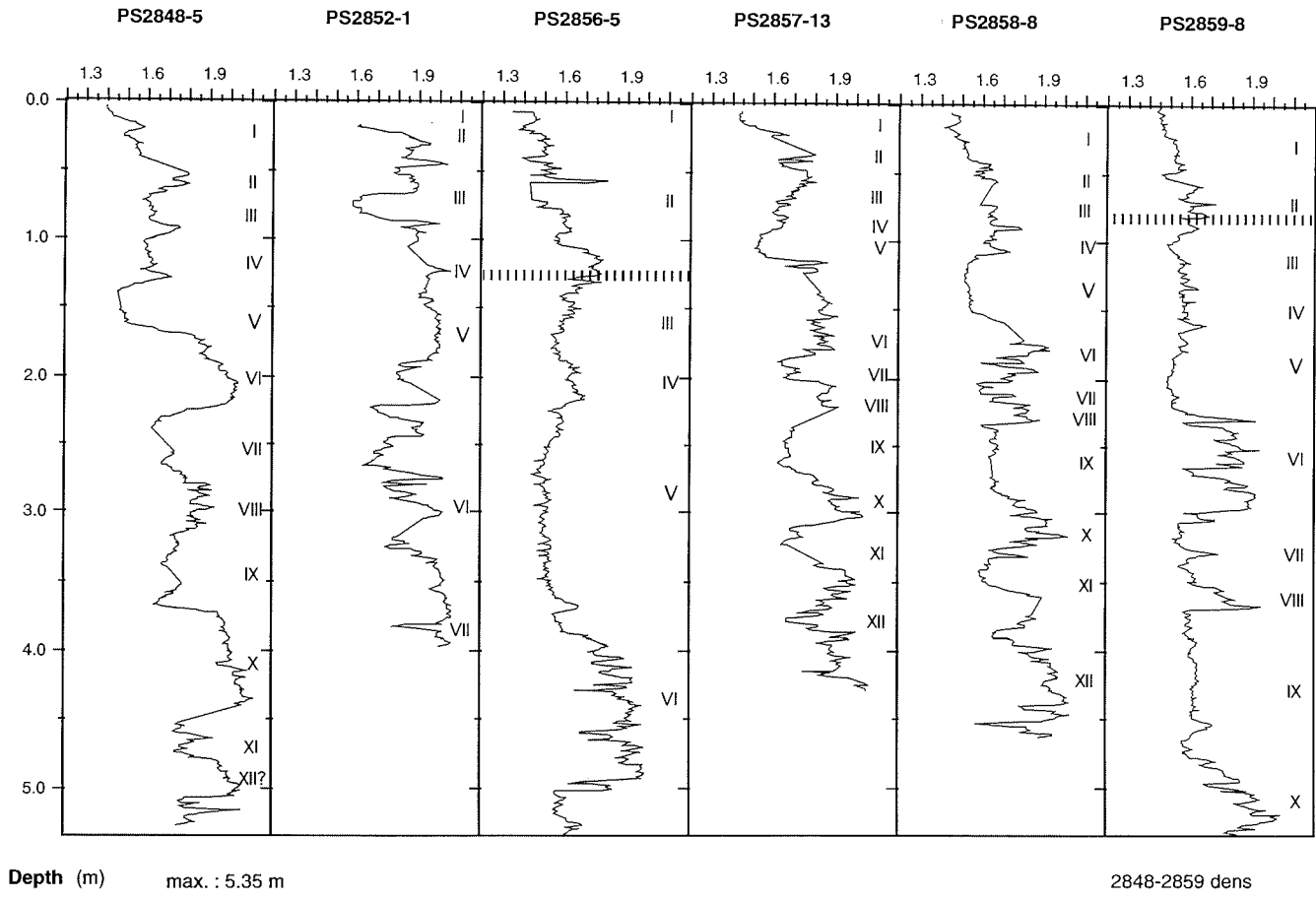


Fig. 7.10: Lateral correlation of wet bulk density data (MSCL) of cores from transects C and D. Roman numerals indicate estimated preliminary oxygen isotope stages as described in Chapter 7.4. Note that cores PS2748-5, PS2757-13 and PS2758-8 were not opened and described yet.

7.4 Lithostratigraphy and Sediment Characteristics (C.J. Schubert, J. Knies, M. Levitan, E. Musatov, R. Stein)

In the following we describe the lithostratigraphy and sediment characteristics of surface, near surface (box cores), and longer sediment sequences (gravity and kastenlot cores). Detailed description of the cores are shown in the annex (Chapter 10.3).

Surface Sediments

Surface Sediments of the Transect from the Svalbard Continental Margin to the Greenland Continental Slope (Transect B)

During transect B fourteen box cores were recovered (Station PS2830 to Station PS2847, Fig. 7.11). All surface sediments show a dark grayish brown to yellowish brown to brown colour, and mainly all of them vary from clayey silt to silty clay. Only at core locations near to northern Svalbard (PS2830 and PS2831) and close to the Greenland slope (PS2843, PS2846) coarser sediments, i.e., with a higher sand content, were recovered. Biogenic components which were found in the coarse fraction ($> 63\mu\text{m}$) are listed in Table 7.6. Worm tubes from polychaetes are the dominant component in the surface sediments of core PS2829 from northern Svalbard, and cores PS2836, PS2838, and PS2839 from the Yermak Plateau, whereas in the most western cores from the Fram Strait area and the Greenland continental slope planktic foraminifers and sponges (PS2842) show the highest abundance. Calcareous benthic foraminifers were found in each surface sediment sample, whereas agglutinated foraminifers seem to be restricted to the Yermak Plateau. The relation between biogenic components and rock fragments varies from 95:5 in sediments from the western Yermak Plateau to 20:80 in sediments from the Western Fram Strait (Table 7.6). No general trend between the different core locations could be observed. Highest dropstone abundances (rock fragments $>1\text{mm}$) were recognized on the Yermak Plateau (PS2836) and on the Greenland slope (PS2846). On the Yermak Plateau this seems to be related to higher bottom water current speed which eliminates finer particles, and therefore, enriches the coarser fraction. On the Greenland slope the higher dropstone abundance may represent the proximity to Greenland with its high glacier occurrence, and therefore, high sediment input via icebergs. In the composition of the dropstones, differences occur between the cores east of the Yermak Plateau and those west of the Yermak Plateau. Whereas in the eastern cores sandstones, schists, and siltstones dominate the dropstone assemblage, the western cores are dominated by metamorphic rocks, quartzites, and basalts. The latter are common on Greenland (especially basalt in northern Greenland) and could be used as a hint to the origin of these stones. Siltstones and sandstones, on the other hand, are especially enriched in formations around the Svalbard area. At core location PS2846 the surface was completely covered with mud pebbles and boulders (quartzites, basalts, and black sandstones) both indicative for sea-ice and/or iceberg transport.

Table 7.6: Composition of coarse fraction (>63µm) of surface sediments PS2829 to PS2848.

	Western Fram Strait PS2848 (2628m)	Greenland slope PS2846 (532m)	Western Fram Strait PS2842 (3216m)	West of Yermak Plateau PS2838, PS2839 (2226, 2905m)
biogenic particles	plankt. forams, polychaetes, calc benth. forams, sponges,	plankt. forams, calc. benth. forams, sponges	sponges, plankt. forams, calc. benth. forams	polychaetes, agglut. benthic forams, calc. benth. forams, sponges, plankt. forams
biogenic/rock particles	90:10	40:60	20:80	95:5
rock assemblage	/	metamorphic rocks, schists, quartzites	metamorphic rocks quartzites, basalt	quartzites, basalt
dropstone abundance	/	++	-	--
grain size	fine	coarse	fine	coarse/fine
	Yermak Plateau PS2836 (635m)	East of Yermak Plateau PS2832 (2070m)	off Svalbard PS2829 (450m)	
biogenic particles	polychaetes, plankt. forams, agglut. benthic forams, bivalves, calc. benth. forams, sponges	calc. benth. forams, agglut. benthic forams, sponges, polychaetes	polychaetes, bivalves, sponges ostracodes, calc. benth. forams	
biogenic/rock particles	80:20	85:15	60:40	
rock assemblage	sandstones, schists, siltstones	sandstones, schists, shales, quartzites	sandstones, schists	
dropstone abundance	++	n.d.	n.d.	
grain size	medium	coarse	coarse	

Table 7.7: Composition of coarse fraction (>63µm) of surface sediments PS2849 to 2860.

	Western Fram Strait PS2849 (3261m)	Western Yermak Plateau PS2853 (2061m)	Western Yermak Plateau PS2855, PS2856 (1455m, 929m)	Yermak Plateau PS2857 (824m)
biogenic particles	plankt. forams, calc. benth. forams, aggl. benth. forams, sponges, bivalves	plankt. forams, sponges, calc. benth. forams, aggl. benth. forams	agglut. benthic forams, plankt. forams, calc. benth. forams, sponges	plankt. forams, sponges, agglut. benthic forams, calc. benth. forams, bivalves
biogenic/rock particles	90:10	30:70	20:80	70:30
rock assemblage	/	/	quartzites	quartzites
dropstone abundance	/	/	/, --	-
grain size	fine	medium	fine, medium	medium
	Yermak Plateau PS2858 (939m)	Eastern Yermak Plateau PS2859 1197m)	Eastern Yermak Plateau PS2860 (1993m)	
biogenic particles	plankt. forams, agglut. benthic forams, sponges, calc. benth. forams, bivalves	planktic forams, sponges, agglut. benthic forams, calc. benth. forams, bivalves	planktic forams, aggl. benth. forams, calc. benth. forams, sponges, bivalves	
biogenic/rock particles	80:20	80:20	50:50	
rock assemblage	quartzites	quartzites	quartzites	
dropstone abundance	+	-	+/-	
grain size	medium	fine	fine	

Surface Sediments of the Transect from the Greenland Continental Slope to the Svalbard Continental Margin (Transects C,D)

During transects C and D 13 box corers were recovered (PS2847 to PS2861, Fig. 7.12). All surface sediments from stations PS 2847 to PS2857, i.e. from Fram Strait to the top of the Yermak Plateau, show a yellowish brown to brown colour, whereas stations PS2858 to PS2861 from the eastern Yermak Plateau show dark grayish colours. Sandy silty clays, clays (PS2854), and foram-rich mud (PS2850) with bioturbated surfaces are indicative for the western cores. Bioturbated sandy silty clays were described for surface sediments of the eastern cores. Highest biogenic abundance was recognized in the western Fram Strait (PS2849; 90:10, biogenic:rock particles) which most likely is the result of open-water conditions, and at the more shallower stations of the eastern part of the Yermak Plateau (Table 7.7). In all but stations PS2855 and PS2856 where agglutinated benthic foraminifers dominated the biogenic components, planktic foraminifers were found as the dominant biogenic component. Other biogenic components were calcareous benthic foraminifers, sponge spicules, and bivalves in varying composition. Polychaetes, a major component in surface sediments of transect B, are missing. Interestingly, no rock fragments were found in the western surface sediments (PS2849, PS2853). In the more eastern surface sediments only quartzites as bigger rock fragments (dropstones?) were recognized. In general, it seems that surface sediments of transects C and D are somewhat finer than surface sediments of transect B.

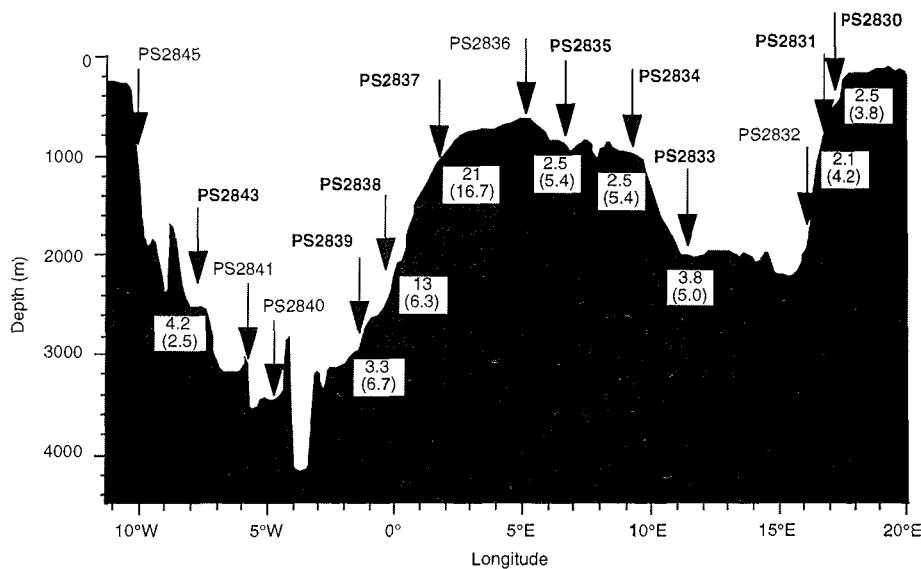


Fig. 7.11: Depth profile of transect B showing geological stations with estimated Holocene and -in parentheses- Stage 2 sedimentation rates (cm/ky). Bold numbers indicate positions where gravity- or Kastenlot-cores were taken.

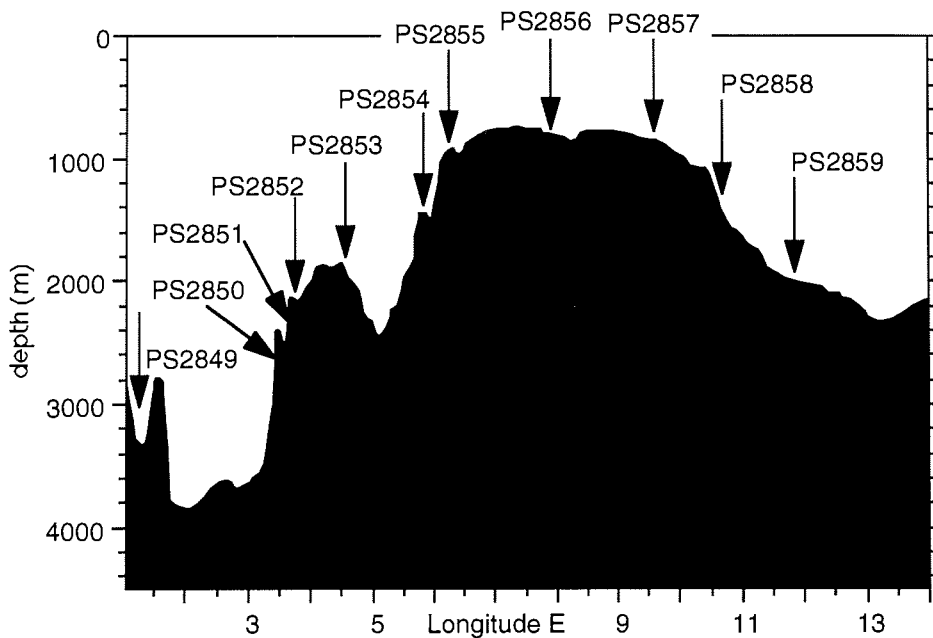


Fig. 7.12: Depth profile of transect D showing geological stations.

Surface Sediments North of Svalbard and Molloy Deep

Dark brown bioturbated sandy silty clays are indicative for surface sediments north of Svalbard (PS2862-PS2867; Fig. 7.6). Surface sediments of the Molloy Deep are very dark grayish brown silty clays, and bioturbation is missing indicating the absence of benthic organisms.

Near-Surface Sediments (Box Cores)

Giant box core sediments were recovered on all transects (81-82° N) across the Yermak Plateau to the eastern Greenland margin and in the Molloy Deep (Fig. 7.6). As a first result, we suggest that all sedimentological characteristics can be related to typical environmental settings of the northern Greenland/ Norwegian Sea.

Yermak Plateau and Northern Svalbard Margin

Uppermost sediments on the Yermak Plateau and the northern Svalbard margin are very soft, bioturbated and of dark brown to dark yellowish brown colour. Beyond, a very distinct layer of well consolidated silty clayey mud was often described as hard ground sediments (Fig. 7.13). These deposits indicating a very low rate of sedimentation are remarkably oxidized and contain a few amount of ice-rafted material. The lowermost mostly homogenous sediments are of dark gray to grayish brown colour and are slightly enriched in ice-rafted material. In contrast to sediments from the East Greenland margin foraminifers are very rare throughout the cores.

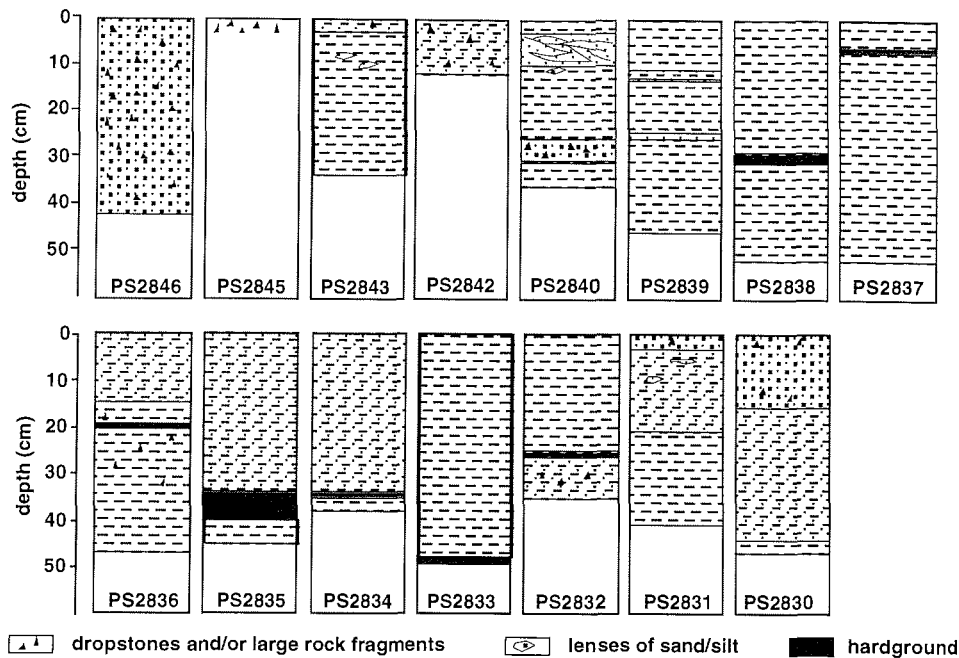


Fig. 7.13: Lithology of box cores (GKG) of transect B.

A short transect from the Yermak Plateau to the northwestern coast of Spitsbergen indicates typical sedimentological and geochemical features. The uppermost centimeters are characterized by very soft, bioturbated and brown colours indicating well oxygenated bottom waters. A decrease in thickness from 6 to 3 cm is observed from the lower to the upper slope. Beyond this distinct layer we described a very homogenous, dark gray to gray sequence of silty clay mud, which may indicate suboxic conditions due to enhanced degradation of marine organic matter.

Fram Strait

Deep-sea sediments in the Fram Strait area were often described as ranging from clay to silty clay. They are mostly homogenous and very soft. The colour often had a yellowish brown to brown touch. The sediments are mostly rare of ice-rafted material, only turbidite-like deposits of well-sorted, coarse-grained sand are interbedded. Throughout the cores numerous foraminifers are obvious.

In the southern Fram Strait, the deepest box core (5416 m) taken during the ARK-XIII/2 cruise, was recovered in the Molloy Deep. Similar to deeper stations in the northern Fram Strait, sediments were very soft and of grayish to brown colour. Classical turbidite sequences were observed throughout the core with typical fining-upward structures.

East Greenland Margin

A remarkable amount of ice-rafted material and rock fragments up to 20 cm in diameter (basalts and metamorphic rocks) were found in near-surface sediments on the East Greenland continental margin. The material is mostly sub- or non-rounded. The sediments were described as silty sand with significant amounts of gravel and dropstones which indicate the nearby glacial transport by sea ice and icebergs. Sediments were of brown colour, indicating well-oxygenated bottom waters. Finer particles are eliminated due to enhanced bottom water current speed. Surprisingly, a lot of benthic and planktic foraminifers were observed in surface sediments and throughout the cores indicating seasonally open-water conditions and moderate surface-water productivity.

Longer Sediment Sequences (Gravity- and Kastenlot-Cores)

Ten of the longer sediment cores were opened and described in detail using smear-slide (see Table 10.4, Chapter 10.3) and coarse-fraction analyses. For correlation of the cores the logging data were consulted (see Chapter 7.3). As mentioned above, it is possible to classify the study areas in different sedimentological environments (Northern Svalbard, Yermak Plateau, Fram Strait, and Greenland continental slope). Since we have only recovered one core (PS2839-5) from the Fram Strait area in close proximity or even on the western flank of the Yermak Plateau it is discussed together with the Yermak Plateau cores.

Northern Svalbard, Yermak Plateau, and Fram Strait

The cores taken in this area (stations PS2830 to PS2839 on the southern transect B and PS2856 and PS2859 on the northern transect D) are characterized by clay, clayey silt or sandy silty clays. Layers dominated by sands only occur in core PS2830-5 at about 250 cm core depth expressing the proximity to the continental margin of Svalbard with high direct input of coarse-grained material (Fig. 7.14). It is obvious that the cores recovered in greater distance from the coast (PS2834-5, PS2835-6, PS2837-5, and PS2839-5) show higher contents of clay. The sand content decreases to < 25%, mainly < 10%, and the silt content varies between 10 and 40%. Sediment colours vary from dark gray over brown and yellowish brown, to olive brown. Colour banding is quite common in all of the cores. Numerous dropstones were recognized in all cores which indicates the input by sea ice or icebergs. Dropstones in this area, in comparison to the western cores from the Fram Strait and Greenland margin where basalts and metamorphic rocks occur, are dominated by sandstones, claystones, and shales. Metamorphic rocks only occur sporadically. This gives a first hint on the origin of the dropstones, i.e. metamorphic and basalts indicate supply from the Greenland margin, whereas other stones originated from Svalbard or the Siberian side of the Arctic Ocean.

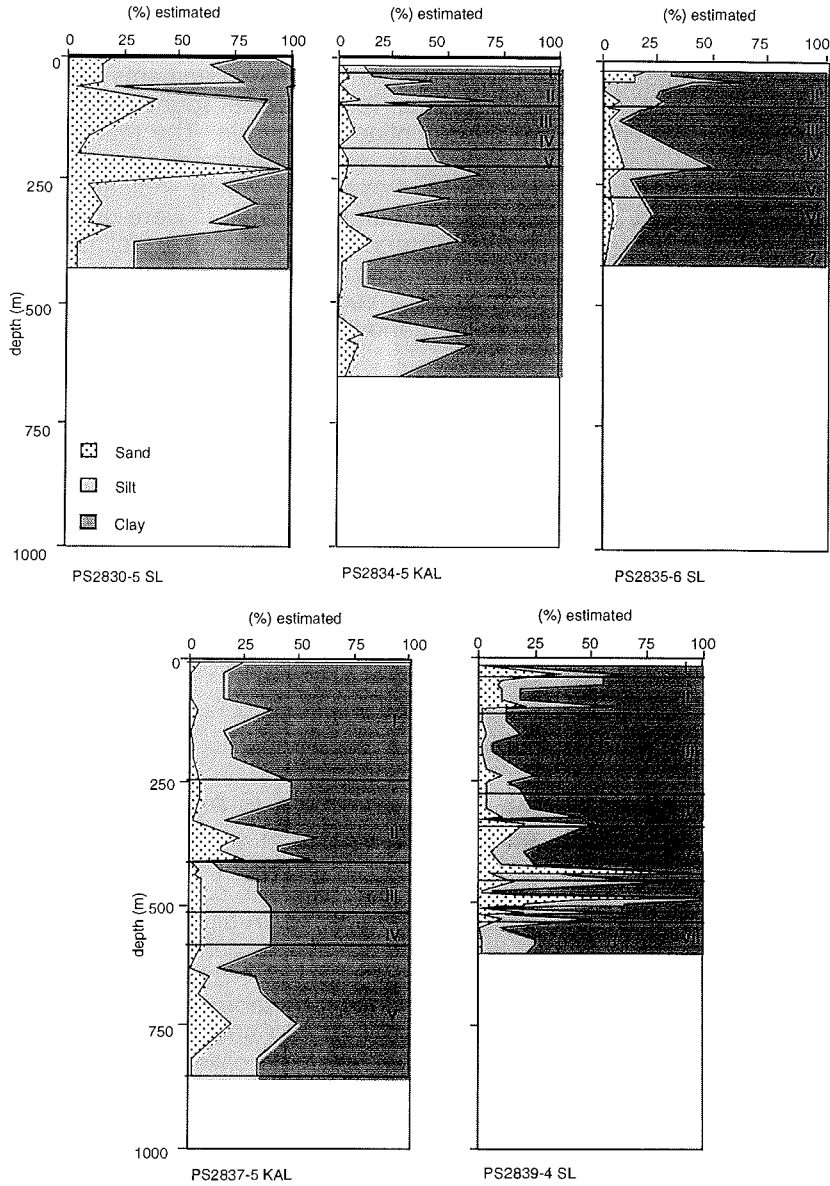


Fig. 7.14: Estimated grain-size distribution from smear-slide analyses of gravity and kastenlot cores from transect B. Numbers indicate oxygen isotope stages; stratigraphy is based on lithology, biogenic abundance and assemblages, and core logging data.

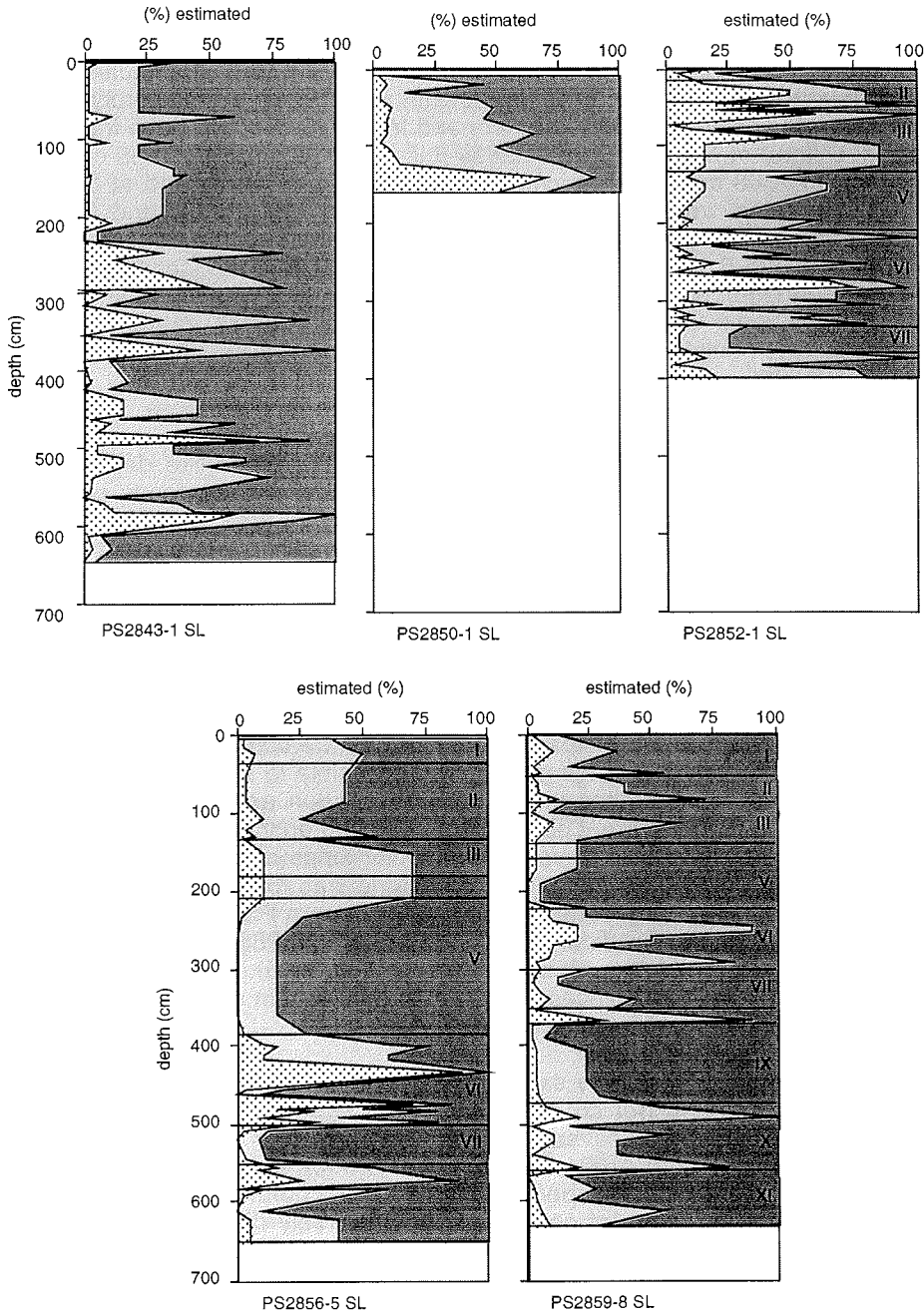


Fig. 7.15: Estimated grain-size distribution from smear-slide analyses of gravity and kastenlot cores from transect D. Numbers indicate oxygen isotope stages; stratigraphy is based on lithology, biogenic abundance and assemblages, and core logger data.

Core PS2830-5 shows mainly dark brown or grayish brown colours. The surface is bioturbated and weak mottling is seen in the uppermost 50 cm. Dropstones occur in 2 cm (red claystone), 31 and 41 cm (dark gray quartzites?), 66 cm (black shale), 348 cm (black claystone), and 395 cm (metamorphic rock). Lamination is shown from 53 to 163 cm and from 316-378 cm. Shell fragments were described at 325 cm. Core PS2834-5 is highly bioturbated (0-35 cm, 120-232 cm, 260-368 cm, 483-508 cm, 521-525 cm, 543-574 cm and at 602-612 cm). Dropstones were found at 93 cm, 104 cm (claystone), and 395 cm (sandstone). Shell fragments occur at 278 cm, foraminifers and shells at 286-310 cm. PS2835-6 shows dropstones at 192 (shale?), 365 cm (sandstone), and 494 cm (quartzite). A sulfidic lense of 0.6 cm in diameter was found at 435 cm. PS2837-5 reveals only one dropstone at 412 cm (black sandstone), but numerous black sulphidic spots are common in a dark olive silty clay interval from 207 to 386 cm. Core PS2839-5 shows some intervals with silty sand or sand and is therefore slightly more coarse-grained than core PS2837-5. Several dropstones were found in this core at 39 cm, 102 cm, 164.5 cm, 249 cm, 292 cm, 306 cm, 325 cm, 382 cm, and 470 cm. Turbidite-like deposits are common from 508 to 440 cm. The high occurrence of dropstones could be explained by the proximity to the Greenland coast, an area with high iceberg calving. The turbidite-like structures seem to be either related to the core location on the Yermak Plateau slope with sliding from the top of the plateau or with high current speeds in this relatively narrow strait.

Core PS2856-5 from the northern transect D includes coarser sediments (Fig. 7.15), i.e., contains more sand than the southerly cores. Only below 587 cm a finer silty clay layer occurs. This may be related to the exposed position of the core on top of the Yermak Plateau where currents are common, eliminating the more fine-grained material. Until now, it is not possible to say whether the sand layers described as turbidites in the core description are really turbidites or layers related to higher current speed. More detailed onshore investigations are necessary. In 203 to 225 cm a vertical triangular lense of silty clay may be the relict of a huge polychaete trace. One dropstone was found at 422 cm (4x4x1 cm, black sandstone). In general, the sediments in core PS2859-8 from 2000 m water depth are somewhat finer than those in core PS2856-5. Nevertheless it contains numerous turbidites (?) below 234 cm (Fig. 7.15). Dropstones occur at 270 cm and 576 cm. Coal pieces of 0.5 cm and 1.2 cm in diameter were found at 494 cm and 503 cm, respectively.

In all of the cores, a dark gray sandy silty clay layer containing one or several dropstones, was found (for correlation of cores see Fig.7.16). This layer has been already described by several authors who worked on cores from the Fram Strait area (Hebbeln et al., 1994; Elverhøi et al., 1995). In these publications the layer is characteristic for a period with high accumulation rates and the presence of high amounts of organic matter. Sparsely distribution of planktic foraminifers at the beginning of this layer indicates a permanently closed sea-ice cover. Higher C/N ratios than in the previous period suggest a shift in the provenance area. The high amount of organic-rich material is related to an input of Jurassic rock fragments from the Spitsbergenbanken and the central Barents Sea. Therefore, it is assumed that the Barents Sea Ice Sheet extended beyond the present day coast line onto the shallow shelf and high amounts of fine-grained terrigenous material were supplied at that time. Increased amounts of IRD are interpreted as higher calving rates of the ice sheet when reaching deeper parts of the Barents Sea. The age of this layer was determined in

several cores and lies between 21 and 23 kyr. Above this layer a sediment sequence with cottage cheese structure was observed in our cores and interpreted as a time with high input of particles from sea ice during melting processes.

The comparison and correlation of the cores using smear-slide and coarse-fraction data, lithological description, and core logging data with published core data from this area allowed to establish a first stratigraphic model which is incorporated in the grain-size distribution figure (Fig. 7.14 and 7.15). Numbers indicate oxygen isotope stages 1 to 6 (below stage 6 the determination of age boundaries becomes extremely difficult because no comparison with published cores reaching only until stage 6, was possible). Nevertheless, in core PS2856-5 we assume the sediment sequence to reach back as far as oxygen isotope stage 11 (Fig. 7.15). According to the logging data, the (not-opened) cores PS2848-5, PS2857-13, and PS2858-8 may even reach back as far as oxygen isotope stage 12 (cf. Fig. 7.10).

Besides core PS2837-5 showing very high sedimentation rates all other cores display very similar sedimentation rates during the different oxygen isotope stages. In Figure 7.17 a comparison between core PS1295-5 from the Fram Strait area, which was dated by oxygen isotopes and AMS ^{14}C methods, and two cores from this expedition is shown. The good correlation between core PS1295-5 and core PS2839-4 is obvious and, thus, gives confidence in our age model. Also the very high sedimentation rates of core PS2837-5, most likely induced by sliding from the top of the Yermak Plateau or transport by currents to this position, is obvious. In Figure 7.11 estimates of sedimentation rates during the Holocene and oxygen isotope stage 2 for selected cores from transect B are shown. In general, Holocene sedimentation rates for the Yermak Plateau cores show values between 2.1 and 3.8 cm/kyr; PS2837-5, however, has much higher sedimentation rates (21 cm/kyr). In oxygen isotope stage 2 sedimentation rates are usually higher (3.8 to 5.4 cm/kyr), only core PS2837-5 has a somewhat lower sedimentation rate (16.7 cm/kyr) than in the Holocene.

Based on our age model, the results of smear-slide analyses (see Table 10.4, Chapter 10.3) and the information we obtained from previous publications (Hebbeln et al. 1997, Elverhøi et al., 1995) the following paleoceanographical reconstruction is possible. It has to be taken into account, however, that no oxygen isotope stratigraphy exist so far; all statements are therefore preliminary. In general, the cores from the southerly transect B (PS2837-5 and PS2839-4) show much higher abundances of coccoliths (also abundances of foraminifers seem to be higher) than in the cores from the northern transect D (PS2856-5 and PS2859-8). This may indicate that, although there is only a 1° shift in latitude, the inflowing Atlantic water mass was weakening drastically and regions with open water were diminished giving rise to decreasing abundances of foraminifers and coccoliths. To support this assumption more detailed quantitative analyses of the cores have to be performed. In the southerly cores the abundance of ice-rafted debris (IRD) and/or rock fragments are of minor importance; only in stage 6 we found higher abundances (Fig. 7.18). This is explained by a much broader and thicker ice coverage especially over the shelves and adjacent land areas (high iceberg production) than for instance during the last glacial period (stage 2). During the uppermost stage 5 and 3 also a slightly increased dropstone occurrence was recognized (no sample of stage 4 was examined).

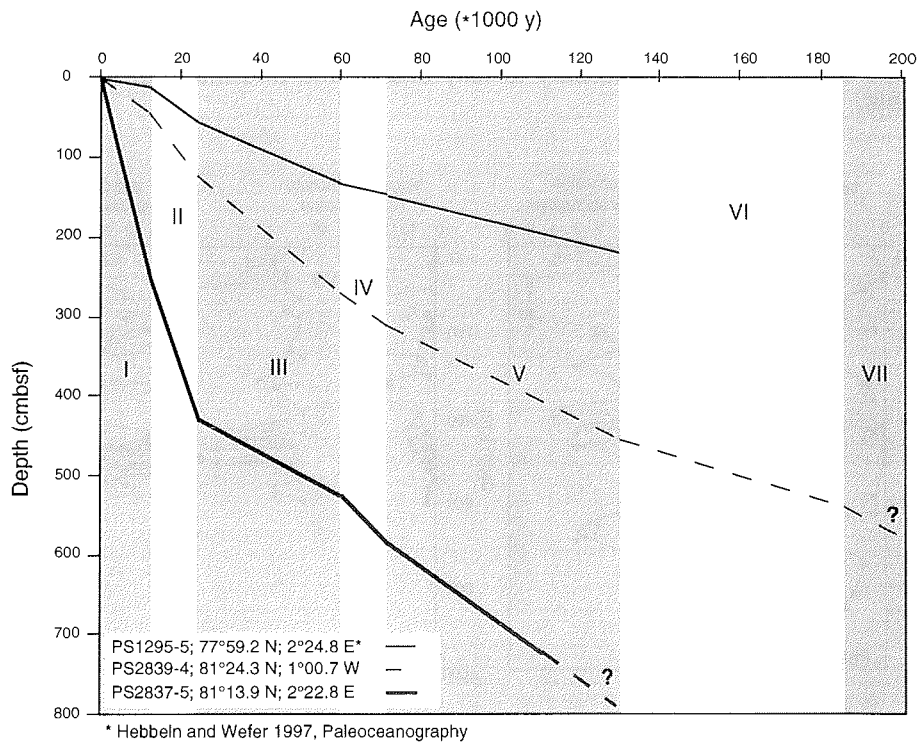


Fig. 7.17: Age-depth diagram of cores PS1295-5, PS2839-4, PS2837-5. Roman numbers indicate oxygen isotope stages.

In the northern cores much higher abundances of dropstones/rock fragments were observed (Fig. 7.19). Additionally, the glacial/interglacial pattern is much better reflected. During glacial stages the abundance of dropstones/rock fragments is much higher (especially stage 2, 6, and 10), whereas during interglacials the amount is diminished. Biogenic components like foraminifers and coccoliths in the southern cores are high during stage 5, especially in the uppermost part (5a?), in stage 2 and in the lowermost Holocene. During these times the inflow of warm Atlantic water diminished the ice cover and open water areas gave rise to higher biogenic production. In general, there is also a good agreement between foraminifers and coccoliths, especially in core PS2837-5. In some periods, however, differences in abundances of foraminifers and coccoliths occur. For instance, during stage 6 and 7 short pulses of high coccolith abundance were not accomplished by higher occurrences of foraminifers in core PS2839-4. This may be explained by only very short periods of open water, i.e., weak inflows of Atlantic water. In core PS2856-5 coccolith abundances are especially high during stage 2, 5, and 7, but also during the lowermost stage 6 and uppermost stage 3 higher abundances were observed. The foraminifers abundance follows the coccolith one. This can be interpreted that Atlantic water still reached areas as far north as this position during these periods. In the more western core PS2859-8 high abundances of biogenic components were observed during stage 2, 7, 9, and 10. In the lower

part of this core (below stage 6), however, the stratigraphic model is weak and should not be overinterpreted. Further investigations, especially an oxygen isotope stratigraphy, is necessary to fully understand and interpret the given signals.

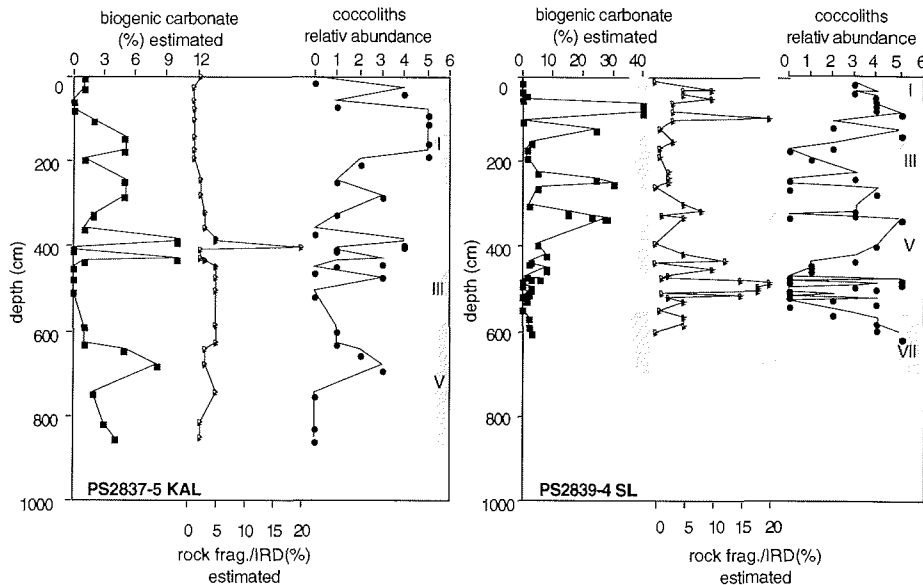


Fig. 7.18: Estimates of biogenic carbonate, coccolith abundances, and rock fragments, based on smear-slide counts.

One objective of the expedition was to recover older (Tertiary) pre-glacial sediments cropping-out at the eastern part of the Yermak Plateau. Two gravity cores PS2850-1 and PS2852-1 were taken for this purpose. The main difference between core PS2850-1 and the other cores is the stiffness of the sediments implying a much higher consolidation of the sediments. Below 9 cm of soft brown sediments (Holocene), very stiff, colourful sediments were recovered. More coarse-grained material was found from 130 to 150 cm. Smear-slide investigation revealed only sparse amount of foraminifers in the uppermost centimeters, coccoliths were completely absent which made an age estimation impossible. Further investigations may reveal an older age but until now no conclusion about the age could be drawn.

Core PS2852-1 was recovered at a very steep slope position which is obvious from the inclined lithological boundaries (angle 8°). It is characterized by changes of clayey silt, silty sand and sandy silt. It shows the same pattern as the other cores from the northern transect D (Fig. 7.17). Additionally, it could be correlated with the other cores by lithology, wet bulk density and magnetic susceptibility. Thus, an older age of this core sequence is less probably.

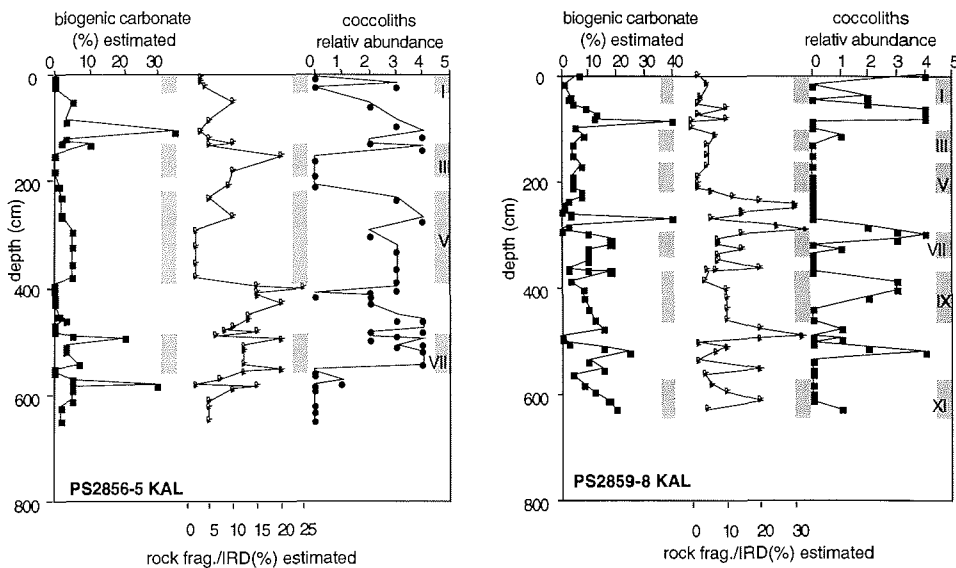


Fig. 7.19: Estimates of biogenic carbonate, coccolith abundances, and rock fragments of cores PS2856-5 KAL and PS2859-8 SL, based on smear-slide counts.

Greenland Continental Slope

Sediments recovered from the Greenland continental slope look completely different from those recovered from the other areas. Whereas sediments from the area off Svalbard, Yermak Plateau, and Fram Strait are dominated by brown to gray colours, the sediments from the east Greenland continental slope show more reddish brown and olive green colours. The marker horizon determined in all long sediment cores from the Svalbard to Fram Strait area is also missing in core PS2843-1. Therefore, it was not possible to correlate the Greenland continental slope core with the other cores. The more reddish colours can be related to input of material from Greenland where Devonian red shales are known. Smear-slide investigations revealed coccolith abundances only until 120 cm core depth; below they were absent which also shows the independent character of this core. In general, sediments were much coarser mainly below 220 cm and revealed more sandy silts and silty sands than cores from the other regions (Fig. 7.17). Turbidites, especially below 480 cm, are common and indicate direct input from the continental shelf or slope areas. Dropstones were found in 249 cm (7x5x2 cm, well rounded black shale), 456 cm (1.5x1x0.2, black shale), and 468 cm (2x1.5x0.3 cm, well rounded gray sandstone).

7.5 Aerosols

(V. Shevchenko)

Numerous studies have shown that aerosols in the Arctic are of importance for atmospheric chemistry and climate (e.g., Barrie, 1986). But up to now aerosols in the marine boundary layer in the high Arctic have been studied little. Here, preliminary results of the studies of aerosol size distribution over the NW Barents Sea and Fram Strait are presented. 66 measurements were carried out during the ARK-XIII/2 Expedition (Fig. 7.20).

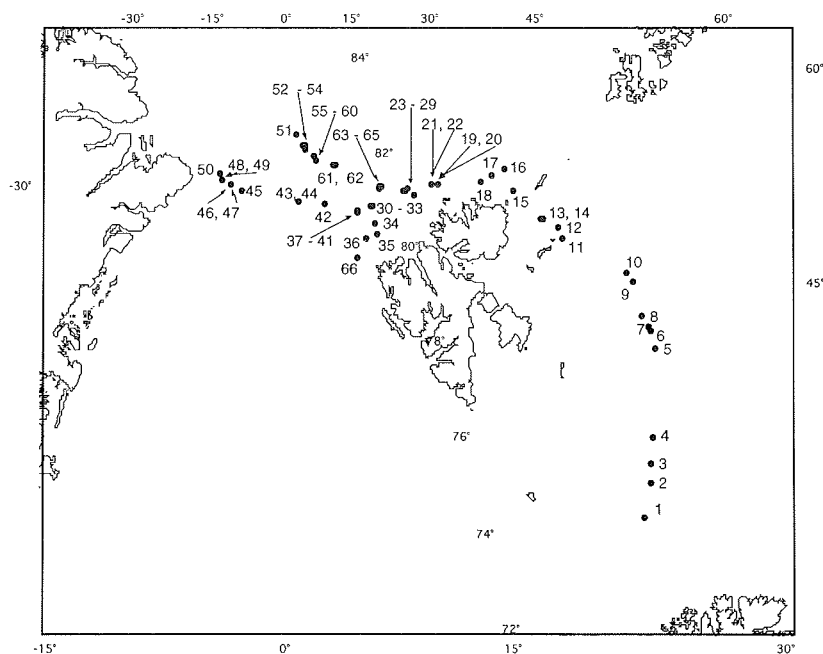


Fig. 7.20: Aerosol sampling stations.

In general, there is a much greater number of small particles (with sizes from $0.5 \mu\text{m}$ to $2 \mu\text{m}$) in comparison to large particles, as it is described elsewhere (O'Dowd et al., 1997). The observed particle size spectra are generally conservative to changes of temperature, relative humidity, wind velocity and direction. However, over the open water in the NW Barents Sea an increase of the wind velocity stimulates the concentration growth of coarse ($>5 \mu\text{m}$) particles in the spectrum (Fig. 7.21 and 7.22). This could testify the input of sea salt particles from the sea surface microlayer by wind and the importance of these particles for the chemical composition of marine aerosols, as it has been shown in other regions (O'Dowd et al., 1997). We will identify the input of wind blown sea salt after the elemental analysis of aerosol samples in the home laboratory.

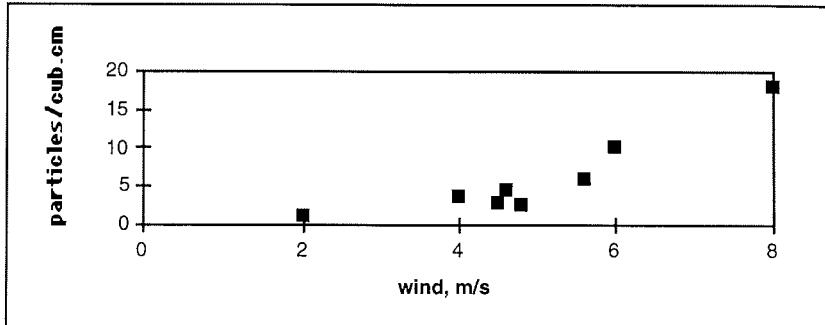


Fig. 7.21: Correlation between wind velocity and concentration of aerosol particles $> 5 \mu\text{m}$ in the northwestern Barents Sea.

In ice-covered areas we find an increase of concentrations of fine particles (from $0.5 \mu\text{m}$ to $2 \mu\text{m}$), especially at low temperature (Fig. 7.22). Growth of concentration of particles from $1 \mu\text{m}$ to $2 \mu\text{m}$ at temperature of about -3°C can be explained by formation of ice microcrystals. A more detailed study of the parameters of aerosol size distribution and controlling factors will be carried out later in comparison with other areas.

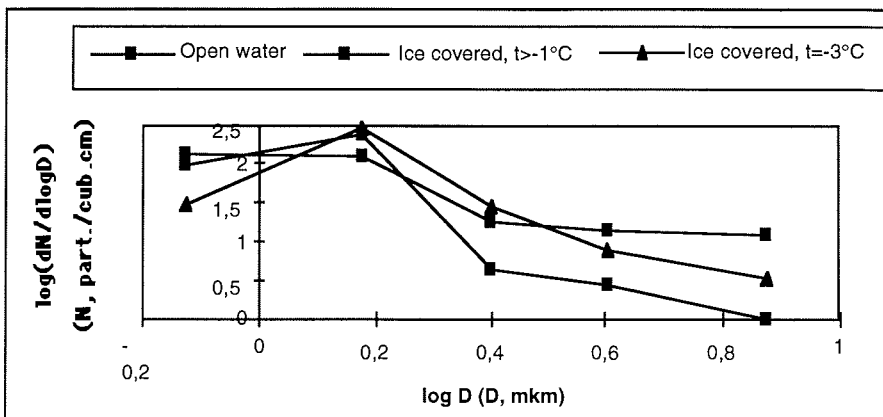


Fig. 7.22: Typical particle size distribution in the study area. Series: 1 - over the open water; 2 - over the ice covered sea, $t > -1^\circ\text{C}$; 3 - over the ice covered sea, $t = -3^\circ\text{C}$.

8 Geochemistry (M. Rutgers v.d. Loeff, E. Damm, M. Kühn, A. Maibaum)

8.1 Early Diagenesis

The rates of early diagenetic reactions within the surface sediment were and will be measured by profiles of oxygen and the trace metals in the pore water of the sediment.

8.1.1 Trace Metals (M. Kühn)

A large fraction of biogenic detritus reaching the sea-floor is degraded directly at the sediment-water-interface (Bender & Heggie, 1984). This decomposition of organic matter results in a release of the adsorbed and incorporated metals into the overlying bottom water (see also 8.2.3.1) as well as into porewater. The process of metal uptake from porewater seems to be the primary link between particulate flux and metal accumulation in the sediment, thus decoupling transport from burial processes for many trace metals. Once liberated into porewater, the mobility of a particular metal depends on its chemical characteristics, the prevailing redox conditions, the chemical composition of the porewater and the nature of the particulate phases present in the sediment.

The studies of the trace metals in the pore water of the samples from ARK-XIII/2 will be performed from multicorer samples. The pore water of the first three cm on the top of the sediment was gained with the help of a centrifuge. The acidified samples will be analysed by trace-matrix-separation combined with ICP-MS and AAS. The results will help to interpret the processes occurring in the benthic nepheloid layer which was the main focus concerning the trace metal behaviour during the cruise (see 8.2.3.1).

8.1.2 Oxygen (E. Damm)

Aerobic respiration dominates the remineralisation of organic matter in Arctic sediments. Thus oxygen uptake is controlled by the availability of degradable organic matter in the sediment.

O₂ profiles were measured in MUC-cores of 24 stations with water depths ranging from 255 m to 5500 m (Annex Table 10.3). Immediately after the return of the multicorer on deck, the cores were brought into the cooled laboratory and measured by using a commercial microelectrode (type 737 Clark style micro-oxygen-electrode). The sediment cores were split into 1-2cm slices and centrifuged. The pore water was collected and filtered (pore diameter 0.45 µm) from equivalent levels from two or three cores. Then pore water samples were frozen for later analysis of nutrients.

Oxygen penetration depths are indicated in the measured profiles (Fig.8.1).

Steep gradients of O_2 concentration were only measured at the shallow stations of the Svalbard shelf. There, O_2 was depleted and the suboxic zone was reached after 1-3 cm. This region is influenced by Atlantic water masses with a higher supply rate of organic matter and a higher benthic flux (see Chapter 5.5).

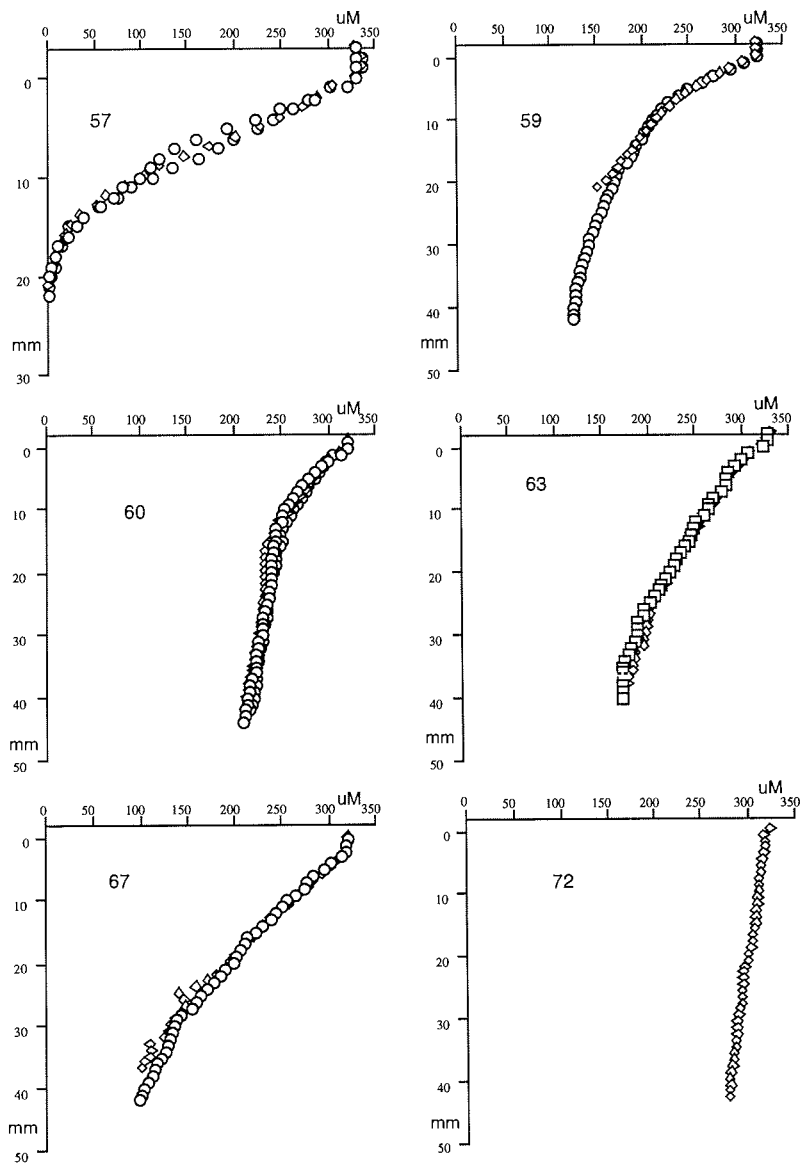


Fig. 8.1: Oxygen concentration profiles in sediments at the transect B from the Svalbard shelf to the Greenland shelf

At the slope stations O_2 was not completely consumed (Fig. 8.1). This type of profile is caused by a low input of organic matter, all of which is degraded in the oxic zone of the sediment. The weakest gradients were determined at the deepest part in the western Fram Strait. This region is dominated by the outflow of cold Arctic deep water and is characterized by a limitation of supply of organic matter (Fig. 8.1) (see Chapter 4). The profiles of O_2 concentration show some differences between the western and the eastern part of the Yermak Plateau. These different degradation rates could be created by the West Spitsbergen Current and processes described below (see 8.2.1 transmissiometry).

8.2 The Benthic Nepheloid Layer (M. Rutgers v.d. Loeff)

The bottom water of the ocean often has a somewhat higher load of suspended particles than the clear water at intermediate depths. On one hand this may imply that there is an important long-range transport of sediments by bottom currents. On the other hand, there may be a continuous exchange of these suspended particles with the seafloor by resuspension and settling. In any case, early diagenetic reactions usually taking part in the surface sediment are known to start to a certain extent already in this early near-bottom suspended phase. Thus, the occurrence of a benthic nepheloid layer (BNL) and the dynamics of the particles at the sediment-water interface have implications for long-range particle transport and for sediment-water exchange and early diagenetic reactions.

8.2.1 Transmissiometry (M. Rutgers v.d. Loeff)

We measured the distribution of the BNL by monitoring the light transmission with a Chelsea transmissometer mounted on the Rosette and connected to the CTD. The system worked very reliably and the data have been used throughout as a selection criterion for water sampling. According to Gardner et al. (1993) there is a good linear relationship between beam attenuation and suspended load. However, the slope of the relationship does depend on the type of particles. Using Gardner's algorithm for the NE Atlantic, we have preliminarily converted the data to suspended load. The data may have to be adjusted after weighing of our filters at AWI. A BNL was observed at nearly all stations.

In the open ocean, the calibration according to the Gardner algorithm can make use of the transmission in the clear water minimum as the transmission of virtually particle-free water. In the Barents Sea, transmission similarly reached a maximum between the plankton-dominated upper water layer and the BNL, but this maximum was lower than measured in clear open-ocean water of intermediate depths. Consequently, the conversion of transmission values to suspended load had to be based here on transmission measurements in air and on the observations later on in the open ocean. The clear-water transmission readings of the instrument were very stable.

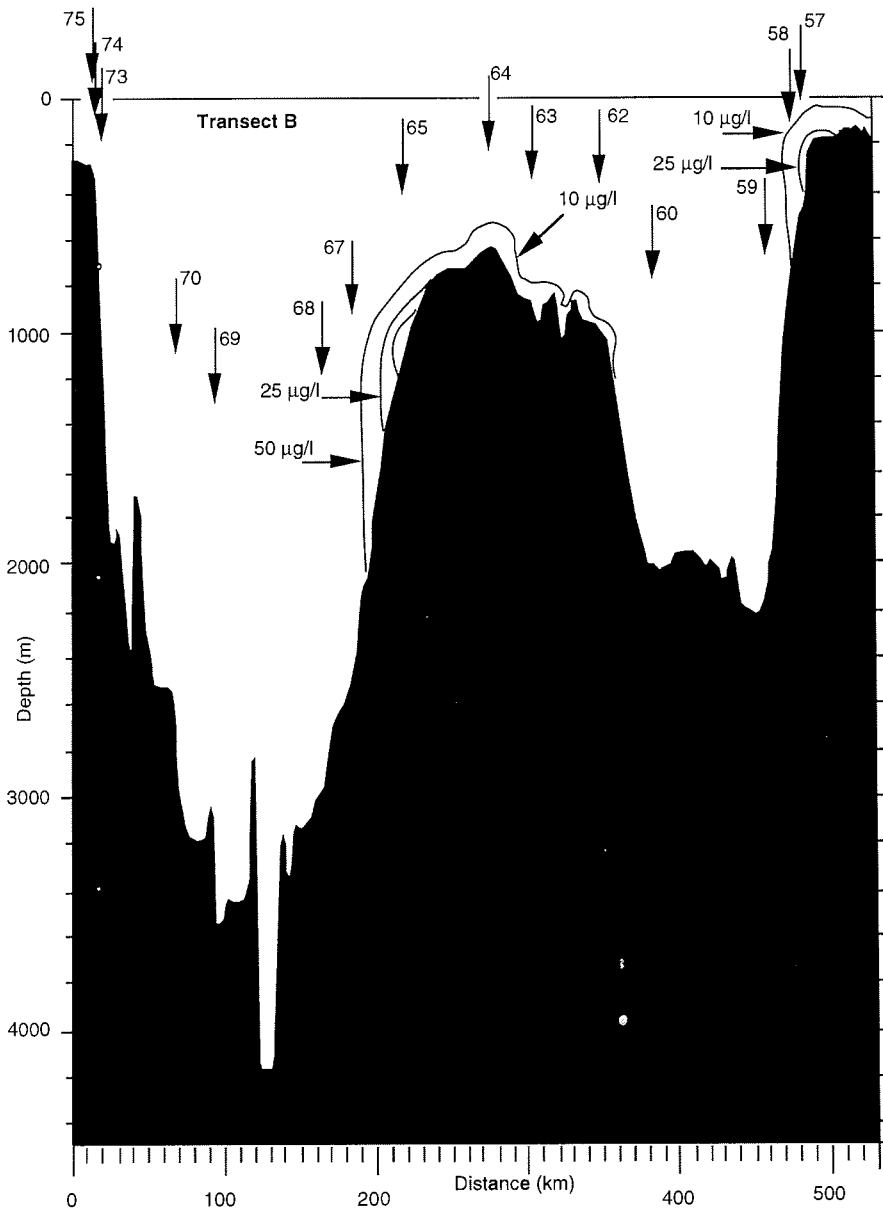


Fig. 8.2: Benthic nepheloid layer (BNL) as observed at transect B. The inventory of the suspended particulate matter is plotted in $\mu\text{g/l}$.

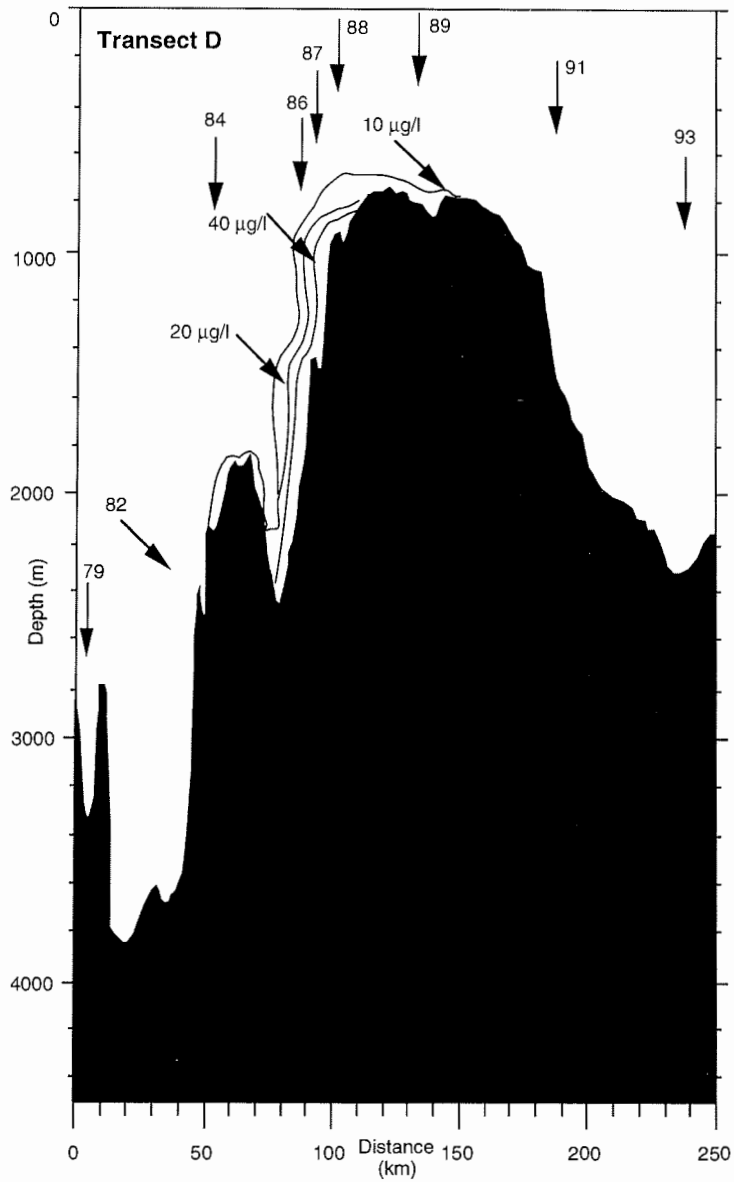


Fig. 8.3: Benthic nepheloid layer (BNL) as observed at transect D. The inventory of the suspended particulate matter is plotted in $\mu\text{g/l}$.

In Figures 8.2 and 8.3 the intensity/inventory of the suspension in the BNL is plotted for the various transects. We observed:

- a high turbidity of bottom waters on the shelf
- a well-developed BNL in the eastern range of Fram Strait, collapsing to a complete absence on the Greenland side and the steep Greenland slope
- a remarkable asymmetry at the Yermak plateau with higher suspended load on the western side than on the eastern side, observed on both transects B and D.

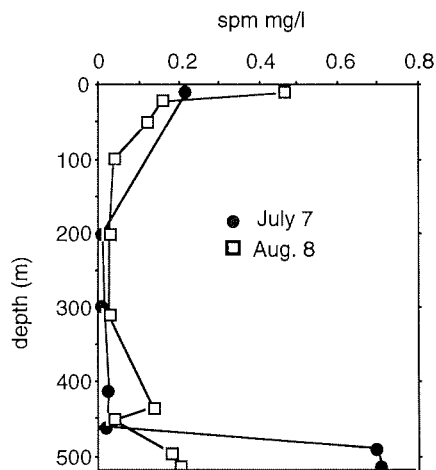


Fig. 8.4: Suspended particulate matter (in mg/l as estimated from transmissometry using the algorithm of Gardner, 1993) at station 61 during deployment (filled circles) and recovery (open squares) of the multisampler.

These observations are explained tentatively in the following way: On the Greenland side, clear deep Arctic water is flowing south. The coarse sediments are indicative for high current speeds, but there is not sufficient fine material available to be resuspended. On the Yermak plateau there is sufficient turbulence, created presumably both by tides and residual currents, to create a well-mixed near-bottom layer where material is resuspended or kept in suspension. We explain the high loads on the western flank as related to the West Spitsbergen Current, forced to the right by the Coriolis acceleration. Topography prevents the basin east of the Plateau to be flushed from the south. In effect there may be a (weak) return flow from the north into this basin, (Chapter 4), in accordance with the transmissometry data and the biological observations (Chapter 5).

8.2.2 Sediment-Water Exchange (Scavenging of ^{234}Th) (M. Rutgers v.d. Loeff)

^{234}Th is a natural tracer that is well-suited to study transport of particles in the ocean on a time scale of months. It is produced by ^{238}U which is an accurately known composite of seasalt, and decays with a half-life of 24.1 days. If ^{234}Th is depleted in the bottom water with respect to ^{238}U , this is indication of particle exchange between the bottom water and the surface sediment. In order to determine the distribution of ^{234}Th in the deep water column, we collected 15-20l samples with the Rosette, which were filtered by air pressure. In the filtrate, Th was precipitated quantitatively with MnO_2 which was subsequently filtered as well. The two filters with the particulate and dissolved fractions, respectively, were counted on board with a beta counter. A depletion of ^{234}Th was found nearly everywhere, and the distribution of this depletion is very similar to the distribution of suspended particle matter (SPM). This implies that the nepheloid layer cannot be explained exclusively by long-range transport, but must be maintained by a constant exchange with the seafloor. The average residence time of particles in the near-bottom water can be estimated to be a couple of months. One of the aims we have in mind for the future is to link these observations with the observations of the biologists on the distribution of bottom fauna and on its feeding mechanisms. The widespread occurrence of filter-feeding organisms shows the importance of biota in sedimentation; whereas it is also known that organisms may play a key role in resuspending particles.

A more detailed description of the near-bottom particle transport requires time-series observations. Moreover, a theoretical analysis of the behaviour of ^{234}Th has shown that a budget has to be made of the isotope that includes supply from mid-water depth as well as accumulation in the sediment. To arrive at such an approach, we have deployed a filtration- and adsorption device, the so-called multisampler, together with a sediment trap. This setup, complemented by a sampling of the surface sediment (MUC), should allow us to determine all relevant parts of the Th-budget. The multisampler was programmed to sample the bottom water every 3 days for 4 hours, with a more frequent sampling in the later phase of the deployment. We gave priority to long pumping times, accepting the risk of power failure in the last phase of the deployment. The instrument worked properly over 8 cycles.

Originally, it was planned to deploy the instruments at a depth of 2000m, but ice conditions forced us to shallower depth on the shelf edge of Spitsbergen. It turned out that an unusually intense nepheloid layer was present at this position (Fig. 8.4). Although the intensity of the BNL was three times higher than anywhere else observed on this expedition, the depletion of ^{234}Th was similar. This implies that a large part of the suspended load is not involved in a recent sedimentation-resuspension cycle. We hypothesize that the water is derived from the Barents Shelf, and that the original depletion has had enough time (several half-lives) to grow towards equilibrium during its transport north. Indeed, intense nepheloid layers have been observed before along the shelf/slope around 75°S (Thomsen et al., 1995). Thus, it is likely that our instruments have monitored the

transport of sediment-laden bottom waters produced during winter freezing on the Barents shelf. This process was studied closer to one of its origins, at Storfjord, by Schauer (1995). The particulate fraction collected by the instrument was counted on-board and showed that the intensity of the BNL had remained consistently high during the entire deployment (Fig. 8.5).

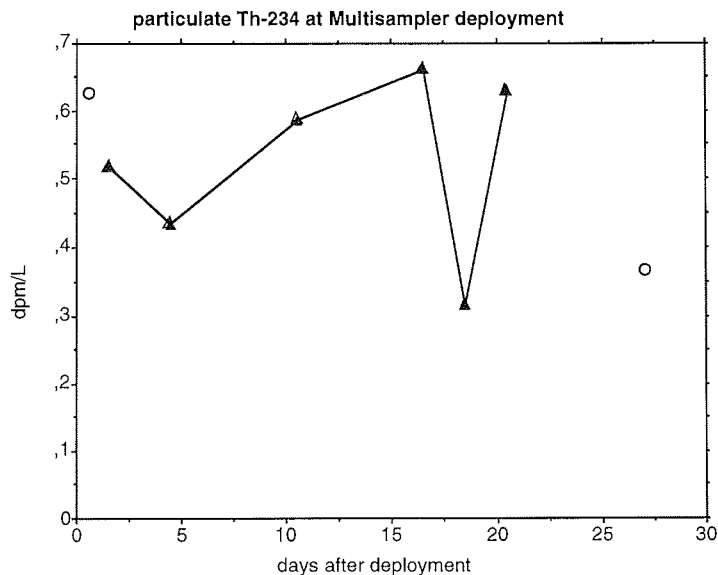


Fig. 8.5: Particulate ^{234}Th activity in the BNL at station 61 as measured with the multisampler (filled triangles) and with Rosette casts (open circles).

8.2.3 Early Diagenetic Reactions in the Suspended Phase (M. Rutgers v.d. Loeff)

The study of particle dynamics in the BNL, based on modelling and measurements of light transmission and ^{234}Th depletion as described above, are meant to provide the basis for further studies on turnover rates of constituents of fresh sediments near the sediment-water interface. Two types of constituents will be investigated: trace metals and biomarkers.

8.2.3.1 Trace Metals (M. Kühn)

The transport of trace metals to the sediments is strongly controlled by the abundance, production, sinking and decomposition of particulate matter. Besides terrigenous material originating from river and atmospheric input, particles are

produced primarily by phytoplankton in the surface water of the oceans. Together with the nutrients, metals are taken up actively or passively by these primary producers and are incorporated into their cells. The bulk of the phytoplankton is grazed upon by zooplankton and the undigested residues are packaged into faecal pellets and aggregates ("marine snow") which sink in rates typically ranging from 50 to 300 meters per day (Gersonde & Kuhn, 1993). Upon sinking through the water column, metals can be released from particles by the degradation of organic matter or dissolution of the inorganic carrier phases (metal oxides, opal, calcite). The vertical and horizontal distributions of dissolved metals in sea-water are a reflection of the whole range of chemical, oceanographic and sedimentary controls on their supply to, distribution in and removal from the ocean.

Once resuspension and bioturbation rates are known from the radionuclide measurements, the turnover rates of other trace elements can be calculated when their concentration gradients in the bottom water are known. Our main interest is the turnover of substances that are released in relation to the decay of organic matter in the surface sediment or in the bottom water. This includes elements that were components of or adsorbed to the degraded organic material (e.g. Cu, Cd, REE), or secondary reaction products of diagenetic reactions in the sediment (Mn, methane).

Water samples were taken from different depths in the water column (mainly in the BNL) with special close-open-close bottles on a plastic coated wire to minimize the risk of contamination. The samples from in and outside the BNL and the additional bottom water sample of the MUC were processed in the clean room laboratory container. The dissolved trace metal concentration will be determined by trace-matrix separation with the cation-exchange resin Chelex-100 (Pai et al., 1990) and liquid-liquid extractions (Danielsson et al., 1978) followed by Atomic Absorption Spectroscopy (AAS) and Inductively Coupled Plasma Mass Spectroscopy (ICP-MS) analysis.

8.2.3.2 Organic Constituents (Biomarker) (M. Rutgers v.d. Loeff)

Particulate organic material has been collected with *in-situ* pumps at 9 stations (Chapter 7.2.2). At two additional stations (93 and 99) samples collected with the Rosette were filtered for the same purpose. The difference in composition between particles suspended in the BNL and particles collected from the surface sediment, coupled to the particle cycling model, can be used to estimate turnover rates of organic constituents.

8.3 Radium Sampling (M. Rutgers v.d. Loeff)

^{228}Ra (5.8 y half-life) is a powerful tracer for water masses that have been in extensive contact with the sediment, especially on the continental shelf. Surface

waters in the Transpolar Drift are known to carry a strong ^{228}Ra signal from the Siberian shelf, but the Barents slope, the Yermak Plateau and the Greenland coast are additional potential sources. During this expedition we took samples for the analysis of Radium isotopes. Samples of surface water could be taken with the ship's seawater supply by adsorption on MnO_2 -impregnated fiber. Deep-water samples (approx. 60l), were collected with the Rosette from selected water masses, and Radium was coprecipitated with BaSO_4 for later analysis by gamma spectroscopy.

8.4 Surface Observations on Export Production. (M. Rutgers v.d. Loeff)

The ^{234}Th scavenging technique, used here primarily for studying particle dynamics in the BNL, has been developed originally to study the export of particles from the euphotic zone. We made such measurements with limited depth resolution during the present cruise. Briefly, the interpretation of the data is based on the following: A developing plankton bloom provides reactive surface area and results initially in a transfer of ^{234}Th activity from the dissolved to the particulate phase. Subsequently, when particles sink out this results in a depletion of total (dissolved + particulate) ^{234}Th with respect to its parent ^{238}U in the surface water. The results give a very clear picture of the development of plankton blooms in the study area (Fig. 8.6):

- Although ice algae were observed throughout (see Chapter 5.1), the water layer just beneath the thick ice cover (stations 77-91) showed no sign of a developing bloom, let alone of a sinking of particles. The depletion of total ^{234}Th remained within 5% of ^{238}U , equivalent to an export flux of $67 \text{ dpm m}^{-2} \text{ d}^{-1}$ from the upper 20 m. This corresponds with two short deployments of sediment traps at 20m depth under ice floes (Bauerfeind, section..), where we measured a flux of $80\text{-}100 \text{ dpm m}^{-2} \text{ d}^{-1}$. After POC analyses these rates can be converted to flux rates of organic carbon.
- The plankton bloom observed in the unexpectedly ice-free water mass off NE Greenland is clearly reflected in an increase in particulate ^{234}Th , but only at station 72a a significant export production has occurred. At stations 73 and 74, ^{234}Th is still close to equilibrium with its parent.
- At the mooring station on the Spitsbergen shelf, total ^{234}Th was depleted by 29% on July 7, implying that a massive bloom had sunk out in a period of 1-2 months before we arrived there. During recovery on August 3, a similar depletion was measured (22% at 10m, 28% at 20m depth), in agreement with the high particle fluxes registered by the sediment trap during the last week of the deployment (Chapter 5.4). The highest depletion in the surface water on transect D (26%) was observed at station 94 near the ice edge, implying that the classical bloom at the marginal ice zone had already resulted in a large particle export.

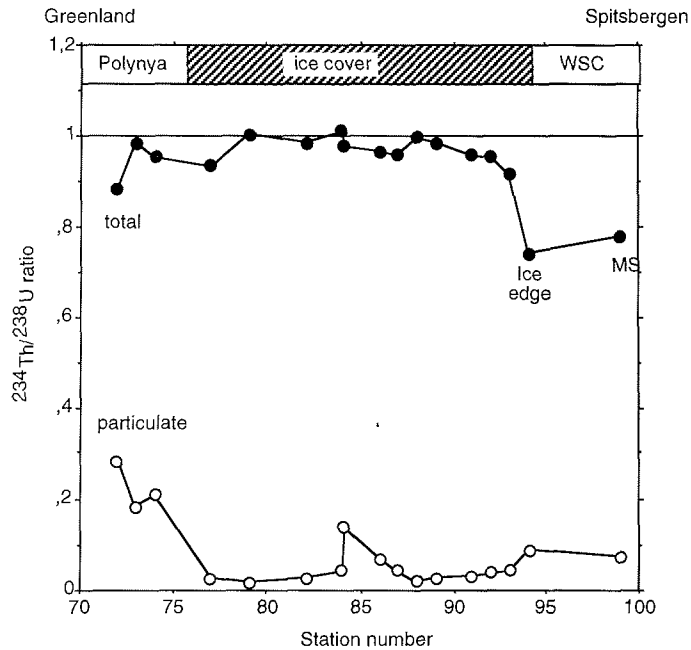


Fig. 8.6: Particulate (open circles) and total (particulate + dissolved, closed circles) $^{234}\text{Th}/^{238}\text{U}$ activity ratio in surface waters along transect D, showing a large depletion of total ^{234}Th at the southern part with largest depletion, indicating the largest recent export of particles near the ice edge. At $82^{\circ}10'\text{N}$, near station 84A with heavy ice cover where a short sediment trap was deployed for 3 days (see Chapter 5.4), high particulate activity shows a plankton bloom, but the total activity close to equilibrium shows the absence of significant export.

8.5 Methane (E. Damm)

Methane could be released to the ocean from the sea floor. However the sea-air exchange of methane is reduced in the ice-covered ocean. Thus methane will be removed by microbial consumption in the oxic water column, and so methane likely has a considerable effect on the marine carbon cycle (Reeburgh et al., 1992; Cranston, 1994; Lammers et al., 1995).

Methane was measured in the water column in order to attempt a preliminary estimate of the methane flux. Water samples were taken with the Rosette from different water depths at 27 stations and immediately analysed on board for methane. The dissolved gases were extracted from the water using a combined vacuum and ultrasonic method (Schmitt et al. 1991) and analysed for methane by gas chromatography.

The methane profiles show differences between the western and eastern Fram Strait which is probably related to different water currents. Background values are at the Greenland shelf and slope (Fig 8.7 A) and seem to characterize the deep Arctic water coming from the north to the western Fram Strait . The profiles at the Svalbard shelf and slope are more inhomogeneous (Fig.8.7 B). This is likely connected with the mixture of water masses in this region (Chapter 4).

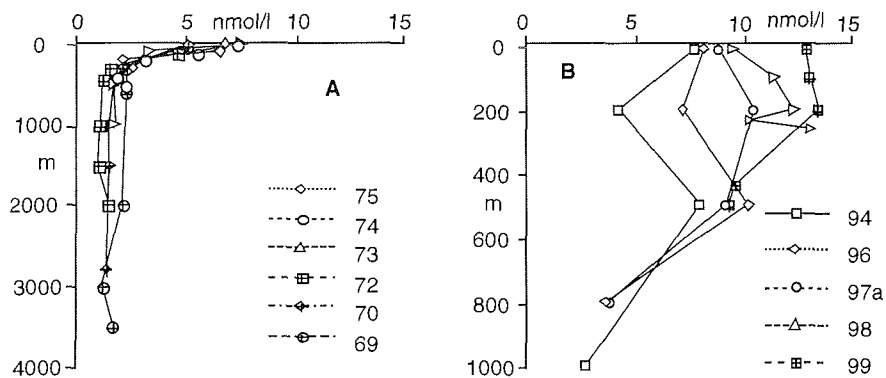


Fig 8.7: Methane concentration profiles of Fram Strait, the Greenland shelf and the Svalbard shelf.

9 References

- Abelmann, A., 1992. Diatom assemblages in Arctic sea ice - indicator for ice drift pathways. *Deep-Sea Res.*, 39, 2, pp. S525-S538.
- Anisimova, N.N., 1989. Distribution patterns of echinoderms in the Eurasian sector of the Arctic Ocean. In: Herman, Y. (ed.): *The Arctic Seas*. Van Nostrand, NY, pp 281-301.
- Arar, E.J. and Collins, G.B., 1992. In vitro determination of Chl a and phaeophytin in marine and freshwater phytoplankton by fluorescence.- U.S.EPA, Cincinnati, 14 pp.
- Barrie, L.A., 1986. Arctic air pollution: an overview of current knowledge. *Atmos. Environ.*, 20, P. 643-663.
- Bender, M.L. and Heggie, D.T., 1984. Fate of organic carbon reaching the sea floor: A status report. *Geochim. Cosmochim. Acta*, 48, 977-986.
- Bourke, R.H., Weigel, A.M., and Paquette, R.G., 1988. The westward turning branch of the West Spitsbergen Current. *J. Geophys. Res.* 93, 14065-14077.
- Brown, R.G.B., 1989. Seabirds and the arctic marine environment, in Rey, L. and Alexander, V.: *Proceedings of the sixth conference of the Comité Arctique International 13-15 May 1985*.
- Bursa, A. Phytoplankton in coastal waters of the Arctic Ocean at Point Barrow. *Arctic*, 16: 239-262.
- Carmack, E.C., Macdonald, R.W., Perkin, R.G., McLaughlin, F.A., and Pearson, R.J., 1995. Evidence for warming of Atlantic Water in the southern Canadian Basin of the Arctic Ocean: Results from the Larsen-93 expedition, *Geophys. Res. Letters*, 22, 1061-1064.
- Carmack, E.C., Aagaard, K., Swift, J.H., Perkin, R.G., McLaughlin, F.A., Macdonald, R.W., and Jones, E.P., 1995. Thermo-haline transitions Extended abstract IUTAM conference, Broome, Australia 8pp.
- Childress, J.J. and Mickel, T.J., 1980. A motion compensated shipboard precision balance system. *Deep Sea Res.* 27, 965-970.
- Cranston, R.E., 1994. Marine sediments as a source of atmospheric methane, *Bulletin of Geological Society of Denmark*, 41 pp.101-109.
- Danielsson, L.G., Magnusson, B., and Westerlund, S., 1978. An improved metal extraction procedure for the determination of trace metals in sea water by atomic absorption spectrometrie with electrothermal atomization. *Anal. Chim. Acta*, 98, 47-57.
- Dethleff, D., 1995. Sea ice and sediment export from the Laptev Sea flaw lead during 1991/92 winter season. - In: H. Kassens, D. Piepenburg, J. Thiede, L. Timokhov, H. W. Hubberten, and S. Priamikov (eds.): *Russian-German Cooperation: Laptev Sea System. Rep. Pol. Res.*, 176, pp. 78-93.
- Dethleff, D., D. Nürnberg, E. Reimnitz, M. Saarso, and Y. P. Savchenko, 1993. East Siberian Arctic Region Expedition '92: The Laptev Sea - Its significance for Arctic sea-ice formation and transpolar sediment flux. *Rep. Pol. Res.*, 120, pp. 44.
- Elverhøi A, E.S. Andersen, T.M. Dokken, R. Spielhagen, J.I. Svendsen, M. Sørflaten, A. Rørnes, M. Hald, and C.F. Forsberg, 1995. The growth and decay of the Late Weichselian Ice Sheet in western Svalbard and adjacent areas based on provenance studies of marine sediments, *Quaternary Research* , 44, 303-316.
- Franeker, J.A. van, 1990. Methods for counting birds at sea: A plea for comparative research, *Sula* 4, pp 85-89.

- Gardner, W. D., I. D. Walsh, and M. J. Richardson, 1993. Biophysical forcing of particle production and distribution during a spring bloom in the North Atlantic. *Deep-Sea Res. II*, 40, 171-195.
- Garrison, D.L. and Buck, K.R., 1986. Organism losses during ice melting: a serious bias in sea ice community studies. *Polar Biol.*, 6, 237-239.
- Gascard, J.-C., Richez, C., and Roauault, C., 1995. New insights on large-scale oceanography in Fram Strait: the West Spitsbergen Current. In "Arctic Oceanography, marginal ice zones and continental shelves" (W.O. Smith Jr. and J.M. Grebmeier eds.), AGU 49, Washington D.C., 131-182.
- Gersonde, R. and Kuhn, G., 1993. Der Meeresboden, Struktur und Sedimente. In: L.-A. Meyer-Reil and M. Köster (eds), *Mikrobiologie des Meeresbodens*. Fischer, Jena, pp. 11-37.
- Gradinger, R., 1996. Occurrence of an algal bloom under Arctic pack ice. *Mar. Ecol. Prog. Ser.*, 131, 301-305.
- Gradinger, R., Spindler, M., and Henschel, D., 1991. Development of Arctic sea-ice organisms under graded snow cover. *Polar Res.*, 10, 1: 295-307.
- Gradinger, R., Spindler, M. and Weissenberger, J., 1992. On the structure and development of Arctic pack ice communities in Fram Strait: a multivariate approach. *Polar Biol.*, 12, 727-733.
- Grant, P.J., 1982. Gulls – A Guide to Identification.
- Grobe, H., 1987. A Simple Method for the Determination of Ice-Rafted Debris in Sediment Cores. *Polarforschung* 57 (3), 123-126.
- Harrison, P., 1983. Seabirds – an identification guide.
- Hebbeln, D and G. Wefer, 1997. Late Quaternary paleoceanography in the Fram Strait, *Paleoceanography*, 12, 49-65.
- Horner, R., 1985. Ecology of sea ice microalgae. In: Horner, R.A. (ed.). *Sea ice biota*. CRC Press, Inc., Boca Raton, Florida, pp. 83-103.
- Horner, R., Ackley, S.F., Dieckmann, G.S., Gulliksen, B., Hoshiai, T., Legendre, L., Melnikov, I., Reeburgh, W.S., Spindler, M., and Sullivan, C.W., 1992. Ecology of sea ice biota. 1. Habitat, terminology, and methodology. *Polar Biol.*, 12, 417-427.
- Hunkins, K., 1990. A review of the Physical Oceanography of Fram Strait. In "The physical Oceanography of Sea Straits" (L.J. Pratt, ed.)
- Joiris, C., 1992. Birds and Mammals. *Ber. z. Polarforsch.* 115, pp.115-117.
- Kögler, F.C., 1963. Das Kastenlot.- *Meyniana* 13, 1 - 7.
- Kowalik, Z. and Proshutinski, 1994. The Arctic Ocean tides, in "The Polar Oceans and Their Role in Shaping the Global Environment", *Geophys. Monogr. Ser.*, vol. 85, edited by O.M. Johannessen, R.D. Muench, and J.E. Overland, pp.137-158, AGU, Washington, D.C.
- Kuhn, G., 1995. Sedimentphysikalische Untersuchungen. In: GERSONDE, R. (Ed.): *Die Expedition ANTARKTIS-XI/2 mit FS "Polarstern" 1993/94.- Berichte zur Polarforschung* 163, 66-74.
- Lammers, S. and E. Suess, 1995. Variations of atmospheric methane supply from the Sea of Okhotsk induced by the seasonal ice cover, *Global Biogeochemical cycle*, 9 (3), pp. 351-358.
- Mehlum, F., 1989. Svalbards fugler og pattedyr.
- Meunier, A., 1910. Microplancton des Mers de Barents et de Kara. *Duc d'Orleans Campagne Arctique de 1907*. Bruxelles. 355 p., pl. 1-37.
- Meunier, A., 1910. Microplancton des Mers de Barents et de Kara. *Duc d'Orleans Campagne Arctique de 1907*. Bruxelles. 355 p., pl. 1-37.
- Nansen, F., 1906. Protozoa on the ice-floes of the North Polar Sea. In: Nansen, F. (ed.). *The Norwegian Polar Expedition 1893-1896. Scientific Results*. Vol. 5. Christiania et al., pp. 1-22, pl. 1-8.

- Niessen, F., 1997. Physical Properties in Marine Sediments. In: Kuhn, G. (Ed.): Die Expedition ANTARKTIS-XI/4 mit FS "Polarstern" 1994. Berichte zur Polarforschung (in press).
- Nowaczyk, N.R., 1991. Hochauflösende Magnetostratigraphie spätquartärer Sedimente arktischer Meeresgebiete. Berichte zur Polarforschung 78, 187p.
- Nürnberg, D., I. Wollenburg, D. Dethleff, H. Eicken, H. Kassens, T. Letzig, E. Reimnitz, and J. Thiede, 1994. Sediments in Arctic sea ice - entrainment, transport and release. Mar. Geol., 119, pp. 185-214.
- O'Dowd, C.D., Smith, M.H., Consterdine, I.E., and Lowe, J.A., 1997. Marine aerosol, sea-salt, and the marine sulphur cycle: A short review. Atmos. Environ., 31, p. 73-80.
- Okolodkov, Y. B., 1989. Sea-ice algae of the East Siberian Sea in May 1987. Novit. Syst. Plant. non Vascul., 26, 36-41. (In Russian).
- Okolodkov, Y. B., 1996. Vertical distribution of algae and nutrients in the first-year ice from the East Siberian Sea in May 1987. Botanical Journal, Russian Acad. Sci., 81, 7, 34-40.
- Okolodkov, Y.B., 1992b. Cryopelagic flora of the Chukchi, East Siberian and Laptev seas. Proceedings of the NIPR Symposium on Polar Biology, 5, 28-43.
- Okolodkov, Y.B. and Dodge, J.D., 1996. Biodiversity and biogeography of planktonic dinoflagellates in the Arctic Ocean. J. Exp. Mar. Biol. Ecol., 202, 19-27.
- Okolodkov, Y.B., 1990. Sea-ice algae of the Chukchi Sea in March-April 1988. Novit. Syst. Plant. non Vascul., 27, 16-20. (In Russian).
- Okolodkov, Y.B., 1992a. Sea-ice algae of the Laptev Sea. Novit. Syst. Plant. non Vascul., 28, 29-34. (In Russian).
- Okolodkov, Y.B., 1993. Dinoflagellates from the Norwegian, Greenland and Barents seas and the Faroe-Shetland Islands area collected in the cruise of the r/v "Oceania", in June-July 1991. Polish Polar Res., 14, 9-24.
- Okolodkov, Y.B., 1997. A new combination and new species of *Gymnodinium*, *Gyrodinium* and *Protoperidinium* (Dinophyceae) from the Arctic and N.E. Atlantic. Botanical Journal, Russian Acad. Sci., 82, 5, 97-106.
- Okolodkov, Y.B., 1997. Biodiversity of planktonic and sea-ice algae in the marginal ice zone of the northern Barents Sea and Svalbard waters. In: Falk-Petersen, S. and Hop, H. (eds.). Ecological processes in the marginal ice-zone of the northern Barents Sea. ICE-BAR 1996 Cruise Report. Norsk Polarinstitut Rapportserie.
- Osterkamp, T. E. and Gosink, J. P., 1984. Observations and analysis of sediment laden sea ice. - In: Barnes, P. W., Schell, D. M. and E. Reimnitz (Eds.), The Alaska Beaufort Sea: Ecosystem and Environment: San Francisco, Academic Press, pp. 73-94.
- Padman, L., 1995. Small-Scale Physical Processes in the Arctic Ocean. In "Arctic Oceanography, marginal ice zones and continental shelves" (W.O. Smith Jr. and J.M. Grebmeier eds.), AGU 49, Washington D.C. 97-129.
- Pai, S.C., Fang, T.-H., Chen, C.-T.A., and Jeng, K.-L., 1990. A low contamination Chelex-100 technique for shipboard pre-concentration of heavy metals in seawater. Marine Chemistry, 29, 295-306.
- Peck, L. S. and Uglow, R.F., 1990. Two methods for the assessment of the oxygen content of small volumes of seawater. J. Exp. Mar. Biol. Ecol. 141, 53-62.
- Perkin, R.G. and E.L. Lewis., 1984. Mixing in the West Spitsbergen Current, J. Phys. Ocean., 14, 1315-1325.

- Pfirman, S.L., D. Bauch, and T. Gammelsrød, 1994. The northern Barents Sea: water mass distribution and modification. In "The Polar Oceans and Their Role in Shaping the Global Environment", Geophys. Monogr. Ser., vol. 85, edited by O.M. Johannessen, R.D. Muench and J.E. Overland, pp.77-94, American Geophys. Union, Washington, D.C.
- Piepenburg, D. and Schmid, M., 1996. Brittle star fauna (Echinodermata: Ophiuroidea) of the Arctic northwestern Barents Sea: composition, abundance, biomass and spatial distribution. *Polar Biol.* 16: 383-392.
- Piepenburg, D. and v. Juterzenka, K., 1994. Abundance, biomass and spatial distribution pattern of brittle stars (Echinodermata: Ophiuroidea) on the Kolbeinsey Ridge north of Iceland. *Polar Biol.* 14, 185-194.
- Piepenburg, D. Blackburn, T.H., Dorrien, C. F. von, Gutt, J., Hall, P.O.J., Hulth, S., Kendall, M.A., Opalinski, K.W., Rachor, E., and Schmid, M.K., 1996. Partitioning of benthic community respiration in the Arctic (northwestern Barents Sea). *Mar. Ecol. Progr. Ser.* 118, 199-213.
- Quadfasel, D., Sy, A. and Rudels, B., 1993. A ship of opportunity section to the North Pole: Upper ocean temperature observations. *Deep-Sea Res.*, 40, 777-789.
- Quadfasel, D., Sy, A., Wells, D., and Tunik, A., 1991. Warming in the Arctic, *Nature*, 350, 385.
- Rachor, E., 1997. Scientific Cruise Report of the Arctic Expedition-ARK XI/1 of RV "Polarstern" in 1995, Reports on Polar Research, 226, 157 pp.
- Reeburgh, W.S., S.C. Whalen, and M.J. Alperin, 1992. The role of methylophony in the global methane budget, in *Microbial Growth on C-1 Compounds*, edited by J.C. Murrell and D. Welley, pp.1-14, Intercept, Andover, Hampshire.
- Reimnitz, E., J. R. Clayton, E. W. Kempema, J. R. Payne, and W. S. Weber, 1993. Interaction of rising frazil with suspended particles: tank experiments with applications to nature. - *Cold Reg. Sc. Techn.*, 21, p. 117-135.
- Reimnitz, E., M. McCormick, K. McDougall, and E. Brouwers, 1993. Sediment-export by ice rafting from a costal polynya, Arctic Alaska. *Arctic Alp. Res.*, 25, 2, pp. 83-98.
- Rudels, B., Jones, E.P., Anderson, L.G., and Kattner, G., 1994. On the intermediate depth waters of the Arctic Ocean. In "The Polar Oceans and Their Role in Shaping the Global Environment." Geophys. Monogr. Ser., vol. 85, edited by O.M. Johannessen, R.D. Muench and J.E. Overland, American Geophysical Union, Washington, pp33-46.
- Schauer, U., 1995. The release of brine-enriched shelf water from Storfjord into the Norwegian Sea. *J. Geophys. Res.*, 100, 16015-16028.
- Schubert, C.J., 1995. Organischer Kohlenstoff in spätquartären Sedimenten des Arktischen Ozeans: Terrigener Eintrag und marine Produktivität. *Berichte zur Polarforschung* 177, 178pp.
- Sournia, A., Chrétiennot-Dinet, M.-J. and Ricard, M., 1991. Marine phytoplankton: how many species in the world ocean? *J. Plankton Res.* 13: 1093-1099.
- Spiess, V., 1992. Digitale Sedimentechographie - Neue Wege zu einer hochauflösenden Akustostratigraphie.- *Berichte aus dem Fachbereich Geowissenschaften der Universität Bremen*, 35, 199pp.
- Stein, R., Schubert, C., Vogt, C., and Fütterer, D.K., 1994. Stable isotope stratigraphy, sedimentation rates, and salinity changes in the latest Pleistocene to Holocene central Arctic Ocean. *Mar. Geol.*, 119, p. 333-355.

- Thomsen, L., G. Graf, K. von Juterzenka, and U. Witte, 1995. An *in situ* experiment to investigate the depletion of seston above an interface feeder field on the continental slope of the western Barents Sea. *Mar. Ecol. Progr. Ser.*, 123, 295-300.
- Weber, M.E., Niessen, F., Kuhn, G., and Wiedicke, M., 1997. Calibration and application of marine sedimentary physical properties using a multi-sensor core logger. *Marine Geology* 136, 151-172.
- Wulff, A., 1919. Über das Kleinplankton der Barentssee. *Wiss. Meeresuntersuch. N. F.*, 13. Abt. Helgoland, 1, 95-124.

Table of Content

- 10 **Annex****
- 10.1 Station List
- 10.2 Weather Data
- 10.3 Geological Data Tables and Graphical Core Description
- 10.4 General Guidelines for Data and Sample
 Distribution and Publications
- 10.4.1 Physical Oceanography
- 10.4.2 Marine Biology
- 10.4.3 Sea-Ice Sedimentology and Water Chemistry
- 10.4.4 Marine Geology
- 10.4.4.1 Sediment Sample Distribution Guidelines for ARK-XIII/2
 Material
- 10.5 List of Participants

10.1 Station List

Explanations:

CTD	- Conductivity temperature depth probe
ISP	- <i>In-situ</i> -pumps
APSN	- Apstein net
MN	- Multi net
BN	- Bongo net
GKG	- Großkastengreifer (big box corer)
MUC	- Multi corer
SL	- Schwerelot (Gravity corer)
MC	- Metalcast
KAL	- Kastenlot
AGT	- Agassiz trawl
EBS	- Epibenthos Sledge
FS	- Fotoschaukel (Seafloor imaging)
OFOS	- Ocean Floor Observation System
PRWS	- Pressure Retaining Water Sampler
VVG	- Van-Veen-Grab
LB	- Letterbottle

The data in the station list represent:

ice stations:		beginn and end of work on ice
geological stations:	(MUC, GKG, SL, KAL) (ISP)	bottom contact
biological stations:	(GKG, MUC, AGT) (BN, MN) (APSN) (OFOS, FS, EBS, AGT) (CTD)	on depth bottom contact on depth water contact begin of transect, end of transect on depth
oceanographic stations:		

Station	AWI-No.	Date	Time (GMT)	Latitude	Longitude	Depth	Activity
Barents Sea							
44/039		27.06.1997	09:27	75°59,9'N	32°59,4'E	300m	CTD
			10:18	75°59,5'N	32°59,5'E	291m	MN
			11:05	75°59,1'N	32°58,9'E		APSN
			10:59	75°59,1'N	32°58,9'E	290m	MN
			11:30	75°58,9'N	32°58,5'E	150m	BN
			11:55	75°58,8'N	32°58,1'E	250m	MN
44/040			15:14	76°20,0'N	33°29,1'E	266m	CTD
44/041			16:57	76°30,1'N	33°35,1'E	185m	CTD
44/042	PS2822-1		18:34	76°39,2'N	33°33,0'E	119m	CTD
	PS2822-2		19:02	76°39,0'N	33°34,0'E	110m	MN
			19:05	76°38,9'N	33°34,1'E		APSN
	PS2822-3		19:23	76°38,9'N	33°34,2'E	120m	MN
	PS2822-4		19:46	76°38,8'N	33°34,1'E	100m	BN
	PS2822-5		20:12	76°38,7'N	33°33,8'E	153m	GKG (bio)
	PS2822-6		20:50	76°38,3'N	33°34,6'E	152m	MUC
			21:25	76°38,1'N	33°33,5'E	begin of trawl	EBS
			21:35	76°38,1'N	33°33'E	hieven	
44/043			23:40	76°50,2'N	33°46,4'E	92m	CTD
44/044		28.06.1997	01:24	76°59,9'N	33°59,3'E	143m	CTD
44/045	PS2823-1		03:45	77°16,2'N	33°34,7'E	137m	CTD
	PS2823-2		04:09	77°16,3'N	33°34,4'E	120m	MN
	PS2823-3		04:31	77°16,4'N	33°34,3'E	120m	BN
	PS2823-4		04:35	77°16,5'N	33°34,4'E	145m	VVG
	PS2823-5		05:09	77°16,6'N	33°34,4'E	140m	VVG
	PS2823-6		05:25	77°16,7'N	33°34,4'E	142m	VVG
	PS2823-7		05:47	77°16,8'N	33°34,2'E	145m	MUC
44/046			08:00	77°21,8'N	34°37,5'E	170m	CTD
			08:30	77°21,8'N	34°37,1'E	begin of trawl	AGT
			08:40	77°21,9'N	34°38,5'E	hieven	
44/047	PS2824-1		10:25	77°34,4'N	34°41'E	195m	CTD
				77°34,2'N	34°40,8'E		APSN
	PS2824-2		11:04	77°34,2'N	34°40,8'E	190m	MN
	PS2824-3		11:30	77°34,1'N	34°40,1'E	190m	MN
	PS2824-4		12:10	77°34,1'N	34°39,5'E	190m	BN
	PS2824-5		12:40	77°34,19'N	34°38,58'E	213m	GKG (bio+geo)
	PS2824-6		13:12	77°34,30'N	34°40,31'E	212m	MUC (bio)
	PS2824-7		13:49	77°34,30'N	34°37,9'E	begin of trawl	EBS
			13:59	77°34,10'N	34°36,7'E	hieven	
	PS2824-8		14:55	77°34,4'N	34°40,1'E	211m	FS
			14:58	77°34,5'N	34°39,8'E	hieven	
	PS2824-9		15:22	77°34,8'N	34°42,2'E		Hydrophon i. w.
			15:24				Mooring recovered
			16:40	77°35,2'N	34°42'E		4 Benthoskugeln o. D.
			16:43				4 Benthoskugeln o. D.
			16:50				Sedimenttrap o. D.
			16:52				2 Benthoskugeln and Releaser o. D.
			21:21	77°55,2'N	33°20,2'E		Icegroup on ice
			21:25	77°55,2'N	33°20,2'E		Icegroup on board
44/048			22:40	75°59,5'N	32°58,7'E	139m	CTD
			23:06	75°59,6'N	32°58,3'E	130m	MN
			23:28	77°59,7'N	32°57,8'E	135m	BN

Station	AWI-No.	Date	Time (GMT)	Latitude	Longitude	Depth	Activity
	PS2825-1		23:47	77°59,6'N	32°57,7'E	137m	VVG (bio)
	PS2825-2	29.06.1997	00:09	77°59,6'N	32°57,7'E	137m	VVG (bio)
44/049			03:24	78°15,7'N	33°00,9'E	156m	CTD
44/050	PS2826-1		07:08	78°37,2'N	32°08,2'E	281m	CTD
	PS2826-2		08:21	78°37,1'N	32°08,0'E	286m	MC
	PS2826-3		08:59	78°37'N	32°07,5'E	280m	CTD
	PS2826-4		09:36	78°36,9'N	32°07'E	280m	MN
	PS2826-5		10:00	78°36,8'N	32°05,9'E	260m	BN
	PS2826-6		10:36	78°36,8'N	32°05,7'E	278m	CTD
	PS2826-7		11:16	78°36,7'N	32°05,1'E	260m	VVG (bio)
	PS2826-8		11:56	78°36,7'N	32°04,7'E	286m	VVG (bio)
			12:10	78°36,7'N	32°04,1'E		MUC (stop)
	PS2826-9		12:54	78°36,65'N	32°03,75'E	290m	MUC
	PS2826-10		13:46	78°37,2'N	32°03,7'E	begin of trawl	EBS
			14:51	78°37,4'N	32°03,7'E	hieven	
44/051			17:50	78°59,7'N	31°20,1'E	185m	CTD
44/052	PS2827-1		22:27	79°26,8'N	30°29,6'E	310m	CTD
	PS2827-2		23:02	79°26,6'N	30°29,6'E	310m	MN
	PS2827-3	30.06.1997	23:35	79°26,5'N	30°29,5'E	309m	MN
	PS2827-4		00:29	79°26,4'N	30°29,3'E	309m	MN
	PS2827-5		01:38	79°26,24'N	30°28,23'E	335m	GKG (bio/geo)
44/053			05:39	79°54,6'N	29°58,5'E	273m	CTD
44/054	PS2828-1		12:20	80°20,8'N	29°03,1'E	332m	CTD
			12:10-12:17	80°20,8'N	29°03,0'E		APSN
	PS2828-2		13:13	80°20,7'N	29°03,0'E	330m	MN
	PS2828-3		13:50	80°20,7'N	29°02,5'E	320m	MN
	PS2828-4		14:31	80°20,8'N	29°02,0'E	301m	BN
	PS2828-5		15:10	80°20,85'N	29°01,35'E	375m	VVG (bio)
	PS2828-6		15:35	80°20,97'N	29°01,1'E	375m	VVG (bio)
	PS2828-7		16:01	80°21,0'N	29°00,9'E	353m	MUC (bio)
44/055			21:50	80°43,6'N	29°29,3'E		Icegroup on ice
		01.07.1997	00:40	80°43,6'N	29°29,3'E		Icegroup on board
	PS2829-1		22:10	80°43,6'N	29°29,3'E	452m	CTD
			22:55	80°43,4'N	29°29,5'E	452m	MC
	PS2829-2		00:18	80°43,2'N	29°29,5'E	430m	MN
	PS2829-3		01:05	80°43,0'N	29°29,4'E	420m	MN
			01:45	80°42,0'N	29°29,2'E	401m	BN
	PS2829-4		02:30	80°42,74'N	29°28,9'E	453m	VVG
	PS2829-5		02:59	80°42,70'N	29°28,81'E	452m	VVG
	PS2829-6		03:26	80°42,66'N	29°28,53'E	450m	MUC (bio)
	PS2829-7		05:23	80°42,9'N	29°21,2'E	begin of trawl	EBS
			05:31	80°42,9'N	29°21,4'E	hieven	
	PS2829-8		07:16	80°41,4'N	29°24,4'E	410m	OFOS
			09:00	80°42,4'N	29°23,6'E	hieven	
North of Svalbard							
44/056		02.07.1997	21:55	81°03,7'N	20°07,5'E	167m	CTD
44/057		03.07.1997	09:40	80°59,2'N	18°32'E		Icegroup on ice
			12:00				Icegroup on board
	PS2830-1		19:41	80°58,7'N	17°25,12'E	503m	CTD
			19:45-20:03	80°58,7'N	17°24,9'E		APSN
			20:17	80°58,7'N	17°24,9'E	507m	MC
	PS2830-2		21:59	80°58,5'N	17°27,5'E	500m	MN
	PS2830-3		22:32	80°58,5'N	17°27,7'E	500m	MN
	PS2830-4		23:25	80°58,5'N	17°27,1'E	450m	BN
	PS2830-5	04.07.1997	00:55	80°58,46'N	17°28,81'E	513m	SL (4.50m)
	PS2830-6		01:36	80°58,54'N	17°29,67'E	517m	GKG (bio)

Station	AWI-No.	Date	Time (GMT)	Latitude	Longitude	Depth	Activity
	PS2830-7		02:14	80°58,57'N	17°30,50'E	509m	GKG (bio)
	PS2830-8		02:49	80°58,61'N	17°31,17'E	500m	GKG (geo)
	PS2830-9		03:51	80°58,68'N	17°32,56'E	494m	MUC (bio)
	PS2830-10		04:34	83°58,7'N	17°33,5'E	488m	MUC (bio)
44/058	PS2831-1		08:15	81°06,2'N	16°54,2'E	965m	CTD
	PS2831-2		09:18	81°06,1'N	16°55,3'E	960m	MN
	PS2831-3		10:32	81°06'N	16°56,2'E	500m	MN
	PS2831-4		12:25	81°05,8'N	16°57,1'E	900m	BN
	PS2831-5		13:24	81°05,66'N	16°57,96'E	942m	GKG (bio)
	PS2831-6		14:15	81°05,65'N	16°58,12'E	937m	GKG (bio)
	PS2831-7		15:02	81°05,64'N	16°58,36'E	934m	GKG (geo)
	PS2831-8		15:53	81°05,66'N	16°58,41'E	932m	FS
			16:14	81°05,7'N	16°58,5'E	hieven	
	PS2831-9		17:07	81°05,7'N	16°58,6'E	917m	MUC (bio)
	PS2831-10		18:08	81°05,7'N	16°58,6'E	917m	MUC (geochem+geo)
	PS2831-11		19:52	81°04,0'N	17°08,4'E	begin of trawl	EBS (bio)
			19:57	81°04,2'N	17°08,1'E	hieven	
	PS2831-12		21:49	81°06'N	16°52'E	1024m	SL (6.25m)
44/059	PS2832-1	05.07.1997	01:09	81°06,0'N	16°11,6'E	2044m	CTD
			00:51	81°06,0'N	16°11,9'E		Icegroup on ice
			02:01	81°06,1'N	16°12,9'E		Icegroup on board
	PS2832-2		03:07	81°06,3'N	16°14,3'E	2027m	MC
	PS2832-3		04:19	81°06,5'N	16°16,1'E	200m	CTD
	PS2832-4		05:21	81°06,6'N	16°17,6'E	2001m	ISP
			07:43			hieven	
			04:44	81°06,6'N	16°16,9'E		APSN
	PS2832-5		09:51	81°06,7'N	16°18,1'E	2000m	MN
	PS2832-6		11:09	81°06,6'N	16°17,1'E	300m	MN
	PS2832-7		11:40	81°06,6'N	16°16,9'E	500m	MN
			12:58	81°06,3'N	16°15,3'E		Icegroup on ice
			15:12	81°06,3'N	16°14,3'E		Icegroup on board
	PS2832-8		14:01	81°06,3'N	16°15,1'E	1500m	BN
	PS2832-9		15:53	81°06,5'N	16°15,1'E	500m	MN
	PS2832-10		17:16	81°06,6'N	16°14,6'E	2048m	GKG (empty)
	PS2832-11		18:29	81°06,6'N	16°13,8'E	2054m	GKG (bio)
	PS2832-12		19:44	81°06,7'N	16°13,1'E	2065m	GKG (bio+geo)
	PS2832-13		21:25	81°06,8'N	16°11,8'E	2070m	MUC (geochem+geo)
	PS2832-14		23:05	81°06,8'N	16°10,3'E	2042m	MUC (bio)
		06.07.1997	00:16-0:32	81°06,7'N	16°08,4'E		Recovery of trap
44/060	PS2833-1		12:48	80°58,3'N	11°52,2'E	1950m	CTD
	PS2833-2		14:38	80°58,1'N	11°51,8'E	1945m	MC
	PS2833-3		15:51	80°58,1'N	11°51,1'E	300m	CTD
	PS2833-4		16:31	80°58,2'N	11°50,8'E	500m	MN
	PS2833-5		17:30	80°58,3'N	11°50,0'E	1964m	GKG (geo)
	PS2833-6		18:47	80°58,4'N	11°49,1'E	1969m	SL (3.50m)
	PS2833-7		20:33	80°58,5'N	11°47,4'E	1976m	MUC (geochem+bio)
	PS2833-8		21:40	80°58,6'N	11°46,4'E	1972m	OPOS
		07.07.1997	00:22	80°58,7'N	11°45,5'E	hieven	
44/061			13:41	80°09,3'N	10°26,5'E	509m	CTD
			14:47	80°09,5'N	10°23,7'E	523m	MC
			15:20	80°09,8'N	10°23,5'E		Multisampler
			16:42	80°10,47'N	10°24,48'E		deployed
			17:15	80°10,3'N	10°21,7'E	200m	CTD
			17:30	80°10,4'N	10°21,9'E		APSN
			17:57	80°10,6'N	10°22,9'E	520m	MN
Yermak Plateau							
44/062	PS2834-1	08.07.1997	15:07	80°54,2'N	09°53,1'E	996m	CTD
	PS2834-2		18:22	80°54,2'N	09°52,5'E	980m	ISP
			19:15	80°54,5'N	09°51,0'E	hieven	
	PS2834-3		20:10	80°54,5'N	09°50,7'E	500m	MN

Station	AWI-No.	Date	Time (GMT)	Latitude	Longitude	Depth	Activity
	PS2834-4		20:18	80°54,6'N	09°50,1'E	950m	BN
	PS2834-5		22:30	80°54,8'N	09°49,4'E	1024m	KAL (6.71m)
	PS2834-6		23:25	80°54,9'N	09°49,4'E	1001m	GKG (geo)
	PS2834-7	09.07.1997	00:35	80°55,00'N	09°49,4'E	1029m	MUC (geochem+bio)
			02:00	80°55,13'N	09°50,30'E	998m	OFOS
			04:31	80°55,5'N	09°53,1'E	hieven	
44/063	PS2835-1		20:55	81°03,4'N	07°17,3'E	891m	MUC
	PS2835-2		22:24	81°03,9'N	07°16,8'E	896m	OFOS
		10.07.1997	00:09	81°04,4'N	07°17,3'E	hieven	
	PS2835-3		02:24	81°05,4'N	06°59,8'E	833m	CTD
			02:29	81°05,5'N	07°00,1'E		div. Handnetze
	PS2835-4		03:23	81°05,6'N	07°00,6'E	500m	MN
			04:07	81°05,8'N	07°01,8'E	winch problems/working stop	SL
	PS2835-5		10:04	81°06,1'N	07°04'E	847m	GKG (geo+bio)
	PS2835-6		11:05	81°06,1'N	07°04'1E	855m	SL (5.49m)
44/064	PS2836-1		19:18	81°07,7'N	05°35,1'E	632m	CTD
			19:15	81°07,7'N	05°35'E		Icegroup on ice
	PS2836-2		19:46	81°07,7'N	5°34,7'E	640m	MC
	PS2836-3		20:59	81°07,7'N	05°34,1'E	200m	CTD
			21:55	81°07,7'N	05°34,2'E		Icegroup on board
	PS2836-4		21:18	81°07,7'N	05°34,1'E	630m	ISP
			21:24	81°07,7'N	05°34,1'E		APSN
		11.07.1997	00:12	81°07,7'N	05°36,0'E	hieven	ISP
	PS2836-5		01:14	81°07,7'N	05°36,9'E	501m	MN
	PS2836-6		02:03	81°07,86'N	05°38,86'E	657m	GKG
	PS2836-7		02:42	81°07,93'N	05°40,12'E	647m	GKG
	PS2836-8		03:23	81°08,01'N	05°41,58'E	647m	MUC
	PS2836-9		04:17	81°08,1'N	05°43,7'E	635m	MUC
			05:17	81°08,2'N	05°46,3'E	638m	OFOS
			08:00	81°08,4'N	05°52,4'E	hieven	
44/064a			20:07	81°09,0'N	04°08,3'E	begin of trawl	AGT
			20:17	81°08,9'N	04°09,2'E	hieven	
44/065	PS2837-1	12.07.1997	07:24	81°13,5'N	02°11,5'E	1056m	CTD
	PS2837-2		09:00	81°13,7'N	02°14,5'E	1033m	MC
	PS2837-3		09:52	81°14'N	02°18,4'E	300m	CTD
	PS2837-4		10:16	81°13,9'N	02°20'E	500m	MN
			11:05	81°14'N	02°22'E		Icegroup on ice
	PS2837-5		11:22	81°14'N	02°22,9'E	1023m	KAL (8.76m)
			12:04	81°14,0'N	02°24,7'E		Icegroup on board
	PS2837-6		12:13	81°13,99'N	02°25,07'	1028m	GKG (geo)
	PS2837-7		12:54	81°13,98'N	02°26,77'E	1018m	GKG (bio)
	PS2837-8		13:45	81°13,93'N	02°28,89'E	992m	MUC
	PS2837-9		14:52	81°13,87'N	02°31,29'E	1006m	MUC
	PS2837-10		15:59	81°13,8'N	2°33,5'E	950m	OFOS
			18:15	81°13,5'N	02°37,1'E	hieven	
44/066			23:55	81°16,3'N	01°31,2'E	1381m	CTD
44/067	PS2838-1	13.07.1997	05:33	81°17,7'N	00°14,2'E	2422m	CTD
	PS2838-2		07:57	81°17,7'N	00°18,6'E	2408m	MC
	PS2838-3		10:01	81°17,6'N	00°20,7'E	2396m	CTD
	PS2838-4		11:45	81°17,4'N	00°21,2'E	2410m	ISP
			11:06	81°17,4'N	00°21,2'E		APSN
			13:15	81°17,5'N	00°20,3'E		Icegroup on ice
			14:16	81°17,5'N	00°20,8'E	hieven	ISP
			15:39	81°17,7'N	00°22,4'E		Icegroup on board
	PS2838-5		16:26	81°17,6'N	00°21,6'E	2340m	MN
	PS2838-6		18:03	81°17,9'N	00°25,9'E	300m	MN
			18:40	81°17,8'N	00°26,8'E	496m	MN
			19:46	81°17,8'N	00°28,0'E	1496m	BO
	PS2838-7		21:56	81°17,8'N	00°26,5'E	2271m	SL (5.90m)

Station	AWI-No.	Date	Time (GMT)	Latitude	Longitude	Depth	Activity
	PS2838-8		22:47	81°17,7'N	00°26,7'E	2270m	GKG (geo)
	PS2838-9	14.07.1997	00:39	81°17,66'N	00°26,6'E	2325m	GKG (bio)
	PS2838-10		02:23	81°17,78'N	00°27,71'E	2313m	MUC
	PS2838-11		04:02	81°17,8'N	00°29,1'E	2226m	MUC
	PS2838-12		05:47	81°17,8'N	00°34'E	2119m	OFOS
			07:22	81°17,5'N	00°36,5'E	hieven	
44/068	PS2839-1		12:31	81°25'N	00°58,2'W	2925m	CTD
	PS2839-2		14:58	81°24,4'N	01°02,8'W	1500m	BN
			14:06	81°24,4'N	01°02,8'W		div. ASPN
	PS2839-3		16:38	81°24,3'N	01°02,4'W	500m	MN
	PS2839-4		17:18	81°24,3'N	01°01,4'W	2933	SL (6.15m)
	PS2839-5		19:50	81°24,2'N	00°58,3'W	2926m	GKG (geo)
	PS2839-6		21:08	81°24,2'N	00°57,1'W	2911m	GKG (bio)
	PS2839-7		23:24	81°24,1'N	00°54,9'W	2905m	MUC
Fram Strait							
44/069	PS2840-1	15.07.1997	09:03	81°29,3'N	05°24,6'W	3579m	CTD
	PS2840-2		10:41	81°27,5'N	05°22,9'W	500m	MN
			10:25	81°27,5'N	05°22,9'W		Icegroup on ice
	PS2840-3		12:30	81°26,7'N	05°24,0'W	3297m	PRWS
			13:06	81°26,7'N	05°23,9'W		Icegroup on board
			14:09	81°26,3'N	05°23,0'W	hieven	
	PS2840-4		16:42	81°25,3'N	05°18,5'W	3524m	GKG (geo)
	PS2840-5		19:07	81°23,7'N	05°15,3'W	3547m	MUC (bio+geochem)
			21:57	81°22'N	05°18,4'W	3278m	OFOS
		16.07.1997	00:20	81°21,4'N	05°23,7'W	hieven	
44/070	PS2841-1		05:01	81°31,1'N	06°49,9'W	2675m	CTD
	PS2841-2		07:07	81°31,4'N	06°48,9'W	2731m	MC
	PS2841-3		08:33	81°31,6'N	06°49,3'W	279m	CTD
			08:35	81°31,6'N	06°49,3'W		APSN
	PS2841-4		10:05	81°31,4'N	06°48,8'W	2610m	ISP
	PS2841-5		12:30	81°31,4'N	06°49,8'W	hieven	
			13:10	81°31,6'N	06°49,9'W		Icegroup on ice
	PS2841-6		13:58	81°31,8'N	06°49,8'W	500m	MN
			14:20	81°31,8'N	06°49,8'W		Icegroup on board
	PS2841-7		15:36	81°31,84'N	06°52,25'W	2656m	MUC
44/071	PS2842-1		18:30	81°27'N	06°19,5'W	3122m	KAL (empty)
	PS2842-2		23:10	81°28,3'N	06°19,8'W	3216m	MUC
East Greenland Margin							
44/072		17.07.1997	03:09	81°34,8'N	08°10,5'W	1931m	CTD
			05:23	81°34,9'N	08°10,6'W	1949m	MN
			06:48	81°34,7'N	08°11,5'W	200m	MN
			07:46	81°34,7'N	08°11,3'W	1889m	CTD
			07:58	81°34,7'N	08°11,3'W		APSN
44/072A	PS2843-1		10:41	81°34'N	07°17,8'W	2527m	SL (6.56m)
	PS2843-2		12:13	81°34,02'N	07°20,97'W	2526m	GKG (empty)
44/072B	PS2844-1		14:26	81°34,9'N	08°10,5'W	500m	MN
	PS2844-2		15:45	81°34,84'N	08°10,79'W	1980m	MUC
44/073	PS2845-1		19:07	81°35,0'N	09°49,4'W	1092m	CTD
			19:30	81°35,0'N	09°49,6'W		APSN
	PS2845-2		19:49	81°34,9'N	09°49,7'W	1000m	MN
	PS2845-3		21:25	81°34,5'N	09°50,5'W	986m	GKG (empty)
	PS2845-4		21:15	81°34,7'N	09°51,8'W	932m	MUC
	PS2845-5		23:15	81°53,1'N	09°55,1'W	773m	OFOS
		18.07.1997	01:30	81°35,9'N	10°00,7'W	hieven	
44/074	PS2846-1		02:43	81°35,3'N	10°01,1'W	492m	CTD
	PS2846-2		03:22	81°35,3'N	10°00,8'W	500m	MN
	PS2846-3		04:06	81°35,3'N	10°00,7'W	500m	MN

Station	AWI-No.	Date	Time (GMT)	Latitude	Longitude	Depth	Activity
	PS2846-4		04:54	81°35,2'N	10°00,4'W	521m	GKG
	PS2846-5		05:36	81°35,1'N	10°00,3'W	513m	MUC
44/075			06:23	81°35,2'N	10°08,1'W	273m	CTD
			06:40	81°35,2'N	10°07,9'W		APSN
Fram Strait							
44/076	PS2847-1		14:46	81°53,1'N	04°39,1'W	4100m	CTD
	PS2847-2		16:08	81°52,8'N	04°34,8'W	500m	MN
	PS2847-3		18:21	81°52,3'N	04°32,3'W	4130m	GKG
	PS2847-4		21:00	81°51,1'N	04°19,9'W	4268m	MUC
	PS2847-5		23:53	81°50,3'N	04°12,7'W	4091m	PRWS
		19.07.1997	01:35	81°50,2'N	04°10,2'W	hieven	
44/077	PS2848-1		08:20	82°N	02°25,2'W	2539m	CTD
	PS2848-2		10:35	81°59,9'N	02°25,8'W	500m	MN
	PS2848-3		12:09	81°59,94'N	02°25,81'W	2600m	GKG
	PS2848-4		14:08	82°00,02'N	02°25,92'W	2628m	MUC
	PS2848-5		15:46	82°00,02'N	02°26,27'W	2628m	SL (5.36m)
Nansen Basin							
44/078		20.07.1997	02:30	82°22,4'N	00°11,7'W	3458m	CTD
44/079	PS2849-1		13:36	82°39,2'N	01°26,7'E	3207m	CTD
	PS2849-2		16:19	82°39,3'N	01°26,9'E	3034m	ISP & PRWS
			19:16	82°3,2'N	01°25,6'E	hieven	
	PS2849-3		21:45	82°39,1'N	01°24,8'E	1500m	BN
	PS2849-4		23:15	82°39,1'N	01°24,4'E	500m	MN (geo)
	PS2849-5	21.07.1997	01:50	82°39,1'N	01°24,7'E	3000m	MN
	PS2849-6		04:57	82°39,2'N	01°27,9'E	3238m	GKG (geo)
	PS2849-7		06:46	82°39,1'N	01°29,8'E	3247m	GKG (bio)
			08:30	82°38,8'N	01°30,6'E		Icegroup on ice
	PS2849-8		09:13	82°38,8'N	01°31,1'E	3217m	MUC
			11:00				Icegroup on board
	PS2849-9		11:58	82°38,52'N	01°31,59'E	3261m	MUC
	PS2849-10		14:01	82°38,53'N	01°31,96'E	3262m	SL (4.70m)
44/080		22.07.1997	00:26	82°37,9'N	02°19,7'E	3846m	OFOS
			03:02	82°37,6'N	02°24,7'E	hieven	
Yermak Plateau							
44/081	PS2850-1	23.07.1997	01:56	82°22,8'N	03°40,82'E	2918m	SL (1.65m)
44/082	PS2851-1		05:32	82°22,6'N	03°41,2'E	2743m	CTD
			06:11	82°22,6'N	03°38,8'E		APSN
	PS2851-2		07:21	82°22,5'N	03°36,9'E	2927m	GKG (geo)
	PS2851-3		09:30	82°22,3'N	03°32,6'E	3173m	MUC
44/083	PS2852-1		12:34	82°20,96'N	03°36,79'E	2665m	SL (4.02m)
44/084	PS2853-1		16:34	82°20,0'N	03°50,4'E	2092m	CTD
			18:00	82°19,9'N	03°48,4'E		Icegroup on ice
	PS2853-2		18:30	82°19,9'N	03°48,4'E	1978m	MC
			18:30	82°19,9'N	03°48,4'E		Icegroup on board
	PS2853-3		19:50	82°19,8'N	03°45,2'E	300m	CTD
			20:17	82°19,7'N	03°44,4'E		APSN
	PS2853-4		21:30	82°19,7'N	03°44,1'E	2150m	ISP & PRWS
		24.07.1997	00:15	82°19,4'N	03°39,9'E	hieven	
	PS2853-5		02:48	82°19,4'N	03°39,8'E	2000m	MN
			04:14	82°19,4'N	03°40,9'E	200m	MN
	PS2853-6		05:13	82°19,4'N	03°41,2'E	1200m	BN
	PS2853-7		06:48	82°19,3'N	03°42,1'E	500m	MN
	PS2853-8		07:53	82°19,2'N	03°42,5'E	2045m	GKG (bio)
	PS2853-9		09:02	82°19,1'N	03°42,5'E	2008m	GKG (geo)
			09:33	82°19'N	03°42,5'E		Icegroup on ice
	PS2853-10		10:28	82°18,9'N	03°42,5'E	1977m	MUC
	PS2853-11		12:04	82°18,61'N	03°42,38'E	2061m	MUC

Station	AWI-No.	Date	Time (GMT)	Latitude	Longitude	Depth	Activity
			12:45	82°18,61'N	03°42,38'E		Icegroup on board
	PS2853-12		13:29	82°18,37'N	03°42,35'E	2090m	SL (3.04m)
	PS2853-13		15:43	82°18,17'N	03°42,31'E	2118m	OFOS
			17:29	82°18,2'N	03°39,8'E	hieven	
44/085	PS2854-1	25.07.1997	01:15	82°12,03'N	03°54,029'E	1798m	SL (5.90m)
	PS2854-2		02:32	82°12,02'N	03°54,09'E	1805m	GKG (geo)
44/086			09:08	82°07,4'N	05°00,2'E	1960m	CTD
44/087	PS2855-1		15:38	82°02,6'N	05°18,3'E	1366m	CTD
			16:06	82°02,5'N	05°18,5'E		APSN
	PS2855-2		17:08	82°02,5'N	05°18,0'E	1350m	MN
	PS2855-3		18:03	82°02,5'N	05°17,7'E	100m	MN (geo)
			18:34	82°02,5'N	05°17,7'E	500m	MN
	PS2855-4		19:51	82°02,5'N	05°17,6'E	1294m	BN
	PS2855-5		21:56	82°02,7'N	05°17'E	1450m	FS
			22:28	82°02,7'N	05°17'E	hieven	
	PS2855-6		23:52	82°02,6'N	05°17'E	1452m	SL (4.72m)
	PS2855-7	26.07.1997	00:54	82°02,72'N	05°17,09'E	1454m	GKG (bio)
	PS2855-8		01:47	82°02,74'N	05°17,30'E	1455m	GKG (geo)
	PS2855-9		02:59	82°02,78'N	05°17,64'E	1455m	MUC (geochem)
	PS2855-10		04:10	82°02,92'N	05°18,3'E	1407m	MUC (bio)
44/088	PS2856-1		07:51	81°58,9'N	05°44,8'E	905m	CTD
	PS2856-2		08:59	81°58'N	05°44,9'E	900m	MN (bio)
	PS2856-3		10:05	81°59,1'N	05°44,9'E	900m	BN
	PS2856-4		11:56	81°59,18'N	05°44,53'E	954m	FS
			12:20	81°59,23'N	05°44,52'E	hieven	
	PS2856-5		13:03	81°59,23'N	05°44,56'E	967m	KAL (6.52m)
	PS2856-6		13:55	81°59,25'N	05°44,6'E	965m	GKG (bio)
	PS2856-7		14:42	81°59,24'N	05°44,93'E	961m	GKG (geo)
	PS2856-8		15:32	81°59,26'N	05°45,25'E	959m	MUC (bio)
	PS2856-9		16:32	81°59,3'N	05°45,8'E	929m	MUC (bio)
			17:38	81°59,3'N	05°46,3'E	921m	OFOS
			20:00	81°58,7'N	05°48,8'E	hieven	
44/089	PS2857-1	27.07.1997	03:16	81°53,1'N	07°26,9'E	769m	CTD
	PS2857-2		04:40	81°53,3'N	07°28,9'E	771m	MC
	PS2857-3		05:46	81°53,5'N	07°32,6'E	300m	CTD
	PS2857-4		06:43	81°53,6'N	07°34,5'E	805m	ISP
			09:17	81°54'N	07°43,1'E	hieven	
	PS2857-5		09:48	81°54'N	07°44,5'E	830m	MN
	PS2857-6		10:55	81°54'N	07°47,2'E	800m	BN
	PS2857-7		12:46	81°54,0'N	07°50,1'E	500m	MN
			12:55	81°54,0'N	07°50,9'E		Icegroup on ice
	PS2857-8		13:51	81°54,04'N	07°52,32'E	859m	FS
			14:17	81°54,04'N	07°52,9'E	hieven	
	PS2857-9		14:54	81°54,06'N	07°53,85'E	859m	GKG (bio)
			15:13	81°54,06'N	07°53,85'E		Icegroup on board
	PS2857-10		15:33	81°54,11'N	07°54,83'E	855m	GKG (geo)
	PS2857-11		16:32	81°54,2'N	07°56,4'E	828m	MUC
	PS2857-12		17:19	81°54,2'N	07°57,69'E	824m	MUC
	PS2857-13		18:28	81°54,4'N	07°59,3'E	823m	SL (4.35m)
44/090	PS2858-1		23:00	81°45'N	09°11,6'E	815m	CTD
	PS2858-2	28.07.1997	00:28	81°45,1'N	09°14,6'E	800m	MN
	PS2858-3		01:52	81°45,2'N	09°17,6'E	800m	BN
	PS2858-4		03:24	81°45,47'N	09°25,20'E	919m	FS
			03:28	81°45,5'N	09°25,40'E	hieven	Stop
	PS2858-5		04:14	81°45,3'N	09°28,0'E	907m	GKG (bio)
	PS2858-6		05:07	81°45,3'N	09°39,9'E	932m	GKG (geo)
	PS2858-7		05:59	81°45,N	09°33,5'E	939m	MUC

Station	AWI-No.	Date	Time (GMT)	Latitude	Longitude	Depth	Activity
	PS2858-8		06:53	81°45,4'N	09°35,6'E	955m	SL (4.72m)
	PS2858-9		07:50	81°45,4'N	09°36,8'E	947m	OFOS
			10:20	81°45,3'N	09°40,9'E	hieven	
44/090A			12:34	81°44,8'N	09°47,7'E	begin of trawl	EBS
			12:40	81°44,6'N	09°47,0'E	hieven	
44/090B			15:40	81°45,0'N	10°06,8'E	1800m begin of trawl	AGT
			15:51	81°44,7'N	10°07,2'E	end of trawl	
44/091	PS2859-1		18:41	81°41,7'N	10°19,13'E	1402m	CTD
	PS2859-2		19:24	81°41,1'N	10°21,4'E	1450m	MC
			20:30	81°41,1'N	10°21,4'E		Icegroup on ice
	PS2859-3		21:15	81°40,5'N	10°24,3'E	500m	CTD
			21:50	81°40,5'N	10°24,3'E		Icegroup on board
	PS2859-4		21:59	81°40,3'N	10°25,2'E	1500m	MN
	PS2859-5	29.07.1997	00:00	81°39,9'N	10°26,4'E	200m	MN
			00:36	81°39,8'N	10°26,6'E	500m	MN (geo)
	PS2859-6		02:03	81°39,8'N	10°27,4'E	1400m	BN
	PS2859-7		04:09	81°39,9'N	10°31,4'E	1546m	FS
			04:41	81°39,9'N	10°31,4'E	hieven	
			05:28	81°39,8'N	10°35,9'E		Icegroup on ice
			05:58	81°39,8'N	10°35,9'E		Icegroup on board
	PS2859-8		08:07	81°45,5'N	10°08,7'E	1120m	KAL (6.70m)
	PS2859-9		08:43	81°45,3'N	10°09,7'E	1180m	GKG (bio)
	PS2859-10		09:36	81°45,1'N	10°11,4'E	1180m	GKG (geo)
	PS2859-11		11:10	81°44,8'N	10°11,7'E	1180m	MUC
	PS2859-12		12:17	81°44,81'N	10°12,27'E	1197m	MUC
44/092	PS2860-1		16:44	81°33,7'N	11°30,1'E	1957m	CTD
	PS2860-2		18:46	81°33,6'N	11°34,0'E	1950m	MN
			19:57	81°33,3'N	11°37,2'E	1950	MN
	PS2860-3		20:27	81°33,2'N	11°37,7'E	1200m	BN
	PS2860-4		23:07	81°33,6'N	11°40,5'E	1966m	FS
			23:44	81°33,7'N	11°41,4'E	hieven	
	PS2860-5	30.07.1997	00:52	81°34,11'N	11°43,72'E	2025m	SL (15) (5.26m)
	PS2860-6		02:13	81°34,54'N	11°47,14'E	2031m	GKG (bio)
	PS2860-7		03:30	81°34,88'N	11°51,14'E	2032m	GKG (geo)
	PS2860-8		05:04	81°34,8'N	11°55,5'E	1993m	MUC
	PS2860-9		07:01	81°34,6'N	11°57,6'E	1994m	OFOS
			09:00	81°34,3'N	11°59,7'E	Hieven	
44/093	PS2861-1		16:54	81°16,5'N	13°00,4'E	2261m	CTD
			17:02	81°16,4'N	13°02,7'E		Icegroup on ice
			17:50	81°16,3'N	13°04,9'E		Icegroup on board
	PS2861-2		19:07	81°16,2'N	13°05,1'E	2252m	MC
			19:45	81°16,0'N	13°08,4'E		Icegroup on ice
			21:00	81°16,0'N	13°10,5'E		Icegroup on board
	PS2861-3		20:30	81°16'N	13°09,6'E	200m	CTD
	PS2861-4		22:00	81°16'N	13°10,5'E	2227m	ISP
			00:35			hieven	
	PS2861-5	31.07.1997	03:02	81°17,5'N	13°19,3'E	2250m	MN
	PS2861-6		04:38	81°18,3'N	13°26,6'E	500m	MN
	PS2861-7		05:58	81°18,4'N	13°28,1'E	1500m	BN
	PS2861-8		07:38	81°18,5'N	13°31,3'E	500m	MN
	PS2861-9		09:08	81°19'N	13°38,8'E	2154m	FS
			09:31	81°18,1'N	13°34,4'E	hieven	
	PS2861-10		10:51	81°19,4'N	13°35,8'E	2149m	GKG (bio)
44/093A	PS2861-11		14:27	81°16,35'N	13°03,02'E	2309m	GKG (geo)
	PS2861-12		16:21	81°16,3'N	13°07,4'E	2234m	MUC
	PS2861-13		18:03	81°16,2'N	13°10,5'E	2252m	MUC
	PS2861-14		19:47	81°16,1'N	13°12,1'E	2238m	OFOS
			22:15	81°15,99'N	13°19,34'E	hieven	

Station	AWI-No.	Date	Time (GMT)	Latitude	Longitude	Depth	Activity
North of Svalbard							
44/094	PS2862-1	01.08.1997	09:37	80°35,1'N	11°53,9'E	1020m	CTD
	PS2862-2		10:53	80°34,9'N	11°51,3'E	500m	MN
	PS2862-3		12:14	80°35,04'N	11°50,75'E	1058m	FS
			12:39	80°34,98'N	11°50,21'E	hieven	
	PS2862-4		13:18	80°34,83'N	11°48,71'E	1049m	SL (548.5cm)
	PS2862-5		14:06	80°34,70'N	11°47,34'E	1042m	GKG (geo)
	PS2862-6		14:53	80°34,58'N	11°46,27'E	1036m	GKG (bio)
	PS2862-7		15:50	80°34,58'N	11°45,70'E	1035m	MUC
	PS2862-8		18:09	80°34,3'N	11°36,4'E	begin of trawl	EBS
			18:19	80°34,2'N	11°35,3'E	hieven	
	PS2862-9		20:35	80°33,9'N	11°21,4'E	begin of trawl	AGT
			20:45	80°33,9'N	11°20,6'E	hieven	
	PS2862-10		23:27	80°34'N	11°12,5'E	962m	OFO5
		02.08.1997	01:46	80°34,8'N	11°02,0'E	hieven	
44/095	PS2863-1		03:14	80°33,46'N	10°17,96'E	808m	SL (5.80m)
	PS2863-2		03:55	0°33,47'N	10°17,93'E	807m	GKG (geo)
44/096	PS2864-1		04:53	80°31,8'N	10°22,4'E	762m	CTD
			05:25	80°31,9'N	10°22,7'E		APSN
	PS2864-2		05:55	80°31,8'N	10°22,6'E	500m	MN
	PS2864-3		06:46	80°31,8'N	10°22,3'E	779m	SL (6.37m)
	PS2864-4		07:26	80°31,8'N	10°22,1'E	777m	GKG (geo)
	PS2864-5		08:28	80°31,7'N	10°21,4'E	772m	MUC
	PS2864-6		10:10	80°31,2'N	10°19,6'E	begin of trawl	EBS
			10:20	80°31,1'N	10°19,4'E	hieven	
	PS2864-7		12:16	80°29,63'N	10°17,02'E	begin of trawl	AGT
			12:26	80°29,47'N	10°16,89'E	hieven	
44/097	PS2865-1		13:55	80°29,717'N	10°29,433'E	823m	SL(5) (421.5cm)
	PS2865-2		14:44	80°29,71'N	10°29,33'E	822m	GKG (geo)
44/097A			15:36	80°29,3'N	10°28,6'E	789m	CTD
44/098	PS2866-1		19:11	80°00,0'N	10°52,0'E	258m	CTD
	PS2866-2		19:44	80°00,1'N	10°52,3'E	254m	MN
	PS2866-3		20:18	80°00,2'N	10°52,3'E	269m	GKG
	PS2866-4		20:50	80°00,5'N	10°52,8'E	269m	MUC
44/099	PS2867-1		22:31	80°10,5'N	10°24,0'E	514m	CTD
	PS2867-2		23:55	80°10,6'N	10°23,3'E	513m	MC
	PS2867-3		00:50	80°11,0'N	10°22,3'E	200m	CTD
			01:05	80°11,4'N	10°23,0'E		APSN
	PS2867-4		01:30	80°11,3'N	10°23,1'E	510m	MN
	PS2867-5		02:27	80°11,5'N	10°24,0'E	500m	MN
	PS2867-6		03:19	80°11,7'N	10°25,2'E	491m	CTD
	PS2867-7		03:57	80°11,85'N	10°26,65'E	517m	GKG (bio)
	PS2867-8		04:42	80°12,1'N	10°28,7'E	496m	MUC
	PS2867-9		05:20	80°12,3'N	10°29,9'E	481m	MUC
	PS2867-10		06:31	80°12,1'N	10°32,9'E	begin of trawl	EBS
			06:41	80°12,9'N	10°33,6'E	hieven	
	PS2867-11		07:54	80°11,3'N	10°36,6'E	begin of trawl	EBS
			08:04	80°11,2'N	10°36,9'E	hieven	
			09:05	80°10,4'N	10°23,5'E		Hydrophon i. water
	PS2867-12		09:55	80°09,5'N	10°23,9'E	536m	MUC
			12:17	80°11,0'N	10°24,2'E		Hydrophon i. water released
			12:22	80°11,0'N	10°24,2'E		Mooring
			12:26	80°11,0'N	10°24,2'E		Mooring
			13:18	80°11,0'N	10°25,3'E		Multisampler o. D.
Molloy Deep							
44/100	PS2868-1	04.08.1997	03:00	79°06,2'N	03°06,6'E	5415m	CTD
	PS2868-2		05:30	79°06,3'N	03°07,2'E	5400m	PRWS & ISP
			10:15	79°06,3'N	03°08,7'E	hieven	

Station	AWI-No.	Date	Time (GMT)	Latitude	Longitude	Depth	Activity
			06:55	79°06,3'N	03°07,1'E		APSN
	PS2868-3		13:38	79°05,9'N	03°11,8'E	1500m	BN
	PS2868-4		15:17	79°06,5'N	03°08,5'E	500m	MN
	PS2868-5		17:03	79°06,5'N	03°05,7'E	5416m	GKG (geo)
	PS2868-6		20:21	79°06,1'N	03°02,6'E	5445m	MUC
	PS2868-7	05.08.1997	00:03	79°06,4'N	03°13,6'E	5431m	OFOS
			02:32	79°05,32'N	03°17,79'E	hieven	
44/100A			23:59	79°06,4'N	03°13,3'E		LB
West of Svalbard							
44/101			16:00	79°57,7'N	00°04,0'E	Profilfahrtbeginn	Hydrosweep
			23:33	79°59'N	05°03,5'E	1. Wegpunkt	Hydrosweep
		06.08.1997	05:54	78°46'N	05°05,0'E	2. Wegpunkt	Hydrosweep
			08:41	78°46'N	08°00'E	3. Wegpunkt	Hydrosweep
			08:49	78°44,2'N	08°00,7'E	4. Wegpunkt	Hydrosweep
			10:43	78°44'N	06°01,1'E	5. Wegpunkt	Hydrosweep
			10:53	78°42,2'N	06°00,1'E	6. Wegpunkt	Hydrosweep
			12:44	78°42,0'N	08°00,0'E	7. Wegpunkt	Hydrosweep
			12:54	78°40,0'N	08°00,0'E	8. Wegpunkt	Hydrosweep
			14:47	78°40,0'N	06°00,0'E	9. Wegpunkt	Hydrosweep
			14:56	78°38,0'N	06°00,0'E	10. Wegpunkt	Hydrosweep
			16:52	78°38,0'N	08°00,0'E	11. Wegpunkt	Hydrosweep
			17:04	78°36,0'N	08°00,0'E	12. Wegpunkt	Hydrosweep
			18:55	78°36,0'N	06°00,0'E	13. Wegpunkt	Hydrosweep
			19:07	78°34,0'N	06°00,0'E	14. Wegpunkt	Hydrosweep
			21:04	78°34,0'N	07°59,0'E	15. Wegpunkt	Hydrosweep
			21:06	78°32,2'N	08°00,2'E	16. Wegpunkt	Hydrosweep
			23:08	78°32,0'N	06°00,0'E	17. Wegpunkt	Hydrosweep
			23:19	78°30,0'N	06°00,2'E	18. Wegpunkt	Hydrosweep
		07.08.1997	01:16	78°30,0'N	08°00,2'E	19. Wegpunkt	Hydrosweep
			01:29	78°27,5'N	08°00,0'E	20. Wegpunkt	Hydrosweep
			04:30	78°27,5'N	05°00,0'E	21. Wegpunkt	Hydrosweep
			04:44	78°25,0'N	05°00,0'E	22. Wegpunkt	Hydrosweep
			07:33	78°25,0'N	08°00,0'E	23. Wegpunkt	Hydrosweep
			07:47	78°22,5'N	08°00,0'E	24. Wegpunkt	Hydrosweep
			10:39	78°22,5'N	05°01,0'E	25. Wegpunkt	Hydrosweep
			10:55	78°20,1'N	05°02,0'E	26. Wegpunkt	Hydrosweep
			13:51	78°20,0'N	08°00,0'E	27. Wegpunkt	Hydrosweep
			14:05	78°17,5'N	08°00,0'E	28. Wegpunkt	Hydrosweep
			17:15	78°17,5'N	05°00,0'E	29. Wegpunkt	Hydrosweep
			17:29	78°15,0'N	05°00,0'E	30. Wegpunkt	Hydrosweep
			20:28	78°15,0'N	07°59,9'E	31. Wegpunkt	Hydrosweep
			20:42	78°12,5'N	07°54,2'E	32. Wegpunkt	Hydrosweep
			23:41	78°12,5'N	05°00,0'E	33. Wegpunkt	Hydrosweep
			23:54	78°10,0'N	05°00,0'E	34. Wegpunkt	Hydrosweep
		08.08.1997	02:51	78°10,0'N	08°00,0'E	35. Wegpunkt	Hydrosweep
			03:05	78°07,5'N	08°00,0'E	36. Wegpunkt	Hydrosweep
			06:22	78°07,5'N	05°00,0'E	37. Wegpunkt	Hydrosweep
			06:37	78°05,0'N	05°00,0'E	38. Wegpunkt	Hydrosweep
			09:38	78°05,0'N	07°59,6'E	39. Wegpunkt	Hydrosweep
			09:52	78°02,6'N	07°59,9'E	40. Wegpunkt	Hydrosweep
			13:01	78°02,5'N	05°00,0'E	41. Wegpunkt	Hydrosweep
			13:13	78°00,0'N	05°00,0'E	42. Wegpunkt	Hydrosweep
			16:09	78°00,0'N	08°00,0'E	43. Wegpunkt	Hydrosweep
			16:22	77°57,5'N	08°00,0'E	44. Wegpunkt	Hydrosweep
			20:26	77°57,5'N	04°59,2'E	Ende Profilfahrt	

10.2 Weather Data

DD.MM.	Year	UT	Lat	Lon	DDDF	Bft	Visib.	WX	Weather	Press.	Ta	Td	rF	Tw	Sea	Max.Sea	Speed	
Fr	27.06.97	00	74.4N	29.1E	3009KT	3	10.0km	/		1010.1	2.1	-0.8	81	5.0	/m	/	NE 13kt	
Fr	27.06.97	03	74.9N	30.3E	30012KT	4	10.0km	/		1009.8	1.2	-0.3	90	4.6	/m	/	NE 13kt	
Fr	27.06.97	06	75.5N	31.6E	29013KT	4	20.0km	70	Snow	1009.4	0.7	-1.1	88	4.0	1.0m	990	0.5m	NE 13kt
Fr	27.06.97	09	76.0N	33.0E	29009KT	3	20.0km	70	Snow	1009.3	-0.2	-1.4	92	2.0	0.5m	/	/	NE 13kt
Fr	27.06.97	12	76.0N	33.0E	30011KT	4	4.0km	71	Snow	1010.0	-0.6	-1.9	91	1.7	0.5m	/	/	Station
Fr	27.06.97	15	76.3N	33.5E	29010KT	3	10.0km	22	Recent snow	1009.7	-1.0	-1.6	96	-1.1	0.0m	/	/	N 8kt
Fr	27.06.97	18	76.6N	33.6E	29013KT	4	4.0km	85	Snow shower	1009.6	-0.9	-1.6	95	-1.0	0.0m	/	/	N 8kt
Fr	27.06.97	21	76.6N	33.6E	30006KT	2	10.0km	77	Snow grains	1010.0	-1.3	-1.7	97	-0.9	0.0m	/	/	Station
Sa	28.06.97	00	76.8N	33.8E	29008KT	3	10.0km	/		1010.0	-1.0	-1.4	97	-0.9	/m	/	/	N 3kt
Sa	28.06.97	03	77.2N	33.6E	29005KT	2	10.0km	/		1009.9	-0.9	-2.2	91	-1.7	/m	/	/	N 8kt
Sa	28.06.97	06	77.3N	33.6E	29004KT	2	20.0km	15	/	1010.1	-0.4	-2.3	87	-0.9	0.0m	/	/	N 3kt
Sa	28.06.97	09	77.4N	34.7E	21004KT	2	10.0km	15	/	1010.0	1.0	-4.4	67	-1.6	/m	/	/	NE 3kt
Sa	28.06.97	12	77.6N	34.7E	22005KT	2	20.0km	15	/	1009.8	-0.6	-4.1	77	-1.8	0.0m	/	/	N 3kt
Sa	28.06.97	15	77.6N	34.7E	17005KT	2	20.0km	15	/	1009.2	-1.0	-2.8	88	-1.8	0.0m	/	/	Station
Sa	28.06.97	18	77.7N	34.3E	13006KT	2	10.0km	77	Snow grains	1008.2	-1.4	-2.4	93	-1.9	0.0m	/	/	NW 3kt
Sa	28.06.97	21	77.9N	33.3E	09007KT	3	10.0km	22	Recent snow	1008.1	-1.3	-3.5	85	-1.7	/m	/	/	NW 8kt
Su	29.06.97	00	78.0N	33.0E	07003KT	1	10.0km	/		1008.1	-1.5	-2.8	91	-1.3	/m	/	/	NW 3kt
Su	29.06.97	03	78.2N	33.0E	06003KT	1	10.0km	/		1008.3	-1.6	-3.0	90	-1.8	/m	/	/	N 3kt
Su	29.06.97	06	78.5N	32.4E	09003KT	1	10.0km	15	/	1008.3	-1.1	-2.9	87	-1.8	/m	/	/	N 8kt
Su	29.06.97	09	78.6N	32.1E	06001KT	1	2.0km	85	Snow shower	1008.9	-0.4	-2.2	88	-1.6	/m	/	/	NW 3kt
Su	29.06.97	15	78.7N	31.9E	15003KT	1	10.0km	15	/	1009.3	-0.4	-0.9	96	-1.0	/m	/	/	N 3kt
Su	29.06.97	18	79.0N	31.3E	10005KT	2	0.5km	56	Freezing drizzle	1009.3	-0.1	-0.4	98	-1.7	/m	/	/	N 8kt
Su	29.06.97	21	79.3N	30.9E	09004KT	2	10.0km	7	Very cldy	1009.9	-1.0	-1.1	99	-1.8	/m	/	/	N 8kt
Mo	30.06.97	00	79.4N	30.5E	07003KT	1	10.0km	/		1010.1	-0.7	-1.0	98	-1.6	/m	/	/	NW 3kt
Mo	30.06.97	03	79.6N	30.2E	08004KT	2	10.0km	/		1009.9	-1.1	-1.4	98	-1.9	/m	/	/	N 3kt
Mo	30.06.97	06	79.9N	29.9E	03003KT	1	10.0km	7	Very cldy	1010.2	-0.7	-1.0	98	-1.9	/m	/	/	N 8kt
Mo	30.06.97	09	80.2N	29.4E	04004KT	2	10.0km	85	Snow shower	1010.3	-0.2	-1.1	94	-1.7	/m	/	/	N 8kt
Mo	30.06.97	12	80.3N	29.1E	02002KT	1	4.0km	56	Freezing drizzle	1010.3	-0.2	-0.7	96	-1.7	/m	/	/	NW 3kt
Mo	30.06.97	15	80.3N	29.0E	01003KT	1	4.0km	28	Recent fog	1010.0	0.0	-0.2	99	-1.7	/m	/	/	W ation
Mo	30.06.97	18	80.5N	29.2E	01005KT	2	10.0km	77	Snow grains	1008.9	-0.3	-0.8	96	-1.8	/m	/	/	N 3kt
Mo	30.06.97	21	80.7N	29.6E	36005KT	2	0.5km	47	Fog	1009.0	-0.5	-0.7	99	-1.7	/m	/	/	N 3kt
Tu	01.07.97	00	80.7N	29.5E	01005KT	2	10.0km	/		1008.6	-0.5	-1.2	95	-1.4	/m	/	/	W ation
Tu	01.07.97	03	80.7N	29.5E	35006KT	2	10.0km	/		1007.8	-0.7	-1.4	95	-1.5	/m	/	/	Station
Tu	01.07.97	06	80.7N	29.4E	34007KT	3	4.0km	85	Snow shower	1007.1	-0.1	-1.1	93	-1.7	/m	/	/	Station
Tu	01.07.97	09	80.7N	29.4E	35012KT	4	4.0km	85	Snow shower	1006.3	-0.6	-1.3	95	-1.6	/m	/	/	Station
Tu	01.07.97	12	80.7N	27.9E	32016KT	5	10.0km	77	Snow grains	1005.6	-0.7	-1.2	96	-1.6	/m	/	/	W 3kt
Tu	01.07.97	15	80.8N	26.8E	33014KT	4	20.0km	15	/	1005.6	-0.3	-1.4	92	-1.8	/m	/	/	NW 3kt
Tu	01.07.97	18	80.7N	26.0E	33012KT	4	20.0km	8	Overcast	1005.9	-0.4	-0.6	99	-1.7	/m	/	/	SW 3kt
Tu	01.07.97	21	80.7N	25.3E	32018KT	5	10.0km	8	Overcast	1006.5	-0.4	-1.0	96	-1.7	/m	/	/	W 3kt
We	02.07.97	00	80.8N	24.9E	31018KT	5	10.0km	/		1006.9	-0.8	-1.8	93	-1.0	/m	/	/	NW 3kt
We	02.07.97	03	80.9N	24.4E	30017KT	5	10.0km	/		1007.4	-0.8	-2.0	92	-1.0	/m	/	/	NW 3kt
We	02.07.97	06	80.9N	24.3E	31017KT	5	2.0km	73	Snow	1007.0	-1.0	-1.7	95	-1.7	/m	/	/	Station
We	02.07.97	09	80.9N	23.6E	31018KT	5	2.0km	71	Snow	1008.4	-1.3	-2.2	94	-0.9	/m	/	/	W 3kt
We	02.07.97	12	80.9N	22.9E	32018KT	5	4.0km	71	Snow	1009.5	-1.4	-2.4	93	-1.7	/m	/	/	W 3kt
We	02.07.97	15	80.9N	22.0E	31014KT	4	20.0km	22	Recent snow	1011.1	-1.7	-3.2	89	-1.8	/m	/	/	W 3kt
We	02.07.97	18	81.0N	21.1E	30011KT	4	2.0km	77	Snow grains	1012.1	-2.1	-2.8	95	-1.6	/m	/	/	NW 3kt
We	02.07.97	21	81.1N	20.2E	28010KT	3	4.0km	40	/	1013.3	-3.0	-3.3	98	-1.7	/m	/	/	NW 3kt
Th	03.07.97	00	81.1N	20.1E	27007KT	3	10.0km	/		1014.3	-3.5	-3.8	98	-0.9	/m	/	/	W ation
Th	03.07.97	03	80.9N	19.8E	26008KT	3	10.0km	/		1015.0	-2.1	-2.3	99	-1.0	/m	/	/	S 3kt
Th	03.07.97	06	81.0N	18.6E	25006KT	2	4.0km	77	Snow grains	1015.0	-0.4	-2.3	87	-1.3	/m	/	/	NW 3kt
Th	03.07.97	09	81.0N	18.5E	24003KT	1	20.0km	15	/	1015.7	1.3	-0.8	86	-1.3	/m	/	/	W ation
Th	03.07.97	12	81.0N	18.5E	99001KT	1	10.0km	50	Drizzle	1016.4	0.2	-1.0	92	-1.4	/m	/	/	Station
Th	03.07.97	15	81.0N	18.5E	16007KT	3	50.0km	7	Very cldy	1017.0	-0.3	-1.0	95	-1.6	/m	/	/	Station
Th	03.07.97	18	81.0N	18.2E	11008KT	3	50.0km	7	Very cldy	1017.0	-0.1	-1.4	91	-1.5	/m	/	/	W 3kt
Th	03.07.97	21	81.0N	17.4E	15006KT	2	4.0km	51	Drizzle	1017.8	0.3	-1.5	88	-1.6	/m	/	/	W 3kt
Fr	04.07.97	00	81.0N	17.5E	17006KT	2	10.0km	/		1018.5	0.0	-0.3	98	-1.7	/m	/	/	Station
Fr	04.07.97	03	81.0N	17.5E	20010KT	3	4.0km	/		1019.5	2.5	0.8	88	-1.6	/m	/	/	Station
Fr	04.07.97	06	81.0N	17.3E	20011KT	4	2.0km	51	Drizzle	1020.0	0.6	0.5	99	-1.6	/m	/	/	W 3kt
Fr	04.07.97	09	81.1N	16.9E	23012KT	4	10.0km	8	Overcast	1021.2	0.3	0.1	99	-1.8	/m	/	/	NW 3kt
Fr	04.07.97	12	81.1N	17.0E	24005KT	2	0.5km	51	Drizzle	1022.2	0.0	-0.1	99	-1.8	/m	/	/	Station
Fr	04.07.97	15	81.1N	17.0E	20009KT	3	2.0km	50	Drizzle	1022.6	0.7	0.6	99	-1.6	/m	/	/	Station
Fr	04.07.97	18	81.1N	17.0E	20010KT	3	2.0km	51	Drizzle	1022.5	1.1	0.9	99	-1.8	/m	/	/	Station
Fr	04.07.97	21	81.1N	17.0E	16010KT	3	0.2km	45	Fog	1022.7	0.8	0.6	100	-1.7	/m	/	/	Station

DD.MM. Year	UT	Lat	Lon	DDDD	Bft	Visib.	WX	Weather	Press.	Ta	Td	rF	Tw	Sea	Max.Sea	Speed
Sa 05.07.97	00	81.1N	16.3E	14011KT	4-	10.0km	/		1022.3	0.5	0.5	100	-1.7	/m	/m	W 3kt
Sa 05.07.97	03	81.1N	16.2E	17007KT	3	10.0km	/		1022.2	0.5	0.3	99	-1.6	/m	/m	W ation
Sa 05.07.97	06	81.1N	16.3E	14003KT	1	50.0km	3	Ptly cldy	1021.7	1.0	-0.4	90	-1.6	/m	/m	E ation
Sa 05.07.97	09	81.1N	16.3E	11005KT	2	50.0km	4	Ptly cldy	1021.3	1.5	-0.2	88	-1.6	/m	/m	Station
Sa 05.07.97	12	81.1N	16.3E	11007KT	3	50.0km	6	Pair	1020.7	1.1	-0.6	88	-1.6	/m	/m	Station
Sa 05.07.97	15	81.1N	16.2E	12004KT	2	50.0km	6	Ptly cldy	1020.0	0.2	-1.1	91	-1.7	/m	/m	Station
Sa 05.07.97	18	81.1N	16.2E	06007KT	3	50.0km	6	Cloudy	1019.1	0.9	0.2	95	-1.6	/m	/m	Station
Sa 05.07.97	21	81.1N	16.2E	05006KT	2	50.0km	7	Cloudy	1018.5	0.3	-0.4	95	-1.7	/m	/m	Station
DD.MM. Year	UT	Lat	Lon	DDDD	Bft	Visib.	WX	Weather	Press.	Ta	Td	rF	Tw	Sea	Max.Sea	Speed
Su 06.07.97	00	81.1N	16.1E	08005KT	2	10.0km	/		1018.0	0.0	-0.3	98	-1.6	/m	/m	W ation
Su 06.07.97	03	81.1N	15.2E	07007KT	3	10.0km	/		1018.3	0.3	-1.0	91	-1.8	/m	/m	W 3kt
Su 06.07.97	06	81.0N	14.2E	07007KT	3	50.0km	7	Cloudy	1018.4	1.2	0.2	93	-1.7	/m	/m	SW 3kt
Su 06.07.97	09	81.0N	12.5E	36006KT	2	50.0km	7	Very cldy	1019.2	0.4	0.1	98	-1.7	/m	/m	W 3kt
Su 06.07.97	12	81.0N	11.9E	03003KT	1	50.0km	6	Cloudy	1020.0	0.7	-1.4	86	-1.7	/m	/m	W 3kt
Su 06.07.97	15	81.0N	11.9E	33004KT	2	20.0km	6	Cloudy	1020.6	0.5	-0.3	94	-1.7	/m	/m	Station
Su 06.07.97	18	81.0N	11.8E	99001KT	1	50.0km	3	Ptly cldy	1021.2	1.6	0.1	90	-1.7	/m	/m	Station
Su 06.07.97	21	81.0N	11.8E	99001KT	1	20.0km	7	Ptly cldy	1021.8	2.9	-0.3	79	-1.7	/m	/m	Station
DD.MM. Year	UT	Lat	Lon	DDDD	Bft	Visib.	WX	Weather	Press.	Ta	Td	rF	Tw	Sea	Max.Sea	Speed
Mo 07.07.97	00	81.0N	11.8E	10003KT	1	10.0km	/		1022.0	0.4	-0.5	94	-1.0	/m	/m	Station
Mo 07.07.97	03	80.9N	11.9E	09008KT	3	10.0km	/		1022.0	1.9	0.5	90	-1.1	/m	/m	S 3kt
Mo 07.07.97	06	80.7N	11.9E	07010KT	3	20.0km	7	Very cldy	1021.7	1.2	0.4	94	-1.7	/m	/m	S 3kt
Mo 07.07.97	09	80.5N	11.8E	10006KT	2	20.0km	7	Very cldy	1022.1	1.1	0.7	97	-1.7	/m	/m	S 3kt
Mo 07.07.97	12	80.3N	11.5E	99003KT	1	20.0km	7	Very cldy	1022.4	1.1	0.1	93	-1.7	/m	/m	S 3kt
Mo 07.07.97	15	80.2N	10.4E	99004KT	1	50.0km	7	Very cldy	1022.4	2.9	0.4	84	1.9	0.0m	190 0.5m	Station
Mo 07.07.97	18	80.2N	10.4E	36004KT	1	50.0km	7	Very cldy	1022.3	2.4	0.4	87	2.3	0.0m	190 1.0m	Station
Mo 07.07.97	21	80.4N	10.4E	06003KT	1	50.0km	7	Very cldy	1022.4	0.7	-0.5	92	-1.7	/m	/m	N 3kt
DD.MM. Year	UT	Lat	Lon	DDDD	Bft	Visib.	WX	Weather	Press.	Ta	Td	rF	Tw	Sea	Max.Sea	Speed
Tu 08.07.97	00	80.6N	10.3E	21003KT	1	10.0km	/		1022.1	0.9	-0.4	91	-1.4	/m	/m	N 3kt
Tu 08.07.97	03	80.6N	10.3E	09004KT	2	10.0km	/		1021.5	1.0	-0.3	91	-1.0	/m	/m	Station
Tu 08.07.97	06	80.6N	10.3E	99001KT	1	50.0km	7	Very cldy	1021.1	2.2	0.1	86	-1.7	/m	/m	Station
Tu 08.07.97	09	80.6N	10.4E	09003KT	1	50.0km	7	Very cldy	1021.3	1.1	-0.2	91	-1.7	/m	/m	E ation
Tu 08.07.97	12	80.9N	10.2E	18006KT	2	20.0km	7	Very cldy	1021.2	1.9	-0.9	82	-1.7	/m	/m	N 3kt
Tu 08.07.97	15	80.9N	9.9E	16006KT	2	20.0km	7	Very cldy	1020.8	2.1	-0.3	84	-1.7	/m	/m	NW 3kt
Tu 08.07.97	18	80.9N	9.9E	16008KT	3	20.0km	7	Very cldy	1020.4	1.1	-0.2	91	-1.6	/m	/m	Station
Tu 08.07.97	21	80.9N	9.8E	17007KT	3	20.0km	7	Very cldy	1020.3	1.5	0.5	93	-1.6	/m	/m	W ation
DD.MM. Year	UT	Lat	Lon	DDDD	Bft	Visib.	WX	Weather	Press.	Ta	Td	rF	Tw	Sea	Max.Sea	Speed
We 09.07.97	00	80.9N	9.8E	17009KT	3	10.0km	/		1020.1	2.7	0.6	86	-1.8	/m	/m	Station
We 09.07.97	03	80.9N	9.9E	18011KT	4-	10.0km	/		1019.8	2.8	1.3	90	-1.8	/m	/m	E ation
We 09.07.97	06	80.9N	9.8E	18016KT	5-	0.5km	47	Fog	1019.7	2.5	2.5	100	-1.7	/m	/m	W 3kt
We 09.07.97	09	81.0N	9.5E	20015KT	4+	0.1km	45	Fog	1020.9	1.4	1.4	100	-1.7	/m	/m	NW 3kt
We 09.07.97	12	81.0N	8.8E	18015KT	4+	0.1km	45	Fog	1021.4	1.7	1.6	99	-1.7	/m	/m	W 3kt
We 09.07.97	15	81.0N	7.6E	17016KT	5-	2.0km	50	Drizzle	1020.5	1.6	1.4	99	-1.7	/m	/m	W 3kt
We 09.07.97	18	81.1N	7.3E	19015KT	4+	4.0km	10	/	1020.3	1.8	1.4	97	-1.7	/m	/m	NW 3kt
We 09.07.97	21	81.1N	7.3E	16014KT	4	0.1km	45	Fog	1019.4	1.8	1.7	99	-1.7	/m	/m	Station
DD.MM. Year	UT	Lat	Lon	DDDD	Bft	Visib.	WX	Weather	Press.	Ta	Td	rF	Tw	Sea	Max.Sea	Speed
Th 10.07.97	00	81.1N	7.3E	14016KT	5-	4.0km	/		1018.1	1.6	1.3	98	-1.4	/m	/m	Station
Th 10.07.97	03	81.1N	7.0E	14014KT	4	4.0km	/		1016.0	1.9	1.5	97	-1.3	/m	/m	W 3kt
Th 10.07.97	06	81.3N	7.0E	15010KT	3	4.0km	61	Rain	1013.9	1.4	0.8	96	-1.7	/m	/m	Station
Th 10.07.97	09	81.3N	7.1E	14010KT	3	10.0km	61	Rain	1012.2	2.0	1.5	96	-1.7	/m	/m	E ation
Th 10.07.97	12	81.1N	7.0E	11010KT	3	4.0km	61	Rain	1010.7	1.0	0.4	96	-1.7	/m	/m	W ation
Th 10.07.97	15	81.1N	6.3E	10008KT	3	4.0km	58	Rain and drizzl	1008.9	1.6	1.0	96	-1.7	/m	/m	W 3kt
Th 10.07.97	18	81.1N	5.7E	07006KT	2	2.0km	51	Drizzle	1008.3	0.7	0.3	97	-1.7	/m	/m	W 3kt
Th 10.07.97	21	81.1N	5.6E	27013KT	4	0.1km	45	Fog	1009.3	0.7	0.6	99	-1.7	/m	/m	W ation
DD.MM. Year	UT	Lat	Lon	DDDD	Bft	Visib.	WX	Weather	Press.	Ta	Td	rF	Tw	Sea	Max.Sea	Speed
Fr 11.07.97	00	81.1N	5.6E	23014KT	4	4.0km	/		1011.0	-0.8	-1.2	97	-1.0	/m	/m	Station
Fr 11.07.97	03	81.1N	5.7E	21012KT	4-	4.0km	/		1012.0	-1.1	-1.5	97	-1.0	/m	/m	E ation
Fr 11.07.97	06	81.1N	5.8E	21009KT	3	20.0km	26	Recent snow sho	1012.4	-0.5	-1.5	93	-1.7	/m	/m	Station
Fr 11.07.97	09	81.1N	5.9E	21014KT	4	20.0km	26	Recent snow sho	1013.2	-0.4	-1.8	90	-1.7	/m	/m	E ation
Fr 11.07.97	12	81.1N	5.4E	22015KT	4+	20.0km	15	/	1014.1	0.0	-2.1	86	-1.7	/m	/m	W 3kt
Fr 11.07.97	15	81.2N	4.2E	21014KT	4	20.0km	26	Recent snow sho	1014.3	-0.1	-1.4	91	-1.7	/m	/m	NW 3kt
Fr 11.07.97	18	81.2N	4.2E	20012KT	4-	4.0km	77	Snow grains	1014.4	-0.3	-1.2	94	-1.7	/m	/m	Station
Fr 11.07.97	21	81.1N	4.2E	21012KT	4-	10.0km	22	Recent snow	1014.4	-1.6	-2.9	91	-1.7	/m	/m	S 3kt
DD.MM. Year	UT	Lat	Lon	DDDD	Bft	Visib.	WX	Weather	Press.	Ta	Td	rF	Tw	Sea	Max.Sea	Speed
Sa 12.07.97	00	81.2N	3.5E	19010KT	3	4.0km	/		1011.6	-1.0	-2.0	93	-1.2	/m	/m	NW 3kt
Sa 12.07.97	03	81.2N	3.1E	18019KT	5	10.0km	/		1012.6	-0.6	-0.9	98	-1.1	/m	/m	W 3kt
Sa 12.07.97	06	81.3N	2.2E	19016KT	5-	2.0km	56	Freezing drizzl	1011.7	-1.1	-1.3	99	-1.7	/m	/m	NW 3kt
Sa 12.07.97	09	81.2N	2.3E	20020KT	5+	4.0km	10	/	1011.4	-0.9	-1.2	98	-1.7	/m	/m	S 3kt
Sa 12.07.97	12	81.2N	2.4E	20016KT	5-	0.5km	45	Fog	1011.2	-0.6	-0.8	99	-1.7	/m	/m	Station
Sa 12.07.97	15	81.2N	2.5E	21016KT	5-	10.0km	8	Overcast	1011.1	-0.1	-0.4	98	-1.7	/m	/m	E ation
Sa 12.07.97	18	81.2N	2.6E	21013KT	4	0.2km	49	Freezing fog	1011.0	-0.7	-0.9	99	-1.7	/m	/m	E ation
Sa 12.07.97	21	81.2N	1.9E	21010KT	3	0.1km	49	Freezing fog	1012.0	-1.2	-1.3	99	-1.7	/m	/m	W 3kt
DD.MM. Year	UT	Lat	Lon	DDDD	Bft	Visib.	WX	Weather	Press.	Ta	Td	rF	Tw	Sea	Max.Sea	Speed
Su 13.07.97	00	81.3N	1.5E	17008KT	3	0.2km	/		1012.2	-2.1	-2.4	98	-1.1	/m	/m	NW 3kt
Su 13.07.97	03	81.3N	0.7E	15009KT	3	0.1km	/		1011.8	-2.2	-2.6	97	-1.1	/m	/m	W 3kt
Su 13.07.97	06	81.3N	0.3E	16012KT	4-	0.2km	48	Freezing fog	1011.2	-2.0	-2.2	99	-1.7	/m	/m	W 3kt
Su 13.07.97	09	81.3N	0.3E	17007KT	3	20.0km	28	Recent fog	1011.6	-0.3	-0.6	98	-1.7	/m	/m	Station
Su 13.07.97	12	81.3N	0.3E	15011KT	4-	4.0km	63	Rain	1010.6	0.1	-0.1	99	-1.7	/m	/m	Station
Su 13.07.97	15	81.3N	0.4E	18012KT	4-	2.0km	61	Rain	1009.5	0.3	0.0	98	-1.7	/m	/m	Station
Su 13.07.97	18	81.3N	0.4E	19013KT	4	0.2km	61	Rain	1009.4	0.1	-0.1	99	-1.7	/m	/m	Station
Su 13.07.97	21	81.3N	0.5E	18012KT	4-	4.0km	63	Rain	1009.0	0.4	0.1	98	-1.7	/m	/m	E ation
DD.MM. Year	UT	Lat	Lon	DDDD	Bft	Visib.	WX	Weather	Press.	Ta	Td	rF	Tw	Sea	Max.Sea	Speed
Mo 14.07.97	00	81.3N	0.4E	19013KT	4	10.0km	/		1008.7	0.2	-0.1	98	-1.2	/m	/m	W ation
Mo 14.07.97	03	81.3N	0.5E	20012KT	4-	0.5km	/		1008.5	0.0	-0.3	98	-1.2	/m	/m	E ation
Mo 14.07.97	06	81.3N	0.6E	20009KT	3	2.0km	51	Drizzle	1008.2	-0.2	-0.4	99	-1.7	/m	/m	Station
Mo 14.07.97	09	81.3N	0.2E	17009KT	3	0.2km	61	Rain	1008							

DD.MM. Year UT Lat	Lon	DDDF	Bft	Visib.	WX	Weather	Press.	Ta	Td	rF	Tw	Sea	Max.Sea	Speed
Tu 15.07.97 00 81.4N	0.9W	19013KT	4	1.0km	/		1004.3	-0.2	-0.4	99	-1.6	/	/	/
Tu 15.07.97 03 81.5N	2.2W	25018KT	5	0.5km	/		1005.2	-0.9	-1.3	97	-1.8	/	/	NW 3kt
Tu 15.07.97 06 81.5N	3.9W	31023KT	6	20.0km	15	/	1009.4	-0.8	-1.2	97	-1.6	0.5m	/	W 3kt
Tu 15.07.97 09 81.5N	5.4W	30021KT	5+	2.0km	85	Snow shower	1014.8	-1.5	-2.1	96	-0.6	0.5m	/	W 3kt
Tu 15.07.97 12 81.4N	5.4W	31014KT	4	20.0km	7	Very cldy	1018.0	-0.7	-2.1	90	-0.6	0.0m	/	S 3kt
Tu 15.07.97 15 81.4N	5.4W	30012KT	4-	20.0km	15	/	1019.8	-0.9	-2.5	89	-0.7	0.0m	/	Station
Tu 15.07.97 18 81.4N	5.3W	33008KT	3	50.0km	7	Very cldy	1021.0	-0.7	-2.2	90	-0.8	/	/	E ation
Tu 15.07.97 21 81.4N	5.3W	27002KT	1	20.0km	7	Very cldy	1022.1	-1.1	-4.0	81	-0.8	0.0m	/	Station
DD.MM. Year UT Lat	Lon	DDDF	Bft	Visib.	WX	Weather	Press.	Ta	Td	rF	Tw	Sea	Max.Sea	Speed
We 16.07.97 00 81.4N	5.4W	16002KT	1	10.0km	/		1022.5	-1.9	-3.4	89	-0.5	/	/	W ation
We 16.07.97 03 81.4N	6.3W	12004KT	2	0.1km	/		1022.1	-2.6	-3.4	94	-0.9	/	/	W 3kt
We 16.07.97 06 81.5N	6.9W	15004KT	2	0.5km	41	Fog Patches	1021.2	-3.2	-3.5	98	-0.7	0.0m	/	NW 3kt
We 16.07.97 09 81.5N	6.8W	13005KT	2	0.5km	77	Snow grains	1021.3	-3.1	-3.3	99	-0.8	0.0m	/	Station
We 16.07.97 12 81.5N	6.8W	14004KT	2	0.5km	41	Fog Patches	1020.7	-2.9	-3.4	96	-0.7	0.0m	/	Station
We 16.07.97 15 81.5N	6.9W	14008KT	3	1.0km	41	Fog Patches	1020.0	-2.6	-3.4	94	-0.7	0.0m	/	W ation
We 16.07.97 18 81.4N	6.3W	10007KT	3	0.5km	77	Snow grains	1019.3	-2.8	-3.5	95	-1.6	0.0m	/	SE 3kt
We 16.07.97 21 81.5N	6.3W	10007KT	3	1.0km	77	Snow grains	1018.8	-2.6	-3.3	95	-0.7	0.0m	/	N 3kt
DD.MM. Year UT Lat	Lon	DDDF	Bft	Visib.	WX	Weather	Press.	Ta	Td	rF	Tw	Sea	Max.Sea	Speed
Th 17.07.97 00 81.5N	6.4W	09006KT	2	10.0km	/		1017.8	-2.9	-3.9	93	-1.6	/	/	W ation
Th 17.07.97 03 81.6N	8.2W	07008KT	3	4.0km	/		1016.4	-2.5	-3.4	93	-0.1	/	/	W 8kt
Th 17.07.97 06 81.6N	8.2W	04009KT	3	0.5km	41	Fog Patches	1014.9	-2.1	-2.4	98	-0.3	0.0m	/	Station
Th 17.07.97 09 81.6N	8.1W	03014KT	4	20.0km	8	Overcast	1013.7	-0.8	-1.4	96	-0.3	0.0m	/	E ation
Th 17.07.97 12 81.6N	7.3W	02014KT	4	10.0km	70	Snow	1012.5	-0.4	-1.0	96	-0.4	0.5m	/	E 3kt
Th 17.07.97 15 81.6N	8.2W	35014KT	4	4.0km	71	Snow	1012.0	-0.3	-0.5	99	-0.1	0.0m	/	W 3kt
Th 17.07.97 18 81.6N	9.5W	35018KT	5	0.5km	47	Fog	1011.9	-0.3	-0.5	99	-0.1	1.0m	/	W 3kt
Th 17.07.97 21 81.6N	9.8W	34014KT	4	0.5km	44	Fog	1012.5	-0.3	-0.5	99	-0.1	0.5m	/	W 3kt
DD.MM. Year UT Lat	Lon	DDDF	Bft	Visib.	WX	Weather	Press.	Ta	Td	rF	Tw	Sea	Max.Sea	Speed
Fr 18.07.97 00 81.6N	9.9W	35011KT	4	10.0km	/		1013.1	-0.3	-0.5	99	-0.1	/	/	W ation
Fr 18.07.97 03 81.6N	10.0W	36009KT	3	10.0km	/		1013.3	-0.3	-0.6	98	-0.1	/	/	W ation
Fr 18.07.97 06 81.6N	10.1W	04009KT	3	20.0km	7	Very cldy	1013.9	-0.4	-0.7	98	0.0	0.0m	/	W ation
Fr 18.07.97 09 81.7N	8.4W	03004KT	2	50.0km	7	Very cldy	1013.9	-0.3	-0.6	98	0.2	0.0m	/	E 3kt
Fr 18.07.97 12 81.9N	5.6W	36006KT	2	50.0km	7	Very cldy	1013.8	0.0	-0.5	96	-0.4	0.0m	/	NE 8kt
Fr 18.07.97 15 81.9N	4.6W	03004KT	2	20.0km	7	Very cldy	1014.0	0.1	-1.0	92	-0.8	/	/	E 3kt
Fr 18.07.97 18 81.9N	4.5W	17001KT	1	1.0km	10	/	1014.5	-0.8	-1.1	98	-0.6	/	/	E ation
Fr 18.07.97 21 81.9N	4.3W	18005KT	2	0.5km	56	Freezing drizzl	1014.8	-1.7	-1.9	99	-0.7	/	/	E 3kt
DD.MM. Year UT Lat	Lon	DDDF	Bft	Visib.	WX	Weather	Press.	Ta	Td	rF	Tw	Sea	Max.Sea	Speed
Sa 19.07.97 00 81.8N	4.2W	15005KT	2	0.5km	/		1014.9	-2.1	-2.6	96	0.0	/	/	S 3kt
Sa 19.07.97 03 81.8N	4.1W	13005KT	2	0.2km	/		1015.1	-2.7	-3.3	96	0.0	/	/	E ation
Sa 19.07.97 06 82.0N	3.2W	15007KT	3	0.5km	41	Fog Patches	1015.1	-2.8	-3.2	97	-1.8	/	/	NE 3kt
Sa 19.07.97 09 82.0N	2.4W	14004KT	2	0.5km	41	Fog Patches	1015.4	-2.6	-3.0	99	-1.7	/	/	E 3kt
Sa 19.07.97 12 82.0N	2.4W	12003KT	1	50.0km	40	/	1015.0	-1.3	-1.9	96	-1.8	/	/	Station
Sa 19.07.97 15 82.0N	2.4W	12003KT	1	50.0km	7	Very cldy	1014.8	-0.7	-1.5	94	-1.8	/	/	Station
Sa 19.07.97 18 82.0N	1.8W	99002KT	1	50.0km	15	/	1014.6	-0.7	-1.5	94	-1.7	/	/	E 3kt
Sa 19.07.97 21 82.2N	0.9W	07003KT	1	0.5km	42	Fog	1015.1	-0.6	-0.9	98	-1.8	/	/	NE 3kt
DD.MM. Year UT Lat	Lon	DDDF	Bft	Visib.	WX	Weather	Press.	Ta	Td	rF	Tw	Sea	Max.Sea	Speed
Su 20.07.97 00 82.3N	0.3W	09002KT	1	0.2km	/		1016.0	-0.7	-0.9	99	-1.7	/	/	NE 3kt
Su 20.07.97 06 82.5N	0.1W	19004KT	2	20.0km	40	/	1018.5	-0.5	-0.9	97	-1.8	/	/	N 3kt
Su 20.07.97 09 82.6N	1.0E	20006KT	2	20.0km	40	/	1020.0	0.6	-0.3	94	-1.7	/	/	NE 3kt
Su 20.07.97 12 82.7N	1.5E	16007KT	3	20.0km	7	Very cldy	1021.3	-0.1	-1.0	94	-1.7	/	/	NE 3kt
Su 20.07.97 15 82.7N	1.4E	18005KT	2	50.0km	7	Very cldy	1022.2	0.1	-1.2	91	-1.7	/	/	W ation
Su 20.07.97 18 82.7N	1.4E	17005KT	2	50.0km	4	Fair	1022.9	0.1	-3.6	76	-1.7	/	/	Station
Su 20.07.97 21 82.7N	1.4E	18007KT	3	50.0km	7	Very cldy	1023.4	-0.6	-2.2	89	-1.7	/	/	Station
DD.MM. Year UT Lat	Lon	DDDF	Bft	Visib.	WX	Weather	Press.	Ta	Td	rF	Tw	Sea	Max.Sea	Speed
Mo 21.07.97 00 82.7N	1.4E	17010KT	3	10.0km	/		1023.4	0.1	-1.4	90	-1.2	/	/	Station
Mo 21.07.97 03 82.7N	1.4E	22007KT	3	10.0km	/		1023.9	-0.3	-2.9	83	-1.2	/	/	Station
Mo 21.07.97 06 82.7N	1.5E	23009KT	3	0.2km	41	Fog Patches	1024.3	-2.1	-2.3	99	-1.7	/	/	Station
Mo 21.07.97 09 82.6N	1.5E	21007KT	3	20.0km	40	/	1024.7	-0.6	-1.9	91	-1.7	/	/	S 3kt
Mo 21.07.97 12 82.6N	1.5E	19011KT	4-	50.0km	1	Fair	1024.7	0.3	-2.8	80	-1.7	/	/	Station
Mo 21.07.97 15 82.6N	1.5E	19013KT	4	50.0km	1	Fair	1024.6	0.7	-2.8	77	-1.7	/	/	Station
Mo 21.07.97 18 82.6N	1.8E	19014KT	4	50.0km	1	Fair	1023.9	0.4	-2.2	83	-1.7	/	/	E 3kt
Mo 21.07.97 21 82.6N	2.1E	19014KT	4	50.0km	40	/	1023.4	-0.4	-2.1	88	-1.7	/	/	E 3kt
DD.MM. Year UT Lat	Lon	DDDF	Bft	Visib.	WX	Weather	Press.	Ta	Td	rF	Tw	Sea	Max.Sea	Speed
Tu 22.07.97 00 82.6N	2.3E	19013KT	4	0.2km	/		1023.2	-2.2	-2.5	98	-1.5	/	/	E 3kt
Tu 22.07.97 03 82.6N	2.4E	17015KT	4+	0.5km	/		1022.3	-2.7	-3.1	97	-1.5	/	/	E ation
Tu 22.07.97 06 82.6N	2.5E	19015KT	4+	4.0km	77	Snow grains	1021.4	-1.2	-1.5	98	-1.6	/	/	Station
Tu 22.07.97 09 82.5N	2.7E	18012KT	4-	10.0km	7	Very cldy	1020.6	-0.3	-0.6	98	-1.7	/	/	S 3kt
Tu 22.07.97 12 82.5N	3.2E	10009KT	3	0.2km	46	Fog	1019.4	0.2	0.1	99	-1.7	/	/	E 3kt
Tu 22.07.97 15 82.5N	3.1E	06010KT	3	50.0km	40	/	1017.9	0.2	-0.5	95	-1.7	/	/	W ation
Tu 22.07.97 18 82.5N	3.5E	07017KT	5-	50.0km	3	Fair	1015.4	0.1	-1.7	88	-1.7	/	/	E 3kt
Tu 22.07.97 21 82.4N	3.8E	07014KT	4	50.0km	3	Fair	1014.3	-0.3	-2.1	86	-1.7	/	/	S 3kt
DD.MM. Year UT Lat	Lon	DDDF	Bft	Visib.	WX	Weather	Press.	Ta	Td	rF	Tw	Sea	Max.Sea	Speed
We 23.07.97 00 82.4N	3.8E	05016KT	5-	10.0km	/		1013.6	-0.4	-2.5	86	-0.8	/	/	Station
We 23.07.97 03 82.4N	3.7E	04016KT	5-	10.0km	/		1013.4	-0.4	-2.6	85	-0.8	/	/	W ation
We 23.07.97 06 82.4N	3.7E	04017KT	5-	50.0km	14	/	1013.7	-0.3	-2.7	84	-1.7	/	/	Station
We 23.07.97 09 82.4N	3.6E	03016KT	5-	50.0km	2	Fair	1014.7	-0.3	-2.2	87	-1.7	/	/	W ation
We 23.07.97 12 82.4N	3.6E	03011KT	4-	50.0km	1	Fair	1016.0	-0.1	-1.9	88	-1.7	/	/	Station
We 23.07.97 15 82.3N	3.8E	01012KT	4-	50.0km	1	Fair	1016.6	0.2	-1.6	88	-1.7	/	/	S 3kt
We 23.07.97 18 82.3N	3.8E	02012KT	4-	50.0km	2	Fair	1017.4	0.1	-1.7	88	-1.7	/	/	Station
We 23.07.97 21 82.3N	3.7E	01009KT	3	50.0km	1	Fair	1018.6	0.3	-2.2	83	-1.7	/	/	W ation
DD.MM. Year UT Lat	Lon	DDDF	Bft	Visib.	WX	Weather	Press.	Ta	Td	rF	Tw	Sea	Max.Sea	Speed
Th 24.07.97 00 82.3N	3.7E	36007KT	3	10.0km	/		1019.7	0.0	-2.2	85	-0.8</			

DD.MM.	Year	UT	Lat	Lon	DDDDF	Bft	Visib.	WX	Weather	Press.	Ta	Td	rF	Tw	Sea	Max.Sea	Speed	
Fr	25.07.97	00	82.2N	4.0E	20013KT	4	10.0km	/		1019.3	-0.9	-2.7	88	-0.9	/	/	/	Station
Fr	25.07.97	03	82.2N	5.9E	20008KT	3	10.0km	/		1019.3	-1.4	-2.9	89	-1.6	/	/	/	W 3kt
Fr	25.07.97	06	82.2N	4.6E	20008KT	3	50.0km	2	Fair	1013.9	-1.4	-2.9	89	-1.7	/	/	/	E 3kt
Fr	25.07.97	09	82.1N	5.0E	20007KT	3	50.0km	1	Fair	1019.6	0.1	-2.1	85	-1.7	/	/	/	SE 3kt
Fr	25.07.97	12	82.1N	5.1E	19007KT	3	50.0km	1	Fair	1020.0	0.1	-1.8	87	-1.7	/	/	/	E 3kt
Fr	25.07.97	15	82.0N	5.3E	19008KT	3	50.0km	2	Fair	1020.3	0.2	-2.0	85	-1.7	/	/	/	S 3kt
Fr	25.07.97	18	82.0N	5.3E	20009KT	3	50.0km	3	Fair	1020.0	0.3	-1.5	88	-1.7	/	/	/	Station
Fr	25.07.97	21	82.0N	5.3E	19009KT	3	50.0km	2	Fair	1020.6	0.1	-1.5	89	-1.8	/	/	/	Station

DD.MM.	Year	UT	Lat	Lon	DDDDF	Bft	Visib.	WX	Weather	Press.	Ta	Td	rF	Tw	Sea	Max.Sea	Speed	
Sa	26.07.97	00	82.0N	5.3E	19009KT	3	10.0km	/		1020.8	0.7	-4.1	70	-1.8	/	/	/	Station
Sa	26.07.97	03	82.0N	5.3E	18008KT	3	10.0km	/		1020.1	-0.5	-3.3	81	-0.7	/	/	/	Station
Sa	26.07.97	06	82.0N	5.4E	15011KT	4	50.0km	14	/	1019.7	-0.6	-3.9	78	-1.7	/	/	/	E 3kt
Sa	26.07.97	09	82.0N	5.7E	14011KT	4	50.0km	1	Fair	1019.2	1.1	-2.3	78	-1.7	/	/	/	E 3kt
Sa	26.07.97	12	82.0N	5.7E	18013KT	4	0.1km	47	Fog	1018.4	0.3	0.1	99	-1.7	/	/	/	Station
Sa	26.07.97	15	82.0N	5.8E	18012KT	4	0.2km	48	Freezing fog	1017.5	-0.4	-0.6	99	-1.7	/	/	/	E 3kt
Sa	26.07.97	18	82.0N	5.8E	18012KT	4	0.2km	50	Drizzle	1016.2	0.0	-0.2	99	-1.7	/	/	/	Station
Sa	26.07.97	21	82.0N	5.8E	19013KT	4	1.0km	56	Freezing drizzl	1014.6	-0.1	-0.5	97	-1.7	/	/	/	Station

DD.MM.	Year	UT	Lat	Lon	DDDDF	Bft	Visib.	WX	Weather	Press.	Ta	Td	rF	Tw	Sea	Max.Sea	Speed	
Su	27.07.97	00	82.0N	6.5E	21017KT	5	10.0km	/		1012.6	-0.8	-1.0	99	-1.4	/	/	/	E 3kt
Su	27.07.97	03	81.9N	7.5E	18013KT	4	0.2km	/		1010.8	-0.1	-0.3	99	-0.8	/	/	/	SE 3kt
Su	27.07.97	06	81.9N	7.6E	21018KT	5	10.0km	15	/	1008.5	-0.9	-1.4	96	-1.7	/	/	/	E 3kt
Su	27.07.97	09	81.9N	7.7E	21019KT	5	20.0km	7	Very cldy	1006.8	-1.3	-1.8	96	-1.7	/	/	/	E 3kt
Su	27.07.97	12	81.9N	7.8E	20019KT	5	20.0km	7	Very cldy	1005.3	-0.9	-1.7	94	-1.7	/	/	/	E 3kt
Su	27.07.97	15	81.9N	7.9E	21019KT	5	10.0km	8	Overcast	1003.1	-0.9	-1.5	96	-1.7	/	/	/	E 3kt
Su	27.07.97	18	81.9N	8.0E	22021KT	5	10.0km	7	Very cldy	1000.8	-1.1	-1.8	95	-1.7	/	/	/	E 3kt
Su	27.07.97	21	81.8N	8.6E	22023KT	6	10.0km	7	Very cldy	999.0	-1.0	-2.0	93	-1.7	/	/	/	SE 3kt

DD.MM.	Year	UT	Lat	Lon	DDDDF	Bft	Visib.	WX	Weather	Press.	Ta	Td	rF	Tw	Sea	Max.Sea	Speed	
Mo	28.07.97	00	81.8N	9.2E	21018KT	5	10.0km	/		998.1	-0.6	-1.9	91	-1.4	/	/	/	E 3kt
Mo	28.07.97	03	81.8N	9.4E	22027KT	6	10.0km	/		996.8	-0.8	-1.7	94	-0.8	/	/	/	E 3kt
Mo	28.07.97	06	81.8N	9.6E	21017KT	5	10.0km	26	Recent snow sho	995.6	-1.1	-1.9	94	-1.7	/	/	/	E 3kt
Mo	28.07.97	09	81.8N	9.7E	23015KT	4	1.0km	73	Snow	994.9	-1.5	-2.6	92	-1.7	/	/	/	E 3kt
Mo	28.07.97	12	81.8N	9.8E	29014KT	4	0.5km	73	Snow	994.8	-2.2	-3.0	94	-1.7	/	/	/	E 3kt
Mo	28.07.97	15	81.8N	10.1E	26021KT	5	4.0km	72	Snow	995.8	-1.7	-2.9	91	-1.7	/	/	/	E 3kt
Mo	28.07.97	18	81.7N	10.3E	28026KT	6	10.0km	8	Overcast	997.8	-1.1	-2.3	92	-1.7	/	/	/	S 3kt
Mo	28.07.97	21	81.7N	10.4E	28027KT	6	4.0km	36	Drifting Snow	1000.3	-1.9	-3.9	86	-1.7	/	/	/	E 3kt

DD.MM.	Year	UT	Lat	Lon	DDDDF	Bft	Visib.	WX	Weather	Press.	Ta	Td	rF	Tw	Sea	Max.Sea	Speed	
Tu	29.07.97	00	81.7N	10.4E	25017KT	5	2.0km	/		1001.6	-1.0	-1.9	94	-1.9	/	/	/	Station
Tu	29.07.97	03	81.7N	10.5E	26019KT	5	10.0km	/		1002.7	-0.5	-2.2	88	-1.9	/	/	/	E 3kt
Tu	29.07.97	06	81.7N	10.6E	25016KT	5	20.0km	14	/	1003.8	-0.3	-1.7	90	-1.7	/	/	/	E 3kt
Tu	29.07.97	09	81.8N	10.2E	23017KT	5	50.0km	7	Very cldy	1004.8	-0.3	-1.6	91	-1.7	/	/	/	NW 3kt
Tu	29.07.97	12	81.7N	10.2E	23018KT	5	50.0km	40	/	1005.9	0.0	-2.3	84	-1.7	/	/	/	S 3kt
Tu	29.07.97	15	81.6N	11.1E	24019KT	5	4.0km	28	Recent fog	1007.0	-0.7	-0.9	99	-1.7	/	/	/	SE 3kt
Tu	29.07.97	18	81.6N	11.6E	22010KT	3	4.0km	50	Drizzle	1007.5	0.4	-0.9	91	-1.7	/	/	/	E 3kt
Tu	29.07.97	21	81.6N	11.6E	22015KT	4	4.0km	51	Drizzle	1007.5	0.2	-0.5	95	-1.7	/	/	/	Station

DD.MM.	Year	UT	Lat	Lon	DDDDF	Bft	Visib.	WX	Weather	Press.	Ta	Td	rF	Tw	Sea	Max.Sea	Speed	
We	30.07.97	00	81.6N	11.7E	23015KT	4	10.0km	/		1007.7	0.3	0.0	98	-1.8	/	/	/	E 3kt
We	30.07.97	03	81.6N	11.8E	22017KT	5	2.0km	/		1007.9	-0.1	-0.5	97	-1.8	/	/	/	E 3kt
We	30.07.97	06	81.6N	12.0E	21012KT	4	2.0km	51	Drizzle	1008.2	0.4	0.0	97	-1.7	/	/	/	E 3kt
We	30.07.97	09	81.6N	12.0E	21015KT	4	2.0km	51	Drizzle	1008.3	0.6	0.2	97	-1.7	/	/	/	Station
We	30.07.97	12	81.5N	12.3E	22016KT	5	1.0km	51	Drizzle	1008.9	0.5	0.2	98	-1.7	/	/	/	SE 3kt
We	30.07.97	15	81.3N	12.9E	23019KT	5	1.0km	50	Drizzle	1009.3	0.7	0.4	98	-1.7	/	/	/	SE 3kt
We	30.07.97	18	81.3N	13.1E	23020KT	5	4.0km	10	/	1009.2	1.1	0.7	97	-1.7	/	/	/	E 3kt
We	30.07.97	21	81.3N	13.2E	23021KT	5	10.0km	3	Fair	1008.8	1.4	-0.2	89	-1.7	/	/	/	E 3kt

DD.MM.	Year	UT	Lat	Lon	DDDDF	Bft	Visib.	WX	Weather	Press.	Ta	Td	rF	Tw	Sea	Max.Sea	Speed	
Th	31.07.97	00	81.3N	13.2E	19022KT	6	10.0km	/		1008.9	1.6	-0.1	88	-1.8	/	/	/	Station
Th	31.07.97	03	81.3N	13.4E	19018KT	5	10.0km	/		1006.9	1.3	0.9	97	-1.8	/	/	/	E 3kt
Th	31.07.97	06	81.3N	13.5E	17021KT	5	10.0km	8	Overcast	1006.0	1.9	0.3	89	-1.7	/	/	/	E 3kt
Th	31.07.97	09	81.3N	13.6E	20029KT	7	4.0km	20	Recent drizzle	1004.6	2.6	2.0	96	-1.7	/	/	/	E 3kt
Th	31.07.97	12	81.3N	13.5E	21031KT	7	4.0km	50	Drizzle	1003.8	2.4	1.7	95	-1.6	/	/	/	W 3kt
Th	31.07.97	15	81.3N	13.1E	22016KT	5	2.0km	51	Drizzle	1004.3	1.0	0.7	98	-1.6	/	/	/	W 3kt
Th	31.07.97	18	81.3N	13.2E	23026KT	6	4.0km	56	Freezing drizzl	1004.3	-0.3	-0.5	99	-1.6	/	/	/	E 3kt
Th	31.07.97	21	81.3N	13.3E	23023KT	6	4.0km	56	Freezing drizzl	1005.1	-1.3	-1.6	98	-1.6	/	/	/	E 3kt

DD.MM.	Year	UT	Lat	Lon	DDDDF	Bft	Visib.	WX	Weather	Press.	Ta	Td	rF	Tw	Sea	Max.Sea	Speed	
Fr	01.08.97	00	81.2N	13.4E	24016KT	5	4.0km	/		1005.5	-0.8	-1.2	97	-1.4	/	/	/	S 3kt
Fr	01.08.97	03	81.0N	13.0E	26013KT	4	0.2km	/		1006.2	-0.1	-0.3	99	-1.3	/	/	/	S 3kt
Fr	01.08.97	06	80.8N	12.8E	26013KT	4	0.2km	51	Drizzle	1006.7	0.2	0.1	99	-1.6	/	/	/	S 3kt
Fr	01.08.97	09	80.6N	12.3E	26012KT	4	0.2km	45	Fog	1007.7	0.0	-0.2	99	-1.6	1.0m	190	1.5m	S 3kt
Fr	01.08.97	12	80.6N	11.8E	27013KT	4	0.2km	49	Freezing fog	1009.2	-0.9	-1.0	99	-1.2	0.5m	200	2.0m	W 3kt
Fr	01.08.97	15	80.6N	11.8E	26015KT	4	0.2km	49	Freezing fog									

DD.MM. Year	UT	Lat	Lon	DDDF	Bft	Visib.	WX	Weather	Press.	Ta	Td	rF	Tw	Sea	Max.Sea	Speed	
Mo 04.08.97	00	79.1N	3.6E	14020KT	5+	0.2km	/		1002.3	4.3	3.9	97	0.9	/	/	/	SW 13kt
Mo 04.08.97	03	79.1N	3.1E	15022KT	6-	0.2km	/		1000.3	4.6	4.3	98	0.6	/	/	/	W 3kt
Mo 04.08.97	06	79.1N	3.1E	15021KT	5+	0.2km	51	Drizzle	998.5	4.6	4.5	99	2.6	1.5m	190 2.0m	Station	
Mo 04.08.97	09	79.1N	3.1E	17024KT	6	4.0km	60	Rain	997.5	3.5	3.1	97	-0.2	1.5m	190 2.0m	Station	
Mo 04.08.97	12	79.1N	3.2E	17021KT	5+	10.0km	21	Recent rain	996.7	3.2	2.5	95	-0.1	1.5m	180 2.0m	Station	
Mo 04.08.97	15	79.1N	3.1E	15014KT	4	0.5km	46	Fog	995.1	3.7	3.5	99	-0.2	1.0m	180 2.0m	Station	
Mo 04.08.97	18	79.1N	3.1E	12015KT	4+	0.2km	53	Drizzle	993.0	3.6	3.5	99	-0.3	1.0m	180 1.5m	Station	
Mo 04.08.97	21	79.1N	3.1E	20011KT	4-	4.0km	21	Recent rain	991.5	3.4	2.9	97	0.6	0.5m	180 1.5m	Station	

DD.MM. Year	UT	Lat	Lon	DDDF	Bft	Visib.	WX	Weather	Press.	Ta	Td	rF	Tw	Sea	Max.Sea	Speed	
Tu 05.08.97	00	79.1N	3.2E	18017KT	5-	4.0km	/		992.0	2.4	2.1	98	4.4	/	/	/	Station
Tu 05.08.97	03	79.1N	3.3E	16019KT	5	4.0km	/		992.0	3.3	0.7	83	3.4	/	/	/	Station
Tu 05.08.97	06	79.2N	2.0E	16010KT	3	2.0km	50	Drizzle	991.6	0.9	0.6	98	-1.3	0.5m	170 1.5m	W 3kt	
Tu 05.08.97	09	79.2N	0.2W	21005KT	2	0.2km	45	Fog	992.5	0.1	0.0	99	-1.2	/	/	/	W 8kt
Tu 05.08.97	12	79.5N	0.3W	28007KT	3	0.1km	49	Freezing fog	993.6	-0.4	-0.5	99	-0.9	/	/	/	N 8kt
Tu 05.08.97	15	79.8N	0.1E	32009KT	3	0.2km	44	Fog	995.0	0.0	-0.1	99	-0.8	/	/	/	N 8kt
Tu 05.08.97	18	80.0N	1.1E	30014KT	4	10.0km	28	Recent fog	996.8	-0.3	-0.5	99	-1.4	/	/	/	NE 3kt
Tu 05.08.97	21	80.0N	3.5E	29013KT	4	0.5km	48	Freezing fog	998.9	-0.4	-0.5	99	-1.2	/	/	/	E 8kt

DD.MM. Year	UT	Lat	Lon	DDDF	Bft	Visib.	WX	Weather	Press.	Ta	Td	rF	Tw	Sea	Max.Sea	Speed	
We 06.08.97	00	79.9N	5.1E	30014KT	4	4.0km	/		1001.3	-0.7	-1.1	97	-0.9	/	/	/	E 8kt
We 06.08.97	03	79.4N	5.1E	29015KT	4+	4.0km	/		1004.9	-0.8	-1.4	96	2.2	/	/	/	S 8kt
We 06.08.97	06	78.8N	5.2E	29006KT	3	50.0km	7	Very cldy	1007.5	0.5	-1.5	86	4.2	0.5m	170 2.0m	S 13kt	
We 06.08.97	09	78.7N	7.8E	26006KT	2	50.0km	15	/	1009.0	1.2	-2.4	77	5.1	0.0m	180 2.5m	E 8kt	
We 06.08.97	12	78.7N	7.2E	19012KT	4-	50.0km	7	Very cldy	1009.4	1.3	-2.2	77	5.2	0.5m	180 2.0m	W 3kt	
We 06.08.97	15	78.6N	6.0E	15015KT	4	20.0km	7	Very cldy	1008.2	2.6	-0.4	81	4.8	0.5m	180 2.0m	SW 3kt	
We 06.08.97	18	78.6N	7.0E	14021KT	5+	10.0km	15	/	1006.8	4.2	2.1	86	5.3	1.0m	190 2.5m	E 3kt	
We 06.08.97	21	78.6N	7.9E	15029KT	7-	1.0km	58	Rain and drizzl	1004.1	4.5	4.2	98	4.9	2.0m	180 2.5m	E 3kt	

DD.MM. Year	UT	Lat	Lon	DDDF	Bft	Visib.	WX	Weather	Press.	Ta	Td	rF	Tw	Sea	Max.Sea	Speed	
Th 07.08.97	00	78.5N	6.7E	14029KT	7-	1.0km	/		999.5	4.9	4.6	98	5.0	/	/	/	SW 3kt
Th 07.08.97	03	78.5N	6.5E	22032KT	7+	4.0km	/		1000.6	3.8	3.4	97	5.0	/	/	/	W 3kt
Th 07.08.97	06	78.4N	6.3E	22025KT	6	10.0km	7	Very cldy	1003.9	3.7	0.5	80	5.0	2.0m	190 3.0m	S 3kt	
Th 07.08.97	09	78.4N	6.8E	17026KT	6+	10.0km	7	Very cldy	1005.1	4.3	1.4	81	5.0	2.5m	190 3.0m	E 3kt	
Th 07.08.97	12	78.3N	6.1E	16028KT	7-	4.0km	10	/	1004.9	3.8	2.3	90	5.0	2.5m	180 2.0m	SW 3kt	
Th 07.08.97	15	78.3N	7.2E	14024KT	6	2.0km	51	Drizzle	1004.5	4.8	4.2	96	5.1	2.0m	190 3.0m	E 3kt	
Th 07.08.97	18	78.2N	5.5E	17022KT	6-	4.0km	10	/	1003.5	4.5	2.6	87	4.3	2.0m	190 3.0m	W 8kt	
Th 07.08.97	21	78.2N	7.7E	16019KT	5	4.0km	10	/	1005.0	4.8	2.8	87	5.1	1.5m	180 3.5m	E 8kt	

DD.MM. Year	UT	Lat	Lon	DDDF	Bft	Visib.	WX	Weather	Press.	Ta	Td	rF	Tw	Sea	Max.Sea	Speed	
Fr 08.08.97	00	78.2N	5.1E	20014KT	4	4.0km	/		1004.0	2.6	1.6	93	4.5	/	/	/	W 13kt
Fr 08.08.97	03	78.1N	8.0E	17019KT	5	4.0km	/		1005.5	4.5	2.2	85	5.0	/	/	/	E 13kt
Fr 08.08.97	06	78.1N	5.4E	18017KT	5-	10.0km	50	Drizzle	1003.9	3.2	2.1	92	4.5	1.5m	190 4.0m	W 13kt	
Fr 08.08.97	09	78.1N	7.4E	18016KT	5-	10.0km	15	/	1005.4	3.9	1.8	86	4.5	1.0m	200 3.5m	E 8kt	
Fr 08.08.97	12	78.0N	6.0E	18009KT	3	4.0km	58	Rain and drizzl	1004.0	2.9	2.4	96	4.4	0.5m	190 3.5m	W 8kt	
Fr 08.08.97	15	78.0N	6.8E	19012KT	4-	10.0km	6	Cloudy	1003.1	2.8	1.1	89	4.5	0.5m	190 3.0m	E 3kt	
Fr 08.08.97	18	78.0N	6.4E	16011KT	4-	20.0km	15	/	1001.7	2.9	0.1	82	4.4	0.5m	200 2.5m	W 3kt	

Abbreviations/Comments

DD.MM. Year	UT	Lat	Lon	Date, Time and Location
DDDF/FF	Bft			Wind direction, speed (Knots and Beaufort)
Visib				Measurement based on light backscattering
WX Weather				WX weather code no. according to SYNOP/FW12
				Weather and clouds according to Synop FW12
Press.				Air pressure in hpa
Ta, Tw				Air/water temperature in deg C
Td				Air dewpoint temperature in deg C
rH				Air relative humidity in %
Sea				Characteristic wave height in m
Max.Sea				Direction and height of swell
ICE				0 no ice visible
				1 Ship is within a lead wider Than 1nm or in fast ice
				2 ice cover less than 3/10, open water or loose drift ice
				3 drift ice cover 4...6/10
				4 drift ice cover 7...8/10
				5 drift ice cover 9/10 or more but <10/10
				6 small fields of drift ice with open water
				7 small fields of dense drift ice
				8 fast ice, open water or loose drift ice seaward of ice edge
				9 fast ice, dense drift ice seaward of ice edge
				/ no data because of darkness or bad visibility
Speed				Direction and speed of ship

Attention: The WX and weather information is only available for data from manual observation. As observations are partly fully automatic, "/" does not necessarily imply that there was no significant weather at this time. The same holds for ICE, sea and swell observation, respectively.

10.3 Geological Tables and Core Descriptions

Legende:**Lithology**

sand



sandy silt



sandy clay



sandy mud



silt



mud



clay



diamicton



foraminiferal ooze



nannofossil ooze



diatomaceous ooze



radiolarian ooze



volcanic ash



chert / porcellanite



pebbles, dropstones



sediment clasts

Structure

bioturbation



stratification



lamination



coarsening upward sequence



fining upwards sequence



sharp boundary



gradational boundary



transition zone

PS2824-5 (GKG)

Central Barents Sea

ARK-XIII/2

Recovery: 0.46 m

77° 34.19' N, 34° 38.58' E

Water depth: 220 m

Depth in core (m)	Lithology	Texture Color	Description	Age
	0		7YR 3/2 2.5YR 4/4 8.5YR 3/3 7.5Y 4/1	0-1.5 cm: dark brown, clay, strong bioturbated 1.5-7 cm: olive brown, clay silty, mottled 7-8 cm: dark brown, silty clay, oxidized layer 8-48 cm: dark gray, silty-sandy clay, homogenous 14-16 cm: oxidized spots 19-25 cm: organic rest, black 44-45 cm: black streaks
1				

PS2827-5 (GKG)

Northwestern Barents Sea

ARK-XIII/2

Recovery: 0.46 m

76° 26.5' N, 30° 28.2' E

Water depth: 325 m

Depth in core (m)	Lithology	Texture Color	Description	Age
	0		7YR 3/2 2.5Y 4/1	0-2 cm: dark brown, clay silty, bioturbated 2-5 cm: dark grayish brown, clay silty, mottled 5-46 cm: dark grayish brown, clay-silty 10-14 cm: worm tubes 14-15 cm: oxidized spots 28-31 cm: oxidized spots 41.5-43.5 cm: pebble conglomerate, sharp boundary, turbidite
1				

PS2830-8 (GKG)

North of Svalbard

ARK-XIII/2

Recovery: 0.24 m

80° 58.6 N, 17° 31.12 E

Water depth: 487 m

Depth in core (m)	Lithology	Texture Color	Description	Age
	0		10YR 4/2 7.5YR4/2	0-12 cm: dark grayish brown, clayey sandy-silty, bioturbated 12-24 cm: brown - dark brown, clayey sandy-silty, bioturbated, oxidized layer
1				

PS2830-5 (SL)

North of Svalbard

ARK-XIII/2

Recovery: 4.50 m

80° 58.45 N, 17°28.81 E

Water depth: 518 m

Depth in core (m)	Lithology	Texture Color	Description	Age
0		10YR4/2	0-12 cm: Dark grayish brown, clayey - sandy silt, bioturbated sharp boundary 2-8 cm: dropstone (red claystone)	II
		7.5YR 4/2	12-53 cm: dark brown, clayey - sandy silt, weak mottling in upper part. Thin lenses of fine-grained sand. The lower boundary is recognised by changing colours. 32 cm: Fragments of shells 30-32 cm: dropstone (metamorphic rock) 41-42 cm: dropstone (metamorphic rock)	
1		10YR 4/2	53-64 cm: dark grayish brown, sandy - clayey silt, laminated, mottling, sharp boundary	III
		2.5Y 3/2	64-68.5 cm: very dark grayish brown, sandy-silty-clayey mud, laminated, mottling, sharp boundary 65-68 cm: dropstone (black shale)	
		7.5YR 4/2	68.5-163 cm: Interbedding of laminae of grayish, grayish brown and brown colours, silty-clayey mud. Decreasing clay content toward the top, laminated (1 to 12 cm thick) weak mottling, gradational boundary.	
		2.5Y 5/2		
		10YR 4/2		
		2.5Y 4/2	163-231 cm: dark grayish brown, clayey mud, homogenous, lower boundary is sharp 173-175.5 cm: tiny black specks of sulphides	
2		2.5Y 4/2	231-234 cm: dark grayish brown, coarse-grained sand with gravel and pebbles, sharp boundaries. Turbidite-like deposits.	
		2.5Y 4/2	234-274 cm: dark grayish brown, sandy-silty clay, faintly stratificated, gradational boundary 235.5 cm: reddish spot of limonite 258-260 cm: dropstone 270-272 cm: dropstone	
		2.5Y 3/2	274-316 cm: very dark grayish brown, sandy silty clay, sharp boundary, rare black specks of sulphides	
3		2.5Y 4/2	301,316 cm: lenses of fine-grained sand 316-330 cm: dark grayish brown, clayey - sandy silt, faintly laminated, boundaries are sharp, recognized by colour and lithological changes 323-326 cm: lense (10YR3/2) 325 cm: shell fragment	
		2.5Y 5/4	330-378 cm: Light olive brown, dark grayish brown sandy silts and dark gray sands. Lamination (1-5 cm). "cottage cheese"-structure in dark gray sands, boundary is gradational 348 cm: dropstone (black claystone)	
		2.5Y 4/2		
		2.5Y 4/1		
		10YR 4/1	378-427 cm: dark gray, containing thin (3-4 mm) light olive brown lenses in the lowermost part of the layer, sandy silty clay, boundaries are gradational, rare black specks of sulphides. 395 cm: dropstone (metamorphic)	
4		2.5Y 5/4	427-433 cm: faint lamination of light olive brown and gray, sandy silty clay, boundaries are gradual, black specks of sulphides	
		2.5Y 4/4	433-450 cm: olive brown, sandy-silty clay, lowermost part of the core is destroyed.	
5				

PS2831-7 (GKG)

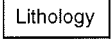
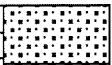
Recovery: 0.39 m

North of Svalbard

81° 5.64 N, 16° 58.35 E

ARK-XIII/2

Water depth: 933 m

Depth in core (m)	Lithology	Texture	Color	Description	Age
	0			10YR 4/2	0-22 cm: dark grayish brown, sandy-silt, bioturbated
			10YR4/1	22-39 cm: dark-brown, silty clay, homogenous, gradual boundary	
1					

PS2832-12 (GKG)

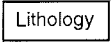
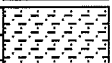
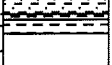
Recovery: 0.33 m

North of Svalbard

81°06.7 N, 16° 12.9 E

ARK-XIII/2

Water depth: 2100 m

Depth in core (m)	Lithology	Texture	Color	Description	Age
	0			10YR 5/3	0-26 cm: yellowish brown, silty-clayey mud, very soft, the upper 3 cm are bioturbated, the layer boundary is sharp
			2.5YR3/2	26-28 cm: "hard ground", oxidized layer of very dense clay, dark reddish brown	
			2.5Y	28-33 cm: dark gray, clay, rather dense, with a lot of non-rounded gravel and pebbles. The upper layer is sharp	
1					

PS2833-5 (GKG)

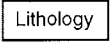
Recovery: 0.49 m

North of Svalbard

80°58.2 N, 11° 49.9 E

ARK-XIII/2

Water depth: 2010 m

Depth in core (m)	Lithology	Texture	Color	Description	Age
	0			10YR 3/6	0-49 cm: dark yellowish brown, clayey silt, very soft, homogenous to the bottom: more silty
1					

PS2834-6 (GKG)

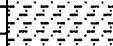
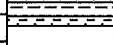
North of Svalbard

ARK-XIII/2

Recovery: 0.43 m

80°54.9 N, 09°49.2 E

Water depth: 1020 m

Depth in core (m)	Lithology	Texture	Color	Description	Age
	0			10YR 4/2	0-35 cm: dark grayish brown, silty-clayey mud, very soft, bioturbated
			10YR4/2 7.5YR3/2	35-40 cm: dark grayish brown interbedding with dark brown. Thickness of lenses: 2-5 cm	
			5YR3/3 2.5Y4/2	40-41.5 cm: dark reddish brown, clayey silt, oxidized layer ("hard ground") 41.5-43.5 cm: dark grayish brown, silty-clayey mud	
1					

PS2834-5 (KAL)

Recovery: 6.71 m

North of Svalbard

80° 54.8 N 09° 49.4 E

ARK-XIII/2

Water depth: 1010 m

	Lithology	Texture Color	Description	Age
0		10YR4/2	0-35 cm: dark grayish brown, silty-clayey mud, bioturbated, very soft, sharp boundary	
		7.5YR3/2	35-40 cm: dark brown, silty-clayey mud, faintly interbedding with dark grayish brown mud, sharp boundaries	
1		5YR3/3	40-41.5 cm: dark reddish brown, clayey silt, very dense -oxidized layer ("hard ground")	
		7.5YR3/2	41.5-50 cm: faint interbedding of dark brown and dark grayish brown, silty-clayey mud, sharp boundaries	
		10YR4/2		
		5Y4/2	50-57 cm: olive gray, silty-clayey mud, sharp boundaries	
		2.5Y4/4	57-64.5 cm: dark gray, silty clayey mud, gradual boundary	
		2.5Y5/5	64.5-67.5 cm: gray, silty clayey mud, very soft, sharp boundary	
		5Y4/2	67.5-81.5 cm: olive gray, silty clayey mud, gradual boundary	
		5Y4/3	81.5-88 cm: olive, sandy-clayey silt, containing yellowish-red spots of limonite, sharp boundary	
		2.5Y4/4	88-94 cm: olive brown, sandy silt with clasts of dry clay and gravel, pieces of black coal, sharp boundaries	
		5Y4/1	94-99 cm: very dark gray, sandy-silty clay, sharp boundaries	
2		5Y5/1	99-112 cm: gray, sandy-silty-clayey mud, gradual boundary	
		5Y5/1	104 cm: dropstone (claystone)	
		2.5Y4/4	112-120.5 cm: olive brown, silty clayey mud, sharp boundary	
		10YR3/3	120.5-126 cm: dark brown, silty clay, very strong mottling	
		5Y5/1	126-132 cm: gray, silty clay, thin lenses of olive brown clay, gradual boundary.	
		2.5Y4/4		
		2.5Y4/4	132 -161 cm: olive brown, sandy-silty clay, mottling. gradual boundary.	
		5Y5/1		
		2.5Y5/2	161-171 cm: grayish brown, silty clay, mottling, gradual boundary	
		2.5Y4/4	171-234 cm: olive brown, silty clay with some amount of fine-grained sand, - traces of polychetaes (?), gradual boundary	
3		10YR3/3	234-258.5 cm: dark brown, olive brown, dark grayish brown sandy silty clay laminated ("cottage-cheese"), sharp boundary.	
		2.5Y4/4		
		2.5Y4/2		
		7.5Y4/2		
		7.5Y5/2	258.5-261 cm: brown, sandy-silty clay with thin lenses enriched by black sulphides, boundaries are sharp	
		10YR4/1		
		10YR5/1	261-336.5 cm: banding, sandy-silty clay, dark gray, gray, brown, olive brown, and reddish brown colours interbedding with olive sandy silts ("cottage cheese"), sharp boundary, reddish spots enriched by limonite, black specks of sulphides, mottling	
		2.5Y4/4		
		5YR4/3	278 cm: tiny shell fragments	
		5Y4/3	286-310 cm: foram shells	
4		10YR5/1	336.5-364 cm: banding, gray, dark gray sandy-silty clay, mottling, sharp boundary	
		10YR4/1		
		2.5Y4/4	364-368 cm: olive brown, sandy-clayey silt, mottling, gradual boundaries.	
		2.5Y4/2	368-372 cm: dark grayish brown, sandy-clayey silt, sharp boundary	
		2.5Y4/4	372-373 cm: olive brown, sandy-silt ("cottage-cheese")	
		5Y3/1	373-377 cm: very dark gray, dark gray clayey-sandy silt (colour banding)	
		5Y4/1	377-398 cm: gray, dark gray, very dark gray (colour banding), sandy-silty clay, sharp boundaries	
		5Y4/1	394-396 cm: dropstone (sandstone)	
		5Y5/1	398-484 cm: dark gray, gray, olive gray (colour banding), silty clay, black specks of sulphides, traces of polychetaes, sharp boundaries	
		5Y4/2		
5		2.5Y4/2	484-509 cm: dark grayish brown, olive brown, dark brown, very dark gray (colour banding), sandy-silty clay, many spots and specks of sulphides, sharp boundaries, mottling, weak bioturbation	
		2.5Y4/4		
		10YR3/3		

ARK-XIII/2

	Lithology	Texture	Color	Description	Age
5			10YR4/1 10YR5/1	509-554 cm: dark gray, gray (colour banding), sandy-silty clay, gradual boundary, black spots and specks of sulphides, traces of polychetae (521-525 cm; 543-554 cm; bioturbation)	
			2.5Y4/4 2.5Y3/2 2.5Y4/2 7.5YR4/ 7.5YR4/ 10YR4/4	554-578 cm: olive brown, very dark grayish brown, dark grayish brown (colour banding), sandy-clayey silts, mottling, sharp boundary, small specks of sulphides	
			2.5Y3/2 2.5Y4/ 10YR4/1 10YR3/1	578-646 cm: Colour banding, interbedding of silty clay and sandy-clayey silt, spots and speck of limonite and sulphides (details: see handwriting description)	
6			5Y4/3	646-674 cm: olive, silty clay, spots of sulphides and limonite, sharp boundary	
				End of Core	
7			5Y4/3		
				End of core-catcher	
8					
9					
10					

PS2835-5 (GKG)

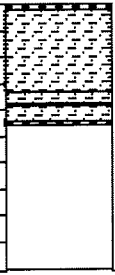
Recovery: 0.46 m

Yermak Plateau

81°06.1 N, 07°01.2 E

ARK-XIII/2

Water depth: 868 m

Depth in core (m)	Lithology	Texture	Color	Description	Age
	0			10YR3/6 10YR3/4	0-2 cm: dark yellowish brown, silty clay, bioturbated 2-33 cm: dark yellowish brown, clayey mud, gradual lower boundary
			10YR4/2 7.5YR3/2	33-38 cm: dark grayish brown interbedded with dark brown (colour banding), silty clayey mud	
			5YR3/3 2.5Y4/2	38-44 cm: dark reddish brown, silty clayey mud, stiff oxidized layer ("hard ground") 44-46 cm: dark grayish brown, silty clayey mud, homogenous	
1					

PS2835-6 (SL)

Yermak Plateau

ARK-XIII/2

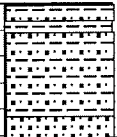
Recovery: 5.51 m

81° 06.1 N 07° 04.3 E

Water depth: 867 m

Depth in core (m)	Lithology	Texture Color	Description	Age
0		10YR4/4	0-31 cm: brown with dark brown layers (27-29 cm), sandy-silty clay, gradual boundary, homogenous	
		7YR4/4	31-35 cm: brown with dark brown layers, sandy-silty clay, sharp boundary	
		10YR4/4	35-42.5 cm: brown with interbedded changing colours (7.5YR4/4/7.5YR5/6)	
		7YR4/3	three hardgrounds (2-3 mm thick at 36, 38.5, 40 cm)	
		10YR4/1	42.5-66 cm: gray layer, sandy silty clay, soft, homogenous, gradual boundary	
		10YR6/3	66-79 cm: gray light, sandy-silty mud, foram rich	
		2.5Y5/4	79-94 cm: gradual boundary to yellow brown olive, first banded than mottled layer ("cottage-cheese"-structure), sandy silty mud, foram rich, sharp boundary	II
1		2.5Y4/	94-99 cm: dark gray, sandy silty clay, (20 ka 14C dated)	
		2.5Y6/1	99-106.5 cm: light gray, sandy silt, light bioturbation, sharp boundary	
		2.5Y6/6	106.5-150 cm: yellow gray, sandy silt, bioturbation (decreasing from bottom to top)	III
		10YR5/4	150-187 cm: yellow brown to brown with dark brown layers (172-178 cm), sandy silt	
		2.5Y5/4	187-206 cm: yellow gray to gray, sandy silty clay	
2		2.5Y5/	206-220 cm: light gray, silty clayey mud, soft, gradual boundary, slight bioturbation	
		2.5Y6/6	220-307 cm: yellow gray to the bottom more yellowish colours, sandy clayey silt	
		2.5Y6/8	288-307 cm: more sandy, strongly bioturbated	
3		5YR5/4	307-330 cm: gray section with changing colours from red gray (312-313 cm) to dark gray (116-117 cm)	
		10YR4/1	307-316 cm: clayey silt	
		2.5Y5/6	316-330 cm: sandy silt with lots of forams	
		2.5Y6/2	330-402 cm: yellow grayish olive layers, change over this section, sandy silty clay	
		2.5Y5/2	334 cm: sulfidic lense	
		2.5Y5/4	338-352 cm: foram rich layer	
		5YR5/3	365 cm: dropstone	
4		2.5Y5/	402-455 cm: gray layer, sandy clayey silt, homogenous, dark sulfidic spots (420-447 cm)	
		5Y5/3	455-472 cm: yellow olive to gray colours, sandy silt, to bottom more bioturbated	
		2.5Y5/	472-483 cm: gray and olive alternation	
		5Y5/4	483-505 cm: olive yellow gray, sandy silty gray	
5		5Y5/3	495 cm: dropstone (quartzite)	

ARK-XIII/2

Lithology	Texture	Color	Description	Age
		2.5Y5/ 2.5Y6/ 5Y5/6	505-511 cm: dark gray, sandy silty clay, gradual boundary to lighter gray slightly finer section (511-544 cm), homogenous, soft 544-551 cm: more yellow olive colored, sandy silt	
End of core				

PS2836-6 (GKG)

Recovery: 0.50 m

Yermak Plateau

81°38.8 N, 05°07.8 E

ARK-XIII/2

Water depth: 647 m

Depth in core (m)	Lithology	Texture Color	Description	Age
	0		10YR4/2	0-4 cm: dark grayish brown, sandy-silty mud, very soft, bioturbated, gradual
		10YR4/3	4-16 cm: brown, sandy-clayey mud, bioturbated, gradual boundary	
		10YR3/3	16-20 cm: dark brown, sandy-clayey mud, sharp boundary, bioturbation, mottling	
		5YR3/3	20-21 cm: dark reddish brown, sandy-silty-clayey mud, very stiff ("hard ground")	
		10YR4/2	21-41 cm: dark grayish brown, sandy-clayey mud (Colour banding: dark brown), yellow spots of limonite, mottling, bioturbation, gradual boundary	
1		10YR4/1	41-50 cm: dark gray, sandy clayey mud, homogenous	

PS2837-6 (GKG)

Recovery: 0.49 m

Yermak Plateau

81°14.0 N, 02°25.0 E

ARK-XIII/2

Water depth: 1027 m

Depth in core (m)	Lithology	Texture Color	Description	Age
	0		10YR3/3	0-5 cm: dark brown, silty clay, gradual boundary, bioturbated
		7.5YR3/2	5-7 cm: dark brown, clayey silty mud, sharp boundary (oxidized layer)	
		2.5YR4/2	7-9 cm: dark grayish brown, silty clay, gradual boundary	
		5Y3/2	9-49 cm: dark olive gray, silty clay, homogenous	
1				

PS2837-5 (KAL)

Yermak Plateau

ARK-XIII/2

Recovery: 8.76 m

81°13.99 N 02°22.85 E

Water depth: 1042 m

Depth in core (m)	Lithology	Texture	Color	Description	Age
0				Uppermost 9 cm of the core are destroyed, correlation with GKG 2837-6	
			5Y3/2	9-207 cm: dark olive gray, silty-clay, homogenous, gradual lower boundary	
			5Y3/2	207-258 cm: dark olive gray silty clay, homogenous with numerous black sulphide spots (Ø =1mm to 1cm), lower boundary gradual	
			5Y3/2	258-278 cm: dark dark olive gray silty-clay, homogenous, gradual lower boundary	
			5Y3/2	278-326 cm: dark olive gray silty clay, homogenous with numerous black sulphide spots (Ø =1mm to 1cm), lower boundary gradual	
			5Y3/2	326-354 cm: dark olive gray silty clay, homogenous with few black sulphide spots (Ø =1mm to 3mm), lower boundary gradual	
			5Y3/2	354-386 cm: dark olive gray silty clay, homogenous with numerous black sulphide spots (Ø =1mm to 1cm), lower boundary gradual	
4			2.5Y5 2.5Y4/2	386-405 cm: gray, sandy-silty-clayey mud, yellowish-reddish spots of limonite (402.5 cm), sharp boundaries. Sediments are coarser than overlying sediments, abundant foraminifers	II
			5Y4/3	405-409.5 cm: olive, clayey-sandy silt, "cottage-cheese" structure, mottling, sharp boundaries	
			5Y4/1	409.5-416 cm: very dark gray, sandy-clayey silt, homogenous, sharp boundaries	
			5Y4/2 10YR4/4 7.5YR4/4	412 cm: dropstone (black sandstone) 416-453 cm: Colour banding: olive gray, dark yellowish brown, brown, sandy-clayey silty mud, rare specks of sulphides, sharp boundaries	III
5			5Y3/2	453-564 cm: dark olive gray, silty clay, homogenous, gradual boundary	

ARK-XIII/2

	Lithology	Texture	Color	Description	Age
5				453-564 cm: dark olive gray, silty clay, homogenous, gradual boundary	
			5Y3/2	564-611 cm: dark olive gray (s.a.), silty clay with small specks and spots of sulphides, sharp boundary	
6			5Y4/2 10YR4/4	611-632 cm: Colour banding: olive gray, dark yellowish brown, sandy-clayey-silty mud, sharp boundaries	
			5Y3/2	632-653 cm: dark olive gray, silty clay with a few amount of sand, homogenous, gradual boundary, black spots appear in underlying deposits	
			5Y3/2	653-700 cm: dark olive gray (s.a.), silty clay, black sulphides (0.5-1.5 cm thick), boundaries are gradual	
7			5Y3/2	700-782 cm: olive gray, silty clay interbedding with black lenses (0.5-1.5 cm thick) of black sulphides, gradual boundaries	
			5Y3/2	782-828 cm: olive gray (s.a.), silty clay with a few amount of sand. The layer contains much less spots and lenses of black sulphides than overlying and underlying deposits, gradual boundaries	
8			5Y3/2 2.5YR2.5	828-876 cm: olive gray (s.a.) silty clay interbedding with thin (0.5-1 cm) and thick (2-3 cm) lenses of black sulphides.	
				The whole interval 632-876 cm shows one sequence of deposits with various amounts of sulphides	
9					
10					

PS2838-8 (GKG)

Western Yermak Plateau

ARK-XIII/2

Recovery: 0.51 m

81°17.7N, 00°26.7 E

Water depth: 2326 m

Depth in core (m)	Lithology	Texture	Color	Description	Age
	0			10YR4/3	0-2 cm: upper 2 cm are destroyed during coring
			7.5YR3/2	2-12 cm: brown, clay, very soft, gradual boundary	
			10YR4/3	12-15 cm: dark brown, clay, gradual boundary	
			10YR4/3	15-17 cm: brown, clay, gradual boundary (s.a.)	
			7.5YR3/2	17-20 cm: dark brown, clay with thin lenses of brown clay, sharp boundary	
			2.5Y5/	20-28 cm: gray, clay, homogenous, sharp boundary	
			10YR4/4	28-29.5 cm: dark yellowish brown, clay, oxidized layer, sharp boundary	
			2.5Y5/	29.5-30.5 cm: gray, clay, homogenous (same as 20-28 cm), sharp boundary	
			10YR3/4	30.5-31.5 cm: dark yellowish brown, clay, oxidized layer, sharp boundary	
1			2.5Y5/	31.5-51 cm: gray, clay, homogenous (33-33.5 cm: lense of brown clay)	

PS2839-5 (GKG)

Western Yermak Plateau

ARK-XIII/2

Recovery: 0.39 m

81° 24.22 N 00° 58.36 W

Water depth: 2991 m

Depth in core (m)	Lithology	Texture	Color	Description	Age
	0			7.YR3/4	0-39 cm: dark brown, clay, very soft, homogenous, abundant foraminifers
1					

PS2839-5 (SL)

Western Yermak Plateau

ARK-XIII/2

Recovery: 6.08 m

81° 24.28' N, 01° 0.71' W

Water depth: 2991 m

Depth in core (m)	Lithology	Texture Color	Description	Age
0		7.5YR3/4	0-38 cm: dark brown, clay, very soft, homogenous, forams, sharp boundary mottling in the lower part	I
		10YR3/2	38-40 cm: thin lamination of very dark grayish brown, silty sand, sharp boundary "cottage-cheese"-structure 39 cm: dropstone 40-42 cm: dark yellowish brown, sandy silt, "cottage-cheese", sharp boundary	
		7.5YR3/4	42-54 cm: colour banding, dark brown, dark yellowish brown, clayey sandy silt, sharp boundary	II
		10YR4/4	48 cm: lense of black clayey silt	
		2.5Y4/1	54-64 cm: dark gray, sandy-silty-clayey mud, homogenous, spots of sulphides sharp boundary	II
		2.5Y5/2	64-74 cm: grayish brown, sandy-silty-clayey mud, gradual boundary, homogenous, spots of sulphides	
1		2.5Y4/4	74-100 cm: olive brown, silty clay, homogenous, lot of forams (82-86 cm), sharp boundary	II
		2.5Y4/2	100-104.5 cm: colour banding, dark grayish brown, olive gray, thin lamination of sandy silt, "cottage-cheese", specks and spots of sulphide, sharp boundary	
		5Y4/2	102 cm: dropstone	II
		2.5Y4/4	104.5-111 cm: colour banding, very dark grayish brown, dark olive gray, clay, specks of sulphides, sharp boundary (Leithorizont)	
		5Y3/2	111-153 cm: colour banding, olive-dark gray-grayish brown, clay, sharp boundary	II
			153-187 cm: colour banding, brown-olive colours (brighter than upper layer), clay, silty clay, sharp boundary	
			164.5 cm: dropstone	III
		2.5YR3/5	187-246 cm: colour banding, dark gray-olive colours, clay, silty clay, specks and spots of sulphides, gradual boundary	
2		5Y4/2		III
		5Y4/4		
		7.5YR4/2	246-264 cm: colour banding, brown-dark grayish brown colours, silty clay, sharp boundary	III
		10YR4/2	249 cm: dropstone 262 cm: lot of sulphides	
		2.5Y4/4	264-302 cm: colour banding, olive brown, dark grayish brown, grayish brown, silty clay, weak mottling, sharp boundary	III
		2.5Y4/2	292 cm: dropstone	
		2.5Y5/4		III
		5Y3/1	302-312 cm: very dark gray, sandy silty clay, sharp boundary	
		5Y4/1	306 cm: dropstone	III
		2.5Y4/4	312-440 cm: colour banding, olive brown, dark grayish brown, olive, dark brown, silty clay, mottling, extremely sharp boundary	
		2.5Y4/2	325 cm: dropstone	III
		5Y4/3	320-325 cm: a lot of forams	
		7.5YR4/3	330-340 cm: lense of silty sand	III
			382 cm: dropstone	
3		2.5Y4/4	440-445 cm: olive brown, coarse sand, sharp boundary are erosional, turbidite- like deposits	III
		5Y4/3	445-446 cm: olive, silty clay, sharp boundary	
		5Y3/2	447-475 cm: dark olive gray, clayey-sandy-silty mud, coarser than overlying deposits, weak mottling, sharp boundary	III
		5Y4/3	475-489 cm: colour banding, olive gray-dark gray, silty clay, weak mottling, sharp boundary is erosional	
		5Y4/1	489-492 cm: dark grayish brown, coarse grained quartz sand, forams, sharp boundary, turbidites	III
		5Y4/2	492-497 cm: olive brown - dark grayish brown colours, silty sand, "cottage cheese", sharp boundary, turbidites	
4		2.5Y4/4		III
		5Y4/3		
5		5Y4/3		III

ARK-XIII/2

	Lithology	Texture	Color	Description	Age	
5			2.5Y3/	497-512 cm: very dark gray, sandy silt, sharp boundary		
			5Y4/1	512-513.5 cm: dark gray, silty clay, sharp boundary		505-508 cm: turbidite
			5Y4/2	513.5-523 cm: olive gray-olive, clayey-sandy-silty-mud, forams, specks of sulphides, sharp boundary		
			5Y4/3			
			2.5Y4/4	523-548 cm: colour banding, olive brown-dark grayish brown, forams, spots and specks of sulphides, sharp boundary		
			2.5Y4/2	525 cm: silty sandy lense		
			5Y4/1	548-563 cm: dark gray, clay, spots of sulphides, homogenous, gradual boundary		
			2.5Y4/2	563-591 cm: colour banding, dark grayish brown-olive gray clay, spots of sulphides, gradual boundary		
6		5Y4/2	591-608 cm: colour banding, olive gray-olive brown, clay, more bright colours than overlying deposits, specks and spots of sulphides			
	5Y4/3					
	End of core			(for more detailed colour descriptions: see handwriting core-descriptions)		
7						
8						
9						
10						

PS2840-4 (GKG)

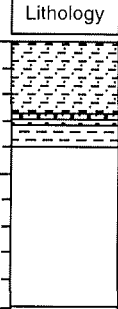
Recovery: 0.40 m

Fram Strait

81°25.3 N 05°18.7 W

ARK-XIII/2

Water depth: 3588 m

Depth in core (m)	Lithology	Texture	Color	Description	Age
	0			10YR4/4	0-27 cm: dark yellowish brown, silty clay with spots and lenses of dark grayish brown silty sand, bioturbation, mottling, sharp boundary
			10YR4/4	27-29 cm: dark yellowish brown and brown, thin lamination of sandy-clayey silt, sharp boundary, turbidite-like deposits	
			10YR3/2	29-31.5 cm: dark yellowish brown (upper part), dark grayish brown, coarse-grained sand, turbidites, sharp boundary	
			10YR4/4	31.5-40 cm: dark yellowish brown, clay, homogenous	
1					

PS2843-2 (GKG)

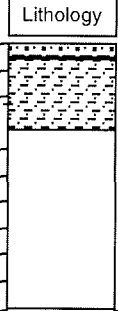
Recovery: 0.32 m

East Greenland Margin

81°34.0 N 07°20.0 W

ARK-XIII/2

Water depth: 2526 m

Depth in core (m)	Lithology	Texture	Color	Description	Age
	0			10YR4/4	0-5 cm: dark yellowish brown, sandy-silty clay, bioturbated, gradual boundary
			10YR8/4	9-32 cm: very pale brown, silty clay 5-15 cm - bioturbated; 15-32 cm - decreasing bioturbation	
1					

PS2843-1 (SL)

East Greenland Margin

ARK-XIII/2

Recovery: 6.54 m

81° 34.04' N, 07° 17.64' E

Water depth: 2527 m

	Lithology	Texture Color	Description	Age
0		10YR4/4	:0-5 cm: dark yellowish brown, sandy silty clay, bioturbated, gradual boundary	
		10YR5/3	:5-37.5 cm: brown, silty clay, very soft, weak mottling, sharp boundary,	
		10YR4/3	:37.5-49.5 cm: brown, silty clay, mottled, sharp boundary	
		7.5YR4/4	:49.5-50 cm: brown, strong oxidized layer (hard ground), silty clayey mud, sharp boundary	
		10YR5/2	:50-55 cm: grayish brown, silty clay mottled gradual boundary	
		10YR4/3	:55-72 cm: brown, silty clay, weak mottling, sharp boundary	
1		5Y4/2	:72-75.5 cm: olive gray, sandy silty clay with gravel, mottling, sharp boundary	
		10YR4/3	:75.5-104 cm: brown, silty clay, weak mottling, sharp boundary	
		10YR4/3	:104-150 cm: colour banding, brown, dark yellowish brown, grayish brown, silty clay, weak mottling, gradual boundary	
		10YR5/3		
	10YR4/4			
	2.5YR5/2			
		10YR4/3	:150-191 cm: brown, silty clay, strong mottling (increasing from bottom to top) sharp boundary	
		10YR4/4	:191-206 cm: dark yellowish brown, clay, weak mottling, sharp boundary	
2		2.5YR5/2	:206-207 cm: grayish brown, silty clayey mud, gradual boundary	
		5Y4/2	:207-215 cm: olive gray, sandy silty clayey mud, mottling (decreasing from bottom to top), gradual boundary	
		10YR5/3	:215-245 cm: colour banding, brown, yellowish brown, silty clay, mottling, sharp erosional boundary	
		10YR5/4		:230 cm: enriched specks of sulphide
		10YR4/3	:245-254.5 cm: grayish brown with spots and lenses of dark grayish brown, sandy silt, sharp boundary	
		7.5YR4/2		:246-252 cm: well rounded dropstone (black shale)
		10YR5/3	:254.5-290 cm: colour banding: yellowish brown-brown, silty clay, mottling, sharp boundary. In the lower part several inclined lenses (2-5) of sand	
		10YR5/4		
3		10YR4/3	:290-295 cm: dark yellowish brown, coars- grained sand, faintly laminated, turbidites, sharp boundary	
		7.5YR4/2		
		10YR4/4	:295-299 cm: brown, clay	
		7.5YR4/2		:299-302 cm: grayish brown, silty clay interbedded with brown clay
		7.5YR4/2	:302-332 cm: brown, clay (s. 295-299 cm). At depth 326 cm specks of sulphide	
		10YR5/2	:332-338 cm: grayish brown, sandy silty clay interbedded with brown clay.	
		7.5YR4/2	:338-367.5 cm: brown, clay (s. 302-332 cm). At depth 342 cm, thin lense of sandy silt, sharp boundary	
		7.5YR4/2	:367.5-377 cm: colour banding: brown-dark grayish brown, silty clay. At depth	
		2.5YR4/2	:373 cm, lense of silty sand (turbidite), gradual boundary	
		7.5YR4/2	:377-395 cm: brown, silty clay, gradual boundary	
4		10YR4/3	:395-400 cm: colour banding: dark grayish brown-brown, silty clay, gradual boundary	
		2.5YR4/2		:397-398 cm: abundant forams
		7.5YR4/2	:400-413 cm: brown, silty clay, gradual boundary	
		7.5YR5/2	:413-415 cm: colour banding: grayish brown-brown, silty clay, mottling	
		7.5YR4/2	:415-428.5 cm: brown, silty clay, mottling, gradual boundary	
		7.5YR4/2	:428.5-435 cm: brown-dark grayish brown, silty clay, sharp boundary	
		10YR4/3	:435-439 cm: dark gray, clayey sandy silty mud, coarser, lot of specks of sulphides, rare forams	
		10YR4/1	:439-455.5 cm: brown, silty clay, mottling, sharp boundary	
		10YR4/1	:455-457 cm: coarser layer; dropstone (black shale)	
		10YR4/3	:457-463 cm: brown, sandy-silty clay, mottling	
		10YR3/2	:463-473 cm: colour banding: grayish brown-dark brown, sandy silt, gradual boundary, specks of sulphide, rare reddish spots of limonite	
		2.5YR5/2	:473-483 cm: colour banding, sandy silty clay, gradual boundary	
5		10YR4/3	:483-488 cm: brown, sandy silty clay, strong mottling, sharp boundary	

ARK-XIII/2

	Lithology	Texture	Color	Description	Age
5			2.5Y4/2	:488-498 cm: dark grayish brown-brown, sandy silty clay (with sandy layers), sharp boundary, turbidite	
			7.5YR4/2	:498-512 cm: brown, silty clay, strong mottling, sharp boundary, spots and lenses of dark brown	
			5Y5/2	:512-520 cm: olive, clayey sandy silty mud, strong mottling, sharp boundary	
			5Y4/4	:520-524 cm: very dark grayish brown-olive, clayey sandy silty mud, mottling	
			5Y4/3	:524-525 cm: olive, clayey sandy silty mud	
			5Y3/1	:525-540 cm: very dark gray, sandy silt, specks of sulphide, sharp boundary	
			5Y3/2	:540-542 cm: dark olive gray, silty sand, mottling	
			5Y4/1	:542-552 cm: dark gray, silty sand	
			2.5Y4/	:552-554 cm: gray, coarse sand, turbidite	
			10YR4/3	:554-555 cm: dark gray, silty sand	
			10YR4/4	:555-563 cm: brown, silty clay, gradual boundary	
			5Y3/2	:563-569 cm: dark yellowish brown, silty clay, sharp boundary is disturbed	
			5Y3/2	:569-577 cm: dark olive gray (upper part), olive gray (lower part), clayey sandy silt, mottling, sharp boundary	
			2.5Y3/2	:577-585 cm: dark grayish brown, sandy silty clayey mud	
6					
	2.5Y4/3	:594 cm; turbidite), gradual boundary			
	10YR4/3	:596-605 cm: colour banding: brown-grayish brown, silty clay, mottling, gradual boundary			
	5YR4/3	:605-627 cm: reddish brown, clay, weak mottling, sharp boundary			
	10YR4/2	:627-635 cm: lamination of dark grayish brown, coarse-grained sand and grayish brown clayey sandy silt, turbidites			
	10YR5/2	:635-654 cm: colour banding: reddish brown, grayish brown, dark reddish, silty clay			
	5YR5/3				
	10YR5/2				
	End of core				
7					
8					
9					
10					

PS2846-4 (GKG)

East Greenland Margin

ARK-XIII/2

Recovery: 0.42 m

81°35.2 N 10°00.4 W

Water depth: 532 m

Depth in core (m)	Lithology	Texture Color	Description	Age
	0		10YR3/3 10YR4/3 5YR4/3 5YR4/3 10YR4/3 5YR4/3 10YR4/3	0-6 cm: dark yellowish brown, silty sand, bioturbated, gradual boundary 6-25 cm: dark yellowish brown, silty sand, coarser than overlying deposits 16 cm - quartzite dropstone 19-21 cm - sandy silt, reddish brown layer interbedded 21-25 cm - high amount of gravel 23 cm - dropstone 25-31 cm: reddish brown, sandy silt, slightly bioturbated in the bottom; mottling 31-41 cm: dark yellowish brown, silty sand; colour change for more reddish brown downwards 32 cm - bivalvia 37-39 cm - dropstone (coarse-grained sandstone) 41-42 cm: dark yellowish brown, gravel and pebbles with coarse-grained sand: turbidite-like deposits
1				

PS2847-3 (GKG)

Fram Strait

ARK-XIII/2

Recovery: 0.40 m

81°52.0 N 04°29.6 W

Water depth: 4190 m

Depth in core (m)	Lithology	Texture Color	Description	Age
	0		10YR3/4 10YR4/4 10YR3/4 10YR4/4 10YR3/4	0-2 cm: dark yellowish brown, clay, bioturbated 6-10 cm: dark yellowish brown, silty clay 10-27 cm: dark yellowish brown, silty clay, increasing mottling between 22-23 cm 27-33 cm: dark yellowish brown, silty clay, mottling in the upper part 33-40 cm: dark yellowish brown, clay
1				

PS2848-3 (GKG)

Fram Strait

ARK-XIII/2

Recovery: 0.40 m

81°59.94 N 02°25.84 W

Water depth: 2602 m

Depth in core (m)	Lithology	Texture Color	Description	Age
	0		10YR3/3 10YR4/4	0-34.5 cm: dark yellowish brown, sandy silty clay, bioturbated, upper part enriched in foraminifers, sharp boundary 34.5-40 cm: dark yellowish brown, sandy silty clay, lighter than upper layer
1				

PS2849-6 (GKG)

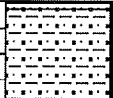
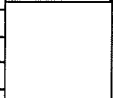
Nansen Basin

ARK-XIII/2

Recovery: 0.37 m

82°39.2 N 01°28.5 E

Water depth: 3293 m

Depth in core (m)	Lithology	Texture	Color	Description	Age
	0			10YR3/4	0-2 cm: dark yellowish brown, sandy silty clay, bioturbated
			10YR4/4	2-37 cm: dark yellowish brown, lighter than above, sandy silty clay	
				7-14 cm: mottling 25-27 cm: spots of sulphide 27-29 cm: mottling	
1					

PS2850-1 (SL)

Northwestern Yermak Plateau

ARK-XIII/2

Recovery: 1.65 m

82° 22.8 N 03° 40.8 E

Water depth: 2958 m

Lithology	Texture Color	Description	Age
	<p>5YR3/3 10YR3/4 2.5Y5/2 5YR4/3 2.5Y4/4 2.5Y5/4 5Y4/4 5Y4/3 2.Y4/2 2.Y4/4 10YR4/3 2.5Y5/ 2.5Y4/</p>	<p>0-9cm: brown, soft, foram rich mud, silty clay, sharp lower boundary is inclined 9-26cm: dark yellowish brown, sandy clayey silt, very stiff, bioturbated, sharp lower boundary is inclined 24.5-27 cm, black spots of sulphide 26-31cm: grayish brown, silty clay, sharp lower boundary is inclined 30-32 cm, weak mottling. 31 cm - dropstone (black claystone) 31-78 cm: colour banding: olive brown, light olive brown, olive sandy silty clayey mud. Reddish brown spots and lenses in the uppermost part, black specks of sulphides. Weak mottling in the lowermost part. 78-95 cm: colour banding: dark grayish brown, olive brown, olive, brown sandy clayey silty mud, stiff. Inclined sharp boundary (94-96 cm). Mottling. 83,88,94 cm - thin (several mm) lenses of sand. 81-84 cm - black spots of sulphides 87-91 cm - reddish spots of limonite 95-165 cm: very dark gray, sandy silty clay with dark gray spots and lenses, very stiff. Rare black specks of sulphides. 122-124 cm, 139-141 cm - lenses (1.0-1.5 cm thick) of coarse sand - turbidites. 113-119 cm - sandy spots. 113, 163 cm - dropstones (sandstone, claystone)</p>	

Depth in core (m)

PS2851-2 (GKG)

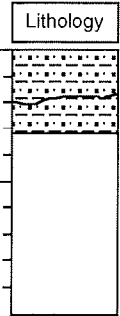
Northwestern Yermak Plateau

ARK-XIII/2

Recovery: 0.31 m

82°22.45 N 03°36.91 E

Water depth: 2997 m

Depth in core (m)	Lithology	Texture	Color	Description	Age
	0			10YR4/3 10YR4/4	0-18 cm: dark yellowish brown, sandy silty clay, many foraminifers between 8-18 cm, erosional discordance 18-24 cm: olive brown, silty sandy clay, mottling, spots of sulphide 24-31.5 cm: olive brown, sandy silty clay, gradual boundary, bioturbated (very stiff material)
1					

PS2852-1 (SL)

Northwestern Yermak Plateau

ARK-XIII/2

Recovery: 4.02 m

82° 20.97 N 03°36.79 E

Water depth: 2663 m

Lithology	Texture Color	Description	Age
	10YR4/4	0-16 cm: dark yellowish brown, sandy silty clay, bioturbated, sharp boundary inclined	
	5Y4/2	16-26 cm: olive gray, silty clay, mottling, sharp boundary inclined	
	2.5Y5/6	26-45 cm: light olive brown, silty sand, bioturbated, "cottage cheese"-structure specks of sulphide, limonite, dropstones (marmoré, claystones, sharp boundary inclined, turbidite	
	10YR5/2	45-56 cm: grayish brown, sandy silt, mottling, sharp boundary inclined, turbidite	
	10YR5/6	56-71 cm: yellowish brown, silty sand, faintly laminated, sharp boundary inclined, turbidites	
	10YR4/4		
	2.5Y5/4	71-94 cm: light olive brown, sandy clayey silt, weak mottling, sharp boundary inclined, specks of sulphide	
	2.5Y4/4	94-130 cm: lamination of olive brown sandy silt and dark yellowish brown sand, strong mottling, sharp boundary inclined, "cottage cheese"- structure, turbidites	
	10YR4/4		
	2.5Y3/2	130-141 cm: very dark grayish brown, sandy silt, laminated with dark yellowish brown coarse sand, sharp boundary, turbidites	
	10YR3/4		
	2.5Y4/4	141-144 cm: dark gray, sandy silt, sharp boundary, lot of gravel	
	5Y4/2	144-150 cm: olive gray, silt, weak mottling, sharp boundary	
	2.5Y3/	150-190.5 cm: very dark gray, sandy silt, homogenous, specks of sulphide, sharp boundary inclined	
	5Y4/1	190.5-194 cm: dark gray, clayey sandy silt, specks of sulphide, sharp boundary	
	5Y4/2	194-204 cm: olive gray, sandy clayey silt, mottled, sharp boundary	
	5Y4/3	204-215 cm: olive, clayey sandy silt	
	5Y4/2	215-222 cm: lamination of olive gray sandy silt and coarse dark yellowish brown sand, turbidites, inclined boundary	
	10YR4/4	218 cm: dropstone (reddish claystone)	
	5Y4/2	222-234 cm: olive gray, sandy clayey silt, interbedded with thin lenses of dark yellowish brown sand, turbidites, sandy lenses are inclined	
	10YR4/4		
	5Y3/2	234-243 cm: dark olive gray, sandy clayey silt, sharp boundaries are fixed by oxidized reddish lenses, "cottage cheese"- structure, turbidites	
	2.5Y4/	243-276 cm: dark gray, silty clay, homogenous, sharp boundary inclined	
	2.5Y4/	276-278 cm: dark gray lense of coarse sand with gravel and pebbles, turbidite	
	5Y4/2	278-300 cm: olive gray, sandy clayey silt, turbidites, sharp boundary inclined	
	5Y3/1	300-305 cm: very dark gray, sandy silt, mottling, sharp boundary, turbidites	
	5Y4/2	305-307.5 cm: olive gray, sandy silt, mottling, sharp boundary, turbidite	
	5Y4/1	307.5-317 cm: dark gray, silty clay, homogenous, sharp boundary	
	2.5Y4/4	317-335 cm: colour banding, interbedding of olive brown, olive and olive gray, sandy silt, reddish spots of limonite in the uppermost part, sharp boundary, turbidites	
	5Y4/3		
	5Y4/2		
	5Y3/1	335-380 cm: very dark gray, sandy silt, turbidites, sharp boundary inclined, lower boundary is fixed by 0.5 cm thick sandy layer	
	5Y4/3	380-383 cm: olive, sandy silty clay, weak mottling, sharp boundary inclined	
	5Y3/1	383-385 cm: very dark gray, coarse sand, sharp boundary inclined, turbidite	
	5Y4/2	385-388 cm: olive gray, sandy silt, weak mottling, sharp boundary inclined, turbidite	
	5Y3/1	388-402 cm: very dark gray, sandy silt, homogenous	
End of core			

PS2853-9 (GKG)

Northwestern Yermak Plateau

ARK-XIII/2

Recovery: 0.30 m

82°19.10 N 03°42.55 E

Water depth: 2048 m

Depth in core (m)	Lithology	Texture Color	Description	Age
	0		10YR3/3 2.5Y4/2 10YR4/4	0-5 cm: dark yellowish brown, sandy silty clay, bioturbated 5-20 cm: olive brown, sandy silty clay, gradual boundary with darker layers between 12 and 15 cm, mottled, foram rich layer (5-6 cm), top of this layer is marked by oxidized (stiff) horizon (see other cores) 20-30 cm: dark yellowish brown, silty sand, gradual boundary, mottled, drop-stones on top, very stiff deposits
1				

PS2854-2 (GKG)

Northwestern Yermak Plateau

ARK-XIII/2

Recovery: 0.49 m

82°12.02 N 03°54.1 E

Water depth: 1806 m

Depth in core (m)	Lithology	Texture Color	Description	Age
	0		10YR4/3 10YR4/3 10YR2/2 2.5Y4/4 10YR3/2 2.5Y4/4 10YR3/3	0-10 cm: brown, clay, bioturbated, very soft, sharp boundary 10-17 cm: thin interbedding of very dark brown and brown silty clay, coal clasts, strong mottling, sharp boundary (oxidized layer) 17-28 cm: colour banding, olive brown, clay, sharp boundary 28-30 cm: lense of olive brown clay, mottling, sharp boundary 30-44 cm: colour banding, olive brown, clay (see 17-28 cm), sharp boundary 44-49 cm: dark brown, clay, homogenous
1				

PS2855-8 (GKG)

Northwestern Yermak Plateau

ARK-XIII/2

Recovery: 0.35 m

82°02.7 N 05°17.3 E

Water depth: 1455 m

Depth in core (m)	Lithology	Texture Color	Description	Age
	0		10YR4/2 2.5Y4/4 2.5Y4/2	0-12 cm: dark yellowish brown, sandy silty clay, bioturbated in the top, mottling, gradual boundary 8-10 cm: strongly oxidized layer 10-12 cm: dark gray layer 12-26 cm: olive brown, silty clay, gradual boundary, mottling 18-19 cm: dark gray layer 26-35 cm: olive brown, sandy silty clay, gradual boundary, mottling 26-28 cm: dark gray layer 30-35 cm: homogenous
1				

PS2856-7 (GKG)

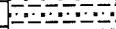
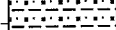
Northwestern Yermak Plateau

ARK-XIII/2

Recovery: 0.44 m

81°59.25 N 05°44.96 E

Water depth: 961 m

Depth in core (m)	Lithology	Texture	Color	Description	Age
	0			10YR4/4	0-16 cm: dark yellowish brown, interbedded with dark brown (oxidized) layers, bioturbated, gradual boundary
				16-17.5 cm: distinctly oxidized layer, very stiff ("hard ground")	
			10YR4/2	17.5-33.5 cm: dark grayish brown, sandy silty clay, mottling, gradual boundary, interbedded with thin yellowish brown layers	
			10YR4/1	33.5-44 cm: dark gray, sandy silty clay, spots of sulfide, homogenous	
1					

	Lithology	Texture Color	Description	Age
5		5YR4/2, 2.5Y4/4 10YR4/4, 2.5Y5/2	497-505cm dark reddish gray, olive brown, grayish brown, dark yellowish brown sandy-silty clay, color banding (bandwidth 0.5-1.0cm)	
		5Y5/3	505-515cm olive sandy-silty clay	
		2.5Y4/1	515-559cm dark gray sandy-silty clay, homogenous. Black spots (0.1-0.5cm, sulphides).	
		2.5Y4/4	559-570cm olive brown, olive gray clayey-sandy silt	
		5Y4/2	570-581 very dark gray clayey-sandy silt	
		5Y3/1	581-587cm brown, dark gray clayey-sandy silt	
		7.5YR5/2	587-608cm dark gray silty clay, homogenous	
6		10YR4/1	608-652cm dark gray silty clay with numerous black spots and lenses (0.5-1.5cm, sulphides)	
		2.5Y4/1		
7				
8				
9				
10				

PS2857-10 (GKG)

Recovery: 0.44 m

Yermak Plateau

81°54.4 N 07°54.8 E

ARK-XIII/2

Water depth: 859 m

Depth in core (m)	Lithology	Texture	Color	Description	Age
	0			10YR3/4	0-38 cm: dark yellowish brown, sandy silty clay, homogenous, very soft, gradual boundary
			10YR3/3	38-44 cm: dark brown, silty clay, oxidized streaks 38-39 cm: strong oxidized layer	
1					

PS2858-6 (GKG)

Recovery: 0.45 m

Yermak Plateau

81°45.52 N - 9°30.91 E

ARK-XIII/2

Water depth: 931 m

Depth in core (m)	Lithology	Texture	Color	Description	Age
	0			10YR4/2	0-2 cm: dark grayish brown, sandy silty clay, bioturbated
			10YR3/3	2-45.5 cm: dark brown, sandy silty clay 38-42 cm: gradual boundary, oxidized lenses	
1					

PS2859-10 (GKG)

Recovery: 0.46 m

Yermak Plateau

81°44.97 N 10°11.14 E

ARK-XIII/2

Water depth: 1180 m

Depth in core (m)	Lithology	Texture	Color	Description	Age
	0			10YR4/2	0-46 cm: dark grayish brown, sandy silty clay, homogenous, surface bioturbated
				35-38 cm: mottling 40-45 cm: dark layers with high amounts of sand interbedded 45-46 cm: strong oxidized layer (hard ground), dropstone (graywacke?)	
1					

PS2859-8 (KAL)

Yermak Plateau

ARK-XIII/2

Recovery: 6.70 m

81° 45.5' N, 10° 08.7' E

Water depth: 1120 m

	Lithology	Texture Color	Description	Age
0		10YR4/3	0-45 cm: brown silty clay, bioturbated in the upper part. 0cm was defined by correlation with the box core ("hard ground" at 46-47 cm)	
		10YR4/3	45-50 cm: brown silty clay and very dark grayish brown sandy silty clayey mud interbedded, at 46-47 cm hardground, dark reddish brown sandy silty clay	
		5Y5/1	50-70 cm: gray silty clay, soft, homogenous. Part of this layer was probably destroyed during coring	
		5Y3/2	70-73 cm: dark olive gray sandy silty clay	
		2.5Y3/2	73-77.5 cm: grayish brown sandy silty clay, very soft	
		5Y3/2	77.5-82 cm: dark olive gray sandy silty clayey mud, spots of reddish limonite, "cottage cheese"-structure	
		10YR5/1	82-86 cm: very dark grayish brown sandy clayey silt, "cottage cheese"-structure	
		10YR4/3	86-91 cm: gray silty clay, homogenous	
		10YR4/3	91-99 cm: brown silty clay	
1		10YR4/3	99-231 cm: dark yellowish brown silty clay, strong mottling	
		10YR4/4	125-140 cm: gray silty clay clasts (2-3 cm)	
		10YR4/3	139-146 cm: brown clay	
2		10YR4/4		
		10YR4/2	231-234 cm: dark grayish brown sandy silty clay	
		2.5Y4/4	234-266 cm: dark grayish brown, olive brown, olive gray sandy silt, turbidites	
		2.5Y4/2	"Cottage cheese"-structure around 252 cm	
		5Y4/1		
		5Y4/2		
		2.5Y4/4	266-275 cm: dark gray silty clay. 270 cm: dropstone (1.0 cm)	
		2.5Y4/4	275-295.5 cm: olive brown sandy silt, turbidites	
		5Y4/2		
3		2.5Y4/4	295.5-356 cm: olive brown, olive gray, gray silty clay. Color banding, several cm thick bands	
		5Y4/2		
		5Y4/3		
		5Y4/3	356-370 cm: olive sandy silt in the uppermost part, very dark gray in the lowermost part. Cottage cheese structure, weak mottling	
		5Y5/2		
		5Y4/3	370-422 cm: olive, olive gray bands of clay, several cm thick	
4		2.5Y4/2	422-450 cm: dark gray clay. Black sulphide spots (0.5-1.0 cm)	
		2.5Y4/2	450-458 cm: dark grayish brown silty clay. Black sulphide spots (0.2-1.0 cm)	
		5Y4/2	458-478 cm: olive gray clay, homogenous	
		5Y4/4	478-488 cm: olive silty clay	
		5Y4/4	488-500 cm: olive, olive gray sandy silts, turbidites, 1-2.5 cm thick bands	
5		5Y4/2	494 cm: coal piece (0.5 cm)	

ARK-XIII/2

Lithology	Texture	Color	Description	Age
	<p>10YR4/3 10YR4/4 7.5YR4/2 2.5Y3/2 2.5Y5/ 2.5Y4/4 5Y4/3 5Y5/1 5Y5/2 10YR3/4 5Y4/3 5Y5/1 5Y5/2 5Y5/1</p>		<p>500-512 cm: olive brown, dark yellowish brown, brown sandy silt 503 cm: coal piece (1.2 cm) 512-518 cm: brown sandy silt, turbidites 518-532 cm: very dark gray and very dark grayish brown sandy silt. Turbidites 1.5-2.5 cm thick 532-562 cm: gray silty clay interbedded with olive brown sandy clayey silty mud 562-611 cm: olive, olive gray, gray clay. Color banding several cm thick, black spots in the lowermost part. 593-595 cm: dark yellowish brown silty clay oxidized layer. 576 cm: dropstone 611-636 cm: dark gray silty clay, homogenous, numerous black spots (sulfides)</p>	

5
6
7
8
9
10

Depth in core (m)

PS2860-7 (GKG)

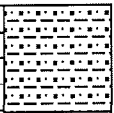
Eastern Yermak Plateau

ARK-XIII/2

Recovery: 0.41 m

81°34.87 N 11°51.13 E

Water depth: 2033 m

Depth in core (m)	Lithology	Texture	Color	Description	Age
	0			10YR4/2	0-41 cm: dark grayish brown, sandy silty clay, homogenous, surface bioturbated
1					

PS2861-11 (GKG)

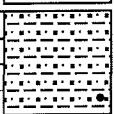
Eastern Yermak Plateau

ARK-XIII/2

Recovery: 0.41 m

81°16.95 N 13°36.15 E

Water depth: 2308 m

Depth in core (m)	Lithology	Texture	Color	Description	Age
	0			10YR4/2	0-39 cm: dark grayish brown, sandy silty clay, homogenous, surface bioturbated and with abundant foraminifers 33 cm: dropstone, quartz (white and rounded) 1*1.5 cm
1					

PS2862-5 (GKG)

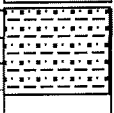
North of Svalbard

ARK-XIII/2

Recovery: 0.41 m

80°34.70N 11°47.36 E

Water depth: 1042 m

Depth in core (m)	Lithology	Texture	Color	Description	Age
	0			10YR3/3 10YR4/2 2.5Y/4	0-8 cm: dark brown, sandy silty clay, homogenous, bioturbated in the top. 8-15 cm: dark grayish brown, silty sandy clay interbedded with very dark brown oxidized layers; mottling. Gradual upper and lower boundaries. 15-41 cm: dark gray, silty sandy clay interbedded with oxidized layers, lenses and spots.
1					

PS2863-2 (GKG)

Recovery: 0.41 m

North of Svalbard

80°33.47N 11°17.93 E

ARK-XIII/2

Water depth: 807 m

Depth in core (m)	Lithology	Texture	Color	Description	Age
	0		10YR3/3	2.5Y4/0	0-5 cm: dark brown, sandy silty clay, bioturbated in the top, sharp boundary. 5-41 cm: dark gray, clayey-silty mud, homogeneous, with black specks of sulphides
1					

PS2864-4 (GKG)

Recovery: 0.40 m

North of Svalbard

80°31.67N 11°22.07 E

ARK-XIII/2

Water depth: 791 m

Depth in core (m)	Lithology	Texture	Color	Description	Age
	0		10YR3/3	2.5Y4/0	0-4 cm: dark brown, sandy silty clay, bioturbated in the top, sharp boundary. 4-40 cm: dark gray, clayey-silty mud
1					

PS2865-2 (GKG)

Recovery: 0.38 m

North of Svalbard

80°29.72N 10°29.27 E

ARK-XIII/2

Water depth: 821 m

Depth in core (m)	Lithology	Texture	Color	Description	Age
	0		10YR3/3	2.5Y4/0	0-3 cm: dark brown, sandy silty clay, bioturbated in the top, sharp boundary. 3-38 cm: dark gray, silty clay, homogenous
1					

PS2868-5 (GKG)

Molloy Deep

ARK-XIII/2

Recovery: 0.46 m

79°06.46N 03°05.75 E

Water depth: 5449 m

Depth in core (m)	Lithology	Texture Color	Description	Age
	0  1	 10YR3/2 2.5Y4/2 2.5Y4/2 2.5Y4/ 2.5Y3/ 5Y4/1	0-4 cm: very dark grayish brown, silty clay, 4-4.5 cm: sandy layer, turbidite 4.5-10 cm: dark grayish brown, silty clay with sandy layers (at 6, 9 and 10 cm) 10-11 cm: oxidized layer, sandy silty clay 11-24.5 cm: dark grayish brown, sandy silty clay (dark brown layer at 23 cm) 24.5-25 cm: oxidized layer 25-31 cm: dark gray, silty clay, homogenous, turbidite 31-33 cm: very dark gray, coarse sandy layer, turbidite 33-46 cm: dark gray, sandy silty clay, more sandy at the top, interbedded with sandy layers (turbidites), strong oxidized layer at 41 cm . . .	

Table 10.1: List of samples of aerosols collected by filtration through AFA-HA filters

No.	Date-time (UTC)	Coordinates		No.	Date-time (UTC)	Coordinates			
		Latitude (N)	Longitude			Latitude (N)	Longitude		
1	27.06-14.35	76°18.4'	33°28.3'E	6	18.07-08.20	81°41.6'	9°01.5'W		
	27.06-14.55	76°20.0'	33°29.0'E		18.07-10.50	81°51.3'	6°34.3'W		
	27.06-15.15	76°20.0'	33°29.0'E		19.07-01.20	81°50.2'	4°10.6'W		
	27.06-18.10	76°37.8'	33°36.5'E		19.07-03.10	81°50.0'	4°07.2'W		
	27.06-21.15	76°38.1'	33°33.7'E		22.07-00.40	82°37.9'	2°20.3'E		
	27.06-23.45	76°50.2'	33°45.9'E		22.07-07.00	82°37.3'	2°31.6'E		
2	29.06-16.40	78°52.9'	31°17.4'E		23.07-04.30	82°22.6'	3°41.4'E		
	29.06-19.00	79°07.0'	31°34.4'E		23.07-09.55	82°22.2'	3°31.7'E		
	30.06-02.00	79°26.8'	30°29.6'E		24.07-16.30	82°18.1'	3°42.0'E		
	30.06-04.00	79°43.6'	30°06.0'E		25.07-08.40	82°07.4'	5°00.4'E		
	30.06-07.15	80°03.2'	29°45.0'E		25.07-15.00	82°02.6'	5°18.4'E		
	30.06-11.10	80°18.3'	29°04.8'E		26.07-04.00	82°02.8'	5°18.1'E		
	30.06-16.30	80°22.2'	29°01.1'E		7	26.07-13.10	81°59.2'	5°44.5'E	
	01.07-12.30	80°42.6'	27°45.0'E			26.07-20.40	81°59.7'	5°48.9'E	
	01.07-18.00	80°42.2'	26°00.5'E	27.07-03.05		81°53.2'	7°56.4'E		
	01.07-23.15	80°45.0'	24°59.1'E	27.07-16.40		81°54.2'	7°56.4'E		
	3	07.07-19.50	80°19.0'	10°20.2'E		27.07-17.07	81°54.2'	7°57.1'E	
07.07-20.45		80°22.7'	10°21.9'E	27.07-18.15		81°54.4'	7°59.1'E		
07.07-21.10		80°23.3'	10°28.6'E	8	29.07-19.00	81°33.4'	11°36.3'E		
07.07-22.25		80°30.8'	10°26.1'E		30.07-01.15	81°34.2'	11°44.5'E		
08.07-17.05		80°54.2'	9°52.2'E		30.07-19.10	81°16.1'	13°08.2'E		
08.07-20.00		80°54.5'	9°50.3'E		31.07-07.25	81°18.5'	13°31.3'E		
08.07-23.05		80°54.9'	9°49.3'E	4	12.07-09.50	81°13.9'	2°18.8'E		
09.07-04.25		80°55.4'	9°53.0'E		12.07-18.30	81°13.5'	2°37.2'E		
11.07-09.45		81°08.2'	5°46.8'E		5	15.07-15.10	81°26.0'	5°22.0'W	
11.07-11.10		81°08.4'	5°39.4'E			15.07-19.25	81°23.5'	5°15.3'W	
4	12.07-09.50	81°13.9'	2°18.8'E			16.07-08.20	81°31.6'	6°49.3'W	
	12.07-18.30	81°13.5'	2°37.2'E			16.07-14.30	81°31.9'	6°48.9'W	
	5	15.07-15.10	81°26.0'			5°22.0'W	17.07-02.35	81°34.8'	8°10.6'W
		15.07-19.25	81°23.5'			5°15.3'W	17.07-08.15	81°34.5'	8°11.5'W
16.07-08.20		81°31.6'	6°49.3'W						
16.07-14.30		81°31.9'	6°48.9'W						
17.07-02.35		81°34.8'	8°10.6'W						
17.07-08.15		81°34.5'	8°11.5'W						

Time and location at the beginning, at intermediate points and at the end of sampling are given.

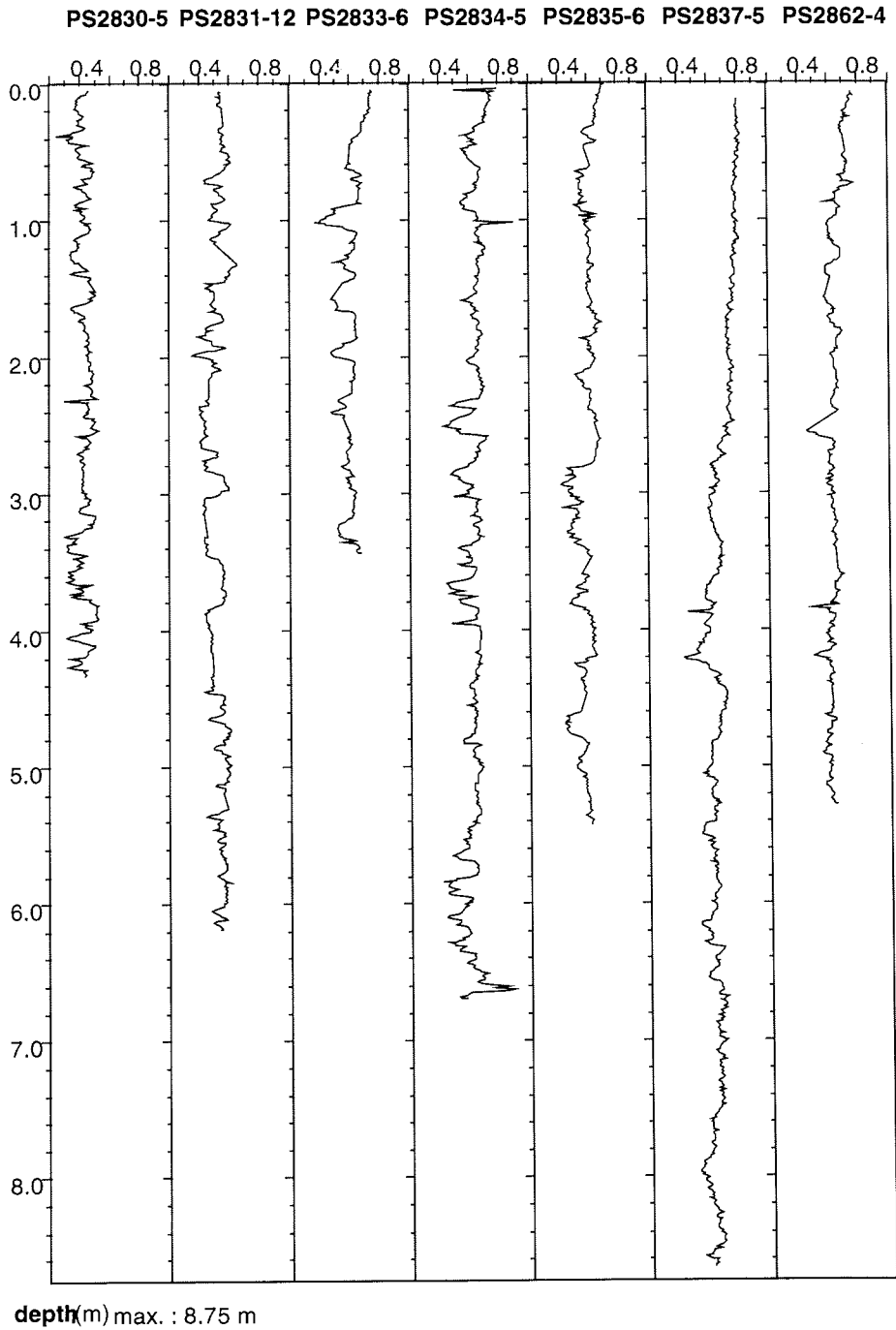
Table 10.2: List of aerosol size measurements
(Measurement times and locations for analyses of particle size
distributions in aerosols of the NW Barents Sea and the Fram Strait)

No.	Date-time (UTC)	Coordinates		No.	Date-time (UTC)	Coordinates	
		Latitude (N)	Longitude			Latitude (N)	Longitude
1	26.06-16.40	73°08.4'	26°00.5'E	54	24.07-16.30	82°18.1'	3°42.0'E
2	26.06-20.00	73°42.1'	27°26.8'E	55	25.07-09.05	82°07.4'	5°00.4'E
3	26.06-21.50	74°01.8'	28°09.8'E	56	25.07-10.10	82°07.3'	5°00.7'E
4	27.06-00.30	74°29.9'	29°15.7'E	57	35.07-15.00	82°02.6'	5°18.4'E
5	27.06-09.15	75°59.8'	32°59.5'E	58	25.07-16.50	82°02.5'	5°18.0'E
6	27.06-15.15	76°20.0'	33°29.0'E	59	25.07-21.25	82°02.7'	5°17.1'E
7	27.06-16.20	76°27.2'	33°35.3'E	60	26.07-02.50	82°02.8'	5°17.6'E
8	27.06-22.25	76°42.1'	33°35.8'E	61	27.07-08.40	81°53.9'	7°41.3'E
9	28.06-08.30	77°21.8'	34°38.7'E	62	27.07-17.05	81°54.2'	7°57.1'E
10	28.06-11.15	77°34.2'	34°40.5'E	63	30.07-21.45	81°16.1'	13°11.6'E
11	29.06-16.40	78°52.9'	31°17.4'E	64	31.07-04.00	81°18.2'	13°25.7'E
12	29.06-19.00	79°07.0'	31°34.4'E	65	31.07-07.20	81°18.5'	13°31.3'E
13	29.06-22.00	79°26.7'	30°33.3'E	66	03.08-15.35	79°58.1'	8°58.2'E
14	30.06-02.00	79°26.8'	30°27.1'E				
15	30.06-10.05	80°14.5'	29°10.7'E				
16	30.06-20.30	80°41.2'	29°31.0'E				
17	01.07-12.30	80°42.6'	27°45.0'E				
18	01.07-18.00	80°42.2'	26°00.5'E				
19	02.07-18.46	81°00.0'	20°54.2'E				
20	02.07-21.10	81°03.3'	20°11.4'E				
21	03.07-19.02	80°58.4'	17°36.8'E				
22	03.07-21.30	80°58.7'	17°25.0'E				
23	04.07-09.15	81°06.1'	16°55.3'E				
24	04.07-23.45	81°05.0'	16°25.1'E				
25	05.07-02.45	81°06.3'	16°14.8'E				
26	05.07-09.25	81°06.7'	16°17.9'E				
27	05.07-15.00	81°06.3'	16°14.4'E				
28	05.07-17.15	81°06.6'	16°14.7'E				
29	05.07-22.00	81°06.8'	16°10.4'E				
30	06.07-14.10	80°58.1'	11°51.7'E				
31	06.07-15.00	80°58.1'	11°51.3'E				
32	06.07-18.15	80°58.3'	11°49.6'E				
33	06.07-23.50	80°58.7'	11°45.6'E				
34	07.07-08.25	80°35.6'	11°42.1'E				
35	07.07-11.25	80°23.9'	11°40.8'E				
36	07.07-19.50	80°19.0'	10°20.2'E				
37	08.07-20.00	80°54.2'	9°52.2'E				
38	08.07-20.00	80°54.2'	9°50.3'E				
39	08.07-23.50	80°54.9'	9°49.3'E				
40	09.07-02.30	80°55.2'	9°50.8'E				
41	09.07-04.25	80°55.4'	9°53.0'E				
42	11.07-10.00	81°08.1'	5°46.7'E				
43	12.07-09.50	81°13.9'	2°18.8'E				
44	12.07-14.25	81°13.9'	2°30.4'E				
45	15.07-15.10	81°26.0'	5°22.0'W				
46	16.07-08.20	81°31.6'	6°49.3'W				
47	16.07-11.00	81°31.3'	6°48.7'W				
48	17.07-02.35	81°34.8'	8°10.6'W				
49	17.07-06.20	81°34.8'	8°11.0'W				
50	18.07-08.48	81°44.0'	8°35.4'W				
51	22.07-05.30	82°37.5'	2°29.4'E				
52	23.07-04.30	82°22.6'	3°41.4'E				
53	23.07-09.55	82°22.2'	3°31.7'E				

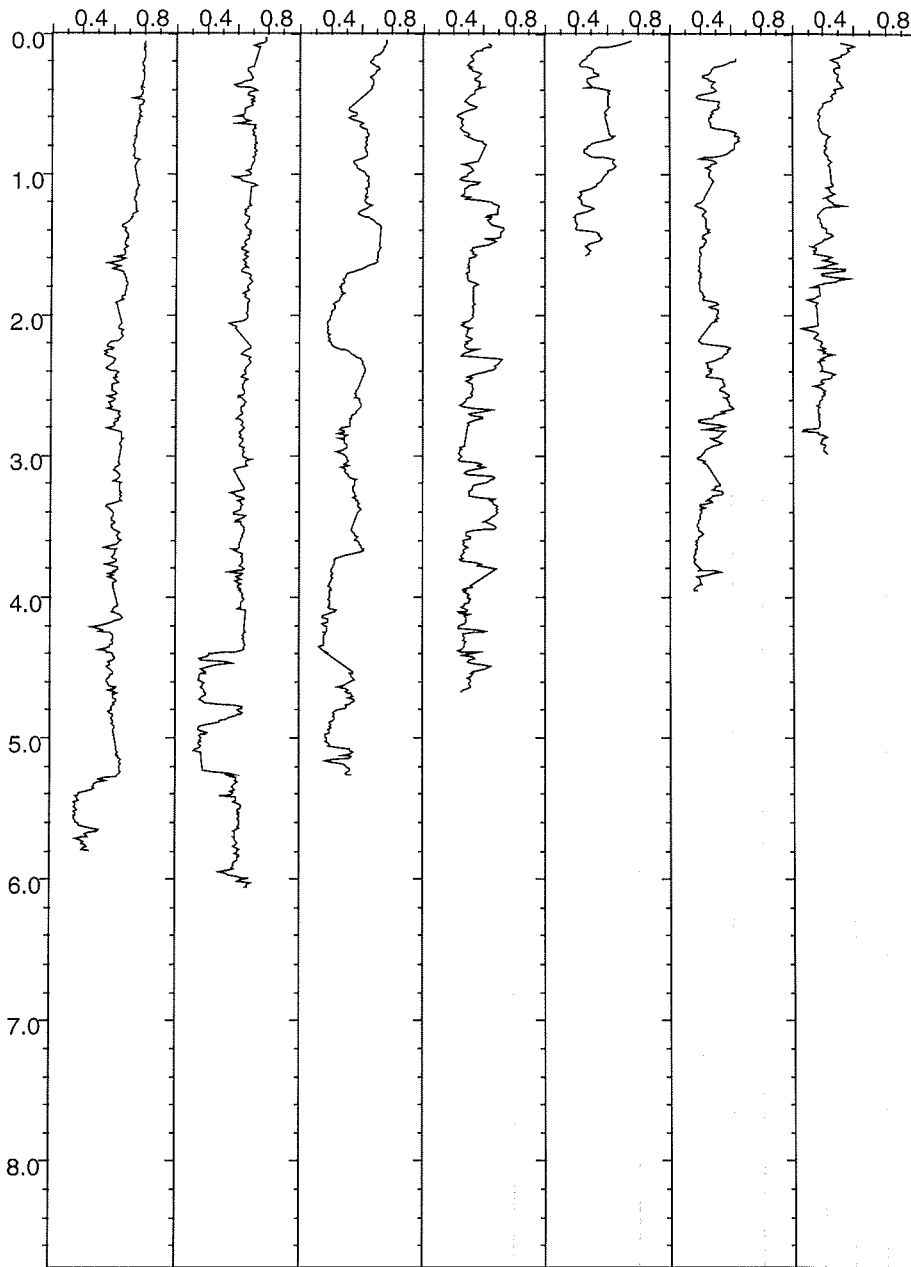
Table 10.3: Samples taken for nitrogen and carbon isotope measurements.

station	position	sample	station	position	sample
2822-5	763861N	Sea water	17	811567N	Meltwaterpond water/algae
	333359E	Copepods		021738E	Sea Ice Sediment
		Surface sediment		811363N	Ice core water/algae
2824-5	773419N	Sea water		023610E	Surface sediment
	343858E	Copepods	18	811778N	Surface sediment
		Surface sediment		002316E	Meltwaterpond water/algae
2827-5	792600N	Surface sediment			Copepods
	302800E		20	815982N	Meltwaterpond water/algae
1		Sea Ice Sediment		011638W	Sea Ice Sediment
2		Sea Ice Sediment	21	820854N	Meltwaterpond water/algae
3	804300N	Sea Ice Sediment		015266W	Sea Ice Sediment
	292940E	Meltwaterpond water/algae	22	815848N	Meltwaterpond water/algae
		Ice core water/algae		023501W	Sea Ice Sediment
		Algae (Melosira?)	23		Sea Ice Sediment
5	804531N	Sea Ice Sediment	24	830611N	Sea Ice Sediment
	213106E			034499W	
6	804403N	Sea Ice Sediment	25	823851N	Meltwaterpond water/algae
	212821E			013191E	Sea Ice Sediment
7	805069N	Sea Ice Sediment	26	821914N	Meltwaterpond water/algae
	210489E			034253E	Sea Ice Sediment
8	805908N	Meltwaterpond water/algae	27	822626N	Meltwaterpond water/algae
	183158E	Ice core water/algae		030472E	Sea Ice Sediment
2830-8	805866N	Surface water	28	822637N	Meltwaterpond water/algae
	172497E	Copepods		044183E	Sea Ice Sediment
2831-7	810564N	Sea water	29	822612N	Meltwaterpond water/algae
	165835E	Copepods		031175E	Sea Ice Sediment
		Surface sediment	30	814993N	Sea Ice Sediment
2832-12	810673N	Sea water		065321E	
	161273E	Copepods	31	815409N	Meltwaterpond water/algae
		Surface sediment		075443E	Sea Ice Sediment
9		Sea Ice Sediment	32	812923N	Meltwaterpond water/algae
	810673N	Ice core water/algae		114070E	Sea Ice Sediment
	161273E		33	814055N	Meltwaterpond water/algae
10	805950N	Sea Ice Sediment		115999E	Sea Ice Sediment
	115917E	Meltwaterpond water/algae	34	813512N	Meltwaterpond water/algae
11	810026N	Sea Ice Sediment		115368E	Sea Ice Sediment
	122325E	Meltwaterpond water/algae	IS	812910N	Sea Ice algae
12	810244N	Sea Ice Sediment		121893E	
	124626E	Meltwaterpond water/algae	35	811603N	Meltwaterpond water/algae
2833-5	805820N	Surface sediment		131070E	Sea Ice Sediment
	114990E				Ice core water/algae
13	805451N	Surface sediment	36	811991N	Meltwaterpond water/algae
	095053E	Sea Ice Sediment		125048E	Sea Ice Sediment
		Meltwaterpond water/algae	37	813003N	Meltwaterpond water/algae
		Ice core water/algae		113769E	Sea Ice Sediment
		Copepods	38	811504N	Meltwaterpond water/algae
14	800768N	Meltwaterpond water/algae		120563E	Sea Ice Sediment
	053411E	Surface sediment			
15	812493N	Meltwaterpond water/algae			
	023152E	Sea Ice Sediment			
16	811964N	Meltwaterpond water/algae			
	013054E	Sea Ice Sediment			

Figure 10.1: Calculated porosity values of logged ARK-XIII/2 sediment cores
(for calculation of porosity see Chapter 7.3)

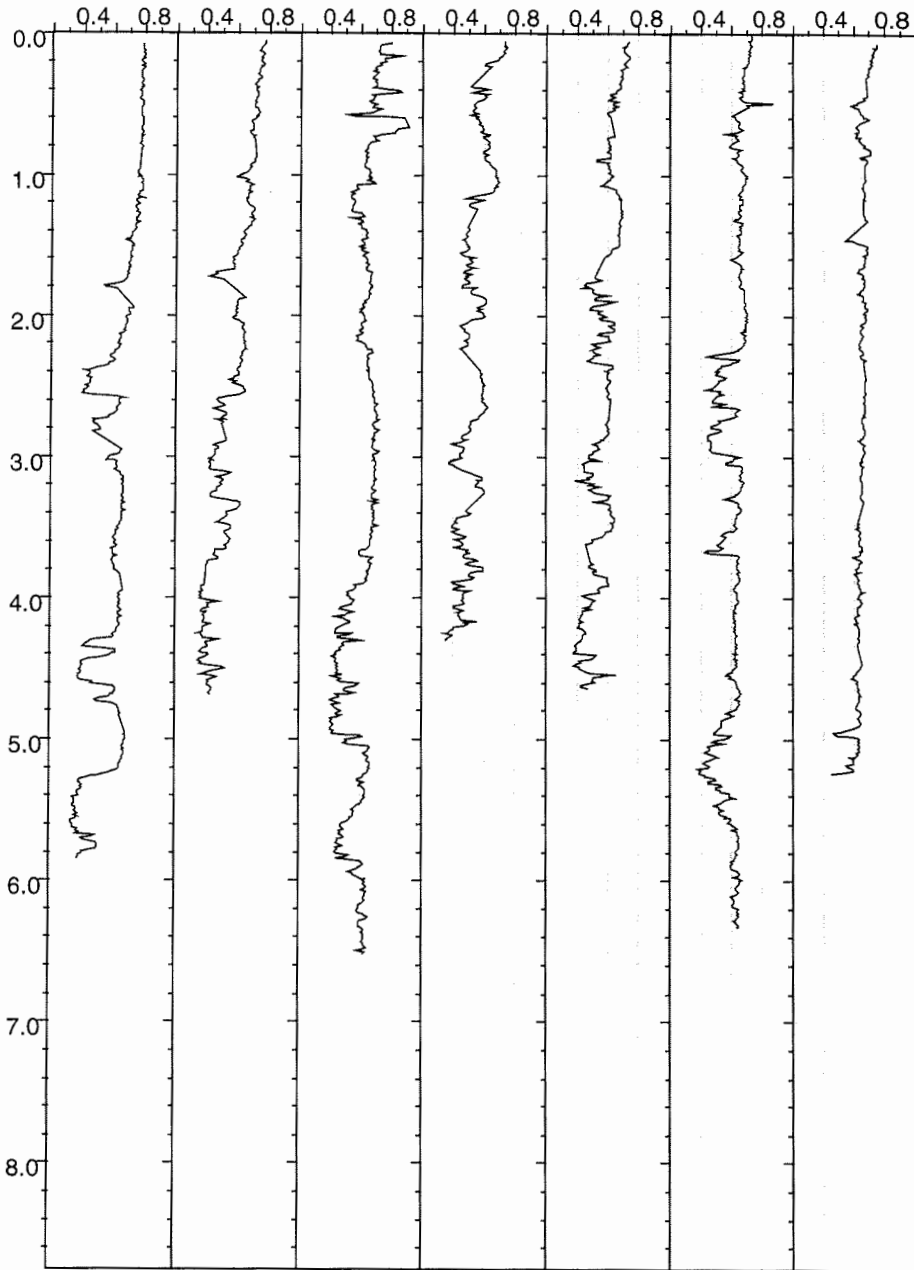


PS2838-7 PS2839-4 PS2848-5 PS2849-10 PS2850-1 PS2852-1 PS2853-12



depth(m) max. : 8.75 m

PS2854-1 PS2855-6 PS2856-5 PS2857-13 PS2858-8 PS2859-8 PS2860-5



depth(m) max. : 8.75 m

Table 10.4: Smear-slide estimates

depth (cm)	sand (%)	silt (%)	clay (%)	quartz (%)	feldspar (%)	forams (%)	Fe ox. (%)	clay min. (%)	rock fragm. (%)	heavy min. (%)	opaque min. (%)	spicules (%)	volc. glass (%)	lithology	plant debris rel. abd.	Cocco rel. abd.
PS2830-5																
7	20	57	17	50	10	5	15	5	0	3	5	1	0	cl. sandy silt		
22	15	50	35	50	15	5	15	5	0	3	5	1	0	snd. clayey silt		
59	15	65	30	50	15	5	15	5	1	3	5	0	1	snd. clayey silt		
66	5	17	77	50	15	5	15	5	1	3	10	0	0	clay		
95	40	50	10	10	40	40	0	5	1	5	2	0	1	foram sandy silt		
165	10	70	20	45	25	15	0	5	5	5	1	0	1	F-rich silt		
202	5	80	15	50	20	10	0	5	5	8	2	0	1	silt		
233	95	5	0	0	0	0	0	0	95	5	0	0	0	sand		
266	10	60	30	50	25	5	0	3	10	3	3	0	0	clayey silt		
305	15	70	15	50	20	2	0	5	15	5	3	0	1	silt		
345	10	55	35	50	20	0	0	5	15	7	2	0	0	clayey silt		
353	20	65	15	50	20	0	0	5	15	7	2	0	0	sandy silt		
382	5	25	70	40	15	5	0	20	10	5	5	0	1	clay		
423	5	25	70	40	15	5	0	23	10	5	2	0	1	clay		
435	5	25	70	40	15	5	0	23	10	5	2	0	1	clay		
PS2834-5																
22	2	10	88	3	5	1	15	75	1	1	1	0	0	clay		
40	5	10	85	5	5	1	15	70	1	2	2	0	0	clay		
43	5	20	75	5	5	0	20	62	2	5	1	0	0	clay		
54	2	40	58	25	20	0	5	36	5	8	1	0	1	silty clay		
61	1	20	79	12	8	0	3	70	1	1	5	0	1	clay		
78	5	20	75	5	5	40	0	40	5	3	2	0	1	foram clay		
86	10	60	30	20	20	0	0	13	40	5	1	0	1	clayey silt		
96	1	20	79	10	10	3	5	65	0	5	5	0	0	clay		

depth (cm)	sand	silt	clay	quartz	feldspar	forams	Fe ox.	clay min.	rock fragm.	heavy min.	opaque min.	spicules	volc. glass	lithol.	plant debris	Cocco
	(%)	(%)	(%)	(%)	(%)	(%)	(%)	(%)	(%)	(%)	(%)	(%)	(%)		rel. abd.	rel. abd.
102	3	40	57	15	10	30	0	40	0	2	3	0	0	foram silty clay		
124	5	30	65	15	10	2	10	55	0	5	3	0	0	silty clay		
155	7	33	60	40	10	5	0	25	12	5	3	0	0	silty clay		
183	1	40	59	20	18	6	6	43	2	3	2	0	0	silty clay		
215	5	40	55	20	18	6	6	40	2	3	5	0	0	silty clay		
240	4	61	35	17	18	0	10	25	19	4	7	0	0	clayey silt		
274	1	25	74	20	20	5	0	50	0	3	2	0	0	clay		
291	8	42	50	15	20	15	0	40	5	3	2	0	0	F-rich silty clay		
324	1	7	92	5	5	1	0	80	5	2	3	0	0	clay		
347	5	40	55	20	15	5	0	45	8	5	2	0	0	silty clay		
375	15	40	45	30	15	2	0	32	10	7	4	0	0	snd. silty clay		
421	2	10	88	10	10	0	0	65	5	5	5	0	1	clay		
468	2	10	88	10	10	1	0	64	5	5	5	0	1	clay		
496	1	40	59	10	10	5	30	40	0	2	3	0	0	silty clay		
533	1	15	84	12	13	0	0	70	0	3	2	0	0	clay		
567	12	48	40	30	20	5	0	30	5	6	4	0	0	clayey silt		
582	5	30	65	15	15	2	0	55	0	8	5	0	0	silty clay		
589	10	50	40	30	20	6	0	35	2	5	2	0	0	cl. silty sand		
653	4	25	71	20	15	2	0	55	3	2	3	0	0	clay		
PS2835-6																
25	20	12	68	12	12	0	20	43	6	5	2	1	1	sandy clay	0	1
33	15	17	68	12	12	0	17	46	6	5	2	1	1	sandy clay	0	0
43	15	50	35	25	20	0	20	25	5	2	1	0	1	clayey silt	3	0
48	2	40	58	30	30	0	0	30	5	2	3	0	1	silty clay	1	0
63	2	25	73	30	25	5	0	55	5	1	1	0	1	clay	0	4
74	5	20	75	10	8	6	10	57	2	1	2	0	0	clay	0	4
88	8	20	72	14	12	0	5	53	10	5	2	0	0	clay	0	3

depth (cm)	sand (%)	silt (%)	clay (%)	quartz (%)	feldspar (%)	forams (%)	Fe ox. (%)	clay min. (%)	rock fragm. (%)	heavy min. (%)	opaque min. (%)	spicules (%)	volc. glass (%)	lithol.	plant debris rel. abd.	Cocco (%)
97,5	3	20	77	10	10	0	2	60	5	8	5	0	0	clay	0	3
104	8	10	82	10	8	10	3	65	0	3	1	0	1	clay	0	4
127	3	5	92	20	15	0	2	55	3	6	1	0	0	clay	1	3
215	10	40	50	17	13	8	15	34	5	5	2	0	0	silty clay	0	5
245	3	10	87	12	10	0	10	60	2	4	2	0	1	clay	0	2
317	6	17	77	20	20	0	0	46	4	7	8	0	3	clay	2	4
421	1	5	94	10	10	0	0	70	2	5	3	0	1	clay	1	0
PS2837-5																
8	5	20	75	10	15	1	5	60	2	3	2	3	0	clay		0
30	1	15	84	5	18	1	5	64	1	4	2	2	1	clay		4
63	1	15	84	5	18	0	5	64	1	4	2	2	1	clay		1
83	1	15	84	5	18	0	5	64	1	4	2	2	1	clay		5
107	4	33	63	5	17	2	5	64	1	4	2	1	1	silty clay		5
149	1	15	84	5	18	5	5	59	1	4	2	2	1	clay		5
182	2	18	80	5	17	5	6	60	1	4	4	1	1	clay		5
201	2	18	80	5	17	1	6	63	1	4	4	1	1	clay		2
253	6	40	54	10	15	5	5	55	2	3	5	1	1	silty clay		1
287	6	40	54	10	15	5	5	55	2	3	5	1	1	silty clay		3
331	2	15	83	5	15	2	5	65	3	2	3	1	1	clay		1
363	23	35	42	5	20	1	5	40	3	5	5	0	0	snd. clayey silt		0
387	15	25	60	10	15	10	5	45	5	5	5	0	0	snd. silty clay		4
392	15	25	60	10	15	10	5	45	5	5	5	0	0	snd. silty clay		4
408	25	30	45	20	25	0	0	30	20	2	3	0	0	snd. silty clay		1
415	1	10	89	7	18	0	0	65	2	3	5	0	0	clay		1
433	5	10	85	5	15	10	0	65	2	2	3	0	0	clay		3
442	3	20	77	10	12	1	0	70	3	3	1	0	0	clay		1
454	7	25	68	10	10	0	5	60	5	5	5	0	0	silty clay		0

depth (cm)	sand (%)	silt (%)	clay (%)	quartz (%)	feldspar (%)	forams (%)	Fe ox. (%)	clay min. (%)	rock fragm. (%)	heavy min. (%)	opaque min. (%)	spicules rel. abd.	volc. glass (%)	lithol.	plant debris rel. abd.	Cocco (%)
477	7	25	68	10	10	0	5	60	5	5	5	0	0	silty clay		3
509	7	30	63	15	15	0	2	60	5	5	3	0	0	silty clay		0
591	7	30	63	14	15	1	2	60	5	5	3	0	0	silty clay		1
633	1	12	87	14	15	1	2	60	5	5	3	0	0	clay		1
648	10	20	70	15	15	5	0	58	3	2	2	0	0	clay		2
684	6	28	66	15	15	8	0	53	3	2	2	0	0	silty clay		3
748	20	30	50	10	10	2	0	40	5	3	30	0	0	snd. silty clay		0
821	2	30	68	15	20	3	0	57	2	2	3	0	0	silty clay		0
855	2	30	68	15	20	4	5	51	2	2	3	0	0	silty clay		0
PS2839-4																
20	0	5	95	4	4	0	5	80	0	3	2	0	0	clay	0	3
37	35	30	35	45	5	0	8	20	10	3	15	0	0	silty clayey sd	tr.	4
40,5	25	30	45	5	2	0	35	32	5	1	20	0	0	sandy silty cl		3
49	10	45	45	30	10	1	5	35	5	4	10	0	0	clayey silt	tr.	4
60	8	47	45	30	20	0	0	30	10	5	5	tr.	0	clayey silt	0	4
69,5	10	8	82	8	7	40	2	25	3	3	10	tr.	0	foram. clay	0	4
87	10	8	82	8	7	40	2	25	3	3	10	tr.	0	foram. clay	0	5
102	20	40	40	40	10	tr.	2	25	20	tr.	3	0	tr.	sandy clayey sl	0	
108	2	10	88	8	4	0	5	73	3	2	5	0	0	clay	0	2
131	2	10	88	4	4	25	2	60	0,5	5	2	0	0	foram-rich cl	0	5
159	3	15	82	8	6	3	8	67	3	5	1	0	tr.	clay	0	2
177,5	1	5	94	4	4	1	9	80	0,5	2	1	0	0	clay	0	0
196	1	5	94	4	4	1	5	80	0,5	2	1	0	0	clay	0	1
229	3	15	82	15	10	5	12	48	2	4	1	0	0	clay	0	3
246	10	15	75	10	5	25	15	33	2	5	2	0	tr.	foram-rich cl	0	0
257	3	10	87	12	10	30	3	35	2	5	3	0	0	foram. clay	0	0
268	3	15	82	20	20	5	5	40	0	3	2	0	0	clay	0	4
308	3	20	77	20	20	2	1	42	5	2	8	0	tr.	clay	0	3

depth (cm)	sand (%)	silt (%)	clay (%)	quartz (%)	feldspar (%)	forams (%)	Fe ox. (%)	clay min. (%)	rock fragm. (%)	heavy min. (%)	opaque min. (%)	spicules (%)	volc. glass (%)	lithol.	plant debris rel. abd.	Cocco rel. abd.
326	10	35	55	25	20	15	0	25	8	5	2	0	tr.	F-rich sl-clay	0	3
332	1	4	95	13	12	23	0	42	1	2	5	0	0	foram-rich cl	0	0
339	20	30	40	20	15	28	0	20	5	2	5	0	0	F-rich sd-sl.cl	0	5
401	5	15	80	20	15	5	5	47	0	3	5	0	0	clay	0	4
427	10	15	75	13	12	8	10	50	5	3	1	0	0	clay	0	3
442	100	0	0	75	10	3	0	0	12	0	0	0	0	sand	0	1
445,5	5	30	65	30	15	2	10	37	0	3	3	0	0	silty clay	0	1
459	15	65	20	20	32	8	0	15	10	5	8	0	2	sandy clayey sl	0	1
475	2	8	90	10	8	1	0	76	2	2	1	0	0	clay	0	0
478	1	5	94	10	8	3	0	73	1	1	2	0	0	clay	0	5
482	1	5	94	10	8	6	3	67	1	1	2	0	0	clay	0	5
487	20	30	50	40	20	0	0	18	15	2	5	0	0	sandy silty cl	0	0
491	100	0	0	70	8	0	0	0	20	2	0	0	0	sand	0	4
495	45	55	0	70	8	0	0	0	20	2	0	0	0	sandy silt	0	3
502	20	45	35	50	8	3	0	22	18	2	2	0	0	sandy clayey sl	0	0
507	20	45	35	50	8	3	0	22	18	2	2	0	0	sandy clayey sl	0	0
511	10	30	60	30	6	2	0	40	18	2	2	0	0	silty clay	0	0
514	1	4	95	12	10	2	0	71	1	1	2	0	0	clay	0	2
520	20	45	35	35	15	0	0	25	15	5	5	0	tr.	sandy clayey sl	1	0
525,5	2	10	88	17	10	1	0	68	2	1	1	0	0	clay	0	4
534	10	40	50	32	25	1	0	35	5	1	1	0	0	silty clay	0	0
555	0	10	90	15	10	0	0	70	0,5	3	2	0	0	clay	0	2
575	1	24	75	20	13	2	0	55	5	tr.	2	0	0	clay	0	4
589	1	24	75	20	13	2	0	55	5	tr.	2	0	0	clay	0	4
605	1	20	79	20	13	3	0	45	0	3	2	0	0	clay	0	5
PS2843-1SL																
3	5	30	65	18	24	5	0	48	3	2	tr.	0	tr.	silty clay	0	2
9	1	20	79	8	16	15	0	51	2	2	3	0	tr.	F-rich clay	0	0
14	1	20	79	10	14	25	0	43	2	1	3	0	0	F-rich clay	0	0

depth (cm)	sand (%)	silt (%)	clay (%)	quartz (%)	feldspar (%)	forams (%)	Fe ox. (%)	clay min. (%)	rock fragm. (%)	heavy min. (%)	opaque min. (%)	spicules (%)	volc. glass (%)	lithol.	plant debris rel. abd.	Cocco rel. abd.
26	1	20	79	10	14	25	0	43	2	1	3	0	0	F-rich clay	0	
43	1	20	79	10	14	20	0	40	2	1	3	0	0	F-rich clay	0	
51	1	20	79	10	14	20	0	40	2	1	3	0	0	F-rich clay	0	
58	1	20	79	10	14	20	0	39	2	1	3	0	1	F-rich clay	0	
67	1	20	79	10	14	30	0	29	2	1	3	0	1	foram. clay	0	
74	10	50	40	8	25	16	0	32	10	5	4	0	tr.	F-rich cl. silt	0	
84	1	20	79	10	14	30	0	28	2	1	3	0	1	foram. clay	0	
100	1	20	79	10	14	30	0	28	2	1	3	0	1	foram. clay	0	
104	8	25	67	10	14	30	0	29	2	1	3	0	1	foram. clay	0	4
108	1	20	79	12	16	18	0	33	2	1	3	0	1	foram. clay	0	
115	1	20	79	12	16	18	0	33	2	1	3	0	1	foram. clay	0	
121	1	20	79	10	14	25	0	30	2	1	3	0	1	F-rich clay	0	5
138	1	34	65	8	12	40	5	30	0	3	1	0	1	foram. silty cl	tr.	
147	1	34	65	11	15	15	2	52	0	3	1	0	1	silty clay	0	
149	2	38	60	10	13	22	0	50	0	3	1	0	1	F-rich silty cl	0	0
164	1	30	69	8	10	25	2	49	0	3	2	0	1	F-rich silty cl	0	0
176	1	30	69	8	10	30	8	38	0	3	2	0	1	foram. silty cl	0	
187	1	30	69	8	10	30	8	38	0	3	2	0	0	foram. silty cl	0	
199	1	30	69	8	10	33	3	36	0	3	5	0	0	foram. silty cl	0	
207	10	15	75	5	7	15	3	54	8	3	5	0	0	foram. silty cl	1	0
219	0	5	95	5	7	33	5	39	6	3	5	0	0	foram. clay	tr.	0
231	0	5	95	5	7	33	5	39	6	3	5	0	tr.	foram. clay	0	
248	30	50	20	15	8	50	0	10	11	5	1	0	0	F clayey sd silt	0	1
256	12	30	58	15	8	50	0	18	3	5	1	0	0	F silty clay	0	
291	50	30	20	35	10	40	0	0	10	5	0	0	0	F silty sand	0	0
296	0	15	85	10	8	35	0	48	2	2	1	0	0	foram clay	0	1
300	8	20	72	20	10	24	3	38	2	2	1	0	0	F-rich clay	0	0
314	0	10	90	5	10	20	5	54	0	2	2	0	tr.	F-rich clay	0	0
334	30	60	10	10	60	10	0	7	5	5	2	0	1	sandy silt	0	1
355	0	10	90	5	10	28	5	46	0	2	2	0	tr.	F-rich clay	0	0

depth (cm)	sand (%)	silt (%)	clay (%)	quartz (%)	feldspar (%)	forams (%)	Fe ox. (%)	clay min. (%)	rock fragm. (%)	heavy min. (%)	opaque min. (%)	spicules (%)	volc. glass (%)	lithol.	plant debris rel. abd.	Cocco rel. abd.
373	45	55	0	10	60	10	0	0	5	5	5	0	1	sandy silt	1	1
385	0	10	90	5	10	20	5	54	0	2	2	0	tr.	F-rich clay	0	0
414	2	15	83	5	10	20	5	54	0	2	2	tr.	tr.	F-rich clay	0	1
422	0	10	90	5	10	20	5	54	0	2	2	tr.	tr.	F-rich clay	0	0
437	15	30	55	20	10	45	5	8	5	5	2	0	tr.	F sandy silt clay	0	1
456	15	30	55	24	12	40	5	8	5	5	2	0	tr.	F sandy silt clay	0	0
461	3	10	87	8	4	20	5	60	0	1	2	0	0	F-rich clay	tr.	0
469	10	50	40	50	5	5	2	18	10	4	4	0	2	clayey silt	0	0
479	5	30	65	8	4	15	8	62	0	2	1	0	0	silty clay	0	
490	70	20	10	40	15	7	0	7	20	5	3	0	3	sand	0	
496	5	30	65	8	4	15	8	62	0	2	1	0	0	silty clay	0	
506	5	30	65	8	4	15	15	55	0	2	1	0	0	silty clay	0	0
513	15	50	35	25	18	0	4	19	18	8	4	0	4	clayey silt	1	
516	15	50	35	25	18	0	4	19	18	8	4	0	4	clayey silt	1	0
522	15	35	50	25	18	0	6	15	18	8	6	0	4	silty clay	1	0
536	3	70	27	40	30	1	0	11	10	5	8	0	3	clayey silt	tr.	1
556	2	35	63	15	12	10	2	50	6	0	3	0	2	silty clay	0	
562	0	8	92	5	5	20	10	56	0	2	2	0	tr.	F-rich clay	0	0
572	7	30	63	15	15	3	2	49	10	3	3	0	0	silty clay	0	
581	12	32	56	20	10	30	5	26	5	3	1	0	0	F silty clay	0	0
584	60	40	0	40	40	5	0	0	10	4	0	0	1	silty sand	0	
594	50	35	15	30	28	15	0	5	10	6	4	0	2	silty sand	0	
612	1	5	94	5	5	30	20	39	0	0	1	0	0	foram clay	0	0
630	3	8	89	5	5	35	5	47	0	2	1	0	0	foram clay	0	0
644	0	4	96	5	5	30	5	51	0	2	2	0	0	foram clay	0	0
PS2850-1																
10	1	4	95	3	1	2	15	40	0	4	0	0	5	nanno clay	0	0
19	5	40	55	20	25	0	10	34	0	3	5	0	3	silty clay	0	0
31	2	10	88	4	10	0	5	80	0	0	1	0	tr.	clay	0	0
39	2	40	58	5	30	0	0	54	10	0	1	0	tr.	silty clay	0	0

depth (cm)	sand (%)	silt (%)	clay (%)	quartz (%)	feldspar (%)	forams (%)	Fe ox. (%)	clay min. (%)	rock fragm. (%)	heavy min. (%)	opaque min. (%)	spicules (%)	volc. glass (%)	lithol.	plant debris rel. abd.	Cocco rel. abd.	comments
50	6	42	52	12	24	0	3	50	8	1	1	0	1	silty clay	0	0	
65	5	40	55	12	20	0	10	50	7	1	tr.	0	tr.	silty clay	0	0	
84	5	60	35	33	27	0	0	25	11	1	2	0	1	clayey silt	0	0	
94	2	55	43	5	8	0	0	30	50	1	4	0	2	clayey silt	0	0	
100	5	45	50	3	2	0	0	25	60	3	5	0	2	silty clay	0	0	
105	7	47	46	11	15	0	0	30	30	5	8	0	1	silty clay	0	0	
123	10	65	25	15	25	0	0	22	20	5	10	0	3	clayey silt	0	0	
139	70	20	10	65	10	0	0	2	15	3	3	0	2	sand	0	0	
158	50	20	30	60	6	0	8	10	8	3	3	0	2	silty clayey sd	0		
PS2852-1																	
2	20	44	36	30	25	0	5	11	20	5	3	0	1	sandy cl. silt	0	0	coal, Dol
8	5	15	80	15	10	4	5	56	5	3	1	0	1	clay	0	0	Dol
20	15	45	40	25	15	2	5	19	30	3	1	0	2	sandy cl. silt	0	1	
30	50	30	20	35	25	0	8	0	25	3	2	0	2	clayey sl. sand	0	0	
34	50	30	20	35	25	0	8	0	25	3	2	0	2	clayey sl. sand	0	0	
45	20	60	20	35	25	2	10	0	20	3	2	0	3	cl. sandy silt	0	0	coal
49	50	50	0	50	28	0	5	0	10	4	3	0	tr.	silty sand	0	0	coal, Dol
54	20	12	68	20	10	3	3	51	10	2	1	0	tr.	sandy clay	0	1	
60	60	40	0	40	25	0	10	0	15	3	3	0	4	silty sand	0	0	
74	2	50	48	15	20	2	1	45	10	2	4	0	1	clayey silt	0	1	coal, Dol
79	10	10	80	20	12	0	10	49	3	2	2	0	0	clay	0	1	mica - 2%
91	50	10	40	40	15	0	2	10	25	3	4	0	1	clayey sand	0	0	coal, FeS2
100	15	70	15	40	15	0	15	9	15	2	3	0	1	silt	0	0	coal
118	15	70	15	40	15	0	15	9	15	2	3	0	1	silt	0	0	coal
125	15	70	15	40	15	0	0	9	14	2	3	0	tr.	silt	tr.	0	coal
141	8	35	57	15	15	0	0	43	15	2	10	0	0	silty clay	0	0	coal
147	15	50	35	25	15	0	0	30	20	2	8	0	0	sandy cl. silt	tr.	0	coal
159	15	50	35	25	15	3	0	27	20	2	8	0	0	sandy cl. silt	tr.	1	coal, Dol
192	5	20	75	15	10	5	0	58	5	2	8	0	2	clay	tr.	1	Dol, coal

depth (cm)	sand (%)	silt (%)	clay (%)	quartz (%)	feldspar (%)	forams (%)	Fe ox. (%)	clay min. (%)	rock fragm. (%)	heavy min. (%)	opaque min. (%)	spicules (%)	volc. glass (%)	lithol.	plant debris rel. abd.	Cocco rel. abd.	comments
197	10	50	40	25	15	5	10	11	20	3	10	0	1	clayey silt	0	0	Dol, coal
208	5	40	55	20	20	0	1	33	15	2	8	0	2	silty clay	0	0	coal
219	60	40	0	55	10	0	0	0	25	3	3	0	2	silty sand	0	0	coal
228	3	15	82	15	15	0	2	57	5	2	3	0	1	clay	0	0	Dol, Glauc, coal
239	10	40	50	25	25	0	0	24	10	3	10	0	3	silty clay	tr.	0	coal
244	5	25	70	15	10	0	0	43	10	4	15	0	3	clay	0	1	Dol, coal
253	20	60	20	25	15	4	8	16	20	4	5	0	3	sandy cl. silt	0	0	Glauc, Dol, coal
264	3	15	82	10	10	6	2	47	6	2	15	0	2	clay	0	0	coal, Dol
275	65	20	15	45	10	5	0	0	25	3	2	0	2	cl. silty sand	0	0	FeS2, Dol
281	75	20	5	45	10	3	0	0	25	2	15	0	tr.	silty sand	tr.	0	coal, Glauc
289	8	60	32	30	20	0	0	0	35	4	8	0	3	clayey silt	tr.	0	coal, Dol, Glauc
298	8	60	32	30	20	0	5	0	30	4	8	0	3	clayey silt	tr.	0	coal, FeS2
300	5	45	50	15	10	5	8	26	10	5	18	0	3	silty clay	tr.	0	coal, FeS2
304	20	65	15	30	18	0	2	4	30	2	13	0	1	sandy silt	tr.	0	coal, Dol
310	1	15	84	10	8	5	5	48	3	2	18	0	1	clay	tr.	0	coal
318	10	60	30	30	25	4	0	6	30	1	2	0	2	clayey silt	0	0	
323	4	45	51	25	20	0	2	24	15	4	8	0	2	silty clay	0	0	coal
329	15	65	20	25	15	0	5	4	25	3	20	0	3	clayey silt	tr.	0	coal, FeS2
332	7	25	68	15	10	0	10	41	5	3	15	0	1	silty clay	0	0	coal
342	5	20	75	10	5	10	0	56	3	3	10	0	3	clay	tr.	0	Glauc, Dol, coal
359	5	20	75	10	5	10	0	56	3	3	10	0	3	clay	tr.	0	Glauc, Dol, coal
374	15	85	0	30	15	15	0	0	15	6	15	0	4	F-rich silt	0	0	Glauc, Dol, coal
382	3	35	62	15	10	0	0	55	5	3	5	0	2	silty clay	0	0	Dol, Glauc
386	10	45	45	20	10	3	0	54	5	3	5	0	3	silty clay	0	0	Glauc, coal

depth (cm)	sand (%)	silt (%)	clay (%)	quartz (%)	feldspar (%)	forams (%)	Fe ox. (%)	clay min. (%)	rock fragm. (%)	heavy min. (%)	opaque min. (%)	spicules (%)	volc. glass (%)	lithol.	plant debris rel. abd.	Cocco rel. abd.	comments
389	15	60	25	30	25	0	0	6	25	3	8	0	3	sandy cl. silt	0	0	Glauc, coal
399	20	60	20	20	15	15	0	7	10	3	15	0	5	F-rich sd.silt	0	1	Glauc, coal, Dol
PS2856-5																	
6	2	35	63	23	15	0	5	50	3	1	2	0	1	silty clay	0	0	
16	2	40	58	23	15	0	5	47	3	1	5	0	1	silty clay	0	3	
24	6	44	50	30	20	0	8	35	4	3	2	0	2	silty clay	0	0	
53	3	40	57	20	25	5	0	28	10	4	5	0	3	silty clay	0	2	
86	3	40	57	25	32	3	0	26	5	3	3	0	3	silty clay	0	3	
107	10	15	75	20	15	35	0	22	3	1	2	0	2	foram clay	0	4	Dt, Rd - tr.
122	3	40	57	25	32	3	0	26	5	3	3	0	3	silty clay	0	2	
129	6	48	46	28	30	2	5	9	10	5	8	0	0	clayey silt	0	2	Glauc
133	2	25	73	20	20	10	0	42	5	1	1	0	1	clay	0	4	
154	10	60	30	20	20	0	8	2	20	5	3	0	2	clayey silt	0	0	
182	10	60	30	25	25	0	5	2	10	5	6	0	2	clayey silt	0	0	Dol
209	10	60	30	25	25	1	5	2	9	5	6	0	2	clayey silt	0	0	
233	1	25	74	15	15	2	0	53	5	4	4	0	2	clay	0	3	
266	0	15	85	10	10	2	0	62	10	2	3	0	1	clay	0	4	coal
295	0	15	85	15	15	5	5	50	2	2	5	0	1	clay	0	2	coal
324	0	15	85	15	15	5	5	47	2	2	8	0	1	clay	0	3	coal
357	0	15	85	15	15	5	5	47	2	2	8	0	1	clay	0	3	coal
382	2	25	73	15	15	5	5	47	2	2	8	0	1	clay	0	3	
397	10	50	40	30	15	0	0	27	15	5	5	0	3	clayey silt	0	3	
402	15	60	25	20	18	0	0	26	25	3	5	0	3	sand. cl. silt	0	2	
410	10	50	40	30	15	0	0	22	15	5	10	0	3	clayey silt	tr.	0	
417	10	50	40	30	15	0	0	22	15	5	10	0	3	clayey silt	tr.	2	
432	90	10	0	40	30	0	0	0	20	5	5	0	tr.	sand	tr.	2	coal

depth (cm)	sand (%)	silt (%)	clay (%)	quartz (%)	feldspar (%)	forams (%)	Fe ox. (%)	clay min. (%)	rock fragm. (%)	heavy min. (%)	opaque min. (%)	spicules (%)	volc. glass (%)	lithol.	plant debris rel. abd.	Cocco rel. abd.	comments
455	3	15	82	10	15	1	0	56	13	2	3	0	tr.	clay	0	3	
462	0	10	90	10	15	3	0	54	13	2	3	0	tr.	clay	0	4	coal
474	70	15	15	43	25	0	0	10	10	4	6	0	2	sand	0	4	
480	15	35	50	25	20	0	0	39	8	3	3	0	2	silty clay	0	3	Glauc
484	30	50	20	25	10	0	25	13	15	4	5	0	3	cl. sandy silt	0	2	Glauc., coal
492	10	30	60	12	10	5	2	56	6	3	5	0	1	silty clay	0	2	Glauc
497	30	50	20	30	15	20	0	4	20	4	5	0	2	cl. sandy silt	0	4	Glauc
510	2	10	88	15	10	3	0	68	12	1	1	0	0	clay	0	3	Dol., Glauc
521	0	8	92	15	10	3	0	68	12	1	1	0	tr.	clay	0	4	Dol., Glauc
545	3	8	89	15	10	7	15	35	12	1	1	0	1	clay	0	4	
555	15	40	55	30	20	0	5	11	20	4	4	0	1	silty clay	0	0	Dol., Glauc
560	8	50	42	35	20	0	0	20	12	3	10	0	tr.	clayey silt	0	0	coal, Dol., FeS
574	25	60	15	35	30	5	0	0	7	3	15	0	5	cl sandy silt	0	1	Dol
583	0	10	90	10	10	30	0	45	2	1	1	0	1	foram clay	0	0	
585	10	50	40	25	15	5	0	20	15	3	15	0	2	clayey silt	0	0	Dol
592	2	40	58	15	15	5	15	32	10	2	5	0	1	silty clay	tr.	0	FeS2, coal
613	0	10	90	15	10	5	3	42	5	3	15	0	2	clay	tr.	0	Glauc., Dol
624	5	35	60	15	10	2	20	30	5	3	13	0	2	silty clay	tr.	0	FeS2
651	5	35	60	15	10	2	20	30	5	3	13	0	2	silty clay	tr.	0	Glauc., Dol
PS2859-8																	
0	1	10	89	8	8	6	10	59	2	2	4	0	1	clay	0	4	Dol, coal
20	10	25	65	15	7	1	10	56	5	2	2	0	1	silty clay	0	0	Dol
42	2	15	83	12	10	3	15	50	3	3	3	0	1	clay	0	2	Dol, coal
49	5	50	48	15	12	2	18	41	3	3	5	0	1	clayey silt	0	0	Dol, coal
54	1	25	74	6	6	4	0	70	2	1	10	0	1	clay	0	2	Dol
63	4	35	61	10	8	9	4	49	10	2	5	0	2	silty clay	0	4	Glauc, Dol
76	4	35	61	10	10	13	0	58	2	3	3	0	tr.	silty clay	0	4	Glauc, Dol
84	12	60	28	25	15	12	18	5	10	5	10	0	0	clayey silt	0	4	Dol

depth (cm)	sand (%)	silt (%)	clay (%)	quartz (%)	feldspar (%)	forams (%)	Fe ox. (%)	clay min. (%)	rock fragm. (%)	heavy min. (%)	opaque min. (%)	spicules (%)	volc. glass (%)	lithol.	plant debris rel. abd.	Cocco rel. abd.	comments
88	5	10	85	5	3	40	5	37	0	2	5	0	tr.	foram clay	0	0	
100	1	8	92	5	3	5	3	80	0	2	2	0	tr.	clay	0	0	Dol
115	10	50	40	20	10	8	15	35	7	3	2	0	tr.	clayey silt	0	1	
134	3	17	80	10	7	4	2	67	5	2	2	0	1	clay	0	0	Dol, coal
153	3	17	80	10	7	4	4	65	5	2	2	0	1	clay	0	0	Dol
172	3	17	80	10	7	7	4	61	5	2	3	0	1	clay	0	0	Glauca
191	0	5	95	6	5	4	8	69	2	1	3	0	2	clay	0	0	Dol
205	0	5	95	6	5	4	8	69	2	1	3	0	2	clay	0	0	Dol
214	0	5	95	6	5	4	5	67	2	1	4	0	2	clay	0	0	Dol
221	8	15	77	10	8	7	8	50	6	3	6	0	2	clay	0	0	Dol
232	8	15	77	10	8	7	8	44	12	3	6	tr.	tr.	clay	0	0	Dol
240	10	50	40	20	15	2	5	27	20	3	8	0	tr.	clayey silt	tr.	0	Glauca, coal
245	20	70	10	30	20	1	4	0	30	5	6	0	4	silt	tr.	0	Glauca, Dol, coal
253	20	70	10	30	20	1	4	0	30	5	6	0	4	silt	0	0	
259	20	30	50	20	15	0	3	31	15	3	10	0	3	sandy sl. clay	tr.	0	coal
265	20	30	50	20	15	3	3	28	15	3	10	0	3	sandy sl. clay	tr.	0	coal
270	10	15	75	6	4	40	8	26	6	2	8	0	tr.	foram clay	tr.	0	coal, Glauca
285	8	60	32	25	20	2	0	17	25	3	8	0	tr.	clayey silt	0	2	mica, coal
293	3	80	17	30	20	0	0	0	33	6	8	0	3	silt	0	3	Glauca, coal
300	5	20	75	15	10	10	5	37	15	3	4	0	1	clay	0	4	Dol
311	2	10	88	10	8	18	1	45	8	2	8	0	tr.	F-rich clay	tr.	3	Dol, coal, mica
320	2	10	88	10	8	18	1	45	8	2	8	0	tr.	F-rich clay	tr.	0	Dol, coal, mica
329	5	20	75	15	10	10	5	37	15	3	4	0	1	clay	0	1	Dol
339	8	35	57	15	7	10	1	45	8	3	10	0	1	silty clay	0	0	Glauca
352	3	30	67	15	7	10	1	45	8	3	10	0	1	silty clay	0	0	
366	30	60	10	30	25	2	5	0	20	5	10	0	3	sandy silt	0	0	coal
368	30	60	10	35	20	10	5	0	7	5	15	0	3	sandy silt	0	0	coal

depth (cm)	sand (%)	silt (%)	clay (%)	quartz (%)	feldspar (%)	forams (%)	Fe ox. (%)	clay min. (%)	rock fragm. (%)	heavy min. (%)	opaque min. (%)	spicules (%)	volc. glass (%)	lithol.	plant debris rel. abd.	Cocco rel. abd.	comments
371	1	10	89	8	8	18	10	42	5	2	6	0	1	F-rich clay	0	0	
390	1	5	94	5	5	3	0	76	4	2	5	0	tr.	clay	0	3	
406	3	20	77	10	8	8	8	46	10	3	5	0	2	clay	tr.	3	FeS2
420	3	20	77	10	8	8	8	40	10	3	9	0	2	clay	0	2	
444	3	20	77	10	8	10	3	45	10	3	9	0	2	clay	0	0	Dol, coal
463	4	25	71	10	8	12	8	38	10	3	9	0	2	clay	0	0	Dol
479	6	45	49	17	10	15	8	18	20	4	5	0	3	F-rich sl.clay	0	1	
493	20	80	0	30	25	0	2	0	32	6	3	0	2	silt	0	0	coal
497	8	45	47	17	10	0	6	36	20	6	3	tr.	2	silty clay	0	1	FeS2
505	1	15	84	5	5	2	2	73	2	3	6	0	2	clay	0	0	
514	10	45	45	10	10	15	5	38	10	3	8	0	1	F-rich cl.silt	0	2	
523	10	25	65	6	10	25	0	39	7	2	8	0	3	F-rich sl.clay	0	4	Glauc
539	1	35	66	6	10	10	0	62	2	4	3	0	3	silty clay	0	0	Dol, Glauc
555	20	60	20	30	20	15	3	0	20	3	5	0	2	F-rich cl.silt	0	0	Dol-2%, Glauc
566	0	15	85	8	8	4	8	63	4	1	3	0	1	clay	0	0	
583	2	25	73	12	12	8	12	36	6	2	12	0	0	clay	0	0	
598	3	15	82	10	8	12	8	49	10	3	9	0	1	clay	0	0	Dol
613	5	50	45	15	15	17	12	5	20	4	10	0	2	F-rich cl.silt	0	0	Glauc
630	8	20	72	10	10	20	12	28	5	3	10	0	2	F-rich clay	0	1	

10.4 General guidelines for data and sample distribution and publications

By mutual understanding participating scientists in "Polarstern" Cruise ARK-XIII/2 agreed on general guidelines for the exchange of material and data obtained during the expedition. Because specific needs vary strongly between disciplines each participating disciplinary group set up its own specific guideline to best meet the specific demands. To optimize information for those not participating in the expedition or associated by shorebased studies a list of potential working titles has been attached.

10.4.1 Physical Oceanography

Principal investigators: B. Rudels (FIMR/AWI), R. Meyer (AWI), V. Ivanov (AARI), D. Hevekerl (IfMHH).

Data distribution, data processing and analysis:

The CTD data will be available for the PI from FIMR, AWI, IfMHH and AARI. Required data will be supplied to other groups involved in water sampling. B. Rudels will be responsible for the calibration and processing of the data in co-operation with IfMHH and AWI.

Tentative titles and publications:

- The hydrography of the northern Fram Strait and the Yermak Plateau. B. Rudels, R. Meyer, V. Ivanov, and D. Quadfasel.
- Interannual variations of thermohaline conditions in Fram Strait in the context of long term climatic oscillations. V. Ivanov, et al.
- Estimating the exchanges through Fram Strait between the Arctic Ocean and the Nordic Seas using geostrophy, balance constraints and energy minimisation. B. Rudels, V. Ivanov, R. Meyer, et al.

10.4.2 Marine Biology

The expedition is regarded a contribution to the ecological research within the AOSGE-project, with special emphasis to processes of subsystem coupling (ice - pelagial - benthal) near and across the marginal ice zone. Accordingly, the material and data collected are to be used especially for purposes of the AOSGE.

Principal investigators and contact persons:

- Sea Ice Biota: M. Spindler, K. Meiners (IPÖ), Q. Zhang (SIO Hangzhou)
- Phytoplankton and Particle Flux: E.-M. Nöthig and E. Bauerfeind (AWI), Y. Okolodkov
- Zooplankton: H.-J. Hirche (AWI), K. Kosobokova (IORAS), H. Auel (IPÖ)

- Macrozoobenthos: E. Rachor, H. Thiel, M. Klages (AWI), K. v. Juterzenka (IPÖ), S. Denisenko (MMBI)
- Meiobenthos, protozoans and biogenic sediment compounds: T. Soltwedel, I. Schewe (AWI), V. Mokievsky (IORAS)
- Microbenthos, bacteria: E. Helmke (AWI)
- Birds: H. Bäsemann, Tromsø

Material:

All samples and data obtained during ARK-XIII/2 are to be labelled with "Polarstern" station numbers, indicating the gear used. Publications should refer to these station numbers. The material will be distributed among the above mentioned investigators and their collaborators; macrofauna material will also be transferred to the ZISP partners in St. Petersburg. Any other use (e.g. by other AOSGE partners) before the end of 1999 is only possible after consent of the principal investigators (underlined above). AWI contact persons have to be informed before such external use.

Tentative titles and publications:

- Athebate dinoflagellates from the waters of Svalbard and the Fram Strait, with description of new species (to be submitted to *Polar Research*).
- A sympagic-planktonic dinoflagellate *Peridiniella catenata* (Levander) Balech: morphology, ecology and biogeography (to be submitted to *Botanica Marina*).
- Protoperidinium falk-petersenii* sp. nov., a new species of thecate dinoflagellates from the European Arctic (to be submitted to *Sarsia*).
- Species range types of marine dinoflagellates based on the distribution of the species recorded from the Arctic (to be submitted to *Grana*).
- Algae in melt pools off Svalbard, the Arctic Ocean (to be submitted to *Botanical Journal, Russian Academy of Sciences*; otherwise, it will be submitted in co-authorship with Marina Carstens, IPÖ, like a paper on the melt pool ecosystem).
- A planktonic flagellate *Birostra noethigae* gen. n., sp. n. from the European Arctic and the NE Atlantic (new genus is questionable; to be submitted to *Sarsia* or *Polar Research*).
- On the grazing impact of heterotrophic protists in Arctic sea ice algal assemblages - R. Gradinger & K. Meiners
- Comparison of sympagic assemblages of different types of Arctic sea ice
R. Gradinger, K. Meiners & Q.Zhang
- The seasonal cycle of ice biota development in Arctic seas
R. Gradinger, K. Meiners & Q.Zhang
- Characterization and biota of small Arctic melt pools

E. Helmke, K.v.Juterzenka, K. Meiners, S. Lischka, Y. Okolodkov, Q.Zhang

-Algae in melt pools off Svalbard (Arctic Ocean)
Y. Okolodkov & M. Carstens (IPOE)

-The response of Arctic sea ice micro-organisms to changes of salinity under different light conditions - Q. Zhang

-Nutrients and primary production along the investigated transects
E.-M. Nöthig, E. Bauerfeind et al.

-Dinoflagellates and other flagellates in Svalbard and Fram Strait waters: Taxonomy, morphology, ecology, biogeography; with descriptions of new species
Y. Okolodkov

-Phytoplankton and particle flux in Svalbard, Fram Strait, Yermak Plateau and northern Barents Sea waters. - E.-M. Nöthig (AWI), E. Bauerfeind & Y. Okolodkov

-Feeding ecology and energy demand of carnivorous copepods (Euchaetidae) in the ice-covered Arctic Ocean - H. Auel

-Mesozooplankton community structure, abundance and biomass across the Yermak Plateau -H. Auel, K. Kosobokova, H.-J. Hirche

-Reproductive biology and egg production in arctic meso- and bathypelagic copepods -K. Kosobokova

-Vertical distribution and seasonal succession of mesozooplankton in the western Barents Sea - K. Kosobokova, H.-J. Hirche, H. Auel

-Seasonal observations on *Calanus glacialis* egg production in the western Barents Sea - K. Kosobokova, H.-J. Hirche

-Zoobenthos larval plankton. - M. Schlüter & E. Rachor

-Carbon flux models for a S-N-transect in the northern Barents Sea (June 1991 compared with May-June 1997) - E. Rachor, M. Klages, K. v. Juterzenka, H.-J. Hirche, K. Kosobokova, H. Auel, E. Bauerfeind, E.-M. Nöthig, E. Helmke, T. Soltwedel, P. Hall/S. Hulth and other participants of the 1991 cruise

-Carbon flux models for the other transect areas - as above

-Bryozoa in the waters off Svalbard. - Nina Denisenko & E. Rachor

-Macrofauna along a transect from Murman coast up to the northern continental slope of the Barents Sea (communities, species composition, abundances, biomass) - S. Denisenko & E. Rachor

-Comparison between Arctic and Antarctic bacterial deep sea communities
E. Helmke

-Temperature and pressure adaptation of the benthic Arctic microflora
E. Helmke

-Reaction of epibenthic echinoderms to organic input - K. v. Juterzenka

-Age determination of crustaceans from the Arctic (and Antarctic) using
Fluorescent Ageing Pigments (FAP). - M. Klages, - running project

-Food fall localization in necrophagous amphipods by means of mechano- and
chemoreception. - M. Klages, - running project

-Benthic energy (carbon) flow budget - M. Klages, T. Soltwedel, E. Damm, K. v.
Juterzenka, H. Thiel, E. Helmke, V. Mokievsky, S. Denisenko, E. Rachor

-Biogeography and general distribution patterns of macro-zoobenthos
communities along the Eurasian continental slopes from the Fram Strait via the
Barents and Kara Seas up to the Laptev Sea - E. Rachor (together with partners
of ZISP, MMBI, IPO)

-Benthic communities in the area of the Yermak Plateau
(including parts of the Fram Strait and of the continental slope off Svalbard) -
larger epifauna, macro-infauna, meiofauna and microbials - H. Thiel, H. Bluhm,
S. Denisenko, E. Helmke, K. v. Juterzenka, M. Klages, V. Mokievsky, E. Rachor, I.
Schewe

10.4.3 Sea-Ice Sedimentology and Water Chemistry

Contact Persons: D. Dethleff (GEOMAR) and V. Shevchenko (IORAS)

-Chemical composition of snow and melt pond water on ice-floes in the NW
Barents Sea and in the Fram Strait in June-July 1997. -M. Kriews, O. Schrems
(AWI), V.P. Shevchenko (IORAS), R. Stein (AWI).

-Characterisation of particulate matter contained in snow cover on ice-floes in the
Fram Strait in July 1997 using electron probe X-ray micro analysis. -V.P.
Shevchenko (IORAS), R. Van Grieken (University of Antwerp), D. Dethleff
(GEOMAR), R. Stein (AWI).

-¹⁰Be deposition to the ice-covered NW Barents Sea and Fram Strait in June-July
1997. -C. Strobl, A. Mangini (University of Heidelberg), V.P. Shevchenko
(IORAS), R. Stein (AWI).

-Sedimentological comparison of Fram Strait ice inclusions and Siberian shelf
surface deposits - Hints to sources and pathways of turbid Arctic sea-ice. -D. Dethleff,
GEOMAR; R. Stein, AWI; M. Levitan, IORAS Moscow; and Shipboard Scientific Party

-Intercomparison of Fram Strait particulate snow content, ice inclusions and surface deposits - New aspects on entrainment and release of ice-transported material. Dethleff, D., GEOMAR; Shevchenko, V., IORAS Moscow; Levitan, M., IORAS Moscow; and Shipboard Scientific Party

-Sediment inclusions in Arctic sea-ice - Possible pre-determined breaking-points or areas of enhanced ice floe stability? -Dethleff, D., GEOMAR; Löwe, P., BSH; Weiel, D. AWI; and Shipboard Scientific Party

10.4.4 Marine Geology

Contact Persons: R. Stein (AWI) and F. Niessen (AWI)

Tentative titles and publications:

-Stable oxygen and carbon isotopes in planktic foraminifers from Arctic ocean surface sediments: Reflection of the low salinity surface water layer.- R. Volkmann & R. F. Spielhagen, GEOMAR

-Barium in Arctic shelf, slope and deep-sea sediments.- D. Nürnberg, GEOMAR

-Physical properties of sediment cores from the northern Fram Strait.- G. Nehrke, GEOMAR

-Coarse fraction and IRD composition of sediment cores from the northern Fram Strait and Late Quaternary ice-rafting history. R. F. Spielhagen & N. Nørgaard-Pedersen, GEOMAR, et al.

-Composition, ventilation and history of water masses at the Barents Sea shelf and northern Fram Strait derived from stable oxygen and carbon isotope data of water samples.- H. Erlenkeuser, Univ. Kiel; R. Volkmann & R. F. Spielhagen, GEOMAR

-Correlation of $\delta^{18}O$ and $\delta^{13}C$ values of the surface waters with values of planktic foraminifers from the surface sediments and from plankton tows.- R. Volkmann, GEOMAR

-Coarse fraction composition of surface sediments obtained during ARK-XIII/2.- R. Volkmann & R. F. Spielhagen, GEOMAR

-Beryllium and Thorium isotopes in sediment cores obtained during ARK-XIII/2.- R. F. Spielhagen, GEOMAR, et al.

-Establishment of a litho- and chronostratigraphy for sediment cores obtained during ARK-XIII/2.-R. Stein, AWI; R. F. Spielhagen, GEOMAR, et al.

-Paleoenvironmental history of the northern Fram Strait during the late Cenozoic.- R Stein, AWI, et al.; N. Nørgaard-Pedersen & R. F. Spielhagen, GEOMAR, et al.

-Planktic foraminifers in ARK XIII/2 sediment cores: Evidence for Late Quaternary environmental changes from micropaleontological analysis. (Abundances and micropaleontology of planktic foraminifers).- R. Volkman, GEOMAR, et al.

-Sr-isotopes in Arctic sediments.- A. Eisenhauer, Göttingen; R. F. Spielhagen, GEOMAR; R. Stein, AWI, et al.

-Elemental composition of aerosols in marine boundary layer over the NW Barents Sea and the Fram Strait in June-July 1997. - V.P. Shevchenko, A.P. Lisitzin (IORAS), R. Stein (AWI), K. Buhlmann (DWD), A.A. Vinogradova (Institute of Atmospheric Physics, Moscow), A.A. Volokh (IMGRE, Moscow).

-Aerosol particle size distribution in marine boundary layer over the NW Barents Sea and the Fram Strait in June-July 1997. - V.P. Shevchenko (IORAS), V.V. Smirnov, A.V. Savchenko (Institute of Experimental Meteorology, Obninsk), R. Stein (AWI).

-Carbon and nitrogen isotope measurements in different components (sea-ice, water, zooplankton, and sediments of the Arctic Ocean. Carsten Schubert et al. (AWI)

-Multi Sensor Core Logging of physical properties of sediment cores from the Arctic Ocean - high resolution stratigraphy and depositional implications. (Niessen, F. and Kleiber, H.-P., AWI).

-Stable oxygen and carbon isotopes in planktonic foraminifers and late Quaternary variability of Arctic Ocean paleoenvironment (R.F. Spielhagen, GEOMAR; R. Stein, AWI)

-Clay mineral distribution and major and minor elements in sediments from the Yermak Plateau and adjacent deep-sea areas: Implications for paleoenvironment, transport processes, and terrigenous sediment source (R. Stein et al., AWI)

-Heavy mineral distribution in late Quaternary sediments from Yermak Plateau and adjacent deep-sea areas: Indicator for source areas and transport mechanisms of terrigenous matter (M. Levitan, M. Behrends, R. Stein, et al.)

-Late Neogene variability of flux and composition of terrigenous matter in the Yermak Plateau and Svalbard continental margin areas and its paleoenvironmental significance - A synthesis (R. Stein, M. Behrends, M. Levitan, et al.)

-Organic carbon flux in late Quaternary sediments from the Yermak Plateau and adjacent deep-sea areas: Terrigenous input versus surface-water productivity (R. Stein, K. Fahl, J. Knies, and C. Schubert, AWI)

-Palynology and biomarker in late Quaternary Arctic Ocean sediments and paleoenvironment (J. Matthiessen, K. Fahl, and R. Stein, AWI)

-Biomarker composition in the water column and underlying sedimentary sequences in the Yermak Plateau and adjacent deep-sea area: Indicator for organic-carbon sources and pathways, and late Quaternary environmental variability (K. Fahl et al., AWI)

-Benthic foraminifer assemblages and their stable oxygen and carbon isotope signal in late Quaternary sediments from the Yermak Plateau and Svalbard continental margin area. (A. Mackensen et al.; AWI)

-Composition of aerosols over the Yermak Plateau and East Greenland and Svalbard continental margin areas in June-August, 1997. (V.P.Shevchenko, et al.).

-Aerosol size distribution over the Yermak Plateau and East Greenland and Svalbard continental margin areas in June-August, 1997. (V.P.Shevchenko, et al.).

10.4.4.1 Sediment sample distribution guidelines for ARK-XIII/2 material

The sample distribution guidelines for ARK-XIII/2 are designed to guarantee a fair distribution of material, to minimize the duplication of scientific effort and maximize the scientific return from these valuable samples.

The Alfred-Wegener Institute (AWI) shall serve as the core repository for all ARK XI/1 sediment samples. AWI will be responsible for the distribution of samples to shipboard and shorebased investigators. AWI will maintain a record of all samples that have been distributed and the nature of the investigations being undertaken. This information will be available to investigators on request.

All cores collected on the expedition will be labelled and recorded according to the AWI and *Polarstern* standard scheme. Samples distributed from these cores will be labelled with a standard identifier which will include a core identifier and the interval from which the sample was removed. This standard identifier should be associated with all data reported; residues of samples should remain labelled so that they can be related to earlier data.

Any investigator wishing to request samples from the expedition shall submit, in writing, a sample request to AWI. The request should contain a statement of the nature of the proposed research, the size and approximate number of samples required to complete the study. Costs associated with the taking and/or receiving samples from the AWI repository shall be accounted for by the requesting party.

For two years following the expedition, sampling shall be limited to shipboard participants and shorebased investigators agreed upon by the geoscience participants during the expedition. Recognizing the tremendous investment of time and energy expended by members of the expedition's scientific party, in general preference shall be given to sample requests from shipboard participants.

For further information, please, contact either the chief scientist of „Polarstern,,
Cruise ARK-XIII/2, Ruediger Stein (AWI) or the curator of the AWI Sediment Core
& Data Repository: Dr. Hannes Grobe,

Alfred-Wegener-Institute for Polar and Marine Research
D-27568 Bremerhaven, Germany
Tel.: +49-471-4831-220
Fax: +49-471-4831-149
e-mail: hgrobe@awi-bremerhaven.de

10.5 Participants ARK-XIII/2

Research Participants

Name	Discipline	Institute
Holger Auel	Biology, Zooplankton	IPÖ
Hinrich Bäsemann	Journalist	Tromsø
Eduard Bauerfeind	Biology, Phytoplankton	AWI
Marion Behrends	Geology, Sedimentology	AWI
Klaus Buhlmann	Meteorology	DWD
Ellen Damm	Geochemistry	AWI
Stanislav Denisenko	Biology, Zoobenthos	MMBI
Dirk Dethleff	Sea Ice Sedimentology	GEOMAR
Wolfgang Dinkeldein	Helicopter-Service	HSW
Horst Ewald	Helicopter-Service	HSW
Kirsten Fahl	Geology, Org. Geochemistry	AWI
Elisabeth Helmke	Microbiology	AWI
Detlef Hevekerl	Oceanography	IfM-HH
Vladimir Ivanov	Oceanography	AARI
Karen v. Juterzenka	Biology, Benthos	IPÖ
Michael Klages	Biology, Zoobenthos	AWI
Ursula Klauke	Microbiology	AWI
Hans-Peter Kleiber	Geology, Sediment physics	AWI
Jochen Knies	Geology, Org. Geochemistry	AWI
Ksenia Kosobokova	Biology, Zooplankton	IORAS
Michael Kühn	Geochemistry	AWI
Friedhelm Kulescha	Biology, OFOS-Techn.	GEOMAR
Uwe Lahrman	Helicopter-Service	HSW
Michael Levitan	Geology, Sedimentology	IORAS
Silke Lischka	Biology, Zooplankton	IPÖ
Axel Maibaum	Geochemistry	AWI
Klaus Meiners	Sea Ice Biology	IPÖ
Ralf Meyer	Oceanography	AWI
Maxim Mitjajev	Geology, Sedimentology	MMBI
Vadim Mokievski	Biology, Benthos	IORAS
Eugene Musatov	Geology, Sedimentology	VNIIO
Gernot Nehrke	Geology, Sedimentology	GEOMAR
Frank Niessen	Geology, Sediment physics	AWI
Yuri Okolodkov	Biology, Phytoplankton	KBI
Eike Rachor	Biology, Zoobenthos	AWI
Bert Rudels	Oceanography	IfM-HH
Michiel Rutgers v.d. Loeff	Geochemistry	AWI
Burkhard Sablotny	Biology, Benthos	AWI
Ingo Schewe	Biology, Benthos	AWI
Detlev Schreiber	Helicopter-Service	HSW
Carsten Schubert	Geology, Org. Geochemistry	AWI
Thomas Soltwedel	Biology, Benthos	AWI
Hartmut Sonnabend	Meteorology	DWD
Vladimir Shevshenko	Geology, Aerosols	IORAS
Ruediger Stein	Chief Scientist (Geology)	AWI
Hjalmar Thiel	Biology, Benthos	AWI
Renate Volkmann	Geology, Foraminifers	GEOMAR

Name	Discipline	Institute
Quing Zhang	Sea Ice Biology	IPO
<u>since 04.08.97:</u>		
Olaf Boehne	Bathymetry	AWI
Birthe Dallmeier-Tiessen	Bathymetry	AWI
Klemens Heidland	Bathymetry	AWI

Institutions

AARI	The State Research Center - Arctic and Antarctic Research Institute, 38 Bering St., St. Petersburg, 199397, Russia
AWI	Alfred-Wegener-Institut für Polar- und Meeresforschung, Columbusstrasse, 27568 Bremerhaven, Germany
DWD	Deutscher Wetterdienst, Seewetteramt Hamburg Bernhard-Nocht-Str. 76, 20359 Hamburg, Germany
GEOMAR	Forschungszentrum für Marine Geowissenschaften, Universität Kiel, Wischhofstr. 1-3, 24148 Kiel, Germany
HSW	Helicopter Service Wasserthal GmbH, Kätnerweg 43, 22393 Hamburg, Germany
IfM-HH	Institut für Meereskunde, Universität Hamburg Tropowitzstr. 7, 22529 Hamburg, Germany
IPO	Institut für Polarökologie, Universität Kiel, Wischhofstr. 1-3, 24148 Kiel, Germany
IORAS	P.P. Shirshov Institute of Oceanology, Russian Academy of Sciences, 23, Krasikova St., Moscow, 117218, Russia
KBI	Komarov Botanical Institute, Russian Academy of Sciences, P-376, Prof. Popov's St., St. Petersburg, 197376, Russia
MMBI	Murmansk Marine Biological Institute, Russian Academy of Sciences, 17, Vladimirskaia Street, Murmansk, 183019, Russia
VNIIO	All-Russian Research Institute for Geology and Mineral Resources (VNIIOKEANGELOGIA), 1, Maklina pr., St. Petersburg, 190121, Russia

Ship's Crew

1.	Kapitän	Ernst-Peter Greve
2.	1. Offizier	Jürgen Keil
3.	1. Offizier	Martin Rodewald
4.	Ltd. Ingenieur	Volker Schulz
5.	2. Offizier	Lutz Peine
6.	2. Offizier	Steffen Spielke
7.	Arzt	Wolfgang Hotz
8.	Funkoffizier	Andreas Hecht
9.	2. Ingenieur	Wolfgang Delff
10.	2. Ingenieur	Henryk Folta
11.	2. Ingenieur	Wolfgang Simon
12.	Elektroniker	Andreas Piskorzynski
13.	Elektroniker	Martin Fröb
14.	Elektroniker	Werner Dimmler
15.	Elektroniker	Helmar Pabst
17.	Bootsmann	Reiner Loidl
18.	Zimmermann	Winfried Neisner
19.	Matrose	Siegfried Moser
20.	Matrose	Andreas Hartwig
21.	Matrose	Andreas Bäcker
22.	Matrose	Jens Bohne
23.	Matrose	Manfred Hagemann
24.	Matrose	Uwe Schmidt
25.	zusl. Matrose	Luis Gil Iglesias
26.	zusl. Matrose	Martinez Pousada
27.	Lagerhalter	Norbert Renner
28.	Masch-Wart	Enrico Arias Iglesias
29.	Masch-Wart	Frank Giermann
30.	Masch-Wart	Günter Fritz
31.	Masch-Wart	Eckard Krösche
32.	Masch.-Wart	Horst Dinse
33.	Koch	Frank Silinski
34.	Kochsmaat/B.	Mario Tupy
35.	Kochsmaat/K.	Heino Hünecke
36.	1. Steward(ess)	Petra Dinse
37.	Stewardess/KS	Claudia Lehmbecker
38.	2. Stewardess	Regine Klemet
39.	2. Stewardess	Maria Schmidt
40.	2. Stewardess	Carmen Lilinski
41.	2. Steward	Wu Mei Huang
42.	2. Steward	Chi Lung Wu
43.	Wäscher	Kwok Yuen Yu
